UNIVERSITY OF SOUTHAMPTON

Faculty of Engineering and Applied Science

School of Electronics and Computer Science

Intelligent Wireless Networking

by

Song Ni

A thesis submitted in partial fulfilment of the requirements for the award of Doctor of Philosophy at the University of Southampton

April 2005

Supervisor: Professor Lajos Hanzo

Dipl Ing, MSc, PhD, FIEEE, FREnd, DSc

Chair of Telecommunications

School of Electronics and Computer Science

University of Southampton

Southampton SO17 1BJ

United Kingdom

This thesis is dedicated to: my parents and Jing

UNIVERSITY OF SOUTHAMPTON

ABSTRACT

FACULTY OF ENGINEERING AND APPLIED SCIENCE
SCHOOL OF ELECTRONICS AND COMPUTER SCIENCE

Doctor of Philosophy

Intelligent Wireless Networking

by Song Ni

In this thesis we have enhanced the achievable performance of the Code Division Multiple Access (CDMA) based Universal Mobile Telecommunication System's (UMTS) Terrestrial Radio Access (UTRA) using both adaptive beamformers and adaptive modulation. A Multi-Carrier CDMA (MC-CDMA) system is also investigated. A specific family of spreading codes, which are known as Loosely Synchronized (LS) codes exhibits a so-called Interference Free Window (IFW), where both the auto-correlation and cross-correlation values of the codes become zero. Hence, LS codes have the potential of increasing the capacity of CDMA networks. The beneficial effect of LS spreading codes on the UTRA-like Frequency Division Duplex (FDD) and Time Division Duplex (TDD) CDMA cellular mobile's network performance was also investigated. More specifically, both single-element antennas, as well as two- and four-element adaptive antenna arrays (AAAs) located at the base stations were used. This work was then extended by investigating the achievable network capacity, when combining Adaptive Quadrature Amplitude Modulation (AQAM) techniques and AAAs. The effect of the cell size as well as that of the Signal-to-Interference plus Noise Ratio (SINR) threshold on the UTRA-like FDD CDMA cellular mobile network's performance was also investigated.

The UTRA TDD CDMA cellular mobile network is potentially more flexible than the FDD mode and hence it has the ability of supporting the asymmetric use of a duplex channel. However, the TDD technique is more vulnerable to cochannel interference than the FDD mode. Hence the attainable performance of the UTRA-like FDD and TDD/CDMA networks was compared in terms of their network capacity, grade of service (GOS) and their mean transmission powers in the context of log-normal shadow faded propagation environments. The key parameters of the UTRA TDD/CDMA Handover (HO) and Power Control (PC) based on the 3rd Generation Partnership Project (3GPP) were studied. A relative pilot power based hard handover technique and a frame-delay based power adjustment model used in power control were developed. A novel Genetic Algorithm (GA) assisted

timeslot scheduling scheme was also proposed, in order to search for the optimal timeslot allocation, which avoided the severe inter-cell interference imposed by using the same carrier for both uplink and downlink transmission in a UTRA TDD/CDMA system. Finally, the performance benefits of GA-assisted timeslot scheduling were quantified.

It was concluded that the joint employment of AAAs and AQAM has the potential of doubling the number of user supported in the FDD mode. Furthermore, AAAs and AQAM hold the promise of improving the number of users by an even higher factor in the TDD mode, which hence approaches the attainable performance of the FDD mode. Additional teletraffic improvements were attained even without multiuser detection by employing LS codes and GA-aided slot-scheduling.

Acknowledgements

I would like to express my gratitude to my supervisor Prof. Lajos Hanzo whose continuous guidance as well as his timely advice contributed greatly to the completion of this thesis. Over the past three year or so, his enthusiasm in searching for new ideas in wireless communications has always inspired and motivated me to reach new heights.

Special thanks are due to my colleagues in the Wireless Communications Research group, who always provided prompt help and advice throughout my entire research at Southampton. There are simply too many to mention here and all of them should be given equal credit. Thank you everybody.

Last but not least, I wish to thank my family for their continuous support. Most importantly, to my wife, Jing.

List of Publications

1. **S. Ni, J.S. Blogh and L. Hanzo** "On the network performance of UTRA-like TDD and FDD CDMA systems using adaptive modulation and adaptive beamforming", Proceedings of the IEEE Vehicular Technology Conference 2003 Spring, Jeju Island, Korea, 22-25 April 2003, vol.1, pp 606 - 610.

2. **S. Ni, H. Wei, J.S. Blogh and L. Hanzo** "Network performance of asynchronous UTRA-like FDD/CDMA systems using loosely synchronised spreading codes", Proceedings of the IEEE Vehicular Technology Conference 2003 Fall, Orlando, Florida, USA, 6-9 Oct 2003, vol.2, pp 1359 - 1363.

3. **S. Ni and L. Hanzo** "Genetic algorithm aided timeslot scheduling for UTRA TDD CDMA networks", IEE Electronics Letters, March 2005, vol.41, no. 7, pp 57 - 58.

4. **S. Ni and L. Hanzo** "Genetically enhanced performance of a UTRA-like time-division duplex CDMA network", To appear in the Proceedings of the IEEE Vehicular Technology Conference 2005 Spring.

5. **S. Ni, J.S. Blogh and L. Hanzo** "Adaptive antenna and adaptive modulation assisted network performance of multi-User detection aided CDMA systems", Submitted to the IEEE Transactions on Vehicular Technology.

6. **S. Ni, Hua Wei and L. Hanzo** "Loosely synchronized spreading code aided network performance of quasi-synchronous UTRA-like TDD and FDD CDMA systems ", Submitted to the IEE Electronics Letters.

7. **S. Ni, Hua Wei and L. Hanzo** "Loosely synchronized spreading code aided network performance of quasi-synchronous next-generation TDD/CDMA systems", Submitted to the IEEE Communications Magazine.

Contents

Chapter 1

Introduction

1.1 Background and Overview

The third generation mobile communication systems such as the Universal Mobile Telecommunication System (UMTS) [1–6] have been designed for supporting a variety of services, such as video telephony, fax, wireless Internet, etc [7, 8]. All these services require flexible and efficient resource allocation methods. The IMT-2000 standard comprises both Frequency Division Duplex (FDD) and Time Division Duplex (TDD) modes [9], in order to support the efficient exploitation of the paired and unpaired band of the allocated spectrum. The FDD mode is intended for applications in both macro- and micro-cell near environments, while supporting medium data rates and high mobility. The TDD mode was contrived for environments having high traffic density and indoor coverage, where the applications require high data rates and tend to create asymmetric wireless Internet traffic [10, 11]. In UMTS Terrestrial Radio Access (UTRA), the different service needs are supported in a spectrally efficient way by a combination of FDD and TDD. The FDD mode is intended for applications in both macro- and micro-cellular environments, supporting data rates of up to 384 kbps and high mobility. The TDD mode, on the other hand, is more suited to micro- and pico-cellular environments, as well as for licensed and unlicensed cordless and wireless local loop applications. It was designed for exploiting the unpaired spectrum - for example in wireless Internet applications, where much of the teletraffic is in the downlink - and supports data rates of up to 2 Mbps. According to the UMTS Forum [12], the percentage of mobile multimedia users increased significantly since 2000. The Third Generation (3G) has been rolled Wideband Code Division Multiple Access (WCDMA) radio access technology out, offering mobile users an evolution for their current mobile voice communication experience to add both video and other attractive new services. By the end of 2004, there were more than 16 million 3G/UMTS customers subscribing to 60 networks based on WCDMA technology in 25 countries. In

2010 about 60% of the traffic in Europe is expected to be created by mobile multimedia applications. The various contributions on the network performance of the UTRA FDD and TDD modes are summarized in Tables 1.1 and 1.2.

In this thesis we characterize the achievable system performance of a UTRA-like FDD and TDD CDMA system employing Loosely Synchronized (LS) spreading codes. LS codes exhibit a so-called Interference Free Window (IFW), where both the auto-correlation and cross-correlation values of the codes become zero. Therefore LS codes have the promise of mitigating the effects of both Inter-Symbol-Interference (ISI) and Multiple-Access-Interference (MAI) in time-dispersive channels. Hence, LS codes have the potential of increasing the attainable capacity of CDMA networks. The performance of a UTRA-like FDD/CDMA cellular network was investigated as a function of various cell sizes and various target SINR thresholds.

We study the performance of a CDMA based cellular mobile network, similar in its nature to the TDD-mode of the proposed UTRA standard. The impact of using adaptive antenna arrays at the base stations was investigated in both non-shadowed and shadowed environments while supporting high data rate users. This work was then extended by the application of adaptive modulation techniques, in conjunction with adaptive antenna arrays. We characterize the capacity of an adaptive modulation assisted, beam-steering aided TDD/CDMA system. In TDD/CDMA the mobiles suffer from interference inflicted by the other mobile stations (MSs) both in the reference cell the MS is roaming in (intracell interference) as well as due to those in the neighboring cells (intercell interference). Furthermore, in contrast to FDD/CDMA, where the Base Stations (BSs) transmit in an orthogonal frequency band, in TDD/CDMA there is additional interference imposed by other BSs of the adjacent cells, since all times-slots can be used in both the uplink and downlink. In return for this disadvantage, TDD/CDMA guarantees the flexible utilization of all the available bandwidth, which meets the demand for the support of asymmetric uplink and downlink services, such as high data rate file download in mobile Internet services, etc. In wireless systems the link quality fluctuates due to either fading- and dispersion-induced channel impairments or as a consequence of the time-variant co-channel interference imposed by the teletraffic fluctuations due to the varying number of users supported. Due to these impairments conventional wireless systems often drop the call. By contrast, a particular advantage of employing adaptive modulation is that the transceiver is capable of automatically reconfiguring itself in a more error-resilient transmission mode, instead of dropping the call.

The key parameters of the UTRA TDD/CDMA handover and power control based on the 3rd Generation Partnership Project (3GPP) standard were studied. A relative pilot power based Hard Handover (HO) and a frame-delay based power adjustment model used in power control were devel-

Year	Author	Contribution
'98	Ojanpera and Prasad [13]	An overview of third-generation wireless personal communications systems was presented.
	Dahlman, Gudmundson, Nilsson and Skold [14]	W-CDMA was presented as a mature technology to provide the basis for the UMTS/IMT-200 standards.
	Brand and Aghvami [15]	Multidimensional PRMA was proposed as a MAC strategy for the UL channel of the UTRA TDD/CDMA mode.
	Markoulidakis, Menolascino, Galliano and Pizarroso [16]	An efficient network planning methodology applied to the UTRA specifications was proposed.
'99	Mestre, Najar, Anton and Fonollosa [17]	A semi-blind beamforming technique was proposed for the UTRA FDD system.
	Akhtar and Zeghlache [18]	A network capacity study of the UTRA WCDMA system was presented.
	Berens, Bing, Michel, Worm and Baier [19]	The performance of low complexity turbo-codes employed in the UTRA TDD mode was studied.
'00	Haardt and Mohr [20]	An overview of UMTS as specified by the 3GPP was presented.
	Holma, Heikkinen, Lehtinen and Toskala [21]	An interference study of the UTRA TDD system based on simulations was provided.
	Aguado, O'Farrell and Harris [22]	An investigation into the impact of mixed traffic on the UTRA system's performance was presented.
'01	Haas and McLaughlin [23]	The "TS-opposing" DCA algorithm was proposed for a TD-CDMA/TDD air-interface.
	Guenach and Vandendorpe [24]	The downlink performance of the conventional RAKE receiver was investigated in the context of the UTRA-WCDMA system.
	Poza, Heras, Lablanca and Lopez [25]	An analytical downlink interference estimation technique was proposed for the UMTS system .
'02	Perez-Romero, Sallent, Agusti and Sanchez [26]	Congestion control mechanisms were proposed and analyzed designed for the UTRA FDD system.
	Allen, Beach and Karlsson [27]	The outage imposed by beamformer-based smart antennas was studied in a UTRA FDD macro-cell environment.

Table 1.1: Contributions on the network performance of UTRA FDD and TDD cellular systems.

Year	Author	Contribution
'02	Ruiz-Garcia, Romero-Jerez and Diaz-Estrella [28]	The effect of the MAC on QoS guarantees was investigated in order to handle multimedia traffic in UTRA system.
	Ebner, Rohling, Halfmann and Lott [29]	Solutions for the synchronization of ad hoc networks based on the UTRA TDD system were proposed.
'03	Agnetis, Brogi, Ciaschetti Detti and Giambene [30]	A frame-by-frame exact DL scheduling algorithm considering different traffic QoS levels was proposed.
	Kao and Mar [31]	An intelligent MAC protocol based on cascade fuzzy-logic-control (CFLC) and designed for the UTRA TDD mode was presented.
	Blogh and Hanzo [32]	The adaptive antenna array and adaptive modulation aided network performance of a UTRA FDD system was investigated.
	Rummler, Chung and Aghvami [33]	A new multicast protocol contrived for UMTS was proposed.
'04	Yang and Yum [34]	A flexible OVSF spreading code assignment designed for multirate traffic in the UTRA system was proposed.
	Sivarajah and Al-Raweshidy [35]	A comparative analysis of different DCA schemes conceived for supporting ongoing calls in a UTRA TDD system was presented.
	Yang and Yum [36]	A power-ramping scheme contrived for the UTRA FDD random access channel was proposed.
'05	Ni and Hanzo [37]	A genetic algorithm aided timeslot scheduling scheme designed for UTRA TDD CDMA networks was proposed.
	Rouse, S. McLaughlin and Band [38]	A network topology was investigated that allows both peer-to-peer and nonlocal traffic in a TDD CDMA system.
	Zhang, Tao, Wang and Li [39]	Developments beyond 3G mobile proposed by the Chinese communications TDD Special Work Group were disseminated.

Table 1.2: Contributions on the network performance of UTRA FDD and TDD cellular systems.

oped. A novel uplink/downlink GA-assisted timeslot scheduling scheme was proposed for the sake of avoiding the severe inter-cell interference caused by using the UTRA TDD/CDMA air interface. The network layer performance of a UTRA-like TDD/CDMA cellular system was quantified.

1.2 Organisation of the Thesis

- **Chapter 2:** In this thesis we will not delve into the basic concepts of CDMA. We characterize the achievable system performance of a UTRA-like FDD CDMA system employing loosely synchronized spreading codes. The achievable network performance was quantified by simulation and it was compared it to that of a UTRA-like FDD/CDMA system using Orthogonal Variable Spreading Factor (OVSF) spreading codes. The trade-offs between the achievable user capacity and the cell size as well as the SINR threshold were then explored. we have also examined the achievable user-load and the overall performance of a MC-CDMA based cellular network benefiting from both adaptive antenna arrays and adaptive modulation techniques.

- **Chapter 3:** This chapter commences with a brief introduction to the UTRA TDD/CDMA network, and then presents network capacity results obtained under various propagation conditions. The performance benefits of adaptive beamforming and adaptive modulation techniques were analyzed. These results were then compared to those acquired, when employing LS spreading codes.

- **Chapter 4:** In this chapter, we studied the effects of the hard handover margin and different power control schemes on the UTRA TDD/CDMA system's performance. Both closed-loop power control as well as open-loop power control schemes were developed based on the 3GPP standard. A frame-delay based power adjustment algorithm was proposed to overcome the channel quality variations imposed by the erratically fluctuating timeslot allocations in the different interfering radio cells.

- **Chapter 5:** In this chapter, we designed a GA-assisted uplink/downlink timeslot scheduling scheme for the sake of avoiding the severe inter-cell interference caused by using the UTRA TDD/CDMA air interface.

1.3 Contributions of the Thesis

- Study of the network performance gains achieved by using loosely synchronized spreading codes in a UTRA-like TDD and FDD CDMA cellular mobile network [40].

- Study of the network performance gains attained by adaptive beamforming and adaptive modulation technologies in a UTRA-like TDD/CDMA cellular mobile network as well as comparing the performance of the UTRA-like TDD and FDD CDMA cellular mobile network [41].

- Demonstrating the benefits of adaptive beamforming and adaptive modulation in the context of MC-CDMA cellular mobile networks.

- Developing a hard handover scheme and a frame-delay based power adjustment algorithm in a UTRA-like TDD/CDMA cellular mobile network.

- Design of a genetic algorithm assisted UL/DL timeslot scheduling scheme in a UTRA-like TDD/CDMA cellular mobile network [37, 42].

Chapter 2

UTRA FDD/CDMA Network Performance

2.1 Effects of Loosely Synchronized Spreading Codes on the Performance of CDMA Systems

2.1.1 Introduction

In this section we characterize the achievable system performance of a UTRA-like FDD CDMA system employing Loosely Synchronized (LS) spreading codes. Current CDMA systems are interference limited, suffering from Inter-Symbol-Interference (ISI), since the orthogonality of the spreading sequences is destroyed by the channel. They also suffer from Multiple-Access-Interference (MAI) owing to the non-zero cross-correlations of the spreading codes. LS codes exhibit a so-called Interference Free Window (IFW), where both the auto-correlation and cross-correlation values of the codes become zero. Therefore LS codes have the promise of mitigating the effects of both ISI and MAI in time dispersive channels. Hence, LS codes have the potential of increasing the capacity of CDMA networks. This contribution studies the achievable network performance by simulation and compares it to that of a UTRA-like FDD/CDMA system using Orthogonal Variable Spreading Factor (OVSF) codes.

In our previous research [43–45], the performance of a UTRA-like FDD CDMA system was quantified, when supported by adaptive beam-steering and adaptive modulation [46]. In [45], the system employed OVSF spreading codes [47], which offer the benefit of perfect orthogonality in an ideal channel. In a non-dispersive channel, all intra-cell users' signals are perfectly orthogonal. However, upon propagating through a dispersive multipath channel this orthogonality is eroded, hence all other users will interfere with the desired signal. Therefore in practice the intra-cell interference is always

non-zero.

We will consider the employment of a specific family of spreading codes, which are known as Loosely Synchronized codes [48]. These codes exhibit a so-called Interference Free Window, where the off-peak aperiodic autocorrelation values as well as the aperiodic cross-correlation values become zero, resulting in zero ISI and zero MAI, provided that the delayed asynchronous transmissions arrive within the IFW. More specifically, interference-free CDMA communications become possible, when the total time offset expressed in terms of the number of chip intervals, which is the sum of the time-offset of the mobiles plus the maximum channel-induced delay spread is within the code's IFW [49]. By employing this specific family of codes, we are capable of reducing the ISI and MAI, since users in the same cell do not interference with each other, as a benefit of the IFW provided by the LS codes used.

2.1.2 Orthogonal Variable Spreading Factor Codes

The spreading codes of the UTRA CDMA system are based on the Orthogonal Variable Spreading Factor technique, which was originally proposed in [47]. Different-length OVSF codes are generated recursively, as shown in Figure 2.1. More specifically, let $C_{SF}(n)$ denote the set of unique, user-specific channelization codes, where SF is the spreading factor of the code, and n is the code-index, where we have $1 \leq n \leq SF$. The codes at the same level of the code-generation tree of Figure 2.1 constitute a set of Walsh functions, which are orthogonal. Furthermore, any two OVSF codes found at different levels of the code tree are also orthogonal, except for the scenario, when one of the two codes is a so-called mother code of the other. For instance, $C_8(2)$ is a descendent of the codes $C_4(1)$, $C_2(1)$ and $C_1(1)$, and hence these three codes are not orthogonal to $C_8(2)$.

The UTRA downlink employs synchronous transmissions within each cell and hence it is capable of exploiting the orthogonality of OVSF codes [50]. The OVSF codes used in the downlink are hence capable of perfectly avoiding intra-cell multiuser interference, provided that no multipath-induced linear distortions are encountered. However, in the presence of wide-band multipath channels channel-induced linear distortion is encountered and hence the orthogonality of the OVSF codes is destroyed, leading to multiuser interference in the downlink [51–54]. More explicitly, the preservation of the OVSF codes' orthogonality is primarily dependent upon the radio channel linking the user population to the base station transmitter. Encountering a high number of multipath components degrades the OVSF codes' orthogonality, unless all the multipath components are resolved, and coherently combined at the receiver.

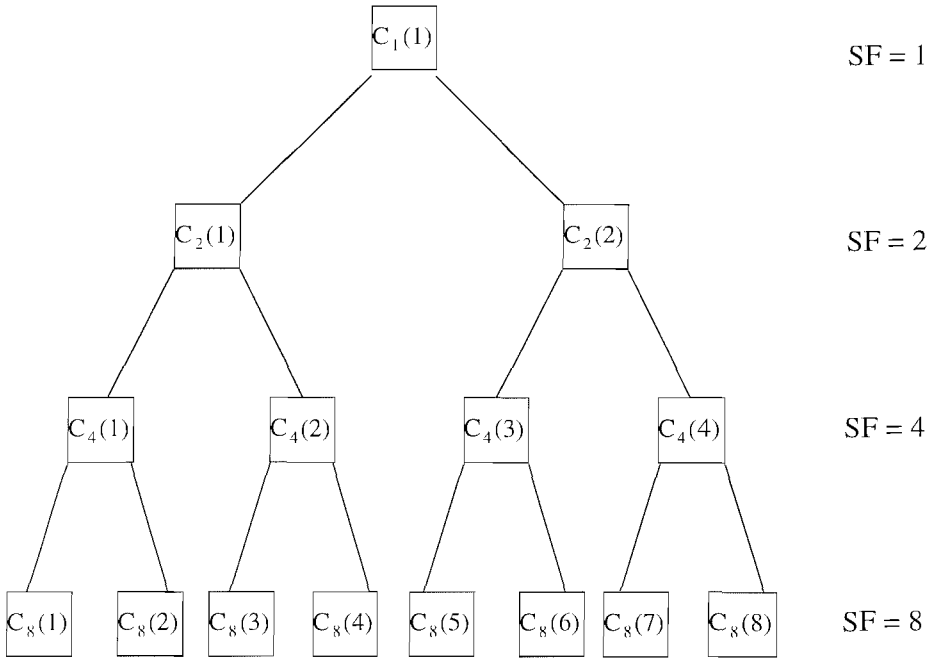

Figure 2.1: OVSF code generation tree-structure.

2.1.3 Loosely Synchronized Codes [40]

There exists a specific family of LS codes [48, 55–57], which exhibits an IFW. Specifically, LS codes exploit the properties of the so-called orthogonal complementary sets [48, 58]. To expound further, let us introduce the notation of LS(N, P, W_0) for denoting the family of LS codes generated by applying a $(P \times P)$-dimensional Walsh-Hadamard matrix to an orthogonal complementary code set of length N, while inserting W_0 number of zeros in the center and at the beginning of the LS code, as shown in Figure 2.2, using the procedure described in [48]. Then, the total length of the LS(N, P, W_0) code is given by $L = 2NP+2W_0$ and the number of codes available is given by $2P$.

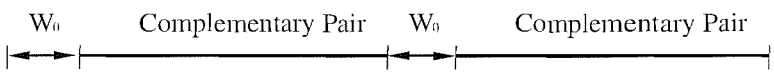

Figure 2.2: The LS code structure.

Since the construction method of binary LS codes was described in [48], we will focus our attention on the employment of orthogonal complementary sets [59, 60] for the generation of LS codes. Firstly, we define a sequence set $\mathbf{c}_1, \ldots, \mathbf{c}_N$, where $\mathbf{c}_n = [c_{n,0}, \ldots, c_{n,L-1}]$ is a spreading sequence having a length of L. These spreading codes exhibit an IFW width of τ_{IFW}, if the cross-correlation of the spreading codes satisfies:

$$R_{jk}(\tau) = \sum_{l=0}^{L-1} c_{j,l} c_{k,(l+\tau) \bmod L} = \begin{cases} L, & for \ \tau = 0, j = k \\ 0, & for \ \tau = 0, j \neq k \\ 0, & for \ 0 < |\tau| \leq \tau_{\mathrm{IFW}}. \end{cases} \quad (2.1)$$

The aperiodic correlation $R_{j,k}(\tau)$ of two sequences $\mathbf{g}_j$ and $\mathbf{g}_k$ has to satisfy Equation 2.1 for the sake of maintaining an IFW of τ_{IFW} chip intervals.

For a given complementary pair $\{\mathbf{c}_0, \mathbf{s}_0\}$ of length N, one of the corresponding mate pairs can be written as $\{\mathbf{c}_1, \mathbf{s}_1\}$, where we have:

$$\mathbf{c}_1 = \tilde{\mathbf{s}}_0^*, \quad (2.2)$$

$$\mathbf{s}_1 = -\tilde{\mathbf{c}}_0^*, \quad (2.3)$$

and where $\tilde{\mathbf{s}}_0$ denotes the reverse-ordered sequence, while $-\mathbf{s}_0$ is the negated version of $\mathbf{s}_0$, respectively. Note that in (2.2) and (2.3) additional complex conjugation of the polyphase complementary sequences is required for deriving the corresponding mate pair in comparison to binary complementary sequences [48]. Having obtained a complementary pair and its corresponding mate pair, we may employ the construction method of [48] for generating a family of LS codes. The LS codes generated exhibit an IFW, where we have $R_{jk}(\tau) = 0$ for $|\tau| \leq min\{N-1, W_0\}$. Hence, we may adopt a choice of $W_0 = N-1$ in order to minimize the total length of the LS codes generated, while providing as long an IFW as possible.

For example, the LS(4,2,3) codes can be generated based on the complementary pair of [59]:

$$\mathbf{c}_0 = +++- \quad (2.4)$$

$$\mathbf{s}_0 = ++--. \quad (2.5)$$

Upon substituting (2.2) and (2.3) into (2.4) and (2.5), the corresponding mate pair can be obtained as:

$$\mathbf{c}_1 = \tilde{\mathbf{s}}_0^* = +-++ \quad (2.6)$$

$$\mathbf{s}_1 = -\tilde{\mathbf{c}}_0^* = +---. \quad (2.7)$$

The generation of this set of the four LS codes can be viewed in Fig 2.3. Upon invoking the 2×2-dimensional Hadamard expansion of [48] in the context of the above orthogonal complementary pairs, we can generate a family of four LS(4,2,3) codes, which are denoted by $\mathbf{g}_p$, $p = 0, \cdots, 3$.

All four different codes of the LS(4,2,3) code family exhibited the same autocorrelation magnitudes, namely that seen in Figure 2.4(a). It can be observed in Figure 2.4(a) that the off-peak autocorrelation $R_p[\tau]$ becomes zero for $|\tau| \leq W_0 = 3$. The crosscorrelation magnitudes $|R_{j,k}(\tau)|$ depicted in Figure 2.4(b)

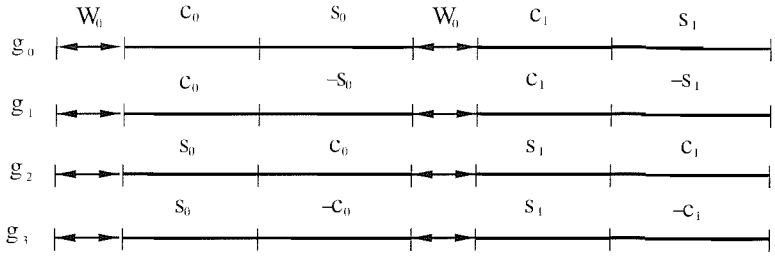

Figure 2.3: Generating four LS codes

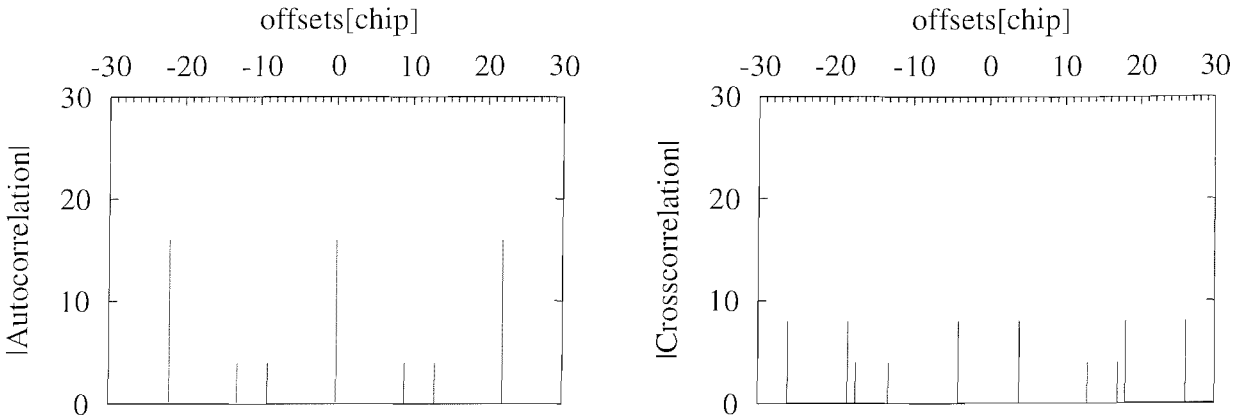

(a) Autocorrelation

(b) Crosscorrelations

Figure 2.4: correlation magnitudes of the LS$(4, 2, 3)$ codes. (a) All four codes exhibit the same autocorrelation magnitude. (b) The crosscorrelation magnitudes of $\mathbf{g}_0$ and $\mathbf{g}_2$.

are also zero for $|\tau| \leq W_0 = 3$. Based on the observations made as regards to the aperiodic correlations we may conclude that the LS(4,2,3) codes exhibit an IFW of ± 3 chip durations.

2.1.4 System Parameters

The cell-radius was 78 m, which was the maximum affordable cell radius for the IFW duration of ± 1 chip intervals at a chip rate of 3.84 Mchip/s. The call duration and inter-call periods were Poisson distributed with the mean values shown in Table 2.1. For our initial investigations we have assumed that the basestations and mobiles form a synchronous network.

Furthermore, the post-despreading SINRs required for obtaining the target BERs were determined with the aid of physical-layer simulations using a 4-QAM modulation scheme, in conjunction with 1/2-rate turbo coding for transmission over a COST 207 seven-path Bad Urban channel [61]. Using this turbo-coded transceiver and LS codes having a spreading factor (SF) of 16, the post-despreading SINR required for maintaining the target BER of 1×10^{-3} was 6.2 dB. The BER which was deemed

Parameter	Value	Parameter	Value
Noisefloor	-100dBm	Pilot power	-9dBm
Frame length	10ms	Cell radius	78m
Multiple access	FDD/CDMA	Number of basestations	49
Modulation scheme	4QAM/QPSK	Spreading factor	16
Min BS transmit power	-48dBm	Min MS transmit power	-48dBm
Max BS transmit power	17dBm	Max MS transmit power	17dBm
Power control stepsize	1dB	Power control hysteresis	1dB
Low quality access SINR	5.2dB	Outage (1% BER) SINR	4.8dB
Pathloss exponent	-2.0	Size of Active BS Set (ABS)	2
Average inter-call-time	300s	Max. new-call queue-time	5s
Average call length	60s	Pedestrian speed	3mph
Max consecutive outages	5	Signal bandwidth	5MHz
Target SINR	6.2dB		

Table 2.1: Simulation parameters.

to correspond to low-quality access, was stipulated at 5×10^{-3}. This BER was exceeded for SINRs falling below 5.2 dB. Furthermore, a low-quality outage was declared, when the BER of 1×10^{-2} was exceeded, which was encountered for SINRs below 4.8 dB. These values can be seen along with the other system parameters in Table 2.1.

2.1.5 Performance Metrics

There are several performance metrics that can be used for quantifying the performance or quality of service provided by a mobile cellular network. The following performance metrics have been widely used in the literature and were also advocated by Chuang [62]:

- New call blocking probability, P_B.
- Call dropping or forced termination probability, P_{FT}. A call is dropped when the lower of the uplink and downlink SINRs dips consecutively below the outage SINR (0.1% BER) a given number of times.
- Probability of a low quality access, P_{low}, quantifies the chances of either the uplink or downlink signal quality being sufficiently poor, resulting in a low quality access (0.5% BER).

- Probability of outage, P_{out}, is defined as the probability that the SINR is below the value at which the call is deemed to be in outage, namely below 4.8 dB, as seen in Table 2.1.

- Grade-Of-Service (GOS) was defined by Cheng and Chuang [62] as :

$$\begin{aligned} GOS &= P\{\text{unsuccessful or low-quality call accesses}\} \\ &= P\{\text{call is blocked}\} + P\{\text{call is admitted}\} \times \\ &\quad P\{\text{low signal quality and call is admitted}\} \\ &= P_B + (1 - P_B) \times P_{low}. \end{aligned} \tag{2.8}$$

Our network performance studies were conducted with aim of maintaining: $P_B \leq 3\%$, $P_{FT} \leq 1\%$, $P_{low} \leq 1\%$ and GOS $\leq 4\%$.

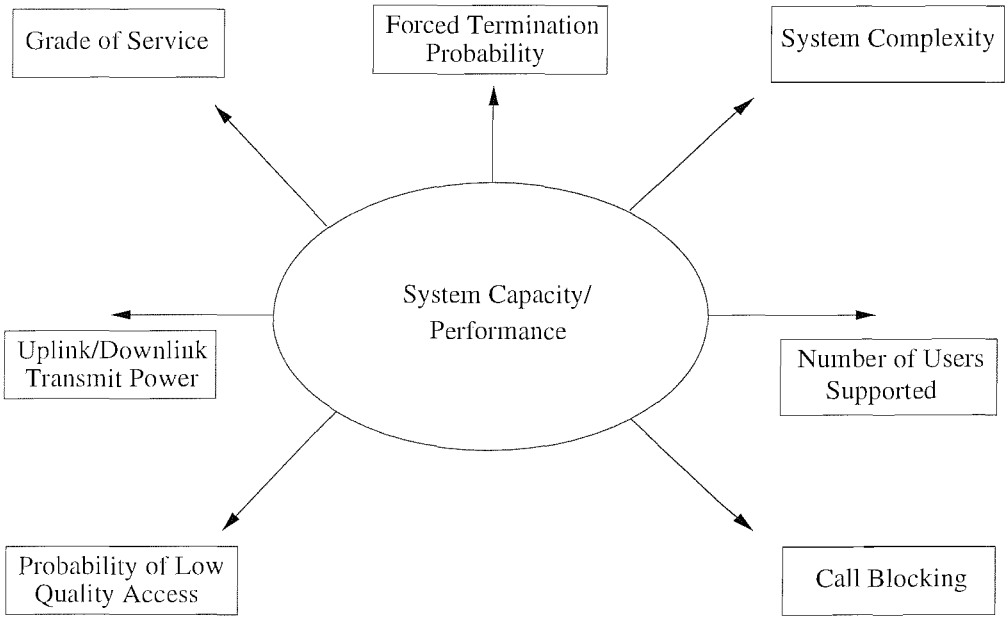

Figure 2.5: System capacity/performance illustration factors.

To elaborate a little further, the design of wireless networks is based on the above-mentioned as well as a range of other often contradictory trade-offs, which are summarized in the stylized illustration seen in Figure 2.5. For example, the figure suggests that it is always possible to reduce the call dropping probability by increasing the call blocking probability, since this implies admitting less users to the system. By contrast, we may admit more users to the system for the sake of reducing the call blocking probability, which however results in an increased call dropping probability. Furthermore, the performance of the entire system may also be improved by increasing the system's complexity upon using more intelligent, but more complex signal processing algorithms, such as the beamforming and adaptive modulation aided transceiver techniques advocated in Chapter 3. Similarly, the genetic algorithm based scheduling techniques of Chapter 5 may be used for reducing the co-channel interference

experienced by the system and hence for increasing the number of users, and/or for improving the call blocking and call dropping performance. Still continuing our discourse in the spirit of Figure 2.5, the number of users supported may also be increased, provided an increased probability of low quality access value may be tolerated. A whole raft of further similar comments may be made in the context of Figure 2.5, which will emanate from our detailed discourse throughout the thesis. Hence we postpone the discussion of these detailed findings to our forthcoming chapters.

2.1.6 Simulation Results

In the investigations of [43], OVSF codes were used as spreading codes. However, the intra-cell interference is only eliminated by employing orthogonal OVSF codes, if the system is perfectly synchronous and provided that the mobile channel does not destroy the OVSF codes' orthogonality. In an effort to prevent intra-cell interference, again, we employ LS codes, which exhibit ideal auto-correlation and cross-correlation functions within the IFW. Thereby, the "near far effect" may be significantly reduced and hence the user capacity of the system can be substantially enhanced. Figure 2.6 compares the BER performance of OVSF codes and LS codes, which were determined with the aid of physical-layer simulations using a 4QAM modulation scheme, 1/2-rate turbo coding and a Minimum Mean Squared Error Block Decision Feedback Equalizer (MMSE-BDFE) based Multi-User Detector (MUD) [63] joint detection for transmission over a COST 207 seven-path Bad Urban channel [64]. The figure illustrates that the achievable BER performance of LS codes is better than that of OVSF codes. For a spreading factor of 16, the post-despreading SINR required for maintaining a BER of 1×10^{-3} was 6.2 dB in case of LS codes, which is almost 2 dB lower than that necessitated by the OVSF codes.

Figure 2.7 shows the forced termination probability associated with a variety of traffic loads measured in terms of the mean normalized carried traffic expressed in Erlangs/km^2/MHz when subjected to 0.5 Hz frequency shadowing having a standard deviation of 3 dB. The average call duration and inter-call duration are 60 s and 300 s, resulting in maximum 0.2 Erlang/user traffic during the busy hour. The UTRA system's bandwidth is 5 MHz, the SF is 16 and given the cell-radius of 150 m as well as the 49-cell simulation area, the *Erlang* capacity is computed by recording all the users' call durations and dividing it by the total of duration of the time-interval over which the statistics were collected, while satisfying the network quality constraints of Section 2.1.5. The figure illustrates that the network's performance was significantly improved by using LS codes. In conjunction with OVSF codes, the "No beamforming" scenario suffered from the highest forced termination probability of the six traffic scenarios characterized in the figure at a given load. Specifically, the network capacity was limited to 152 users, or to a teletraffic load of approximately 2.65 Erlangs/km^2/MHz. With the advent of employing four-element adaptive antenna arrays at the base stations the number of users supported

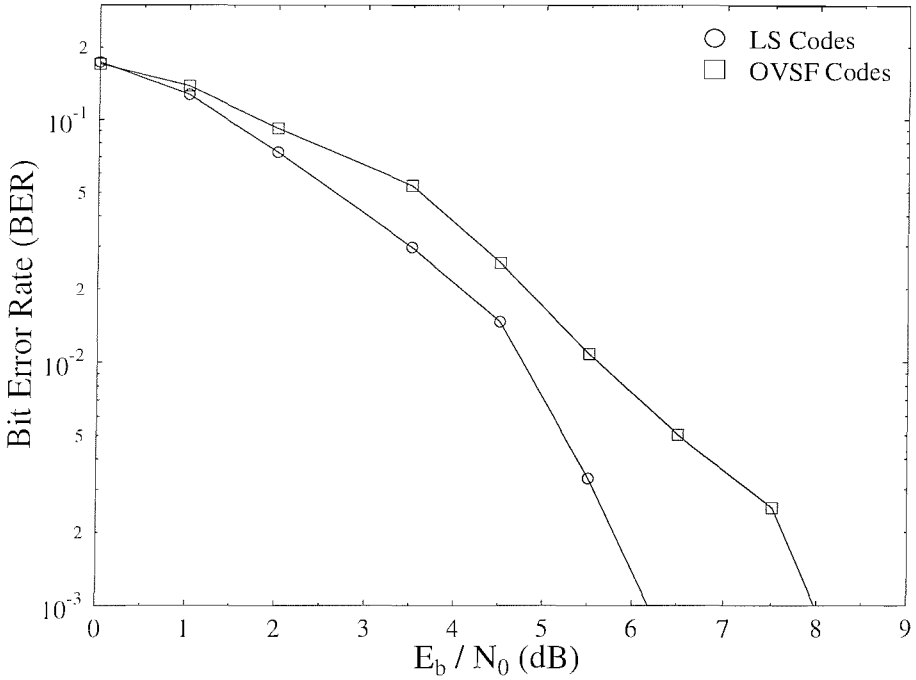

Figure 2.6: BER performance of a UTRA-like system using OVSF codes and LS codes generated with the aid of physical-layer simulations using 4-QAM modulation, 1/2-rate turbo coding and MMSE-BDFE joint detection for transmissions over a COST 207 seven-path Bad Urban channel.

by the network increased to 428 users, or almost to 7.23 Erlangs/km^2/MHz. However, in conjunction with LS codes, and even without employing antenna arrays at the base stations, the network capacity was dramatically increased to 581 users, or 10.10 Erlangs/km^2/MHz. When four-element adaptive antenna arrays were employed in the LS-code based scenario, the system was capable of supporting 800 users, which corresponded to a teletraffic load of 13.39 Erlang/km^2/MHz. This is because the LS codes' perfect auto-correlation and cross-correlation properties allowed the system to essentially eliminate the intra-cell interference, as it was discussed in Sections 2.1.1 and 2.1.3.

The probability of low quality access is depicted in Figure 2.8. As expected, a given P_{low} value was associated with a higher traffic load, when the number of antenna elements was increased. In the case of OVSF codes, it can be seen from the figure that without beamforming the system suffered from encountering more multiuser interference as the traffic loads increased. Hence the probability of low quality access became higher. In conjunction with beamforming, both the intra- and inter-cell interference was reduced and hence the probability of low quality access was reduced as well. However, increasing the number of antenna elements from two to four resulted in an increased probability of a low quality outage with the advent of the sharper antenna directivity. As a benefit of employing LS codes, the intra-cell interference was efficiently reduced and therefore the probability of low quality

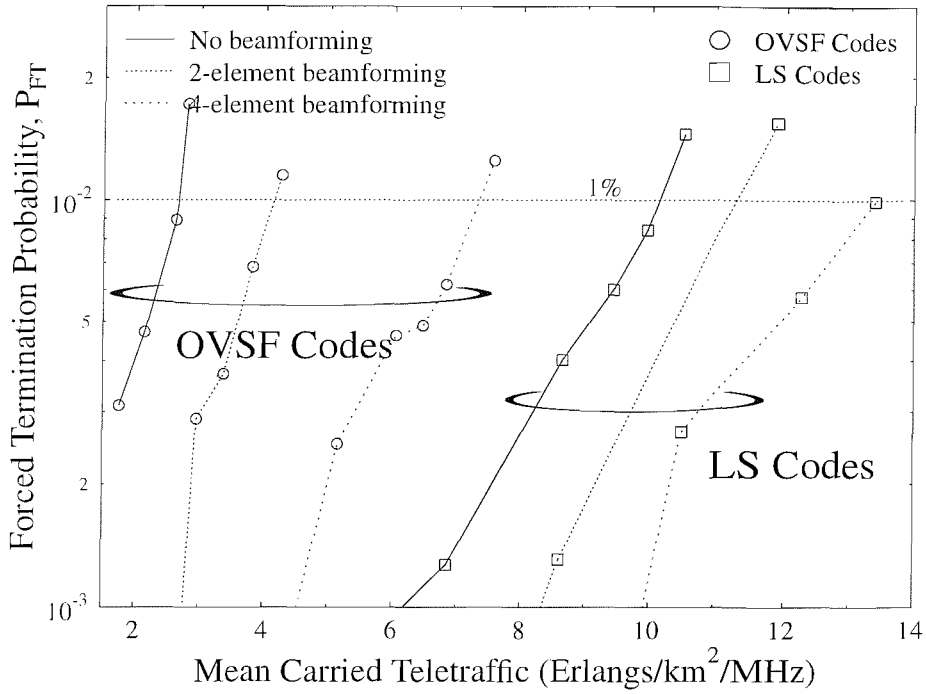

Figure 2.7: Forced termination probability versus mean carried traffic of the UTRA-like FDD cellular network using **LS codes and OVSF codes** both with as well as without beamforming in conjunction with shadowing having a frequency of 0.5 Hz and a standard deviation of 3dB for a spreading factor of SF=16.

access was found to be lower even without beamforming, than that of the system using OVSF codes and employing 2- or 4-element beamforming. Again, owing to the sharper antenna directivity, the probability of a low quality outage increased, when increasing the number of antenna elements from two to four. It should be noted that the probability of low quality access always remained below our 1% constraint in the scenarios studied.

Figure 2.9 shows the achievable Grade-Of Service (GOS) for a range of teletraffic loads. Similar trends were observed regarding the probability of low quality access to those shown in Figure 2.8. The grade of service is better (i.e. lower) when the traffic load is low, and vice versa for high traffic loads.

The mean transmission power versus teletraffic performance is depicted in Figure 2.10. Again, as a benefit of employing LS codes, both the required mean uplink and downlink transmission power are lower than that necessitated by OVSF codes. It is worth pointing out that the employment of adaptive antenna arrays may in fact result in the attenuation of the desired signal, but this is always performed for the sake of maximizing the received SINR, thus ensuring that the effects of interference are mitigated. As a further benefit, invoking adaptive antenna arrays at the basestation reduced the mean uplink transmission power required for meeting the service quality targets of the network. In

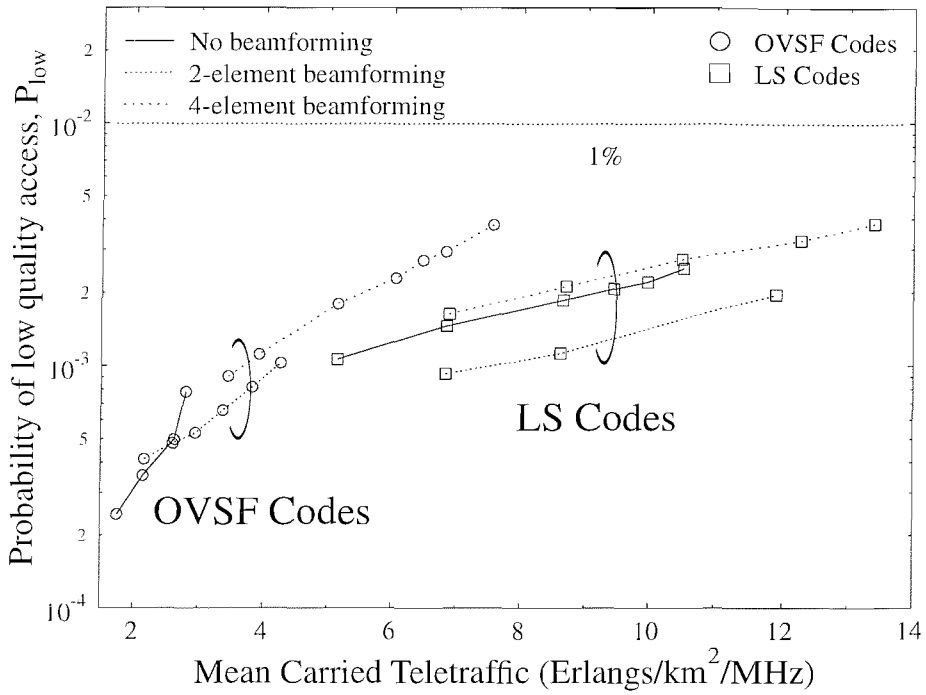

Figure 2.8: Probability of low quality access versus number of users of the UTRA-like FDD cellular network using **LS codes and OVSF codes** both with as well as without beamforming in conjunction with shadowing having a frequency of 0.5 and a standard deviation of 3dB for a spreading factor of SF=16.

Spreading Code	Beamforming	Users	Traffic (Erlangs /km^2/MHz)	Power (dBm) MS	BS
OVSF codes	No	152	2.65	-9.0	-9.0
OVSF codes	2-elements	242	4.12	-8.28	-7.88
OVSF codes	4-elements	428	7.23	-7.45	-5.40
LS codes	No	581	10.1	-8.19	-5.84
LS codes	2-elements	622	10.6	-9.88	-5.53
LS codes	4-elements	802	13.39	-10.57	-4.49

Table 2.2: Maximum mean carried traffic and maximum number of mobile users that can be supported by the network, whilst meeting the network quality constraints, namely $P_B \leq 3\%$, $P_{FT} \leq 1\%$, $P_{low} \leq 1\%$ and GOS $\leq 4\%$. The carried traffic is expressed in terms of normalized Erlangs (Erlang/km^2/MHz) using **OVSF codes and LS codes** in conjunction with shadow fading having a standard deviation of 3 dB and a frequency of 0.5 Hz, for a spreading factor of SF=16.

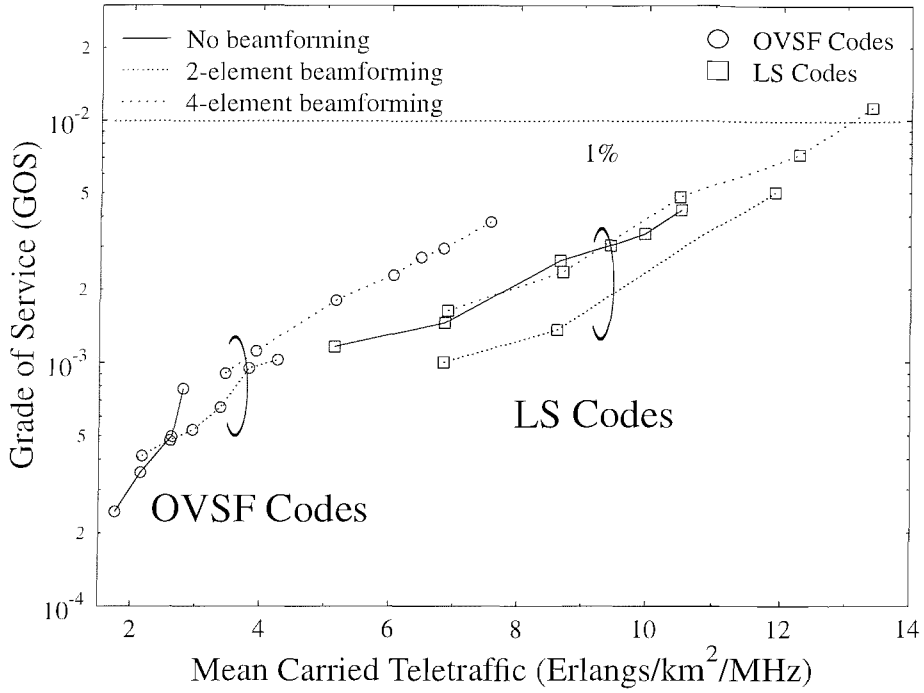

Figure 2.9: Grade-Of-Service (GOS) versus number of users of the UTRA-like FDD cellular network using **LS codes and OVSF codes** both with as well as without beamforming in conjunction with shadowing having a frequency of 0.5 Hz and a standard deviation of 3dB for a spreading factor of SF=16.

OVSF code based scenarios, the basestation suffered from more multiuser interference, as the traffic loads increased. This was particularly true for the intra-cell interference, which required an increased uplink mean transmission power for the sake of reaching the target SINR. By contrast, the LS codes had potential of eliminating the intra-cell interference, ultimately leading to the reduction of the mean transmission power required.

A summary of the maximum user capacities of the UTRA-like networks using OVSF codes and LS codes in conjunction with log-normal shadowing having a standard deviation of 3 dB and a shadowing frequency of 0.5 Hz as well as both with and without beamforming is given in Table 2.2. The teletraffic carried and the mean mobile and base station transmission powers required are also shown in Table 2.2.

2.1.7 Summary

In this section it was demonstrated that the network performance of a UTRA-like CDMA system employing LS spreading codes was substantially better than that of the system using OVSF codes. Explicitly, a low forced termination probability, low mobile and base station transmission power and

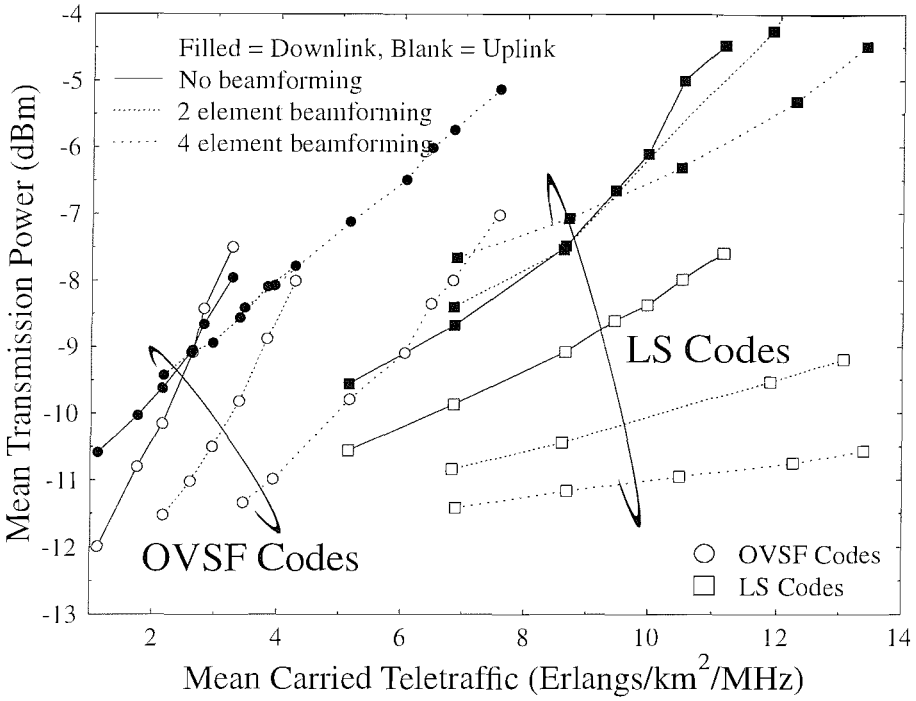

Figure 2.10: Mean transmission power versus number of users of the UTRA-like FDD cellular network using **LS codes and OVSF codes** both with as well as without beamforming in conjunction with shadowing having a frequency of 0.5 Hz and a standard deviation of 3dB for a spreading factor of SF=16.

high call quality has been maintained. In the context of the interference limited 3G CDMA system LS codes [49] might hold the promise of an increased network capacity without dramatic changes of the 3G standards, while dispensing with the employment of high-complexity, power-hungry multiuser detectors. It has to be mentioned, however that the number of available LS codes is limited and hence the system may become code-limited, instead of being interference-limited. Therefore it is necessary to invoke a range of supporting measures for the sake of increasing the number of system users that can be supported. This can be achieved for example by combining time-domain (TD) LS-code based direct-sequence spreading with frequency-domain (FD) OVSF-code based spreading. The employment of FD spreading in the context of multicarrier CDMA has the further advantage of potentially extending the length of the IFW proportionately to the number of FD subcarriers, because the symbols to be transmitted are mapped to a number of parallel subcarriers, where the subcarriers' modulated symbols have an extended duration. Theses physical-layer issues were discussed in [65].

2.2 Effects of Cell Size on the Performance of CDMA Systems

2.2.1 Introduction

In this section we embark on exploring the trade-offs between the achievable user capacity and the cell size. In CDMA systems all signals share the entire bandwidth and the users are differentiated by their unique spreading codes. Naturally, the higher the number of users in a cell, the higher the multiuser interference, which can be modelled by Gaussian noise according to the central limit theorem [9, 66].

Again, in this section we studied the effects of different cell sizes on the user capacity of UTRA-like FDD/CDMA systems, employing cell-radii of 78 m, 150 m, 300 m, 500 m and 800 m. The simulation results were compared for the sake of quantifying how the cell size effects the achievable system performance.

2.2.2 System Model and System Parameters

As in our previous investigations, the mobiles were capable of moving freely, at a speed of 3mph, in random directions, selected at the start of the simulation from a uniform distribution, within the infinite simulation area of 49 wrapped-around traffic cells [43, 67, 68]. In order to facilitate the employment of an infinite simulation area, a tessellating rhombic simulation area was used [43]. More explicitly, mobile stations about to leave the 49-cell simulation area were reflected back to it at a 180^o-rotated angle, which we refer to as being "wrapped around" from one side of the network to the other [43, 67, 68]. The benefit of employing this technique is that a mobile station in call, which leaves the network at its edge, re-enters the network at the opposite side, whilst continuing to inflict Co-Channel Interference (CCI) to the surrounding users, which may be roaming in its vicinity in the network [43]. Figure 2.11 depicts this scenario graphically. By contrast, in the "desert-island"-like scenario of employing no wrap-around, the users near the fringes of the 49-cell simulation area would experience a reduced co-channel interference, resulting in optimistic users capacity estimates.

As in Section 2.1.4 the basestations are assumed to be equipped with the Minimum Mean Squared Error Block Decision Feedback Equalizer based Multi-User Detector (MUD) [61, 63]. The post-despreading SINRs required by this MUD for obtaining the target BERs were determined with the aid of physical-layer simulations using a 4-QAM/QPSK modulation scheme, in conjunction with 1/2 rate turbo coding and MUD for transmission over a COST 207 seven-path Bad Urban channel [64].

Using this turbo-coded MUD-assisted transceiver and a spreading factor of 16, the post-despreading SINR required for maintaining the target BER of 1×10^{-3} was 8.0 dB. The BER which was deemed to correspond to low-quality access, was stipulated at 5×10^{-3}. This BER was exceeded for SINRs

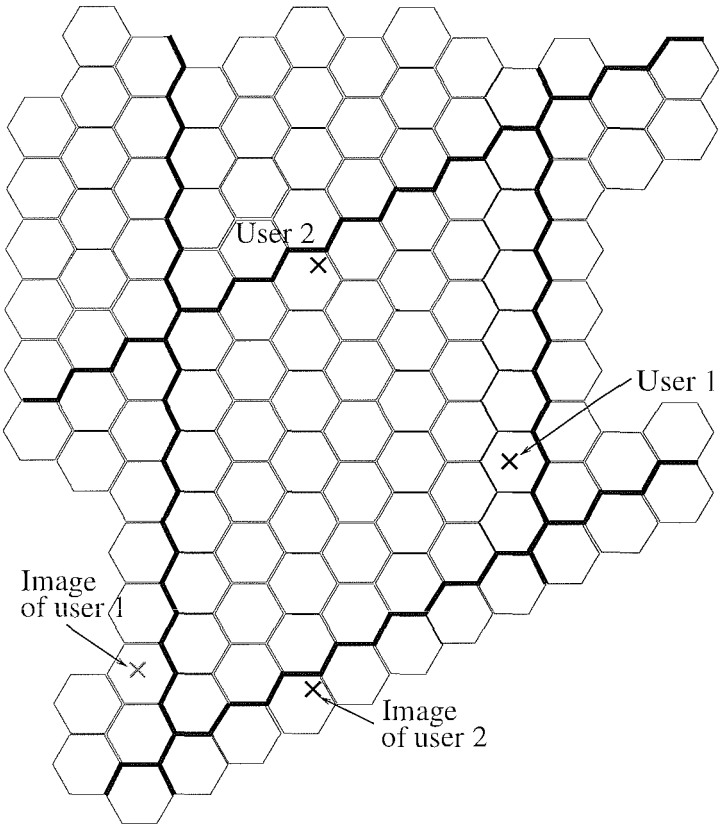

Figure 2.11: The 7x7 rhombic simulation area showing a user and its "wrapped" image [43].

Parameter	**Value**	**Parameter**	**Value**
Noisefloor	-100dBm	Frame length	10ms
Multiple access	FDD/CDMA	Number of basestations	49
Modulation scheme	4QAM/QPSK	Spreading factor	16
Power control stepsize	1 dB	Power control hysteresis	1dB
Low quality access SINR	7.0 dB	Outage (1% BER) SINR	6.6 dB
Target SINR (at BER=0.1%)	8.0 dB	Size of Active Basestation Set	2
Average inter-call-time	300s	Max. new-call queue-time	5s
Average call length	60s	Pedestrian speed	3mph
Maximum consecutive outages	50 ms	Signal bandwidth	5MHz

Table 2.3: Basic simulation parameters.

Cell radius	Maximum BS/MS transmit power	Minimum BS/MS transmit power	Pilot power	Pathloss exponent
78 m	17.5 dBm	-47.5 dBm	-8.5 dBm	-2.0
150 m	21.0 dBm	-44.0 dBm	-5.0 dBm	-3.5
300 m	28.0 dBm	-37.0 dBm	2.0 dBm	-3.5
500 m	32.67 dBm	-32.33 dBm	6.67 dBm	-3.5
800 m	39.7 dBm	-25.3 dBm	13.7 dBm	-3.5

Table 2.4: Signal power parameters

falling below 7.0dB. Furthermore, a low-quality outage was declared, when the BER of 1×10^{-2} was exceeded, which was encountered for SINRs below 6.6 dB. These values can be seen along with the other system parameters in Table 2.3.

As the cell size changes, the minimum Base Station (BS) and Mobile Station (MS) transmit power as well as the pilot power also has to change for the sake of maintaining an adequate coverage. Table 2.4 summarizes the minimum required BS power associated with the different cell radii. We consider the scenario having a cell radius of 78 m to be associated with Line of Sight (LOS) propagation having a path loss exponent [9] of 20 dB/decade.

2.2.3 Simulation Results and Comparisons

We investigated various scenarios having different cell radii and compared the quality of service by using the performance metrics of Section 2.1.5 for estimating how the cell size affected the capacity of the UTRA-like FDD/CDMA system, considered current FDD/CDMA systems are interference limited, suffering from intra-cell interference imposed by the signals transmitted to other mobiles supported by the same basestation, and by the inter-cell interference inflicted by the surrounding base stations. When the cell radius was increased, the maximum/minimum BS/MS transmission powers and the pilot power had to be appropriately adjusted as seen in Table 2.4. Again, observed in Table 2.4 that the cell having a radius of 78 m encountered LOS propagation, which may affect the system's capacity.

2.2.3.1 Network performance using adaptive antenna arrays

Figure 2.12 shows achievable teletraffic capacity versus the cell radius associated with a variety of traffic loads measured in terms of the mean normalized carried traffic expressed in Erlangs/km^2/MHz when subjected to 0.5 Hz frequency shadowing having a standard deviation of 3 dB. The figure illustrates

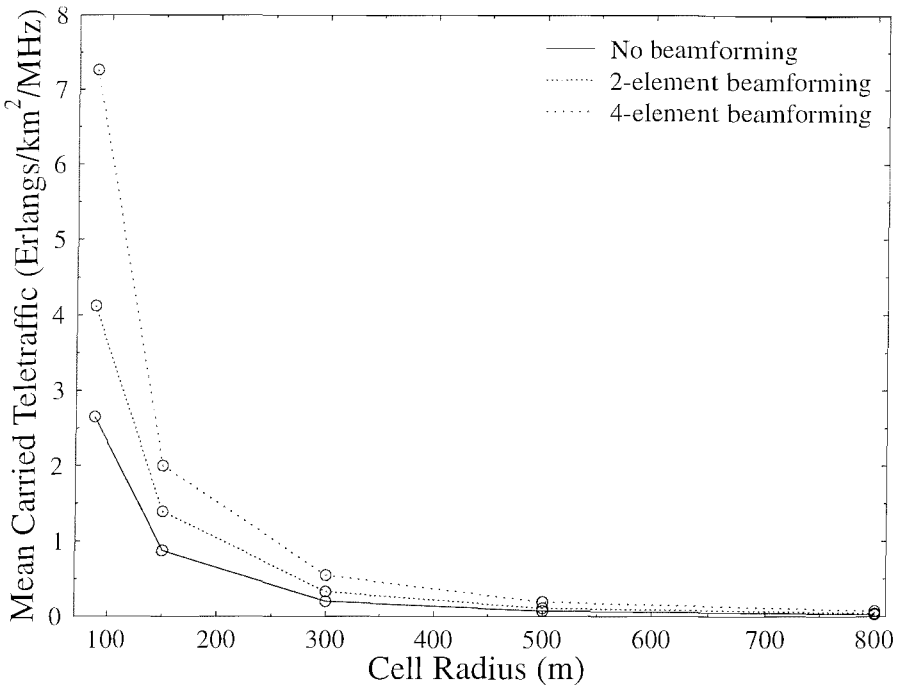

Figure 2.12: Cell radius versus mean carried traffic of the UTRA-like FDD cellular network both with as well as without beamforming in conjunction with shadowing having a frequency of 0.5 Hz and a standard deviation of 3dB for a spreading factor of SF=16.

that the network's user capacity was significantly degraded, when the cell radius was increased, which was mitigated by employing adaptive antenna arrays. The scenario having a cell radius of 78 m in Figure 2.13(a), reached a network capacity of 2.65 Erlang/km^2/MHz even without employing antenna arrays, which is about 94 times to that of the network having a cell radius of 800 m, which may characterized in Figure 2.13(d) and had a capacity of 0.028 Erlang/km^2/MHz. When using "2- or 4-element beamforming", the adaptive antenna arrays have considerably reduced the levels of interference, leading to a higher network capacity. It can be seen in Figure 2.13(a), that scenario having a cell radius of 78 m, the exhibited a network capacity which was increased by 59% to 4.12 Erlang/km^2/MHz with the advent of employing 2-element adaptive antenna arrays at the basestations. Replacing the 2-element adaptive antenna arrays by 4-element arrays led to a further capacity increase of 77%, which is associated with a network capacity of 7.26 Erlangs/km^2/MHz. As it is widely recognized, the high capacity requirements of dense urban environments require a high cell-site density.

The probability of low quality access experienced in different cell radius scenarios is depicted in Figure 2.14, which also exhibited a substantial improvement with the advent of two-element adaptive antenna arrays. Similar performance trends were observed in all four sub-figures of Figure 2.13. At lower traffic loads the probability of low quality access experienced without employing adaptive

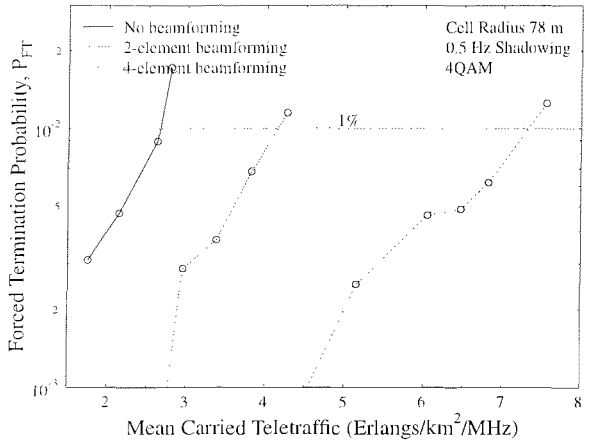

(a) Cell radius is 78 m

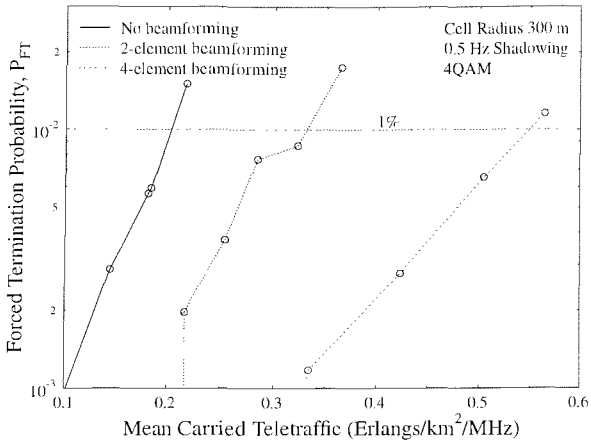

(b) Cell radius is 300 m

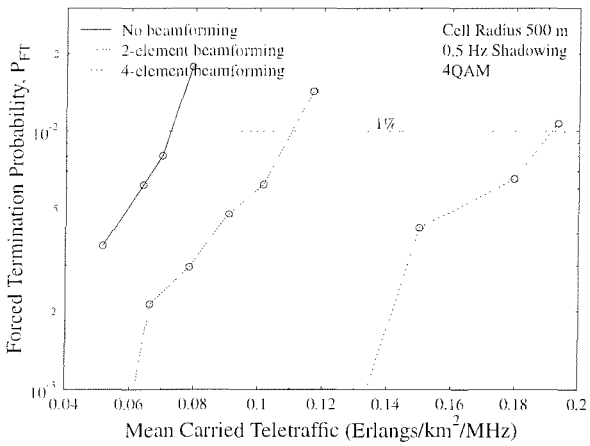

(c) Cell radius is 500 m

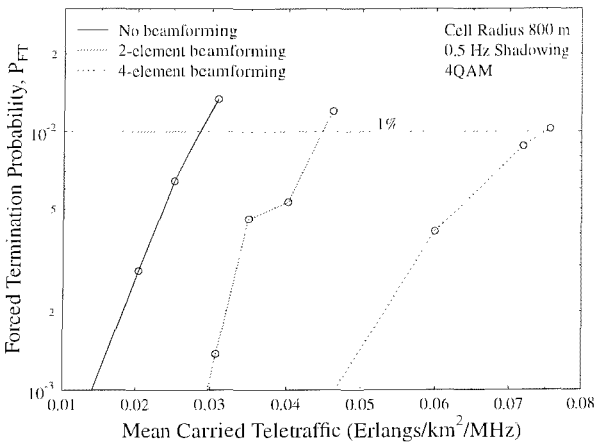

(d) Cell radius is 800 m

Figure 2.13: Forced termination probability versus mean carried traffic of the UTRA-like FDD cellular network both with as well as without beamforming in conjunction with shadowing having a frequency of 0.5 Hz and a standard deviation of 3dB for a spreading factor of SF=16.

antenna arrays is typically better than that of the antenna array-aided scenarios, because of the adaptive antenna arrays' sensitivity to the potentially damaging interfering signals, when a new call commences. This tendency becomes more marked when using 4-element arrays. As the traffic load becomes heavier, the level of multiuser interference increases as well, as seen in Figure 2.14, resulting in a steep rise of the low quality access probability curves, when using no beamforming. By contrast, as expected, using adaptive antenna arrays in case of high traffic loads results in a reduced probability of low quality access. The variation of the cell radius did not dramatically affect the probability of the low quality outage.

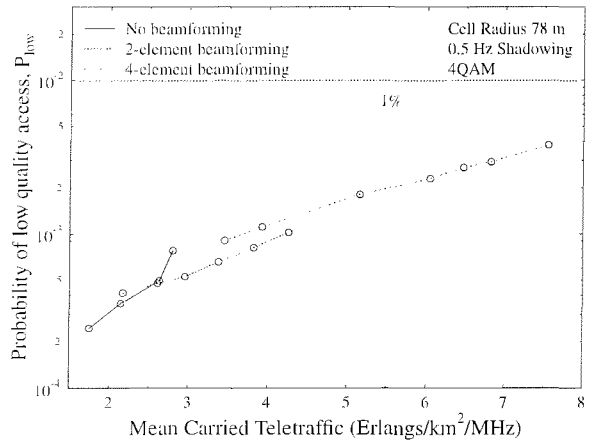

(a) Cell radius is 78 m

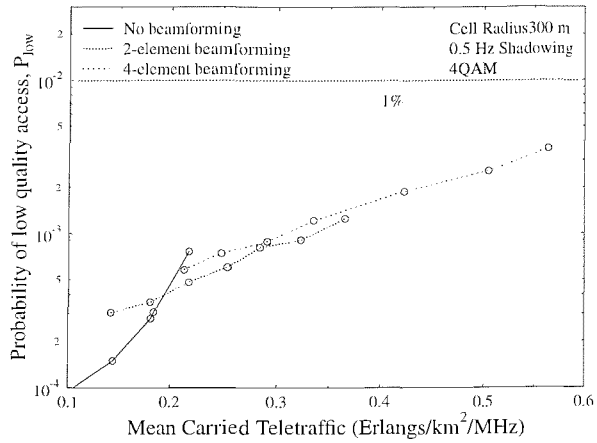

(b) Cell radius is 300 m

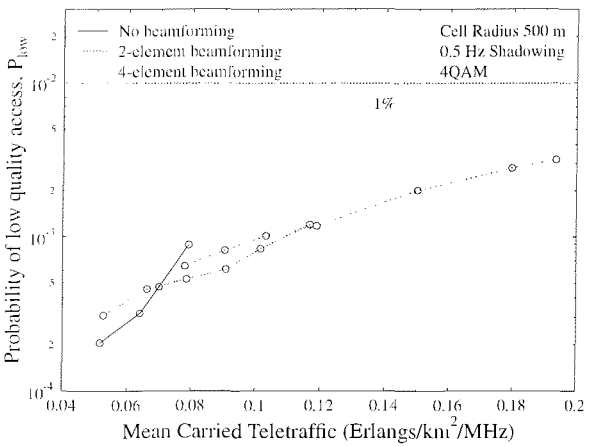

(c) Cell radius is 500 m

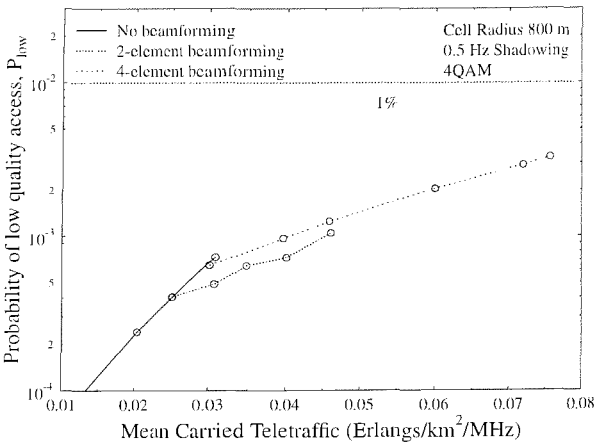

(d) Cell radius is 800 m

Figure 2.14: Probability of low quality access versus mean carried traffic of the UTRA-like FDD cellular network both with as well as without beamforming in conjunction with shadowing having a frequency of 0.5 Hz and a standard deviation of 3dB for a spreading factor of SF=16.

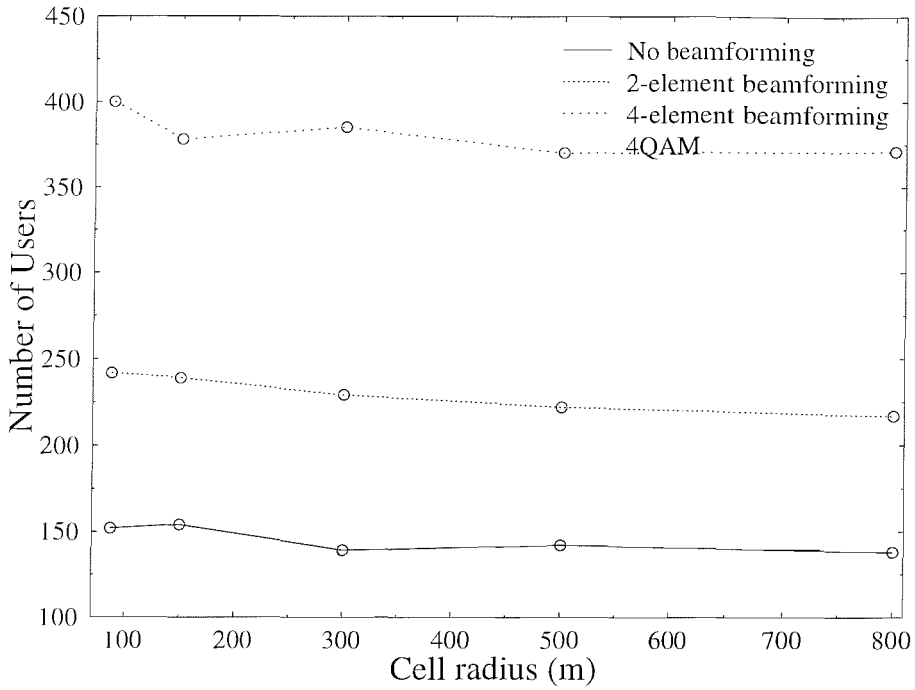

Figure 2.15: Cell radius versus number of users of the UTRA-like FDD cellular network both with as well as without beamforming in conjunction with shadowing having a frequency of 0.5 Hz and a standard deviation of 3dB for a spreading factor of SF=16.

Figure 2.15 portrays the number of users supported versus the cell radius. In this context the "Number of Users" refers to the simulation area of 49 traffic cells as seen in Figure 2.11, although depending on the cell-radius this corresponds to widely different areas expressed in km^2. Figure 2.15 suggests that varying the cell radius does not dramatically affect the number of users supported within the simulation area, since the number of users supported is approximately proportional to the number of base stations. The more base stations there are in a fixed area, the more mobile users can be supported. As we have mentioned at the beginning of this section, CDMA systems are interference limited. Each additional user admitted to the system constitutes one more source of interference. Again, it can be seen from Figure 2.15 that the scenarios carrying higher traffic loads benefitted from the employment of the 2- or 4-element antenna arrays, which substantially enhanced the achievable network capacity.

The mean uplink and downlink transmission power versus cell radius is depicted in Figure 2.16, suggesting that a higher average signal power was required for maintaining an acceptable signal to interference plus noise ratio, as the cell radius increased. When the cell radius increased from 78 m to 800 m, the mean transmission power had to be increased by more than 30 dBm. A summary of the maximum achievable user capacities for the UTRA-like network considered, which was subjected to

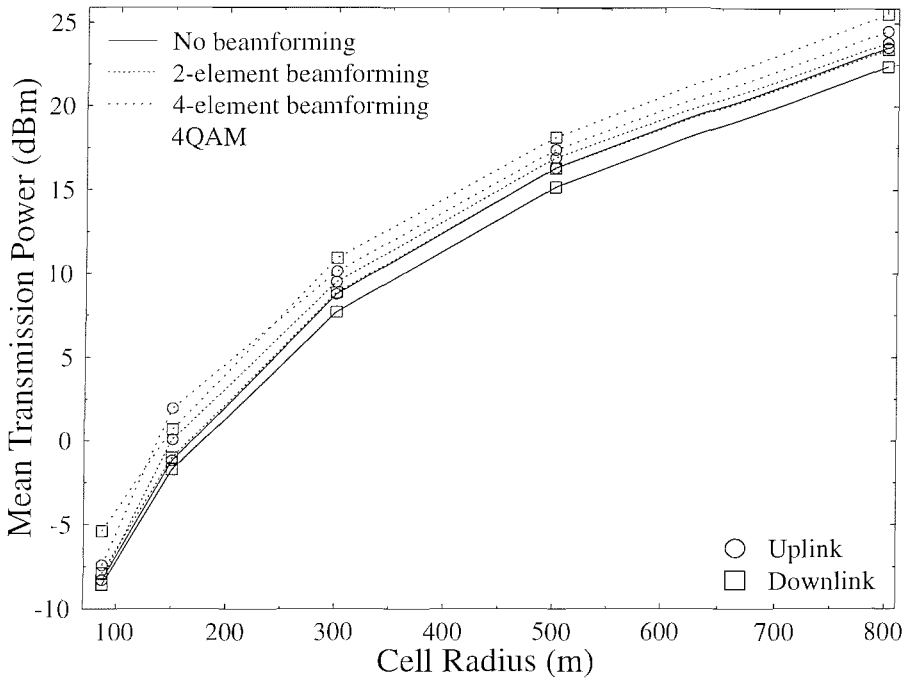

Figure 2.16: Mean uplink and downlink transmission power versus cell radius of the UTRA-like FDD cellular network both with as well as without beamforming in conjunction with shadowing having a frequency of 0.5 Hz and a standard deviation of 3dB for a spreading factor of SF=16.

log-normal shadowing having a standard deviation of 3 dB and a frequency of 0.5 Hz, both with and without employing beamforming, is given in Table 2.5. The teletraffic carried and the mean mobile and base station transmission powers required are also shown in Table 2.5.

Cell radius (m)	Beamforming	Users	Traffic (Erlangs /km^2/MHz)	Power (dBm) MS	BS
78	No	152	2.65	-8.30	-8.57
78	2-elements	242	4.12	-8.28	-7.88
78	4-elements	430	7.26	-7.41	-5.38
150	No	150	0.87	-1.05	-1.51
150	2-elements	239	1.39	-0.43	-0.58
150	4-elements	348	1.99	1.94	0.67
300	No	139	0.19	8.76	7.69
300	2-elements	229	0.32	9.49	8.85
300	4-elements	385	0.54	10.12	10.91
500	No	142	0.07	16.30	15.15
500	2-elements	222	0.10	16.89	16.27
500	4-elements	370	0.19	17.37	18.11
800	No	138	0.02	23.53	22.39
800	2-elements	217	0.04	23.84	23.42
800	4-elements	371	0.07	24.53	25.56

Table 2.5: Maximum mean carried traffic and maximum number of mobile users that can be supported by the network, whilst meeting the network quality constraints, namely $P_B \leq 3\%$, $P_{FT} \leq 1\%$, $P_{low} \leq 1\%$ and GOS $\leq 4\%$. The carried traffic is expressed in terms of normalized Erlangs (Erlang/km^2/MHz) in conjunction with shadow fading having a standard deviation of 3 dB and a frequency of 0.5 Hz for a spreading factor of SF=16. The average transmission power of the MSs and BSs are also summarized.

2.2.3.2 Network performance using adaptive antenna arrays and adaptive modulation

In this section we will quantify the impact of cell radius on the achievable network capacity, while using both adaptive antenna arrays and Adaptive Quadrature Amplitude Modulation (AQAM) [43,46]. AQAM activates the most appropriate modulation mode depending on the near-instantaneous channel quality in order to maximize the achievable data throughput, while maintaining the target bit error ratio.

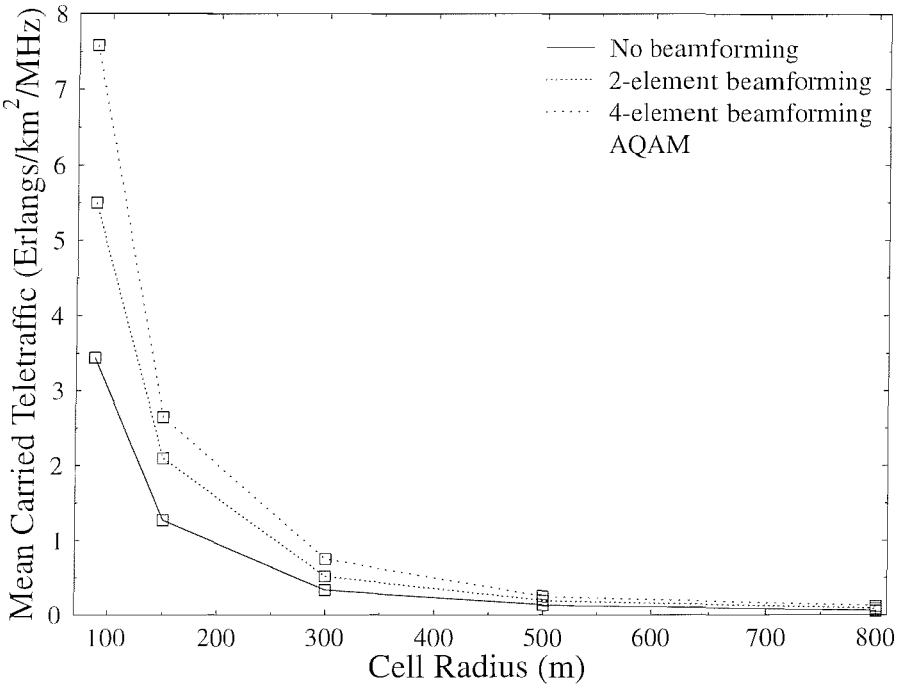

Figure 2.17: Cell radius versus mean carried traffic of the UTRA-like FDD cellular network both with and without beamforming in conjunction with **AQAM** as well as shadowing having a frequency of 0.5 Hz and a standard deviation of 3dB for a spreading factor of SF=16.

Figure 2.17 shows the cell radius associated with a variety of traffic loads in terms of the mean normalized carried traffic expressed in Erlang/km^2/MHz. Similar trends were observed in Figure 2.12, namely that the system's capacity degraded quite dramatically, when the cell size was increased. For the sake of comparison with the fixed-modulation based QPSK scenario of Figure 2.12 we note that the highest AQAM-aided mean carried traffic improvement was achieved by the 2-element AAA. Explicitly, in case of the 78 m cell-radius the 2.4 Erlang/km^2/MHz carried traffic was increased to about 5.5 Erlang/km^2/MHz. Upon comparing Figure 2.13 to Figure 2.18, we observe that a further call dropping probability reduction is achieved, when using AQAM.

The probability of low quality outage was shown in Figure 2.19, which in fact indicates a degrada-

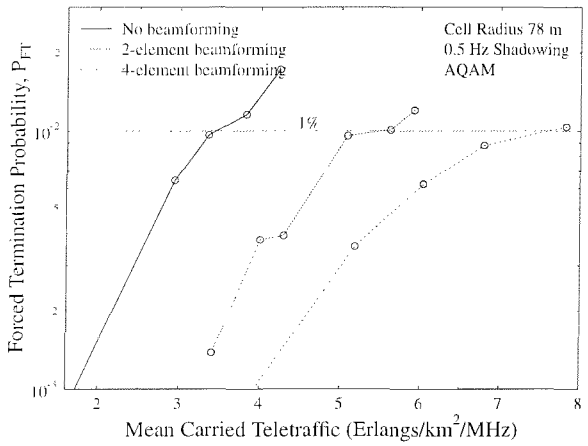

(a) Cell radius is 78 m

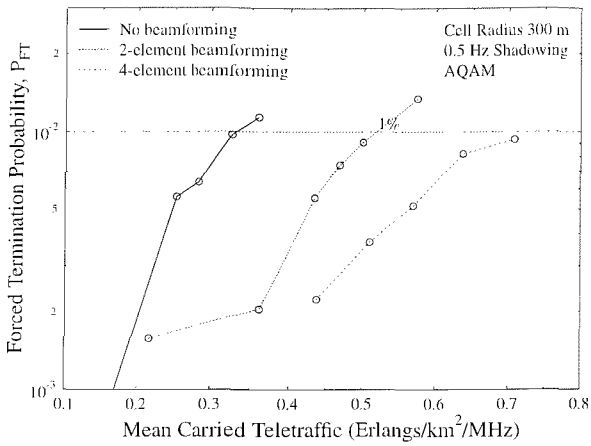

(b) Cell radius is 300 m

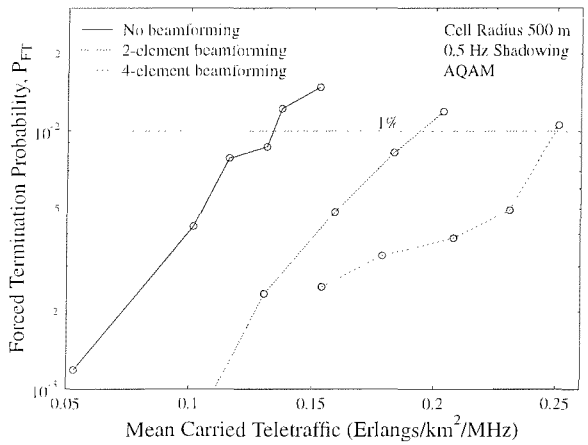

(c) Cell radius is 500 m

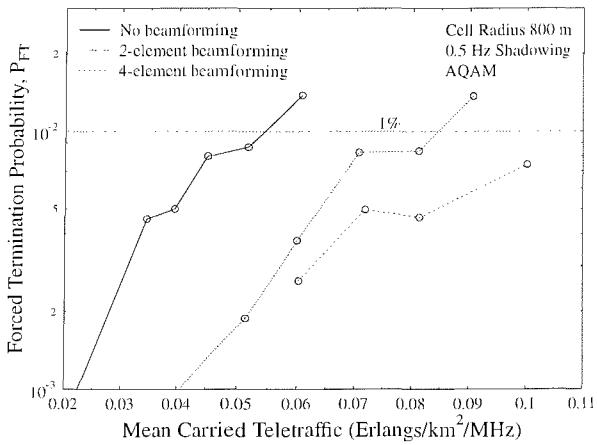

(d) Cell radius is 800 m

Figure 2.18: Forced termination probability versus mean carried traffic of the UTRA-like FDD cellular network both with and without beamforming in conjunction with **AQAM** as well as shadowing having a frequency of 0.5 Hz and a standard deviation of 3dB for a spreading factor of SF=16.

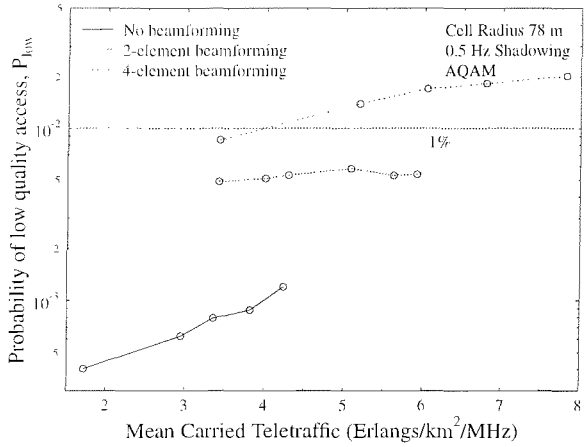

(a) Cell radius is 78 m

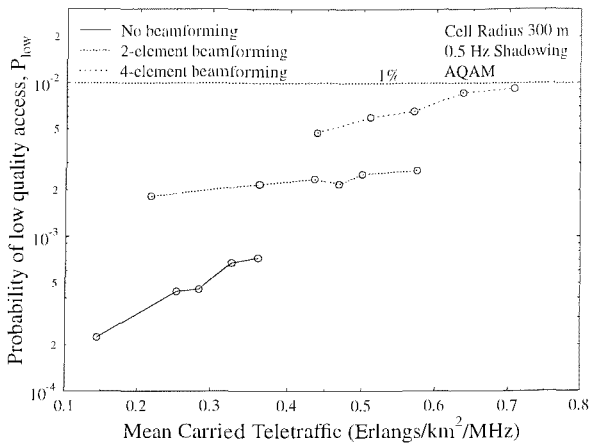

(b) Cell radius is 300 m

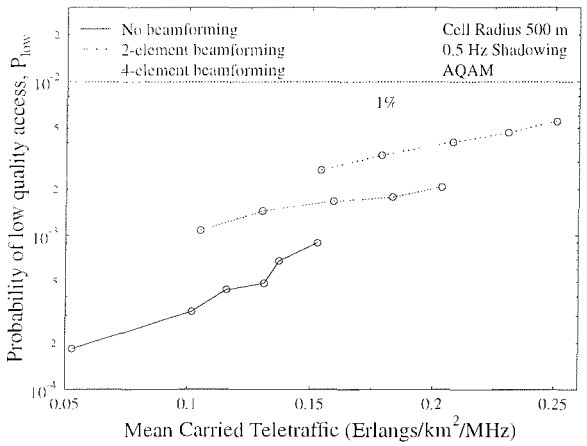

(c) Cell radius is 500 m

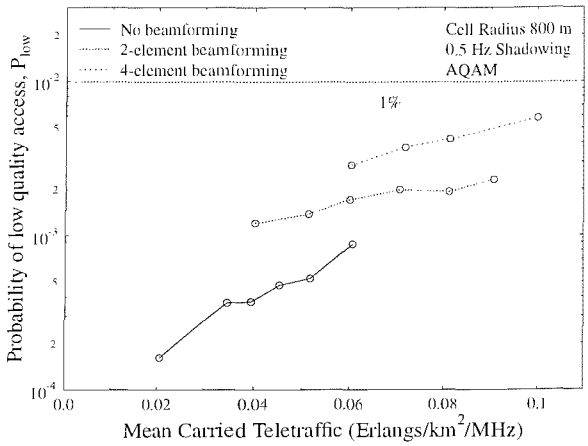

(d) Cell radius is 800 m

Figure 2.19: Probability of low quality access versus mean carried traffic of the UTRA-like FDD cellular network both with and without beamforming in conjunction with **AQAM** as well as shadowing having a frequency of 0.5 Hz and a standard deviation of 3dB for a spreading factor of SF=16.

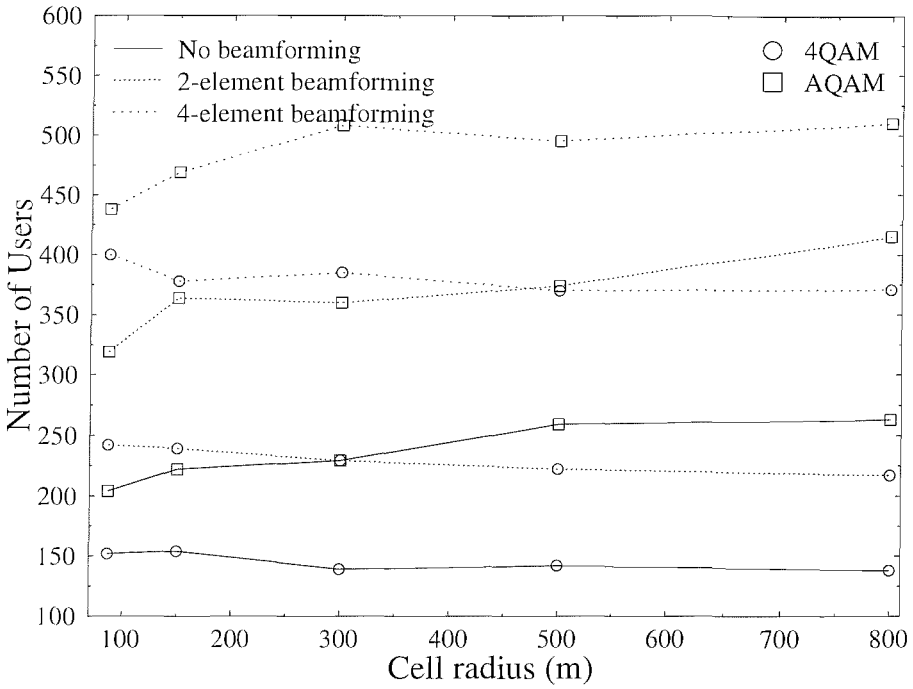

Figure 2.20: Cell radius versus number of users of the UTRA-like FDD cellular network both with and without beamforming in conjunction with **AQAM** as well as shadowing having a frequency of 0.5 Hz and a standard deviation of 3dB for a spreading factor of SF=16.

tion imposed by the employment of adaptive modulation, when compared to the corresponding 4QAM curves seen in Figure 2.14. The increase in the probability of low quality access can be attributed to the employment of less robust, but higher-throughput, higher-order modulation modes invoked by the adaptive modulation scheme, which resulted in an increase of the achievable system capacity. For example, when we use fixed 4QAM modulation mode, as characterized in Figure 2.14, a low quality outage may not occur. By contrast, an outage is more likely to happen for more prolonged periods of time, when a higher-order AQAM mode is invoked, as suggested by Figure 2.19.

Figure 2.20 shows the number of users supported versus the cell radius. From Figure 2.20 we can see that the achievable user capacity of FDD/CDMA employing adaptive modulation was improved in comparison to the system using fixed 4QAM. Figure 2.21 portrays the mean transmission power versus the cell radius. Naturally, the required signal power increased, as the cell radius increased.

2.2.4 Summary and Conclusion

In Section 2.2 we quantified the impact of cell radius on the achievable network capacity of UTRA-like FDD/CDMA systems, while using both adaptive antenna arrays and adaptive modulation. The

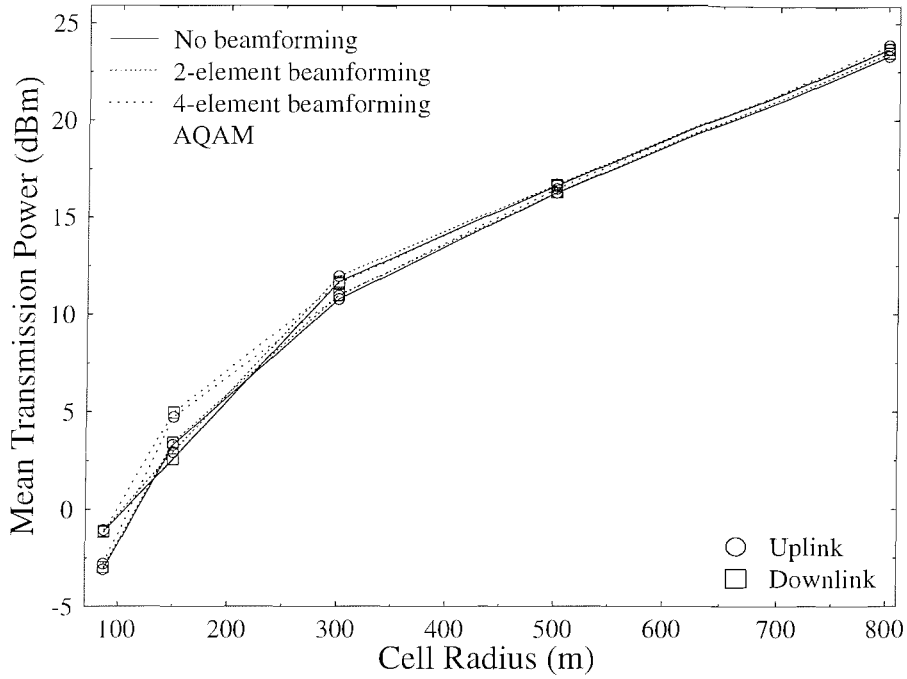

Figure 2.21: Mean transmission power versus cell radius of the UTRA-like FDD cellular network both with and without beamforming in conjunction with **AQAM** as well as shadowing having a frequency of 0.5 Hz and a standard deviation of 3dB for a spreading factor of SF=16.

simulation results demonstrate that the high capacity requirement of dense urban environments necessitates a high cell-site density. The variation of the cell size did not dramatically affect the probability of low call quality access. However, a higher average signal power was required for maintaining an acceptable signal to interference plus noise ratio, as the cell radius increased. Considerable network capacity gains were achieved, employing both 2- and 4-element adaptive antenna arrays in conjunction with adaptive modulation techniques.

2.3 Effects of SINR Threshold on the Performance of CDMA Systems

2.3.1 Introduction

The third generation wireless networks are capable of adjusting the transmission integrity for the sake of providing multimedia services. The term multimedia encompasses a number of diverse media to be combined in novel ways for the sake of communicating using text, voice, video, graphics, images, audio etc [69]. In [70] Acampora and Naghshineh refer to three types of wireless communications services, namely: a) real-time connections using voice and low-rate video, b) non-real-time delay-sensitive connection-oriented services with limited delay bounds, such as using remote login and the File Transfer Protocol (FTP), c) message-oriented, delay-insensitive traffic such as paging, electronic mail, voice mail and fax. These different types of services have diverse the target SINR requirements. As the target SINR requirement are changing, so does the user capacity. In this section we study the effects of the SINR threshold on the user capacity of CDMA systems, since this allows us to directly quantify the impact of more or less error-resilient transceivers on the network's performance.

2.3.2 Simulation Results

This simulation conditions were the same as in Section 2.2.2. Again, mobiles were capable of roaming freely, at a speed of 3mph, in random directions, selected at the start of the simulation from a uniform distribution, within the simulation area of 49 traffic cells. The cell radius was 150 m. The propagation environment was modelled using the a pathloss model having a pathloss exponent of -3.5. The mobile and base station transmit powers were restricted to the range of -44 dBm to +21 dBm for the power control assisted and adaptive modulation based simulations. If a channel allocation request for a new call could not be satisfied immediately, this request was queued for a duration of up 5 s, after which time, if not satisfied, it was classed as blocked.

In the previous Section 2.2 we observed significant performance gains with the advent of employing adaptive antenna arrays at the base station. The CDMA based network considered here has a frequency reuse factor of unity, therefore the level of co-channel interference is high, and hence the adaptive antennas are expected to provide substantial performance benefits. The SINR threshold used by the network control algorithms is determined by the error resilience of the wireless transceiver used, namely, by the SINR value required for maintaining the target BER of the service concerned. For example, if a more error resilient transceiver is used, the SINR requirements may be reduced and hence more users can be supported. The same is true, when the service can tolerate a higher BER.

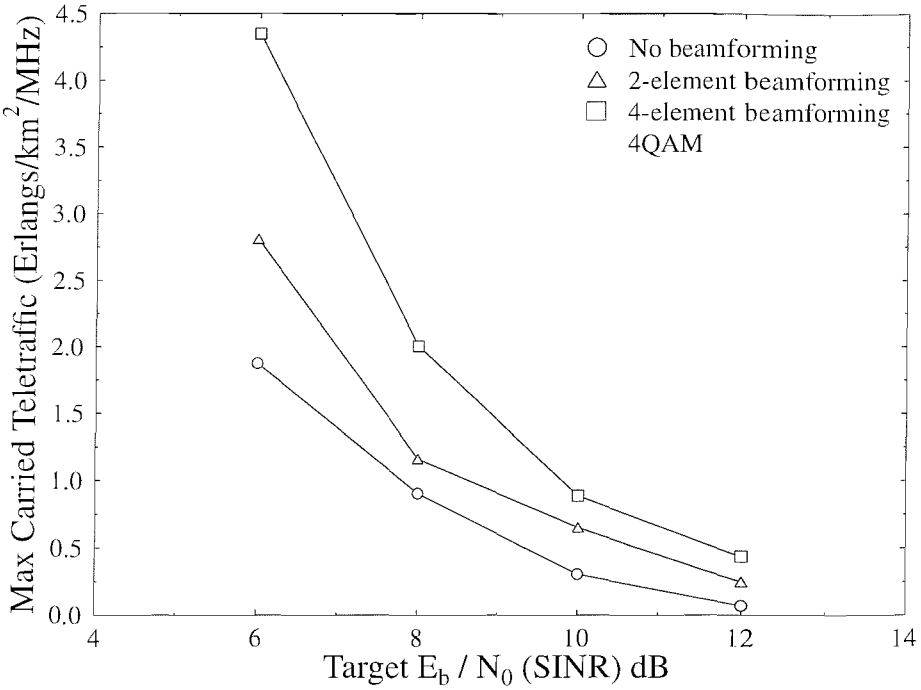

Figure 2.22: Mean carried traffic of the UTRA-like FDD cellular network versus the target SINR threshold both with as well as without beamforming in conjunction with shadowing having a frequency of 0.5 Hz and a standard deviation of 3dB for a spreading factor of SF=16.

Figure 2.22 shows the target SINR threshold associated with a variety of traffic loads measured in terms of the mean normalized carried traffic expressed in Erlangs/km^2/MHz when subjected to 0.5 Hz frequency shadowing having a standard deviation of 3 dB as a function of the target SINR threshold. As expected, the figure illustrates that the network's user capacity degrades, when the target SINR requirement is increased. When the target SINR threshold was 6 dB, it can be seen in Figure 2.23(a) that the network capacity reached 1.87 Erlang/km^2/MHz, which is about 27 times the capacity, when the SINR value was set to 12 dB, as evidenced by Figure 2.23(d), where the corresponding carried traffic was 0.069 Erlang/km^2/MHz without employing antenna arrays at the base station.

When using 2- or 4-element beamforming, the adaptive antenna arrays have considerably reduced the levels of interference, leading to a higher carried traffic. As it can be seen in Figure 2.23(a), when the SINR threshold was 6 dB, the carried traffic increased by 33% to 2.80 Erlang/km^2/MHz with the advent of employing 2-element adaptive antenna arrays at the basestations. Replacing the 2-element adaptive antenna arrays with 4-element arrays led to a further capacity increase of 35%, which is associated with a network capacity of 4.34 Erlangs/km^2/MHz. When the target SINR threshold was increased to 12 dB, it can be observed in Figure 2.23(d) that the carried traffic became extremely poor without the employment of adaptive antenna arrays. This is because the target SINR is high, hence the

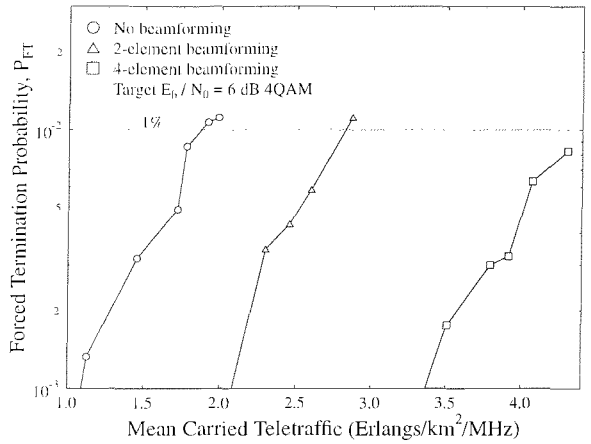

(a) Target SINR of 6 dB

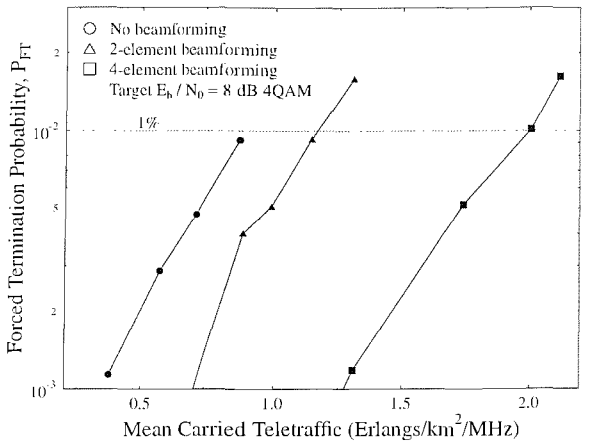

(b) Target SINR of 8 dB

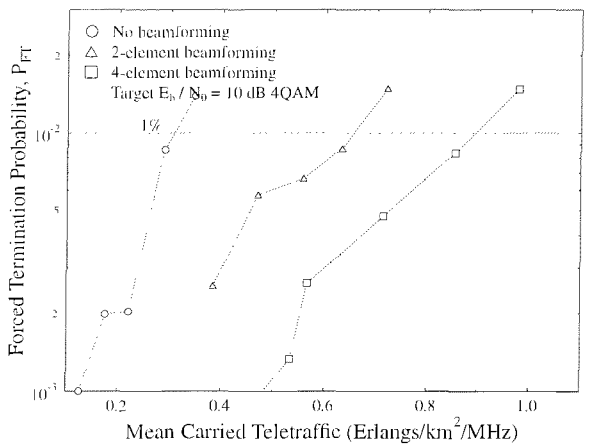

(c) Target SINR of 10 dB

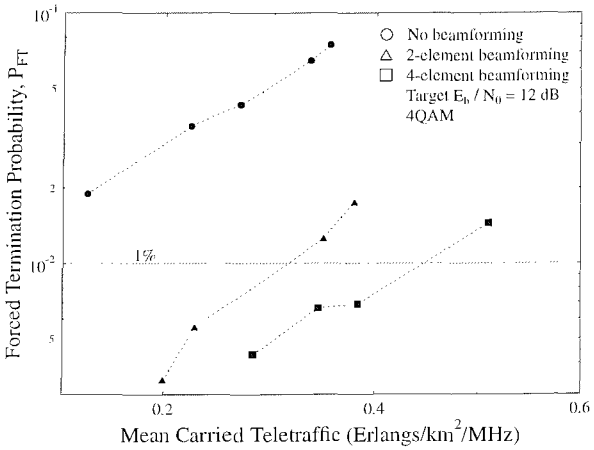

(d) Target SINR of 12 dB

Figure 2.23: Forced termination probability versus mean carried traffic of the UTRA-like FDD cellular network both with as well as without beamforming in conjunction with shadowing having a frequency of 0.5 Hz and a standard deviation of 3dB for a spreading factor of SF=16. This figure demonstrates the effects of the different target SINRs of 6, 8, 10 and 12 dB and may be compared to Figure 2.13, where the effects of different cell radii were studied.

required transmitted power is increased, inevitably increasing the interference level imposed. Hence an error-sensitive transceiver, which requires a high SINR for maintaining the target integrity may lead to an unstable, low-capacity system. The benefits of using adaptive antenna arrays are clearly demonstrated in this scenario. With the advent of using 2- or 4-element beamforming the carried traffic becomes a factor four or eight higher than that of the 'No beamforming' scenario, supporting 43 and 78 users, respectively.

Four different probability of low quality access scenarios associated with various target SINR threshold were presented in Figure 2.24. Specifically, in Figure 2.24(a) and Figure 2.24(b) similar trends were observed, namely that at lower traffic loads the achievable low quality outage performance was worse than that of no beamforming when using adaptive antenna arrays. This likely to be due to the addition of a new source of interference, constituted by a user initiating a new call, which results in an abrupt change in the gain of the antenna in the direction of the desired user, when invoking adaptive antenna arrays. Increasing the number of antenna elements from two to four results in an increased probability of low quality outage due to the sharper antenna directivity. In contrast to Figure 2.24(a) and Figure 2.24(b), Figure 2.24(c) and Figure 2.24(d) portray a better performance, when employing adaptive antenna arrays than that of no beamforming. However, the price to be paid for this is that a network using no adaptive antenna arrays requires a higher transmission power for maintaining the target SINR level, as it will be discussed in more detail in the context of Figure 2.25 and Figure 2.26. This results in a higher overall interference level. In conclusion, in a network having a high target SINR threshold, employment of adaptive beamforming holds the promise of a reduced probability of low quality outage.

The mean transmission power performance versus carried traffic is depicted in Figure 2.25 and Figure 2.26. Figure 2.25 clearly shows the lower levels of transmission power required for maintaining an acceptable SINR, while using adaptive antenna arrays at the base stations. These power budget savings were obtained in conjunction with reduced levels of co-channel interference, leading to superior call quality, as illustrated in Figure 2.23 and Figure 2.24. This phenomenon can be seen more clearly in Figure 2.26, where we recorded the system's mean transmission power when the teletraffic load was 1 Erlang/km^2/MHz. The mean transmission power was increasing rapidly, as the required target SINR was increased. An additional average transmission power of 5 dBm was required, when the target SINR threshold was increased from 6 dB to 8 dB. A further transmission power increment of 5 dBm was necessitated, when the required SINR threshold was increased from 8 dB to 10 dB. Figure 2.27 characterizes the mean transmission power versus SINR threshold performance, when the cellular network achieved the maximum user-capacity values shown in Figure 2.22. A summary of the maximum user capacities of the UTRA-like FDD networks in conjunction with log-normal shadowing

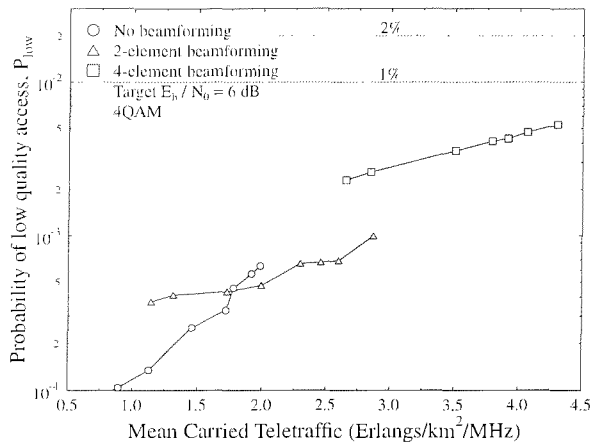

(a) Target SINR of 6 dB

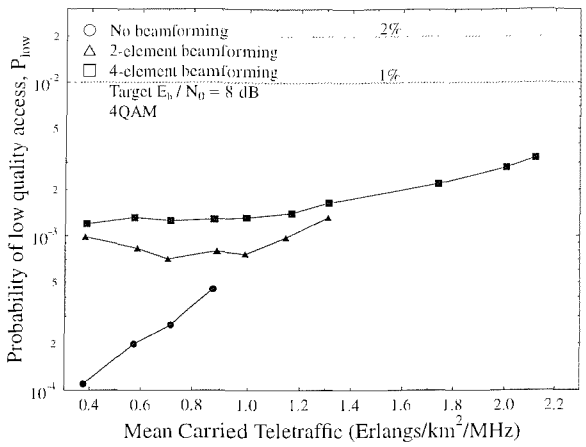

(b) Target SINR of 8 dB

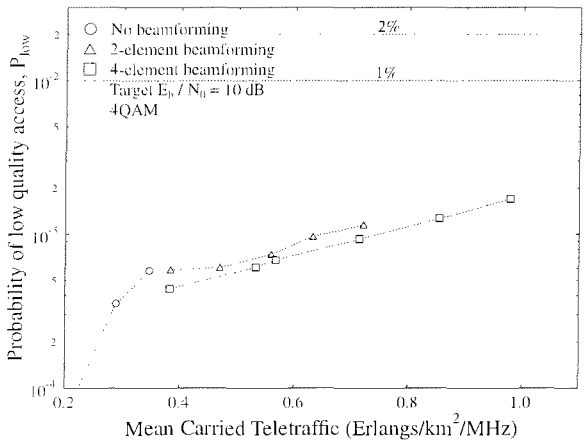

(c) Target SINR of 10 dB

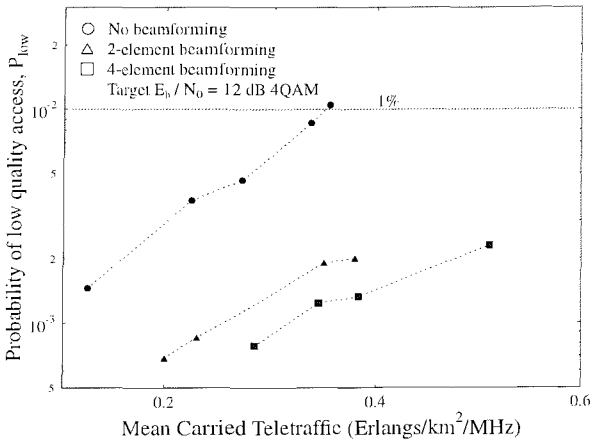

(d) Target SINR of 12 dB

Figure 2.24: Probability of low quality access versus mean carried traffic of the UTRA-like FDD cellular network both with as well as without beamforming in conjunction with shadowing having a frequency of 0.5 Hz and a standard deviation of 3dB for a spreading factor of SF=16. This figure demonstrates the effects of the different target SINRs of 6, 8, 10 and 12 dB and may be compared to Figure 2.14, where the effects of different cell radii were studied.

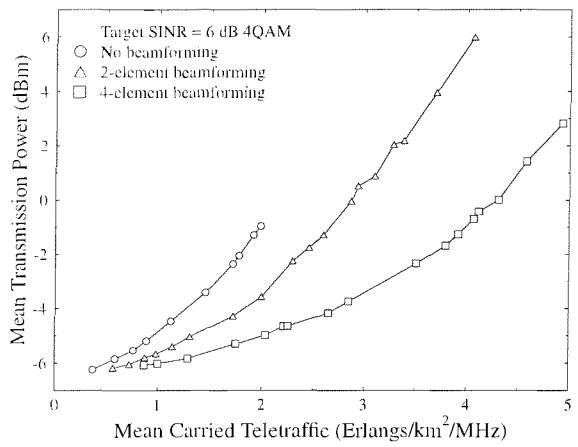

(a) Target SINR of 6 dB

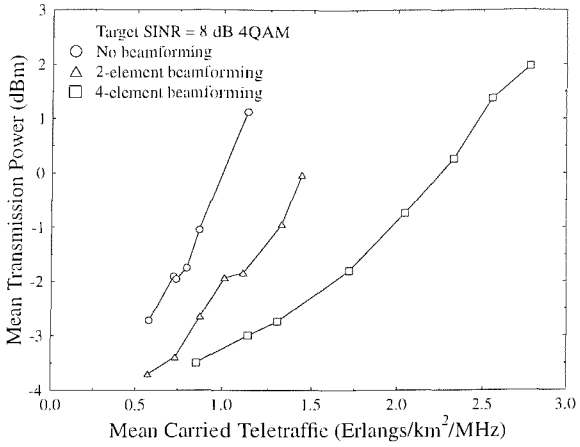

(b) Target SINR of 8 dB

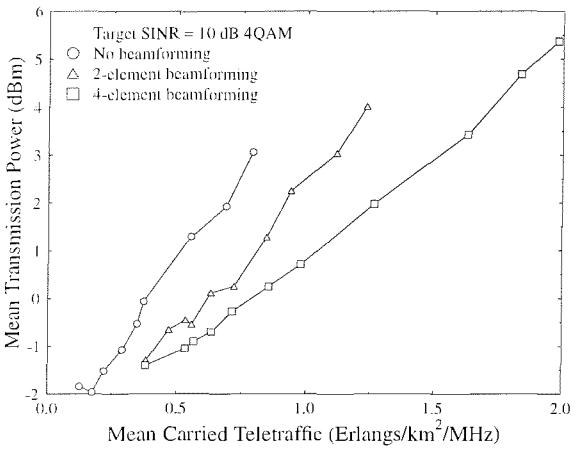

(c) Target SINR of 10 dB

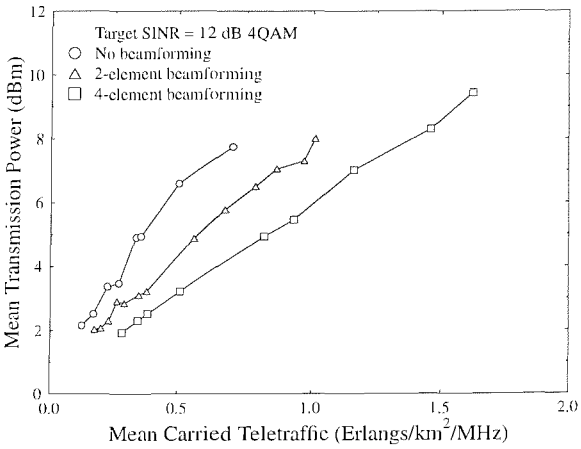

(d) Target SINR of 12 dB

Figure 2.25: Mean transmission power versus mean carried traffic of the UTRA-like FDD cellular network both with as well as without beamforming in conjunction with shadowing having a frequency of 0.5 Hz and a standard deviation of 3dB for a spreading factor of SF=16. This figure demonstrates the effects of the different target SINRs of 6, 8, 10 and 12 dB.

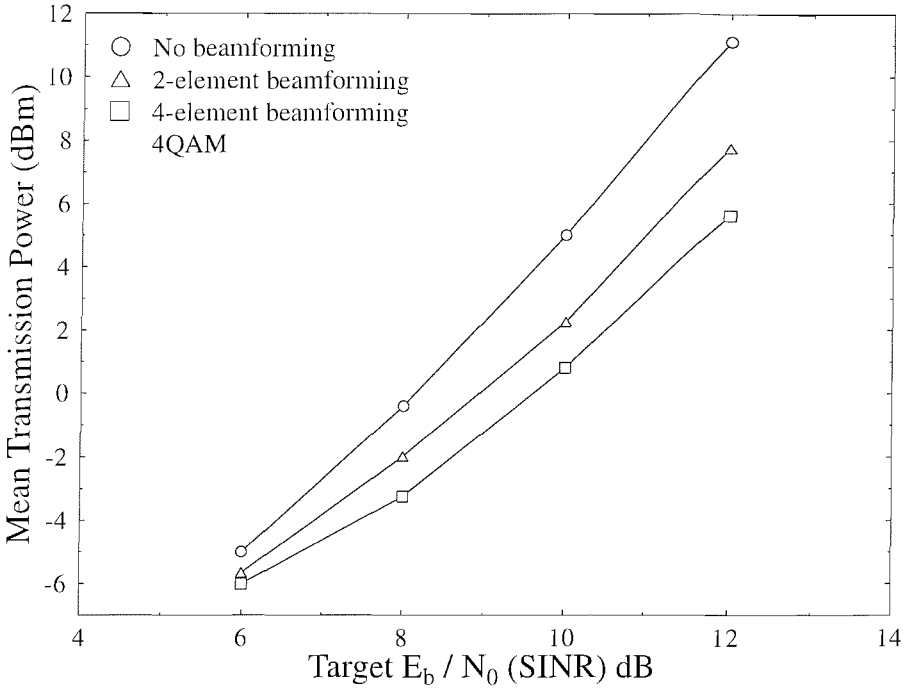

Figure 2.26: Mean transmission power versus target SINR threshold of the UTRA-like FDD cellular network while carried traffic is 1 Erlangs/km^2/MHz, both with as well as without beamforming in conjunction with shadowing having a frequency of 0.5 Hz and a standard deviation of 3dB for a spreading factor of SF=16.

having a standard deviation of 3 dB and a frequency of 0.5 Hz, both with and without employing beamforming is given in Table 2.6. The teletraffic carried and the mean mobile as well as base station transmission powers required for attaining these user capacities are also shown in Table 2.6.

2.3.3 Summary and Conclusion

In this section we studied the effects of the SINR threshold on the achievable user capacity of the UTRA-like FDD/CDMA systems studied, in order to quantify the impact of the error-resilience of the transceivers employed on the network's performance. From the simulation results we observed that increasing the required SINR for the sake of invoking higher throughput, but less error resilient modems may in fact lead to an unstable, easily overloaded, low-capacity system, which is associated with a high power consumption. However, the advantages of using adaptive antenna arrays within a mobile cellular network result in substantial performance improvements in terms of the achievable call quality, mean transmission power and the number of supported users.

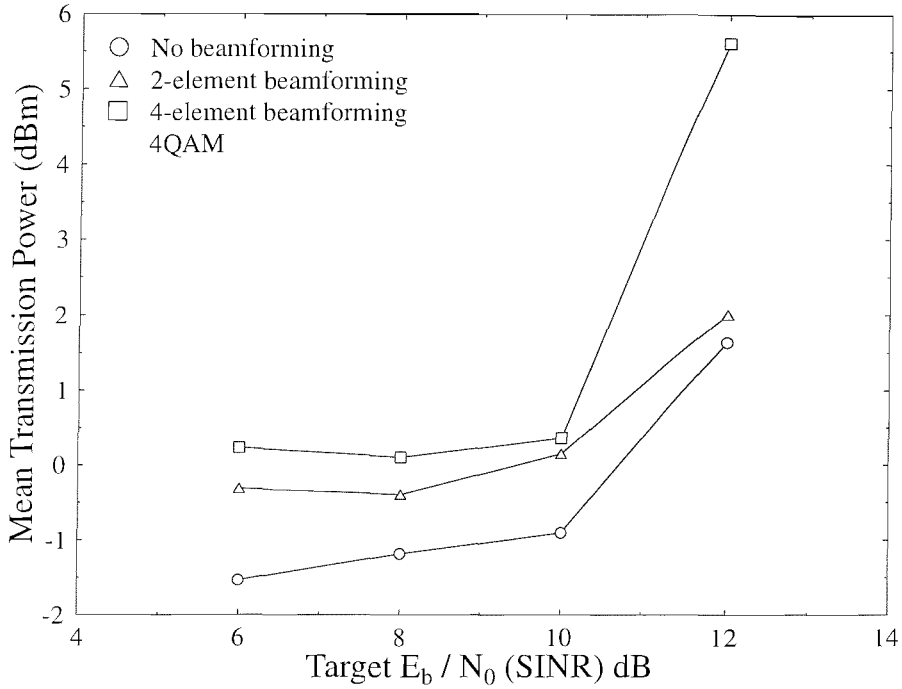

Figure 2.27: Mean transmission power versus target SINR threshold of the UTRA-like FDD cellular network while the maximum user-capacity achieved, both with as well as without beamforming in conjunction with shadowing having a frequency of 0.5 Hz and a standard deviation of 3dB for a spreading factor of SF=16.

2.4 Network-Layer Performance of Multi-Carrier CDMA

2.4.1 Introduction [71]

A range of novel techniques combining DS-CDMA and OFDM have been presented in the literature [71–76].

A DS-CDMA system applies spreading sequences in the time domain and uses Rake receivers for optimally combining the time-dispersed energy in order to combat the effects of multi-path fading. However, in indoor wireless environments the time dispersion is low, on the order of nano seconds, and hence a high chip rate, on the order of tens of MHz, is required for resolving the multi-path components. This implies a high clock-rate, improving a high power consumption as well as a range of implementation difficulties. In order to overcome these difficulties, several techniques have been proposed, which combine DS-CDMA and multi-carrier modulation, such as MC-CDMA [72–74], MC-DS-CDMA [75] and Multi-Tone CDMA (MT-CDMA) [76]. This overview is mainly based on references [77, 78] by Prasad and Hara, as well as on [79] by Scott, Grant, McLaughlin, Povey and Cruickshank.

Target SINR (dB)	Beamforming	Users	Traffic (Erlangs /km^2/MHz)	Power (dBm) MS	BS
6	No	320	1.87	-1.55	-3.03
6	2-elements	489	2.81	-0.31	-1.58
6	4-elements	758	4.34	0.23	0.65
8	No	155	0.90	-1.19	-1.63
8	2-elements	203	1.16	-0.40	-0.56
8	4-elements	350	2.00	0.10	1.46
10	No	53	0.30	-0.91	-0.81
10	2-elements	113	0.65	0.15	1.15
10	4-elements	156	0.89	0.36	1.26
12	No	9	0.07	1.64	1.48
12	2-elements	43	0.25	2.01	2.53
12	4-elements	78	0.44	5.61	2.79

Table 2.6: Maximum mean carried traffic and maximum number of mobile users that can be supported by the network, whilst meeting the network quality constraints, namely $P_B \leq 3\%$, $P_{FT} \leq 1\%$, $P_{low} \leq 1\%$ and GOS $\leq 4\%$. The carried traffic is expressed in terms of normalized Erlangs (Erlang/km^2/MHz) in conjunction with shadow fading having a standard deviation of 3 dB and a frequency of 0.5 Hz for a spreading factor of SF=16.

In MC-CDMA, instead of applying spreading sequences in the time domain, we apply them in the frequency domain, mapping a different chip of a spreading sequence to an individual OFDM subcarrier. Hence each OFDM subcarriers [71] has a data rate identical to the original input data rate and the multicarrier system 'absorbs' the increased chip-rate due to spreading to a wider frequency band. The transmitted signal of the ith data symbol of the jth user $s_i^j(t)$ is written as [72, 80] :

$$s_i^j(t) = \sum_{k=0}^{K-1} b_i^j \, c_k^j \cos\{2\pi(f_0 + kf_d)t\} \, p(t - iT) \ , \tag{2.9}$$

where

- K is the number of subcarriers,
- b_i^j is the ith message symbol of the jth user,
- c_k^j represents the kth chip, $k = 0, \ \cdots \ , K-1$, of the spreading sequence of the jth user,
- f_0 is the lowest subcarrier frequency,

- f_d is the subcarrier separation and
- $p(t)$ is a rectangular signalling pulse shifted in time given by :

$$p(t) \triangleq \begin{cases} 1 & \text{for } 0 \leq t \leq T \\ 0 & \text{otherwise .} \end{cases} \tag{2.10}$$

If $1/T$ is used for f_d, the transmitted signal can be generated using the IFFT, as in the case of an OFDM system [71]. The overall transmitter structure can be implemented by concatenating a DS-CDMA spreader [61] and an OFDM transmitter, as shown in Figure 2.28. At the spreader, the information

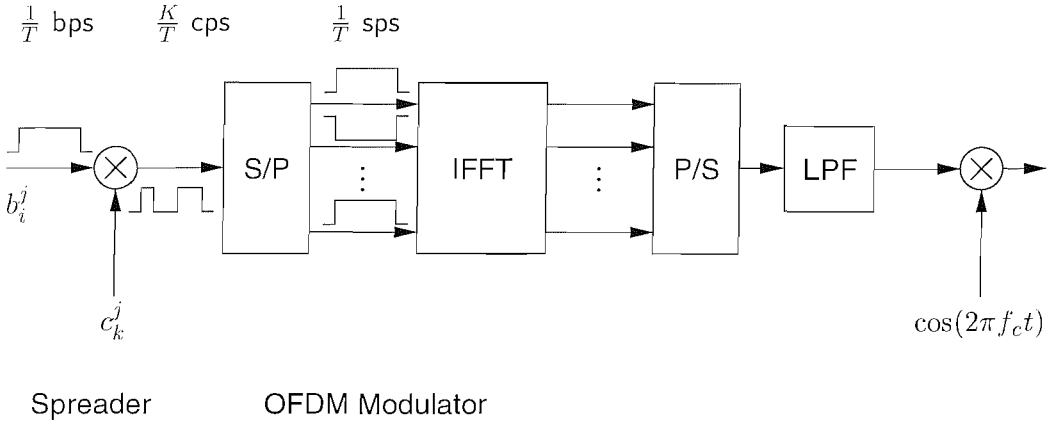

Figure 2.28: Transmitter schematic of MC-CDMA

bit, b_i^j, is spread in the time domain by the jth user's spreading sequence, c_k^j, $k = 0, \cdots, K-1$. In this implementation, high-speed operations are required at the output of the spreader in order to carry out the chip-related operations. The spread chips are fed into the serial-to-parallel (S/P) block and IFFT is applied to these K parallel chips. The output values of the IFFT in Figure 2.28 are time domain samples in parallel form. After parallel to serial (P/S) conversion these time domain samples are low-pass-filtered, in order to obtain the continuous time domain signal. The signal modulates the carrier and is transmitted to the receiver.

Figure 2.29 shows another implementation, which removes the time domain spreader. In this implementation, the spreading sequence is applied directly to the identical parallel input bits. Hence, the high speed spreading operation is not required.

The unique, user-specific spreading sequences in MC-CDMA separate other users' signals from the desired signal, provided that their spreading sequences are orthogonal to each other. Orthogonal codes have zero cross correlation and hence they are particularly suitable for MC-CDMA.

At the MC-CDMA receiver shown in Figure 2.30 each carrier's symbol, *i.e.* the corresponding chip c_k^j of user j, is recovered using FFT after sampling at a rate of K/T samples/sec and the recovered

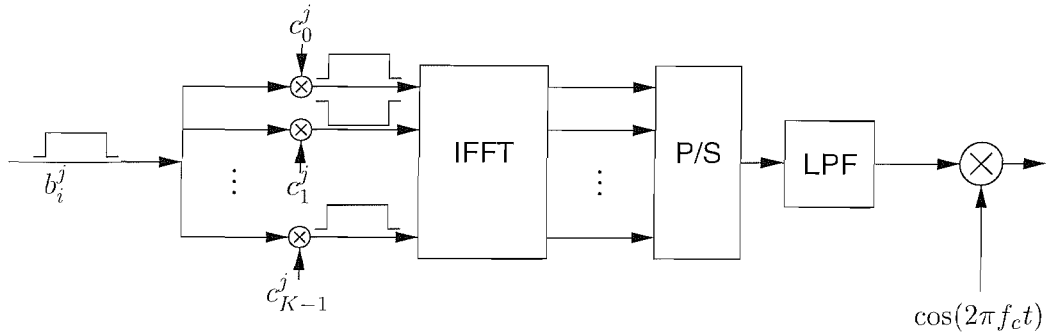

Figure 2.29: Alternative transmitter schematic of MC-CDMA

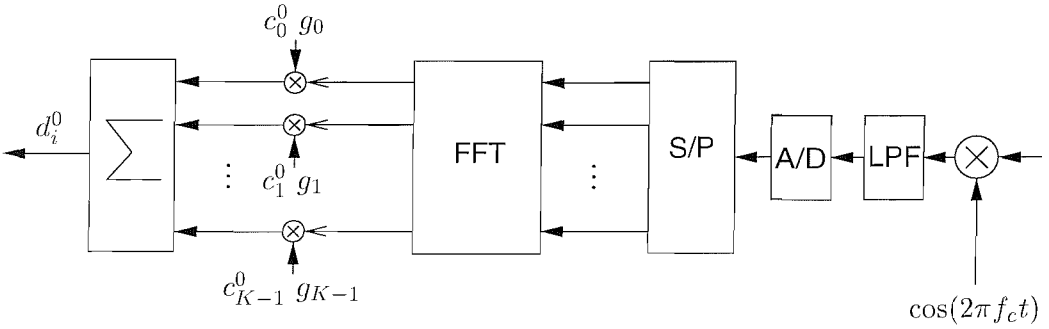

Figure 2.30: Receiver schematic of MC-CDMA

chip sequence is correlated with the desired user's spreading code in order to recover the original information bit, b_i^j. Let us define the ith received symbol at the kth carrier in the downlink as:

$$r_{k,i} = \sum_{j=0}^{J-1} H_k\, b_i^j\, c_k^j + n_{k,i}\ , \tag{2.11}$$

where J is the number of users, H_k is the frequency response of the kth subcarrier and $n_{k,i}$ is the corresponding noise sample. The MC-CDMA receiver of the 0-th user multiplies $r_{k,i}$ of (2.11) by its spreading sequence chip, c_k^0, as well as by the gain, g_k, which is given by the reciprocal of the estimated channel transfer factor of subcarrier k, for each received subcarrier symbol for $k = 0, \cdots, K-1$. It sums all these products, in order to arrive at the decision variable, d_i^0, which is given by :

$$d_i^0 = \sum_{k=0}^{N-1} c_k^0\, g_k\, r_{k,i}\ . \tag{2.12}$$

Without the frequency domain equalization of the received subcarrier symbols discussed in great detail in [61, 81], the orthogonality between the different users cannot be maintained. Several methods have been proposed for advantageously choosing the value of g_k [72, 77, 80]. The associated BER analysis was performed using various equalization methods over both Rayleigh channels and Rician channels by Yee and Linnartz [72]. The comparative summary of numerical results for various equalization strategies was given, for example, by Prasad and Hara [77, 78] and by Hanzo [71] et al.

2.4.2 Simulation Results

In this section simulations using an MC-CDMA [71] based cellular network were conducted in various scenarios employing adaptive antenna arrays [43] as well as adaptive modulation techniques [46]. Network performance results were obtained using 2- and 4-element adaptive antenna arrays in conjunction with adaptive modulation, in the presence of 0.5 Hz frequency shadow fading exhibiting a standard deviation of 3 dB. As in the context of our previous investigations presented in Section 2.2, the expected carried traffic gains were quantified. For the sake of comparing to the achievable network performance to a UTRA-like wideband CDMA system, the similar parameters were adopted to those summarized in Table 2.1. A cell radius of 150 m was assumed, 49 wrapped-around traffic cells constituted the simulation area, as it was shown in Figure 2.11. Figure 2.31 portrays the BER performance of the MC-CDMA system using various modulation schemes for a spreading factor of 16, where the number of subcarriers was also 16. These results were determined with the aid of physical-layer simulations using BPSK, 4QAM and 16-QAM modulation schemes [81], 1/2-rate turbo coding [46] and a Minimum Mean Squared Error Block Decision Feedback Equalizer (MMSE-BDFE) based Multi-User Detector [61, 63] joint detection for transmission over a COST207 Bad-Urban Reduced-mode A (BU-RA) channel [82]. The system was configured to operate at a target BER of 0.1%, a low-quality outage was recorded for BERs in excess of 0.5%, while an outage was declared for BER $\geq$ 1%. Table 2.7 summarizes the corresponding BPSK, 4QAM and 16-QAM SINR thresholds used in our simulations, when employing AQAM [46].

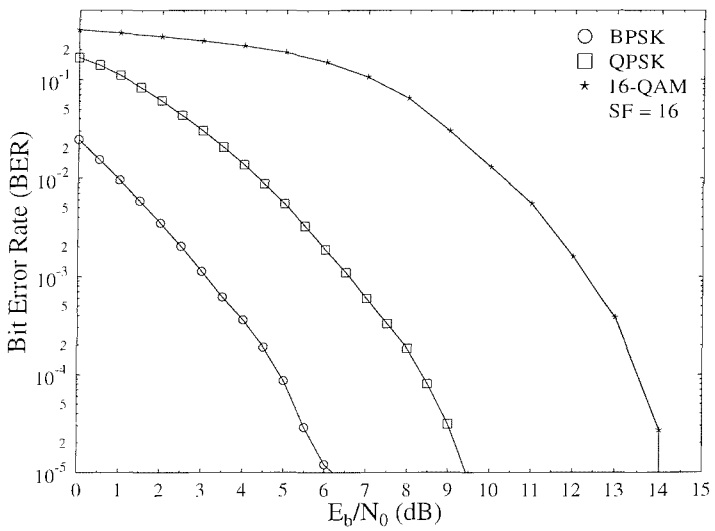

Figure 2.31: BER performance of a MC-CDMA system generated with the aid of physical-layer simulations using BPSK, 4QAM, 16-QAM modulation, 1/2-rate turbo coding and MMSE-BDFE joint detection for transmissions over a COST207 Bad-Urban Reduced-mode A (BU-RA) channel.

SINR Threshold	BPSK	4-QAM	16-QAM
Outage SINR (1% BER)	0.87 dB	4.20 dB	10.3 dB
Low Quality Outage SINR (0.5% BER)	1.60 dB	4.85 dB	11.0 dB
Target SINR (0.1% BER)	2.75 dB	6.15 dB	12.2 dB

Table 2.7: The target SINR, low quality outage SINR and outage SINR thresholds used for the BPSK, 4-QAM and 16-QAM modulation modes of the adaptive modem in MC-CDMA based cellular networks.

Figure 2.32 shows the forced termination probability associated with a variety of traffic loads, measured in terms of the mean normalized carried traffic expressed in Erlangs/km^2/MHz. The figure shows that the carried traffic was significantly improved by using adaptive antenna arrays [43] and adaptive modulation [46]. In Figure 2.32(a), the curve labelled as "No beamforming" presents the achievable carried traffic of the MC-CDMA network without the aid of AAAs and AQAM techniques, which was limited to 323 users, or to a teletraffic load of approximately 1.83 Erlangs/km^2/MHz. However, with the advent of 2- and 4-element adaptive antenna arrays at the base stations, the number of users supported by the network increased by 44% to 466 users and by 127% to 733 users, which corresponded to carried traffic values of 2.72 Erlangs/km^2/MHz and 4.18 Erlangs/km^2/MHz, respectively. When the network employs AQAM techniques without the assistance of adaptive antenna arrays, the attainable performance is characterized by the curve labelled as "No beamforming" in Figure 2.32(b). A carried traffic gain of 60% corresponding to supporting a total of 517 users was achieved compared to the "No beamforming" scenario of Figure 2.32(a). This carried traffic was higher than the carried traffic supported upon 2-element beamforming in the 4QAM scenario of Figure 2.32(a). When both AAAs and AQAM techniques were invoked in the MC-CDMA system, the maximum user capacity reached 869 subscribers, which corresponded to a teletraffic load of 4.98 Erlangs/km^2/MHz, which was attained upon using 4-element beamforming in conjunction with AQAM.

The probability of low quality access versus the mean carried teletraffic load was presented in Figure 2.33, where we observe that the system did not benefit from the application of adaptive antenna arrays, in fact on the contrary. This is likely to be a consequence of the potentially more rapidly fluctuating SINR levels imposed the AAAs, which may experience abrupt SINR level variations as a detriment of their spatial selectivity, which subscribers move in and out of the high-gain beams. This low quality access degradation would be less pronounced in conjunction with omni-directional antennas. Furthermore, Figure 2.33(a) depicted the probability of low quality access without employing adaptive modulation, i.e. when using fixed 4QAM. Upon comparing these results to those obtained in conjunction with adaptive modulation in Figure 2.33(c), the probability of low qual-

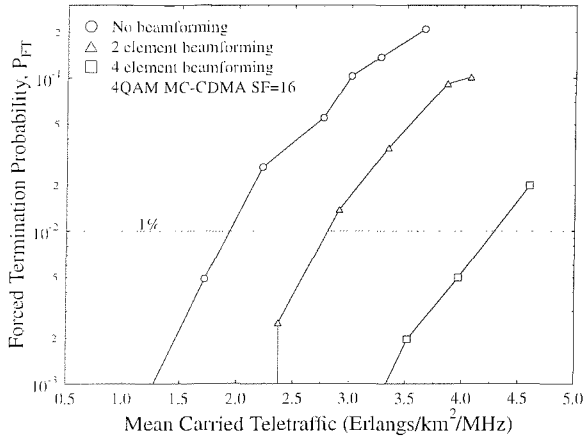

(a) Using adaptive antenna arrays

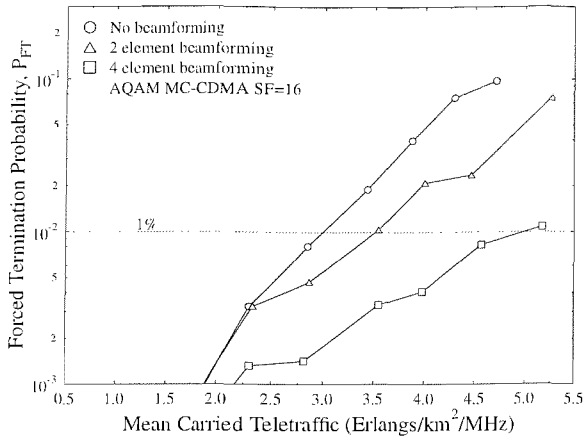

(b) Using AAAs and AQAM

Figure 2.32: Forced termination probability versus mean carried traffic of the MC-CDMA cellular network both with and without beamforming in conjunction with 4QAM and **AQAM** for a spreading factor of SF=16.

ity access degradation imposed by the employment of adaptive modulation can be explicitly seen. This increased probability of low quality access can be attributed to the employment of less robust, but higher-throughput, higher-order modulation modes invoked by the adaptive modulation scheme, which are more vulnerable to sudden SINR changes, than 4QAM. Hence, under given propagation and SINR conditions encountered in the interference-resilient fixed 4QAM modulation mode characterized Figure 2.33(a), a low quality outage event may be avoided. By contrast, when using adaptive modulation invoking a less resilient, but higher-throughput and higher-order modulation mode, the same propagation and SINR conditions may inflict a low quality outage. Upon comparing Figure 2.33(b) to Figure 2.33(d), it can be seen that this scenario was more often encountered in the uplink transmission. This phenomenon will be discussed in more detail in the context of Figure 2.36.

The mean transmission power versus teletraffic performance using both fixed and adaptive modulation in conjunction with AAAs is depicted in Figure 2.34 and Figure 2.35, respectively. The employment of AAAs may result in the attenuation of the desired signal, while maximizing the received SINR, hence the levels of interference are efficiently reduced, ultimately leading to the reduction of the mean transmission power, as seen in Figure 2.34(b) and Figure 2.34(c). Figure 2.35(a) suggests that the mean uplink transmission power was below the mean downlink transmission power when the traffic loads were low, which may be attributed to encountering interfered pilot signals by the mobiles in the downlink. At higher traffic loads the mean required uplink transmission power had to be increased for the sake of maintaining an acceptable SINR, as evidenced by Figure 2.35(b). However, it is seen in Figure 2.35(c) that the mean downlink transmission power requirement was reduced, as the

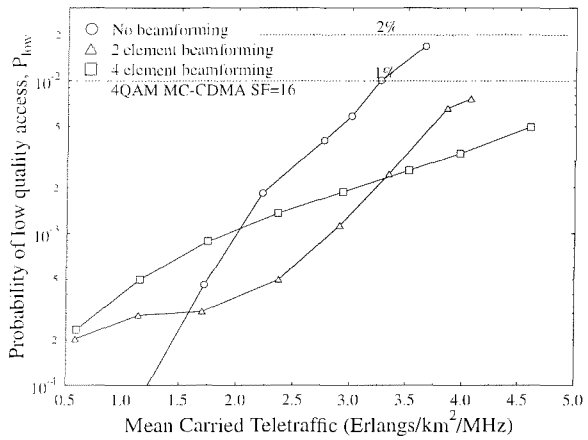

(a) Averaged UL/DL P_{low} for 4QAM and AAAs

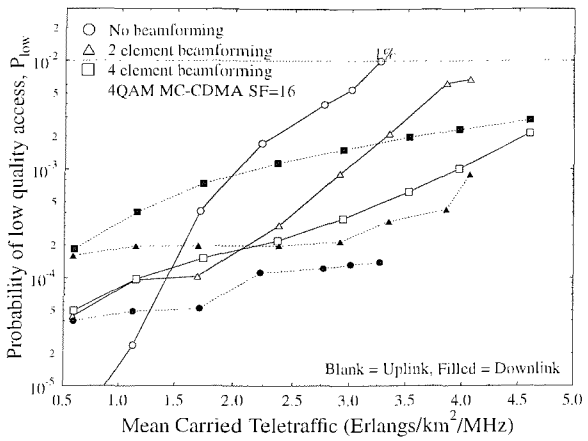

(b) Separate UL and DL P_{low} for 4QAM and AAAs

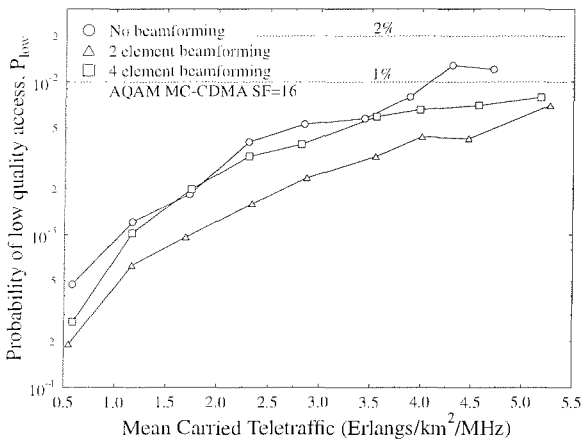

(c) Averaged UL/DL P_{low} for AQMA and AAAs

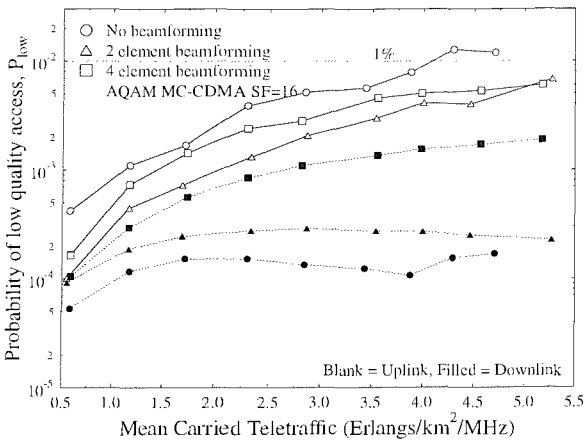

(d) Separate UL and DL P_{low} AQAM and AAAs

Figure 2.33: Probability of low quality access versus mean carried traffic of the MC-CDMA cellular network both with and without beamforming in conjunction with 4QAM and **AQAM** for a spreading factor of SF=16.

traffic load became higher. That is because when the traffic load increased, the level of interference rose, resulting in a low SINR. In this scenario the AQAM control regime is expected to switch from 16-QAM to 4-QAM or from 4-QAM to BPSK, hence requiring a reduced average power level for the network. This hypothesis may be confirmed by examining Figure 2.36, which portrays the mean SINR versus the mean carried teletraffic as well as the discrete histogram modelling the probability density function (PDF) of the mean SINR. From Figure 2.36(a) we observe that the mean SINR of the network reduced as the traffic load became higher. The PDFs suggests that at lower traffic loads typically higher target SINRs were maintained, which facilitated the employment of higher-throughput but more vulnerable modulation modes, such as 16-QAM. By contrast, at higher traffic loads typically low target SINRs were maintained, requiring lower-throughput but more robust modulation modes, such as BPSK.

A summary of the maximum achievable user capacity of the MC-CDMA networks considered in this section under the detrimental effect of a log-normal shadowing having a standard deviation of 3 dB, both with and without employing beamforming in conjunction with AQAM is given in Table 2.8. The teletraffic carried and the mean mobile as well as base station transmission powers required for attaining these user capacities are also shown in Table 2.8.

2.4.3 Summary and Conclusions

In this section we have examined the achievable network capacity and the overall performance of the MC-CDMA based cellular network benefiting from both adaptive antenna arrays and adaptive modulation techniques. We have shown that a substantially increased number of users may be supported, who benefit from a superior call quality, and reduced transmission power requirements for a given number of AAA array elements located at the base stations.

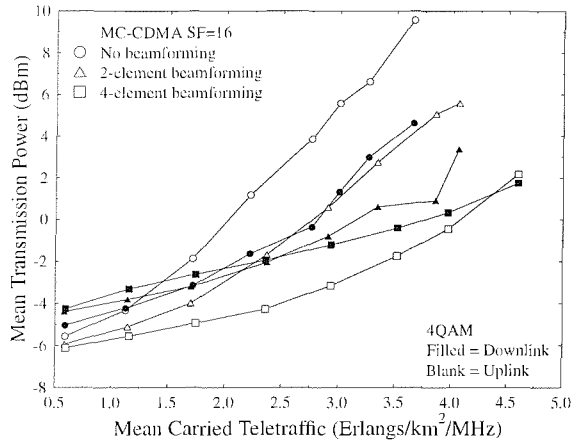

(a) Mean UL and DL Tx. Power

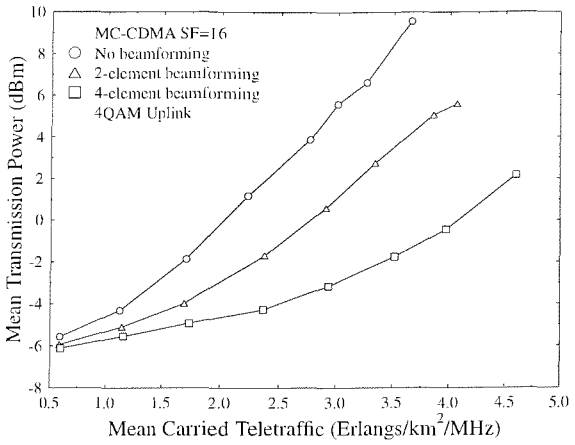

(b) Mean UL Tx. Power

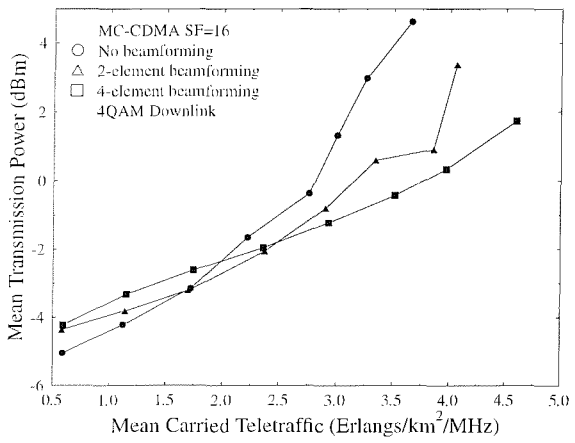

(c) Mean DL Tx. Power

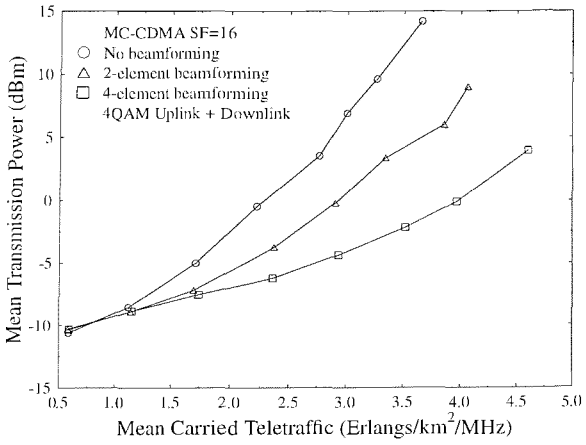

(d) Mean UL+DL Tx. Power

Figure 2.34: Mean transmission power versus mean carried traffic of the MC-CDMA cellular network both with as well as without beamforming for a spreading factor of SF=16.

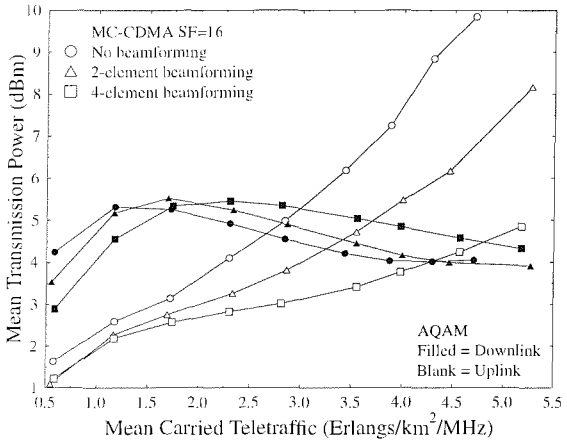

(a) Mean UL and DL Tx. Power

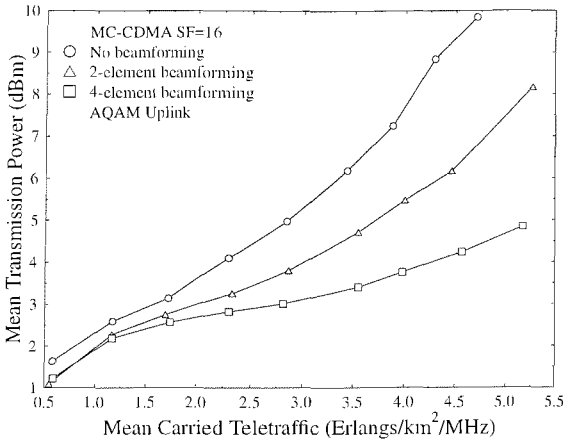

(b) Mean UL Tx. Power

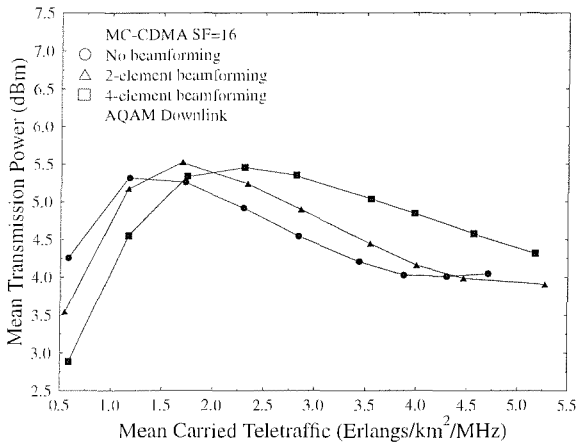

(c) Mean DL Tx. Power

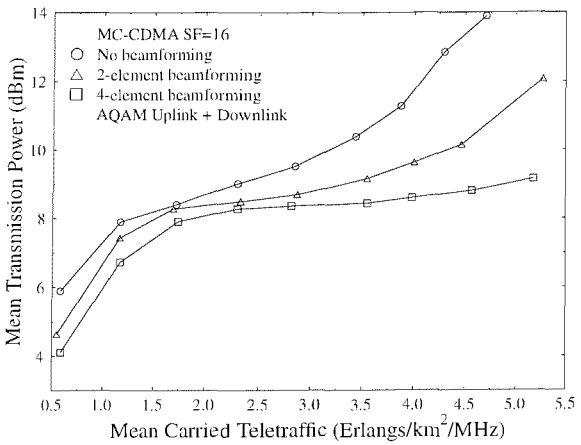

(d) Mean UL+DL Tx. Power

Figure 2.35: Mean transmission power versus mean carried traffic of the MC-CDMA cellular network both with and without beamforming in conjunction with **AQAM** for a spreading factor of SF=16.

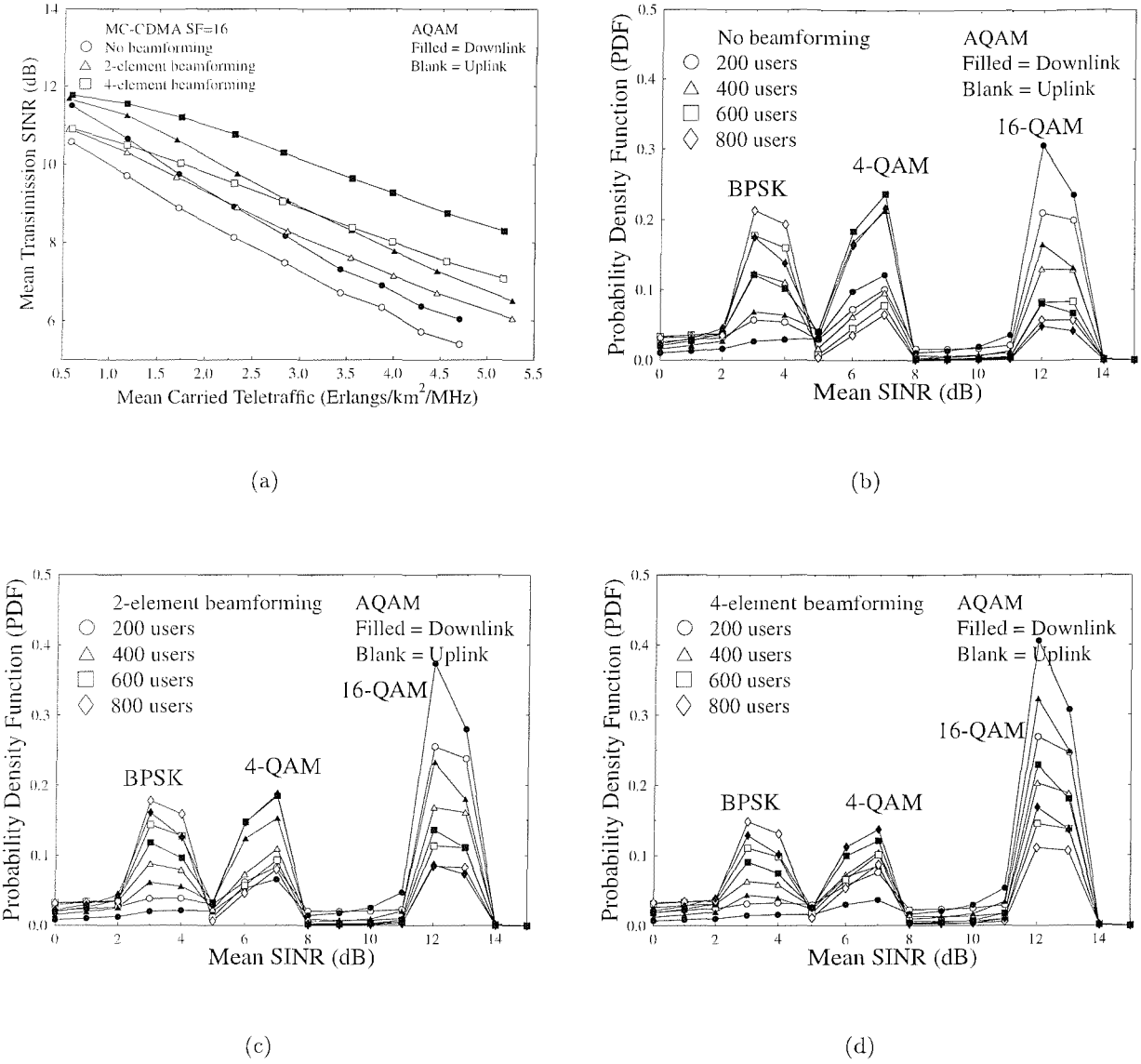

Figure 2.36: Mean SINR versus mean carried traffic and the SINR histogram modelling the probability density function of the MC-CDMA cellular network's SINR both with and without beamforming in conjunction with **AQAM** for a spreading factor of SF=16.

Modulation Mode	Beamforming	Users	Traffic (Erlangs /km^2/MHz)	Power (dBm) MS	BS
4-QAM	No	323	1.83	-1.15	-2.79
4-QAM	2-elements	466	2.72	-0.18	-1.22
4-QAM	4-elements	733	4.18	0.46	0.82
AQAM	No	517	2.95	5.20	4.48
AQAM	2-elements	594	3.50	4.66	4.47
AQAM	4-elements	869	4.98	4.65	4.39

Table 2.8: Maximum carried traffic and maximum number of mobile users that can be supported by the MC-CDMA network, whilst meeting the target network quality constraints, namely $P_{FT} \leq 1\%$, $P_{low} \leq 1\%$ and GOS $\leq 4\%$. The carried traffic is expressed in terms of normalized Erlangs (Erlang/km^2/MHz) in conjunction with shadow fading having a standard deviation of 3 dB and a frequency of 0.5 Hz, whilst employing adaptive modulation techniques [64] for a spreading factor of SF=16. The average transmission power of the MSs and BSs are also summarized.

Chapter 3

UTRA TDD/CDMA Network Performance

3.1 Introduction

In January 1998, the European standardization body created for the definition of the third generation (3G) mobile radio system, namely the European Telecommunications Institute's - Special Mobile Group (ETS ISMG), ratified a radio access scheme referred to as the Universal Mobile Telecommunications System (UMTS) [43]. The UMTS terrestrial Radio Access known as UTRA supports two duplexing modes, namely the Frequency Division Duplexing (FDD) mode, where the uplink and downlink are transmitted on different frequencies, and the Time Division Duplexing (TDD) mode, where the uplink and the downlink are transmitted on the same carrier frequency, but multiplexed in time [43]. UMTS networks will introduce into wide area using a completely new high bit rate radio technology - wideband CDMA (WCDMA).

In UTRA, the different services are expected to be supported in a spectrally efficient manner, either by FDD or TDD. The FDD mode is intended for applications in both macro- and micro-cellular environments, supporting data rates of up to 384 Kbps both at relatively high velocity. The TDD mode, on the other hand, is more suited to micro and pico-cellular environments, as well as for licensed and unlicensed cordless and wireless local loop applications. It makes efficient use of the unpaired spectrum - for example in wireless Internet applications, where much of the teletraffic is expected to be on the downlink - and supports data rates of up to 2 Mbps. Therefore, the TDD mode is particularly well suited for environments generating a high traffic density e.g. in city centres, business areas, airports etc. and for indoor coverage, where the applications require high data rates and tend to have highly asymmetric traffic, again, as in wireless Internet access.

3.2 UMTS Terrestrial Radio Access (UTRA)

A bandwidth of 215 MHz in the region of 2.0 GHz has been allocated for UMTS services in Europe. The paired bands of 1920-1980 MHz (uplink) and 2110-2170 MHz (downlink) have been set aside for FDD W-CDMA systems, and the unpaired frequency bands of 1900-1920 MHz and 2010-2025 MHz for TDD CDMA systems.

A UTRA Network (UTRAN) consists of one or several Radio Network Sub-systems (RNSs), which in turn consist of base stations (referred to as Node BS) and Radio Network Controllers (RNCs). A Node B may serve a single or multiple cells. Mobile stations are known as User Equipment (UE), which are expected to support multi-mode operation in order to enable handovers between the FDD and TDD modes and, prior to complete UTRAN coverage, also to GSM. The two modes differ in a number of ways in the physical layer, but for compatibility and implementation reasons they are harmonized as far as possible, especially in higher layers. More details on the differences and distinctions can be found in [83]. The key parameters of UTRA have been defined in Table 3.1. The harmonization enables the same services to be offered over both modes, while the differences lead to one mode being best utilized in certain system scenarios while the other mode may perform better in other scenarios.

	UTRA FDD	UTRA TDD
Frame structure	15 slots/frame	15 slots/frame
Frame length	10 ms	10 ms
Chip rate	3.84 Mcps	3.84 Mcps
Spreading factor range	4-512	1-16
Frequency bands	1920-1980 MHz (UL)	1900-1920 MHz (UL)
	2110-2170 MHz (DL)	2010-2025 MHz (DL)
Modulation	4-QAM/QPSK	4-QAM/QPSK
Bandwidth	5 MHz	5 MHz
Handover	soft and hard	hard only
Power control update rate	1500 Hz	800 Hz
Dynamic channel allocation	N/A	slow and fast

Table 3.1: Key UTRA parameters for the FDD and TDD modes.

3.2.1 Characteristics of UTRA

The proposed spectrum allocation of UTRA is shown in Figure 3.1. As can be seen, UTRA is unable to utilize the full frequency spectrum allocated for the 3G mobile radio systems during the WARC'92

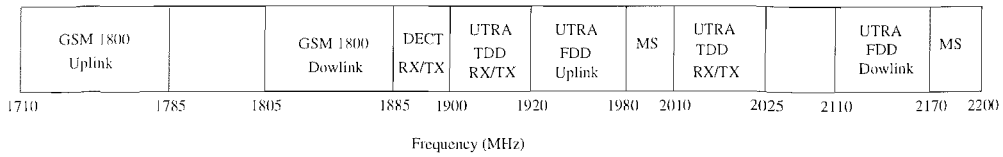

Figure 3.1: The proposed spectrum allocation in UTRA

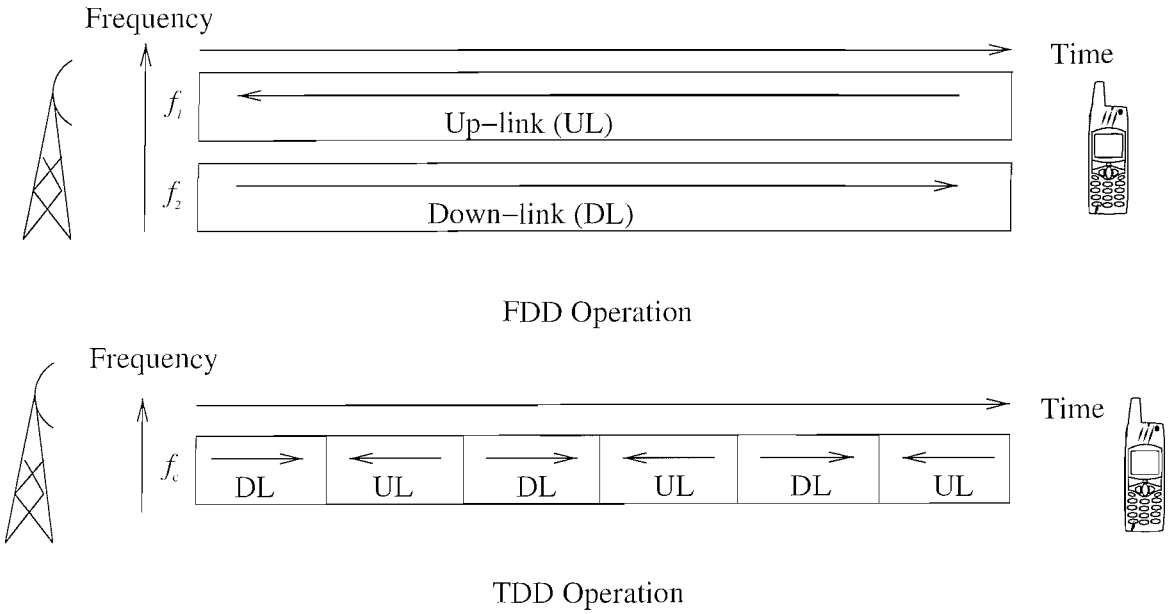

Figure 3.2: Principle of FDD and TDD operation.

conference [9], since those frequency bands have also been partially allocated to the Digital Enhanced Cordless Telecommunications (DECT) system [84]. The frequency spectrum was originally allocated based on the assumption that speech and low data rate transmission would become the dominant services offered by IMT-2000 [43, 85]. However, in recent years a paradigm has been experienced towards services that require high-speed data transmission, such as wireless Internet access and multimedia services. A study conducted by the UMTS Forum [12] forecast that the current frequency bands allocated for IMT-2000 are only sufficient for the initial deployment until the year 2005. According to the current demand estimates, it was foreseen that an additional frequency spectrum of 187 MHz might be required for IMT-2000 in high-traffic areas by the year 2010. Among of numerous candidate extension bands, the band 2520-2670 MHz has been deemed to be the most likely. Unlike other bands, which have already been allocated for use in other applications, this band was allocated to mobile services in all regions. Furthermore, the 150 MHz bandwidth available is sufficiently wide for satisfying most of the forecast spectrum requirements.

Again, the UMTS radio access supports both FDD and TDD operations [43]. The operating principles of these two schemes are augmented here in the context of Figure 3.2.

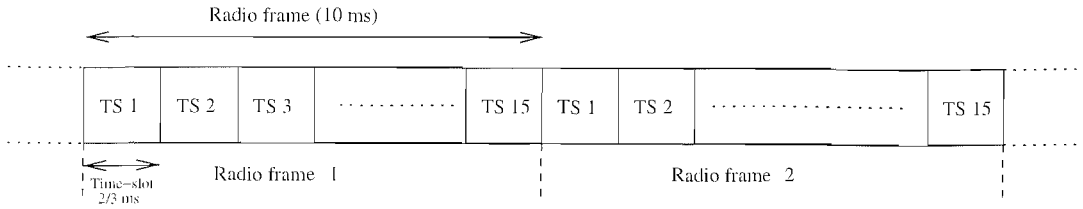

Figure 3.3: UTRA physical channel structure

Specifically, the Uplink (UL) and Downlink (DL) signals are transmitted using different carrier frequencies, namely f_{UL} and f_{DL}, respectively, separated by a frequency guard band in the FDD mode. On the other hand, the UL and DL messages in the TDD mode are transmitted using the same carrier frequency f_{TDD}, but in different time-slots, separated by a guard period. As seen from the spectrum allocation of Figure 3.1, the paired bands of 1920-1980 MHz and 2110-2170 MHz are allocated for FDD operation in the UL and DL, respectively, whereas the TDD mode is operated in the remaining unpaired bands. The parameters designed for FDD and TDD operations are mutually compatible so as to ease the implementation of a dual-mode terminal capable of accessing the services offered by both FDD and TDD operators.

3.2.2 Physical Channels

The transport channels are transmitted using the UTRA physical channels [43, 86, 87]. The physical channels are typically organized in terms of radio frames and time-slots, as shown in Figure 3.3. While in GSM [88] each TDMA user had an exclusive slot allocation, in W-CDMA the number of simultaneous users supported is dependent on the users' required bit rate and their associated spreading factors. The MSs can transmit continuously in all slots or discontinuously, for example, when invoking a Voice Activity Detector (VAD) [88].

As seen in Figure 3.3, there are 15 timeslots within each radio frame. The duration of each timeslot is 2/3 ms, which yields a total duration of 10 ms for the radio frame. As we shall see later in this section, the configuration of the information in the time-slots of the physical channels differs from one another in the UL and DL, as well as in the FDD and TDD modes. In the FDD mode, a DL physical channel is defined by its spreading code and frequency. Furthermore, in the UL, the modem's orthogonal in-phase(I) and quadrature-phase (Q) branches are used for delivering the data and control information simultaneously in parallel [43]. On the other hand, in the TDD mode, a physical channel is defined by its spreading code, frequency and time-slot.

3.3 UTRA TDD/CDMA System

The UTRA TDD mode is partly a result of the original UMTS spectrum allocation, which consists of one paired and two unpaired bands. This led to an ETSI decision in 1998 that not just one but two of the proposed access technologies should be adopted for the UMTS standard. Hence, the FDD mode should be used in paired band and the TDD mode in the unpaired band. The TDD UTRA scheme will be deployed in the unpaired IMT-2000 frequency bands. The so-called band A is the 3G unpaired frequency allocation in Europe: 1900-1920 MHz and 2010-2025 MHz. In the United States so-called band B, namely the PCS spectrum allocation encompasses the range of 1850-1910 MHz and 1930-1990 MHz. Furthermore, the United States also allocated band C, an unlicensed band from 1910 MHz to 1930 MHz. The nominal channel spacing in UTRA is 5 MHz, with a channel raster of 200kHz, which means that the carrier frequency is a multiple of 200 kHz.

There are a few characteristics that are typical of TDD systems and different from the characteristics of FDD systems. These characteristics are listed below.

- *Utilization of unpaired bands* : the TDD system can be invoked in unpaired bands, while the FDD system always requires a pair of bands. It is more likely that in the future unpaired spectrum resources will be made available for UMTS.

- *Possible interference between uplink and downlink* : since both the uplink and downlink share the same carrier frequency in TDD, any timeslot can be used in any direction and hence the signals of the two transmission directions may interfere with each other.

- *Flexible capacity allocation between the uplink and downlink* : in the TDD mode, the uplink and downlink are divided in the time domain. It is possible to control the switching point [89] between the uplink and downlink, as seen in Figure 3.2, and move capacity form the uplink to downlink, or vice versa, if the capacity requirement is asymmetric between the uplink and downlink.

- *Discontinuous transmission* : the mobile and the base station transmissions are discontinuous in TDD. Discontinuous transmissions impose specific requirements on the implementation. Switching between the transmission directions requires a reflecting time, since the effects of switching effects of transients must be avoided. Hence, for the aim of avoiding the overlapping of the uplink and downlink transmissions, a guard period is used at the end of each slot.

- *Uplink/Downlink channel properties* : in case of frequency selective fading the channel's function depends on the frequency and, therefore in the FDD mode the fast fading is typically uncorrelated between the uplink and downlink. Since the same frequency is used both for the

uplink and downlink in the TDD mode, the fast fading properties are more similar in the uplink and downlink. The similarity of the fast fading between the uplink and downlink can be exploited in both power control and adaptive antenna arrays used in TDD.

It is unlikely that any of the service providers would operate standalone wide-area TDD networks, but rather they would invoke the FDD UTRA mode and possibly GSM to provide continuous wide-area coverage, while TDD to serve as a separate capacity-enhancing layer in the network [90]. Furthermore, as a benefit of being able to arbitrarily adjust the UL/DL asymmetry, the TDD mode is also capable of supporting high bit rates, ranging from 144 kbps to 2 Mbps in wireless Internet type applications.

3.3.1 The TDD Physical Layer

The UTRA TDD mode has a similar frame structure to that of the UTRA FDD mode. As seen in Figure 3.3, there are 15 slots in a frame, which has a period of 10 ms. Each slot has 2560 chips and lasts for 0.667 ms. A superframe consists of 72 frames and lasts for 720 ms. A physical channel consists of bursts that are transmitted in the same slot of each frame. For specifying a physical channel explicitly, we also have to define its so-called repetition period, repetition length and superframe offset, which will be exemplified below. The number of frames between slots belonging to the same physical channel is the repetition period of a given physical channel, which must be sub-multiple of 72, i.e. 1,2,3,4,6,8,9,12,18,24,36 and 72. An example is given by the physical channel occupying slot 0 in every 12th frame. The superframe offset defines the repetition period offset within a superframe, with respect to the beginning of the frame. Returning to our example, if the superframe offset is 3, the physical channel will occupy slot 0 in frames 3,15,27,39,..., since it was offset by 3 frames, where the corresponding slots are 12 frames apart. The repetition length defines the number of slots associated with each repetition, and may have values of 1,2,3,4. For the example where the physical channel occupies slot 0, the repetition period is 12, the superframe offset is 3, and say, the repetition length is 4, the physical channel will occupy slot 0 in frames (3,4,5,6,), (15,16,17,18), (27,28,29,30), etc.

3.3.2 Common Physical Channels of the TDD Mode

The UTRA TDD mode employs time division duplexing for creating bidirectional transmission links. Each slot in a frame can be used for carrying either uplink or downlink information. The switching point or points between uplink and downlink slots may be variable, as is the number of slots allocated to each link. At least one slot must be allocated in each direction.

In TDD operation, the burst structure of Figure 3.4 is used for all the physical channels, where each time-slot's transmitted information can be arbitrarily allocated to the uplink or downlink, as

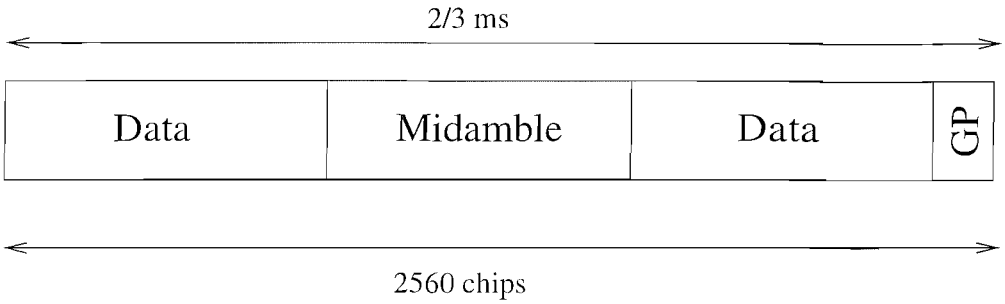

Burst type	Data	Midamble	Guard Period
Burst Type 1	976	512	96
Burst Type 2	1104	256	96

Figure 3.4: Time slot of the physical channels.

shown in the four possible TDD allocations of Figure 3.5. A symmetric UL/DL allocation refers to a scenario in which an approximately equal number of DL and UL bursts is allocated within a TDD frame, while in case of asymmetric UL/DL allocation there is an unequal number of UL and DL bursts, such as services, etc., for example, in "near-simplex" file download from the wireless Internet or in case of video-on-demand.

In UTRA, two different TDD burst structures, known as *Burst Type* 1 and *Burst Type* 2, are defined, which are shown in Figure 3.4. The Type 1 burst has a longer midamble of 512 chips than the Type 2 burst of length 256 chips. However, both types of bursts have an identical *Guard Period* (GP) of 96 chips. The midamble sequences that are allocated to the different TDD bursts in each time-slot belong to a so-called *midamble code set*. The codes in each midamble code set are derived from a unique *Basic Midamble Code*. Adjacent cells are allocated different midamble code sets. This can be exploited to assist in cell identification.

3.3.3 Power Control

Power control of the UTRA TDD mode is performed on a framely basis, for example using a power control update per 10 ms, which is carried out differently for the uplink and downlink.

Specifically, the uplink power control uses an open loop technique, which exploits the similarity of the uplink and downlink channel in a TDD system, in particular as regards to the pathloss. In each cell there is at least one beacon, i.e. a physical channel having a known transmit power. Furthermore,

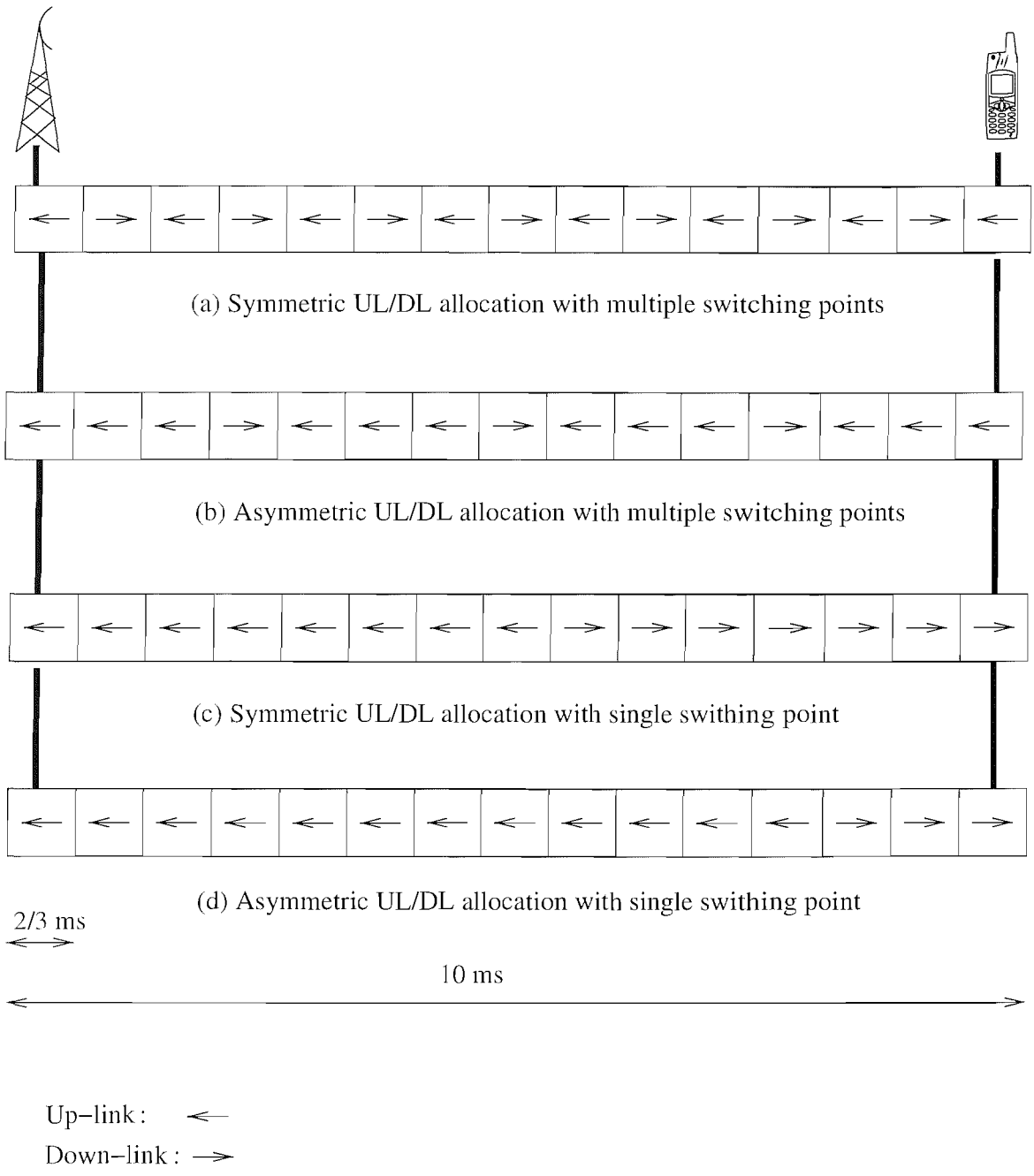

Figure 3.5: Multiple switching points per frame for different slot per frame allocations.

during unallocated uplink timeslots the base station is capable of estimating the uplink interference by exploiting the knowledge of the required target SIR, the MS can set its transmission power in order to fulfill the transmission integrity requirements at the BS. A first-order predictor corresponding to a weighting factor can be used for taking into account the expected delay between the downlink pathloss estimate and the actual uplink pathloss. At the BS, an outer power control loop is used for estimating the SIR of the received signal, which is compared it to the target SIR requirements. Then the necessary MS transmit power is calculated, which is signalled to the MS. This requirement allows the SIR-based outer loop to compensate for the long-term fluctuation of the associated pathlosses.

3.3.4 Time Advance

Timing advance is the mechanism used in UTRA for controlling the transmit time instant of signals from different MSs for mitigating leakage between time slots. During the initial access, the base station estimates the instant of reception for the MSs and advances their instant of transmission by the estimated propagation delay, so that all signals arrive approximately within the expected time window at the BS. The UTRA TDD system can be used in wide area cells, where the employment of this timing advance mechanism is necessary for preventing the up-link burst collisions at the BS receiver. The timing advance operates to a resolution of four chips or 1.04 μs, since the chip-rate is 3.84 Mchip/s. The BS estimates the time offset associated with the PRACH transmissions [43] and calculates the required initial timing advance. The timing advance parameter is transmitted as an 8-bit number, catering for a maximum timing advance of 256 $\times$ 1.04 μs corresponding to the up-link transmissions from the MS. This maximum propagation delay of approximately 256 μs potentially allows for a cell-size of 80 km.

There are proposals to have an enhanced timing advance mechanism with a resolution of one-eighth of a chip period. This potentially holds the promise of quasi-synchronous up-link transmission, which would dramatically decrease the multiple access interference, since all the transmitted codes of the MSs would remain quasi-orthogonal.

When performing a handover to another TDD cell, which is generally synchronized to reference cell, the MS is capable of autonomously applying the right timing advance in the new cell. In any case, the MS has to signal the timing advance it applies to the BS in the new cell.

3.4 Interference Scenario In TDD CDMA

One of the major attractions for the UTRA TDD mode system is that it allows the uplink and downlink capacities to be allocated asymmetrically. The uplink and downlink are transmitted on the same carrier frequency, which creates additional interference scenarios compared to UTRA FDD, and as seen in Figure 3.6, the UL/DL transmission directions of adjacent co-channel BSs may severely interfere with each other. This kind of interference may become particularly detrimental, if the base stations are not synchronized, or if a different ratio of uplink and downlink timeslots is used in adjacent cells, even if the base stations are frame synchronized. Frame synchronization requires an accuracy of a few symbols, rather than an accuracy of a few chips.

The interference between uplink and downlink can also occur between adjacent frequencies. Therefore, the interference between uplink and downlink can take place within one operator's band, and also between two operators.

The interference between uplink and downlink can occur between two mobile stations and between two base stations. In FDD operation the duplex separation prevents the interference between uplink and downlink. In a TDD system there are four types of inter-cell/inter-operator interference. These are:

- MS $\rightarrow$ MS
- BS $\rightarrow$ BS
- MS $\rightarrow$ BS
- BS $\rightarrow$ MS

The interference between a mobile station and a base station is the same both in TDD and in FDD operation. The extent of these interference is dependent on many parameters such as the cell locations and user distributions, however there are two parameters that can greatly affect the system performance and can potentially be managed by the network. There are synchronization between cells, and the asymmetry across the network.

3.4.1 Mobile to Mobile Interference

Mobile to mobile interference occurs in Figure 3.6, at the timeslot 7 the mobile MS_2 is transmitting and the mobile MS_1 is receiving in the same frequency in adjacent cells. Mobile to mobile interference is statistical because the locations of the mobiles cannot be controlled. Therefore, mobile to mobile interference cannot be avoided completely by the network planning.

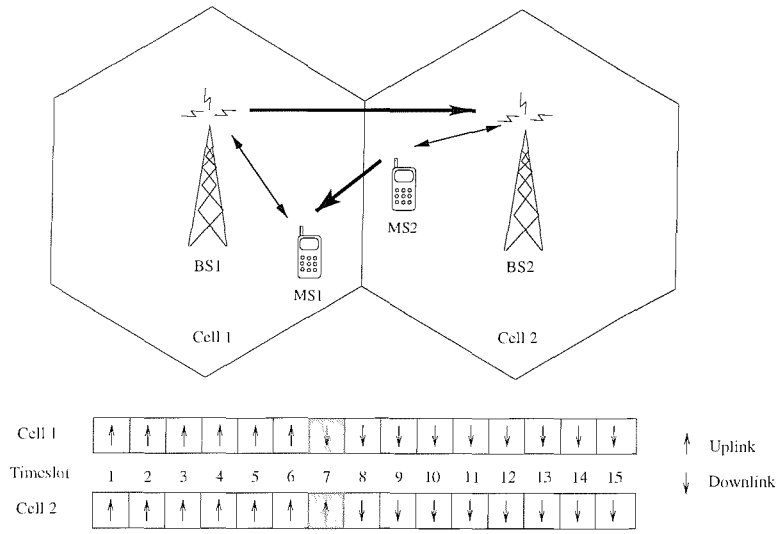

Figure 3.6: MS-to-MS BS-to-BS inter-cell interference

3.4.2 Base Station to Base Station Interference

Base station to base station interference occurs in Figure 3.6, at the timeslot 7 the base station BS_1 is transmitting and the base station BS_2 is receiving in the same frequency in adjacent cells. Base station to base station interference depends heavily on the path loss between the two base stations, and therefore, the network planning greatly affects this interference scenario [91].

3.5 Simulation Results

A number of studies have been conducted, in order to characterise the network capacity of WCDMA-assisted 3G networks [92–94]. *The Timeslot (TS) opposing technique* proposed by Haas, McLaughlin and Povey [23, 95] enables asynchronous cells to overlap without a significant capacity degradation in comparison to the more idealistic scenario, when the base stations of all cells transmit and receive slot-synchronously in the UTRA-TDD system. Furthermore, the Dynamic Channel Allocation (DCA) [96] aided TS-opposing algorithm [23] enables neighbouring cells to adopt different grades of uplink/downlink (UL/DL) asymmetry without inflicting a significant capacity loss. The co-existence of the UTRA-TDD and FDD modes was studied in [97–99], since they are expected to co-exist in the same geographical area. Owing to the presence of increased levels of interference, capacity degradations are expected. It is crucial to estimate this potential capacity degradation and to identify appropriate countermeasures. Power control is a standard technique of improving the performance of wireless systems. Different power control techniques and their application within the UMTS were presented in [100–103]. More specifically, in [100], received signal level-based and interference level-

based power control algorithms were introduced and the achievable system performance was compared by means of simulations. In [101], the UTRA TDD mode was studied in conjunction with an open loop power control algorithm combined with outer loop power control functions, which resulted in an improved rate of successful call establishment in the network. An Optimum Power Control (OPC) method was proposed in [102], which achieved the same performance as Wu's [104] at the cost of a lower complexity. Kurjenniemi [103] studied uplink power control in the context of the UTRA TDD system by the means of system level simulations, demonstrating that the UTRA TDD uplink power control substantially benefited from exploiting accurate interference measurements and hence achieved a high capacity, even in the presence of implementation errors. A pre-Rake smart antenna system designed for TDD CDMA was studied in [105]. The study demonstrated that incorporating an antenna array at the base station significantly improves the achievable capacity by reducing the interference between the uplink and downlink of adjacent cells, which is a consequence of potentially using all timeslots in an arbitrary uncoordinated fashion both in the UL and DL. Conventional single-user detectors, such as the Rake receiver are expected to result in a low network capacity owing to the excessive TDD-induced Multiple Access Interference . By contrast, Multi-User Detectors (MUD) have the potential of increasing the network capacity at the cost of a higher complexity [46, 63, 106].

This section presents our simulation results obtained for a TDD mode UTRA-like CDMA cellular network, investigating the achievable user capacity of the TDD mode in both non-shadowed and shadowed propagation environments. This is in Section 3.5.2 followed by our performance investigations using adaptive antenna arrays, when subjected to both non-shadowed as well as shadowed propagation conditions. Finally, the performance of adaptive modulation techniques used in conjunction with adaptive antenna arrays in shadow faded environments is then characterised in Section 3.5.3.

3.5.1 Simulation Parameters [43]

In this section simulations were conducted for various scenarios and algorithms in the context of a TDD mode UTRA-like CDMA based cellular network in order to study the interactions of the processes involved in such a network. As in the UTRA standard, the frame length was set to 10 ms, containing 15 power control timeslots. The power control target SINR was chosen to give a Bit Error Ratio (BER) of 1×10^{-3}, with a low quality outage occurring at a BER of 5×10^{-3} and an outage taking place at a BER of 1×10^{-2}. The received SINRs at both the mobile and the base stations were required for each of the power control timeslots, and hence the outage and low quality outage statistics were gathered. If the received SINR was found to be below the outage SINR for 75 consecutive power control timeslots, corresponding to 5 consecutive transmission frames or 50 ms, the call was dropped. The post-despreading SINRs necessary for obtaining the target BERs were determined with the aid

of physical-layer simulations using a 4-QAM modulation scheme, in conjunction with 1/2 rate turbo coding and joint detection over a COST 207 seven-path Bad Urban channel [64]. For a spreading factor of 16, the post-de-spreading SINR required for maintaining BER of 1×10^{-3} was 8.0 dB, while for a BER of 5×10^{-3} it was 7.0 dB, and for a BER of 1×10^{-2} was about 6.6 dB. These values can be seen along with the other system parameters in Table 3.2. The pre-de-spreading SINR is related to E_b/N_o and to the spreading factor by

$$SINR = (E_b/N_o)/SF, \tag{3.1}$$

where the spreading factor is given by $SF = W/R$, with W being the chip rate and R the data rate. A receiver noise figure of 7 dB was assumed for both the mobile and the base stations [50]. Thus, in conjunction with a thermal noise density of -174 dBm/Hz and a noise bandwidth of 5 MHz, this resulted in a receiver noise power of -100 dBm. The power control algorithm used was relatively simple, and unrelated to the previously introduced schemes of Section 3.3.3. Furthermore, since it allowed a full transmission power change of 15 dB within a 15-slot UTRA data frame, the power control scheme advocated is unlikely to limit the network's capacity.

Specifically, for each of the 15 timeslots per transmitted frame, both the mobile and base station transmit powers were adjusted such that the received SINR was higher than the target SINR, but less than the target SINR plus a 1 dB hysteresis. When in handover, a mobile's transmission power was only increased, if all of the base stations in the Active Base station Set (ABS) requested a power increase, but was it decreased if any of the base stations in the ABS had an excessive received SINR. In the downlink, if the received SINR at the mobile was insufficiently high, then all of the active base stations were commanded to increase their transmission powers. Similarly, if the received SINR was unnecessarily high, then the active base stations would reduce their transmit powers. The downlink intra-cell interference orthogonality factor α, was set to 0.5 [92–94]. Due to using a frequency reuse factor of one, with its associated low frequency reuse distance, it was necessary for both the mobiles and the base stations to increase their transmitted power gradually when initiating a new call or entering handover. This was required for preventing sudden increases in the level of interference, particularly on links using the same base station. Hence, by gradually increasing the transmit power to the desired level, the other users of the network were capable of compensating for the increased interference by increasing their transmit powers, without encountering undesirable outages. In an FDMA/TDMA network this effect is less noticeable due to the significantly higher frequency reuse distance.

Since a dropped call is less desirable from a user's viewpoint than a blocked call, two resource allocation queues were invoked, one for new calls and the other - higher priority - queue, for handovers. By forming a queue of the handover requests, which have a higher priority during contention for

Parameter	Value	Parameter	Value
Frame length	10 ms	Timeslots per frame	15
Target E_b/N_o	8.0 dB	Outage E_b/N_o	6.6 dB
Low Quality (LQ) Outage E_b/N_o	7.0 dB	BS Pilot Power	-5 dBm
BS/MS Minimum TX Power	-44 dBm	BS Antenna Gain	11 dBi
BS/MS Maximum TX Power	+21 dBm	MS Antenna Gain	0 dBi
Pathloss exponent	-3.5	Cell radius	150 m
Downlink scrambling codes per BS	1	Modulation scheme	4-QAM
Downlink OVSF codes per BS	Variable	Max new-call queue-time	5 s
Uplink scrambling codes per BS	Variable	Average inter-call time	300 s
Uplink OVSF codes per BS	Variable	Average call length	60 s
Spreading factor	16	Data/voice bit rate	Variable
User speed	1.34 m/s	Noisefloor	-100 dBm

Table 3.2: Simulation parameters of the UTRA-like CDMA based cellular network.

network resources than new calls, it is possible to reduce the number of dropped calls at the expense of an increased blocked call probability. A further advantage of the Handover Queueing System (HQS) is that during the time a handover is in the queue, previously allocated resources may become available, hence increasing the probability of a successful handover. However, in a CDMA based network the capacity is not hard-limited by the number of frequency/timeslot combinations available, like in a FDMA/TDMA based network such as GSM. The main limiting factors are the number of available spreading or OVSF codes, or the interference levels in conjunction with the restricted maximum transmit power, resulting in excessive forced termination rates. New call allocation requests were queued for up to 5 seconds, if they could not be immediately satisfied, and were blocked if the request had not been completed successfully within the 5 second.

There are several performance metrics that can be used for quantifying the quality of service provided by a cellular network. The following performance metrics have been widely used in the literature and were also advocated by Chuang *et al.* [68]:

- New Call Blocking probability, P_B,
- Call Dropping or Forced Termination probability, P_{FT},
- Probability of low quality connection, P_{low},
- Probability of Outage, P_{out},

- Grade Of Service, *GOS*.

The new call blocking probability, P_B, is defined as the probability that a new call is denied access to the network. In an FDMA/TDMA based network, such as GSM, this may occur because there are no available physical channels at the desired base station or the available channels are subject to excessive interference. However, in a CDMA based network this does not occur, and hence the new call blocking performance is typically very high.

The forced termination probability, P_{FT}, is the probability that a call is forced to terminate prematurely. In a GSM type network, an insufficiently high SINR, which inevitably leads to dropped calls, may be remedied by an intra- or inter-cell handover. However, in CDMA either the transmit power must be increased, or a soft handover must be performed in order to exploit the available diversity gain.

Again, the probability of a low quality connection is defined as :

$$\begin{aligned} P_{low} &= P\{SINR_{uplink} < SINR_{req} \text{ or } SINR_{downlink} < SINR_{req}\} \\ &= P\{min(SINR_{uplink}, SINR_{downlink}) < SINR_{req}\}. \end{aligned} \tag{3.2}$$

The GOS was defined in [68] as :

$$\begin{aligned} GOS &= P\{\text{unsuccessful or low-quality call access}\} \\ &= P\{\text{call is blocked}\} + P\{\text{call is admitted}\} \times \\ &\quad P\{\text{low signal quality and call is admitted}\} \\ &= P_B + (1 - P_B)P_{low}, \end{aligned} \tag{3.3}$$

and is interpreted as the probability of unsuccessful network access (blocking), or low quality access, when a call is admitted to the system. However, since the new call blocking probability of CDMA based networks is negligible, this metric has been omitted.

In our forthcoming investigations, in order to compare the network capacities of different networks, it was decided to use two scenarios defined as :

- A *conservative scenario*, where the maximum acceptable value for the new call blocking probability, P_B, is 3%, the maximum forced termination probability, P_{FT}, is 1%, and P_{low} is 1%.
- A *lenient scenario*, where the maximum acceptable value for the new call blocking probability, P_B, is 5%, the maximum forced termination probability, P_{FT}, is 1%, and P_{low} is 2%.

In the next section we characterise the capacity of an adaptive modulation [81] assisted, beam-steering aided TDD/CDMA system. In TDD/CDMA the mobiles suffer from interference inflicted

by the other mobile stations (MSs) both in the reference cell the MS is roaming in (intracell interference) as well as due to those in the neighbouring cells (intercell interference). Furthermore, in contrast to FDD/CDMA, where the Base Stations (BSs) transmit in an orthogonal frequency band, in TDD/CDMA there is additional interference imposed by other BSs of the adjacent cells, since all times-slots can be used in both the uplink and downlink. In return for this disadvantage TDD/CDMA guarantees the flexible utilization of all the available bandwidth, which meets the demand for the support of asymmetric uplink and downlink services, such as high data rate file download in mobile Internet services, etc. In wireless systems the link quality fluctuates due to either fading- and dispersion-induced channel impairments or as a consequence of the time-variant co-channel interference imposed by the teletraffic fluctuations due to the varying number of users supported. Owing to these impairments conventional wireless systems often drop the call. By contrast, a particular advantage of employing adaptive modulation is that the transceiver is capable of automatically reconfiguring itself in a more error-resilient transmission mode, instead of dropping the call. Here we study the achievable network performance by simulation and compare it to that of the FDD/UTRA system.

3.5.2 Performance of Adaptive Antenna Arrays aided TDD CDMA System

In this section we study the impact of adaptive antenna arrays on the network's performance. The investigations were conducted using a spreading factor of 16. Given that the chip rate of UTRA is 3.84 Mchips/sec, this spreading factor corresponds to a channel data rate of $3.84 \times 10^6/16 = 240$ kbps. Applying 1/2 rate error correction coding would result in an effective data throughput of 120 kbps, whereas utilizing a 2/3 rate error correction code would provide a useful throughput of 160 kbps. A cell radius of 150 m was assumed, and a pedestrian walking velocity of 3 mph was used.

The advanced UTRA FDD system level simulator [43] employing adaptive antenna arrays at the basestation as well as adaptive modulation [81] was extended to the UTRA TDD mode for evaluating the system's achievable performance. We observed quite significant performance gains as a direct result of the interference rejection capabilities of the adaptive antenna arrays and adaptive modulation invoked. Network performance results were obtained using two and four element adaptive antenna arrays, both in the absence of shadow fading, and in the presence of 0.5 Hz and 1.0 Hz frequency shadow fading exhibiting a standard deviation of 3 dB. The adaptive beamforming algorithm used was the Sample Matrix Inversion (SMI) algorithm [43]. The specific adaptive beamforming implementation used in our TDD/CDMA based network was identical to that used in the network simulations of [43]. Briefly [43], one of the eight possible 8-bit BPSK reference signals was used for uniquely and unambiguously identifying the desired user, while the remaining interfering users-up to seven of-them were assigned the other seven 8-bit reference signals. The received signal's autocorrelation matrix was

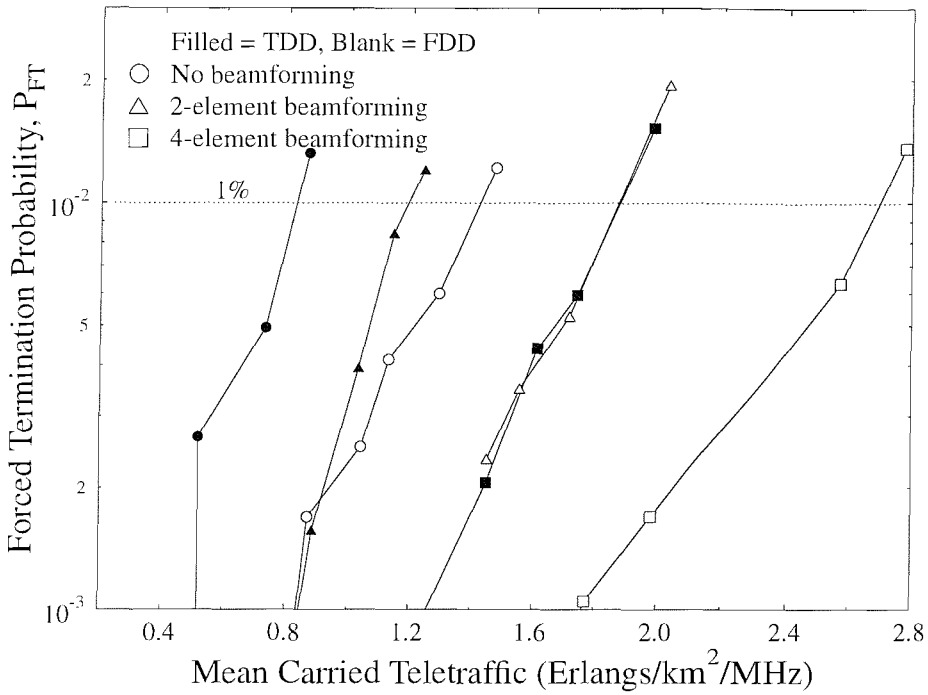

Figure 3.7: Forced termination probability versus mean carried traffic of the UTRA-like FDD and TDD/CDMA based cellular network of Table 3.2 both **with as well as without beamforming and without shadowing** for SF=16.

then calculated, and from the knowledge of the desired user's reference signal the receiver's optimal antenna array weights were determined with the aid of the SMI algorithm. This implementation of the algorithm only calculated the receiver's antenna array weights, namely the antenna array weights used by the base station for receiving the mobiles' uplink transmissions. However, it was demonstrated in [43] that further performance gains are attainable, if the BS's UL and DL array patterns, namely the transmit and receive beamforms are optimised individually. The antenna array weights were re-calculated for every power control step, i.e. 15 times per UTRA data frame, owing to the potential significant changes in terms of the desired signal and interference powers that may occur during one UTRA frame as a result of the maximum possible 15 dB change in the power transmitted by each user.

Figure 3.7 shows the forced termination probability associated with a variety of traffic loads without shadowing, measured in terms of the mean normalised carried traffic expressed in Erlangs/km^2/MHz. The figure suggests that the TDD network's performance was poor in comparison to the FDD mode both with and without employing antenna arrays at the base stations. As expected, the "No beamforming" scenario suffered from the highest forced termination probability of the three beamforming scenarios at a given traffic load, which was valid for both the TDD and FDD modes. Our discussions are focused here on the TDD mode, using FDD as the benchmark. When using "2-element beam-

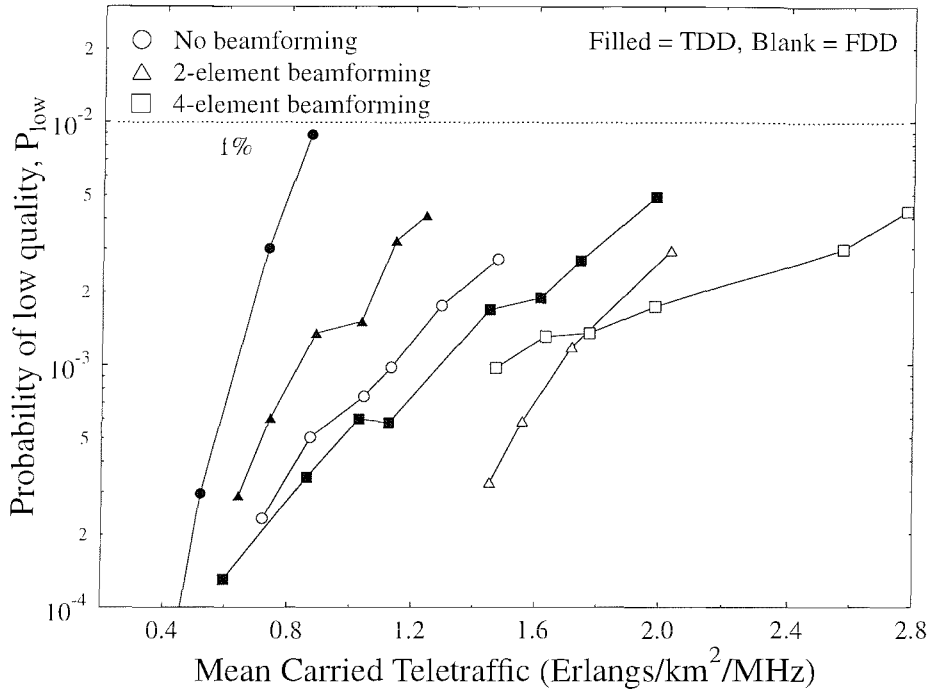

Figure 3.8: Probability of low quality access versus mean carried traffic of the UTRA-like FDD and TDD/ CDMA based cellular network both **with as well as without beamforming and without shadowing** for SF=16.

forming", the adaptive antenna arrays have considerably reduced the levels of interference, leading to a reduced forced termination probability. Without employing antenna arrays at the base stations the network capacity was limited to 142 users, or to a teletraffic load of approximately 0.81 Erlangs/km^2/MHz. However, with the advent of employing 2-element adaptive antenna arrays at the base stations the number of users supported by the network increased by 45% to 206 users, or almost to 1.18 Erlangs/km^2/MHz. Replacing the 2-element adaptive antenna arrays with 4-element arrays led to a further capacity increase of 56%, or 127% with respect to the capacity of the network using no antenna arrays. This is associated with a network capacity of 322 users, or 1.85 Erlangs/km^2/MHz. We can also see in Figure 3.7 that the capacity of the UTRA-like TDD/CDMA cellular system is significantly poorer than that of the UTRA-like FDD/CDMA system under the same propagation conditions. The "TDD 4-element beamforming" scenario has a similar performance to the "FDD 2-element beamforming" scenario. This is because the TDD system suffers from the effects of the extra inter-cell interference, which we alluded to in Section 3.4.

Figure 3.8 portrays the probability of low quality access versus various traffic loads. It can be seen from the figure that higher traffic loads were carried with the aid of the 4-element array at a sufficiently low probability of a low quality, than that achieved using a 2-element array. Again, the user-capacity of the TDD mode is often a factor two lower than that of the FDD mode close to the 1% P_{low} limit

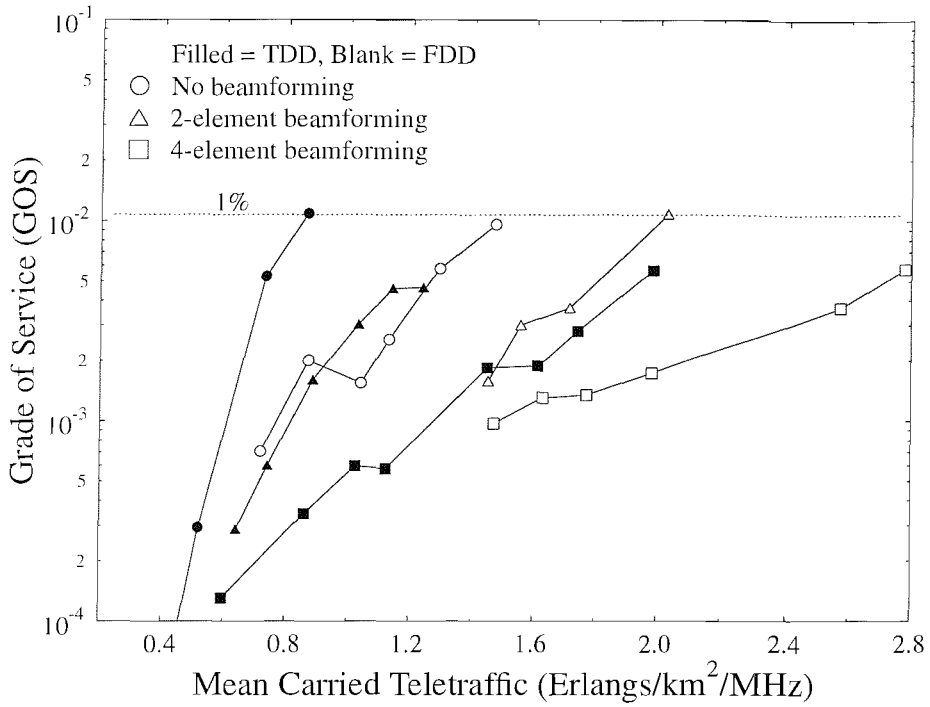

Figure 3.9: Grade-Of-Service (GOS) versus mean carried traffic of the UTRA-like FDD and TDD/CDMA based cellular network both **with as well as without beamforming and without shadowing** for SF=16.

and TDD system is more prone to rapid performance degradation. However, at lower traffic loads the FDD mode performance with four-element was worse than that using two-element. It is because in a network using adaptive antenna arrays, when new calls started, the adaptive antenna arrays are used to null the sources of interference, and the array may reduce the antenna gain in the direction of the desired user, in order to maximise the SINR. This phenomenon was more marked, when using four-element arrays since the directivity, and thus sensitivity to interfering signals is greater.

Figure 3.9 shows the achievable Grade-Of-Service for a range of teletraffic loads. Similar trends were observed regarding the probability of call blocking to those shown in Figure 3.7. The grade of service is better (i.e. lower) when the traffic load is low, and vice versa for high traffic loads. This is mainly attributable to the higher call blocking probability of the "No beamforming" scenario, particularly in the region of the highest traffic loads. As before, the TDD mode is more prone to rapid interference-level fluctuations as well as to avalanche-like teletraffic overload and its teletraffic capacity is up to a factor two lower than that of the FDD mode. Our expectation is that this performance trend may be partially mitigated with the aid of the adaptive modulation techniques of Section 3.5.3 [81], because when the instantaneous SINR is low, we activate a robust, but low-throughput modulation mode, and vice versa.

The impact of adaptive antenna arrays recorded in a propagation environment subjected to shadow

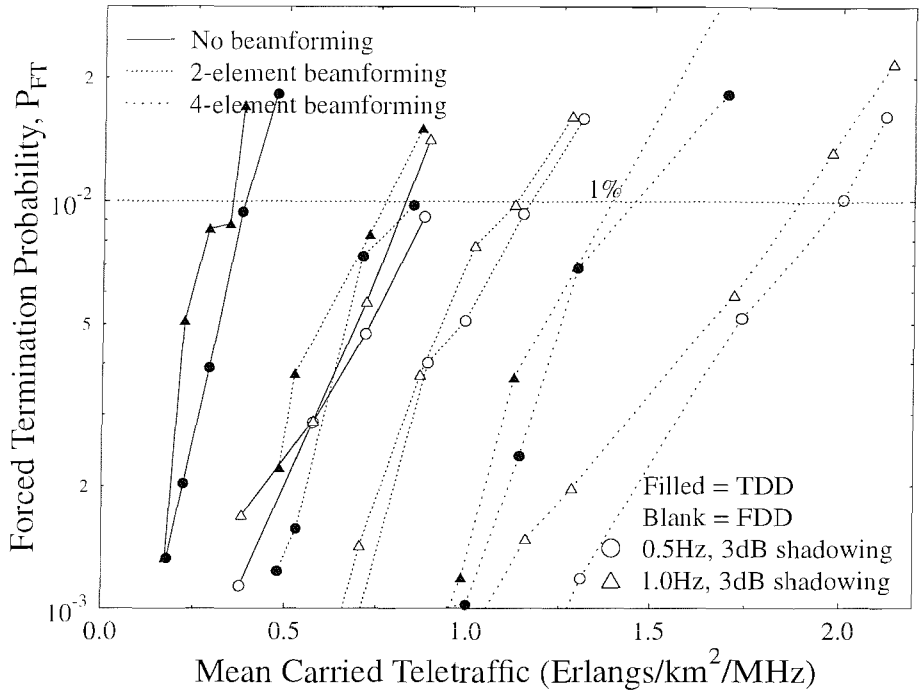

Figure 3.10: Forced termination probability versus mean carried traffic of the UTRA-like FDD and TDD/CDMA based cellular network both **with as well as without beamforming and with shadowing** for SF=16.

fading was then investigated. The associated forced termination performance is shown in Figure 3.10. This figure illustrates the substantial network capacity gains achieved with the aid of both 2- and 4-elements adaptive antenna arrays under shadow fading propagation conditions. Simulations were conducted in conjunction with log-normal shadow fading having a standard deviation of 3 dB, experiencing maximum shadowing frequencies of both 0.5 Hz and 1.0 Hz. As expected, the network capacity was reduced at the higher shadow fading frequency in both the FDD and TDD modes. Without employing adaptive antenna arrays, the TDD network supported just over 71 users and 62 users, when subjected to 0.5 Hz and 1.0 Hz frequency shadow fading, respectively. With the application of 2-element adaptive antenna arrays, these capacities increased by 111% and 113%, to 151 users and 131 users, respectively. The employment of 4-element adaptive antenna arrays led to a TDD network capacity of 245 users at a 0.5 Hz shadowing frequency, and 234 users at a 1.0 Hz shadowing frequency. This corresponded to relative gains of 62% and 78% over the capacity provided in the TDD mode with the aid of two-element adaptive antenna arrays. In comparison to the FDD benchmark we have recorded again up to a factor two lower teletraffic capacity.

The probability of low quality access performance is depicted in Figure 3.11. As expected, a given P_{low} value was associated with a higher traffic load, as the number of antenna elements increased. When the maximum shadow fading frequency was increased from 0.5 Hz to 1.0 Hz, P_{low} also increased.

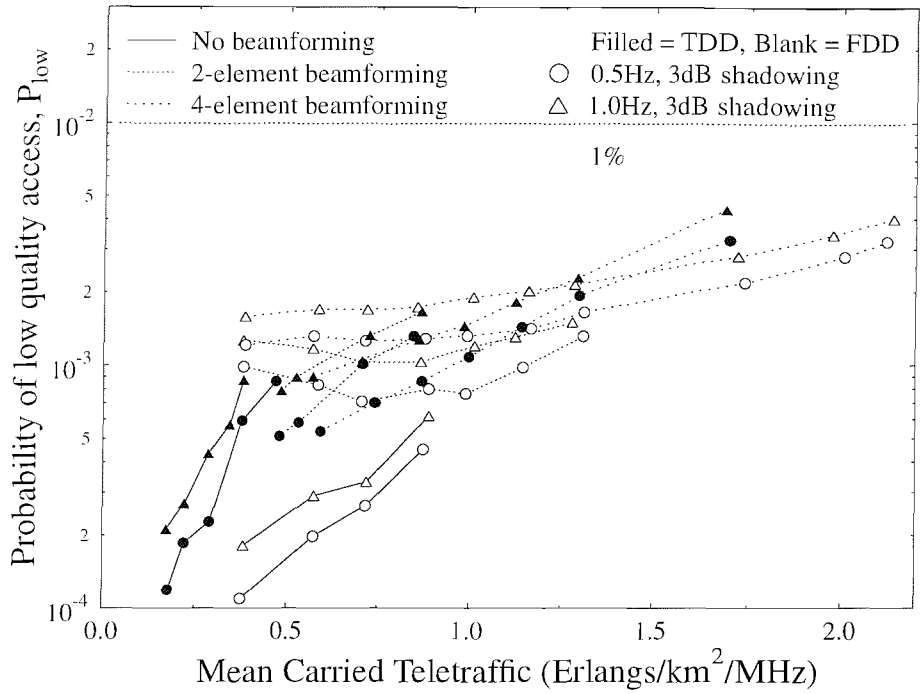

Figure 3.11: Probability of low quality access versus mean carried traffic of the UTRA-like FDD and TDD/CDMA based cellular network both **with as well as without beamforming and with shadowing** for SF=16.

The probability of low quality seen in Figure 3.11 is similar in the scenarios employing adaptive antenna arrays in the UTRA TDD and FDD CDMA systems. It should be noted, however that the probability of low quality access always remained below the 1% constraint of the conservative scenario under the scenarios studied, and the forced termination probability was considerably reduced by the adaptive antenna arrays, as it will demonstrated during our later discussion in the context of Figure 3.13. When using beamforming, the inferiority of the TDD mode was less pronounced than in the context of the previously studied performance metrics.

Figure 3.12 presents the Grade-Of-Service (GOS) for a range of teletraffice loads with and without beamforming as well as in conjunction with shadowing. A summary of the maximum network capacities of the various scenarios considered in this section both with and without shadowing having a standard deviation of 3dB, as well as with and without employing beamforming using two and four element arrays is given in Table 3.3. Throughout this section we have observed that the capacity of the TDD mode was consistently lower than that of the FDD mode owing to the fact that any timeslot may be used both in the uplink and in the downlink. In the next section we will invoke adaptive modulation as a further countermeasure for mitigating this deficiency.

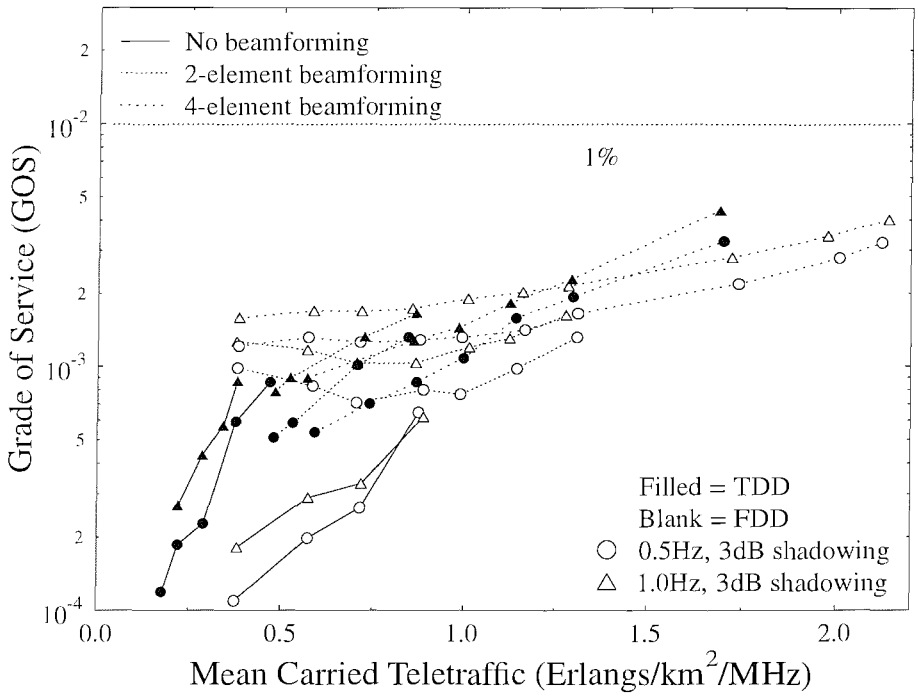

Figure 3.12: Grade-Of-Service (GOS) versus mean carried traffic of the UTRA-like FDD and TDD/CDMA based cellular network both **with as well as without beamforming and without shadowing** for SF=16.

		Conservative scenario			
		Number of Users		Traffic (Erlangs/km^2/MHz	
Shadowing	Beamforming	FDD	TDD	FDD	TDD
No	No	256	142	1.42	0.81
No	2 elements	325	206	1.87	1.18
No	4 elements	480	322	2.75	1.85
0.5 Hz, 3 dB	No	150	72	0.87	0.41
0.5 Hz, 3 dB	2 elements	203	151	1.16	0.87
0.5 Hz, 3 dB	4 elements	349	245	2.0	1.39
1.0 Hz, 3 dB	No	144	62	0.82	0.35
1.0 Hz, 3 dB	2 elements	201	131	1.12	0.75
1.0 Hz, 3 dB	4 elements	333	234	1.88	1.33

Table 3.3: Maximum mean carried traffic and maximum number of mobile users that can be supported by the FDD/TDD network, whilst meeting the conservative quality constraints. The carried traffic is expressed in terms of normalised Erlangs (Erlang/km^2/MHz), for the network described in Table 3.2 both **with and without beamforming, and also with and without shadow fading having a standard deviation of 3 dB** for SF=16. The FDD benchmark results were adopted from [43].

3.5.3 Performance of Adaptive Antenna Arrays and Adaptive Modulation TDD CDMA System

In this section we build upon the results presented in the previous section by applying Adaptive Quadrature Amplitude Modulation (AQAM) techniques [81]. The various scenarios and channel conditions to be investigated here were identical to those of the previous section, except for the application of AQAM. Since in the previous section an increased network capacity was achieved due to using independent up- and down-link beamforming, this procedure was invoked in these simulations. AQAM involves the selection of the appropriate modulation mode in order to maximise the achievable data throughput over a given channel, whilst maintaining a given target the Bit Error Ratio. More explicitly, the philosophy behind adaptive modulation is the most appropriate selection of a modulation mode according to the instantaneous radio channel quality experienced [81]. Therefore, if the SINR of the channel is high, then a high-throughput high-order modulation mode may be employed for exploiting the high instantaneous quality of the radio channel. Similarly, if the channel is instantaneously of low quality, exhibiting a low SINR, a high-order modulation mode would result in an unacceptably high BER or FER, and hence a more robust, but lower throughput modulation mode would be employed. Therefore, adaptive modulation combats the effects of time-variant channel quality, while also attempting to maximise the achieved data throughput, and maintaining a given BER or FER. In the investigations conducted, the modulation modes of the up and downlink were determined independently, thus taking advantage of the lower levels of co-channel interference on the uplink, or of the potentially higher transmit power of the base stations.The particular implementation of AQAM used in these investigations is illustrated in [43].

Comparison Figure 3.13 to Figure 3.10 shows the significant reduction in the probability of a dropped TDD call, achieved by employing adaptive antenna arrays in conjunction with adaptive modulation [43, 46] in a log-normal shadow faded environment. The figure demonstrates that even with the aid of a two-element adaptive antenna array, a substantial forced termination probability reduction was achieved. The single-antenna based TDD network was found to support 153 users, corresponding to a traffic load of 0.875 Erlang/km^2/MHz, when subjected to 0.5 Hz frequency shadow fading. The capacity of the single-antenna aided TDD network was slightly reduced to 152 users, or 0.874 Erlang/km^2/MHz, upon increasing the maximum shadow fading frequency to 1.0 Hz. Upon employing two-element adaptive antenna arrays, the TDD network capacity increased by 109% to 320 users, or to an equivalent traffic load of 1.834 Erlang/km^2/MHz, when subjected to 0.5 Hz frequency shadow fading. When the maximum shadow fading frequency was increased to 1.0 Hz, the number of users supported by the TDD network was 307, or 1.82 Erlang/km^2/MHz, representing an increase of 102% in comparison to the network refraining from using adaptive antenna arrays. It is seen in

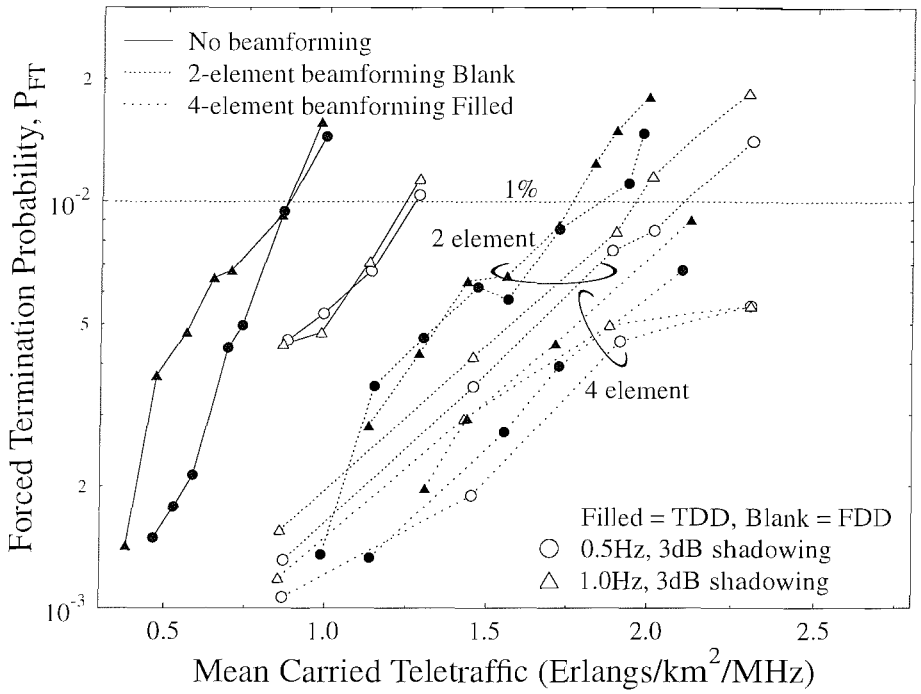

Figure 3.13: Forced termination probability versus mean carried traffic of the UTRA-like FDD and TDD/CDMA based cellular network both **with and without beamforming in conjunction with AQAM as well as with shadowing having a standard deviation of 3 dB** for SF=16.

Figure 3.13 that the forced termination probability of the UTRA-like TDD/CDMA scenarios is close to that of the FDD/CDMA scenarios, when employing adaptive antenna arrays in conjunction with adaptive modulation.

The probability of low quality outage, presented in Figure 3.14, did not benefit from the application of adaptive antenna arrays, in fact on the contrary. Furthermore, recall that Figure 3.11 depicted the probability of low quality outage without adaptive modulation, i.e. using fixed modulation, and upon comparing these results to those obtained in conjunction with adaptive modulation shown in Figure 3.14, the performance degradation owing to the employment of adaptive modulation can be explicitly seen. This is because the increase in the probability of low quality access can be attributed to the employment of less robust, but higher throughput, higher-order modulation modes invoked by the adaptive modulation scheme. Hence, under given propagation conditions and using the interference-resilient fixed 4-QAM modulation mode, as in Figure 3.11, a low quality outage may not occur. By contrast, when using adaptive modulation invoking a less resilient, but higher-throughput and higher-order modulation mode, the same propagation conditions may inflict a low quality outage.

A summary of the maximum user capacities of the FDD and TDD networks considered in this sec-

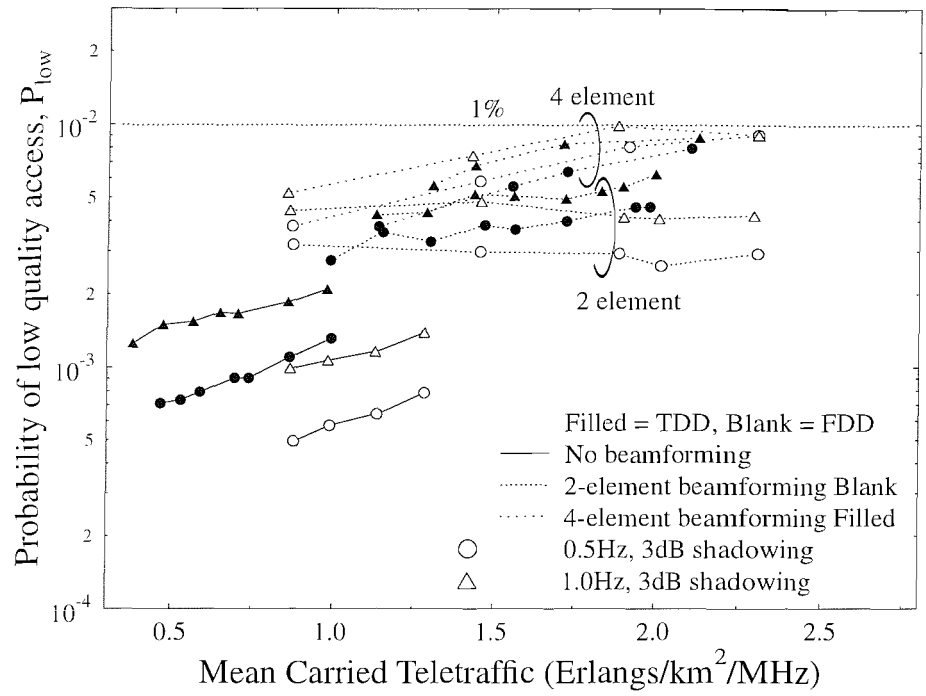

Figure 3.14: Probability of low quality access versus mean carried traffic of the UTRA-like FDD and TDD/CDMA based cellular network both **with and without beamforming in conjunction with AQAM as well as with shadowing having a standard deviation of 3dB** for SF=16.

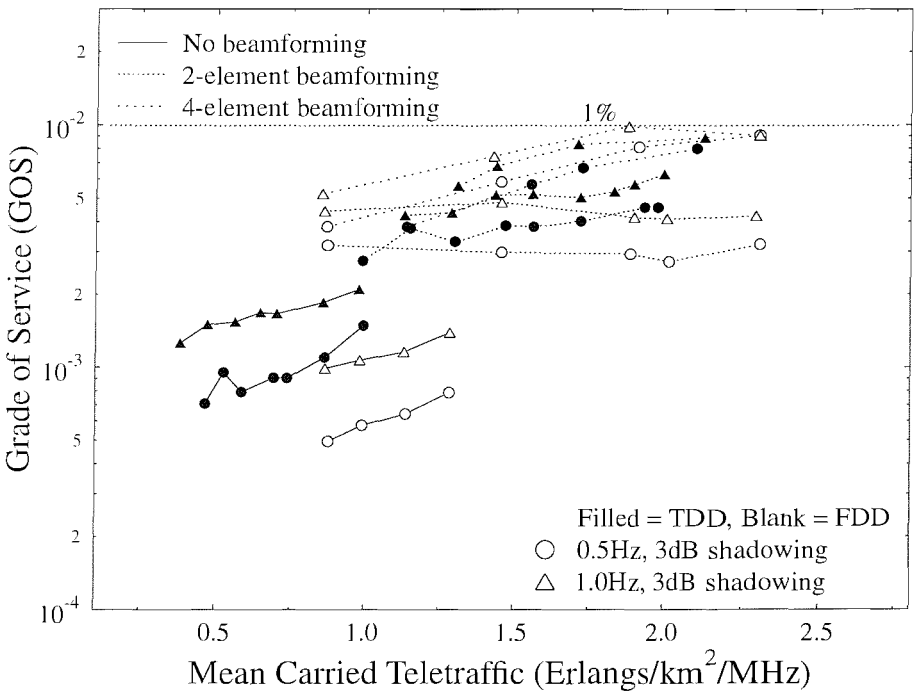

Figure 3.15: Grade-Of-Service (GOS) versus mean carried traffic of the UTRA-like FDD and TDD/CDMA based cellular network both **with and without beamforming in conjunction with AQAM as well as with shadowing having a standard deviation of 3dB** for SF=16.

tion both with and without shadowing having a standard deviation of 3dB as well as with and without employing beamforming using two and four element arrays, whilst employing adaptive modulation is given in Table 3.4.

		Conservative scenario			
		Number of Users		Traffic (Erlangs/km^2/MHz	
Shadowing	Beamforming	FDD	TDD	FDD	TDD
0.5 Hz, 3 dB	No	223	153	1.27	0.875
0.5 Hz, 3 dB	2 elements	366	320	2.11	1.834
0.5 Hz, 3 dB	4 elements	476	420	2.68	2.41
1.0 Hz, 3 dB	No	218	152	1.24	0.874
1.0 Hz, 3 dB	2 elements	341	307	1.98	1.758
1.0 Hz, 3 dB	4 elements	460	393	2.59	2.234

Table 3.4: Maximum mean carried traffic and maximum number of mobile users that can be supported by the FDD and TDD network, whilst meeting the conservative quality constraints. The carried traffic is expressed in terms of normalised Erlangs (Erlang/km^2/MHz), for the network described in Table 3.2 both **with and without beamforming, in conjunction with shadow fading having a standard deviation of 3 dB, whilst employing adaptive modulation techniques** for SF=16. The FDD benchmark results were adopted from [43].

3.6 Loosely Synchronized Spreading Code Aided Network Performance of UTRA-like TDD/CDMA Systems

3.6.1 Introduction

In this section we investigate the achievable capacity of a UTRA-like TDD/CDMA system employing Loosely Synchronized (LS) spreading codes. The family of operational CDMA systems is interference limited, suffering from Inter-Symbol-Interference, since the orthogonality of the spreading sequences is destroyed by the frequency selective channel. They also suffer from Multiple-Access-Interference owing to the non-zero cross-correlations of the spreading codes. By contrast, the family of LS codes exhibits a so-called Interference Free Window (IFW), where both the auto-correlation and cross-correlation values of the codes become zero. Therefore LS codes have the promise of mitigating the effects of both ISI and MAI in time dispersive channels. Hence, LS codes have the potential of increasing the capacity of CDMA networks. This section studies the achievable network performance in comparison

to that of a UTRA-like TDD/CDMA system using Orthogonal Variable Spreading Factor (OVSF) codes.

The air interface of UMTS supports both FDD and TDD mode [43], in order to facilitate an efficient exploitation of the paired and unpaired band of the allocated spectrum. The FDD mode is intended for applications in both macro- and micro-cellular environments, when supporting both medium data rates and high mobility. In contrast to the FDD mode, the TDD mode was contrived for environments associated with a high traffic density and asymmetric uplink as well as downlink indoor coverage. Although the UTRA/TDD mode was contrived for the sake of improving the achievable network performance by assigning all the timeslots on a demand basis to the uplink and downlink [9], this measure may result in an excessive $BS \rightarrow BS$ interference and hence in a potentially reduced number of system users [41, 107]. As seen in Figure 3.6, if BS_1 is transmitting and BS_2 is receiving at the same time in a given timeslot, $BS \rightarrow BS$ interference takes place, provided that these base stations are in adjacent cells. In [41] we demonstrated that the employment of adaptive arrays in conjunction with AQAM limited the detrimental effects of co-channel interference on the UTRA-like TDD/CDMA system and resulted in performance improvements both in terms of the achievable call quality and the number of users supported. However, in comparison to a UTRA-like FDD/CDMA system, the capacity of the UTRA-like TDD/CDMA cellular system was shown to remain somewhat poorer than that of the UTRA-like FDD/CDMA system under the same propagation conditions.

The network performance of the UTRA-like FDD/CDMA systems was quantified in our previous research [40], when supported by adaptive beam-steering [46] and LS [48] spreading codes. It was demonstrated that the network performance of a UTRA-like FDD/CDMA system employing LS spreading codes was substantially better than that of the system using OVSF codes [47]. We consider the employment of this specific family of LS spreading codes in the UTRA-like TDD/CDMA system. The LS spreading codes exhibit a so-called Interference Free Window (IFW), where the off-peak aperiodic autocorrelation values as well as the aperiodic cross-correlation values become zero. With the advent of the IFW we may encounter both zero ISI and zero MAI, provided that all the delayed asynchronous transmissions arrive within the IFW. More specifically, interference-free CDMA communications become possible, when the total time offset expressed in terms of the number of chip intervals, which is the sum of the time-offset of the mobiles plus the maximum channel-induced delay spread is within the code's IFW [49]. By employing this specific family of codes, we are capable of reducing the ISI and MAI, since users in the same cell do not interference with each other, as a benefit of the IFW provided by the LS codes used.

3.6.2 LS Codes in UTRA TDD/CDMA

There exists a specific family of LS codes [48], which exhibits an IFW, where both the auto-correlation and cross-correlation values of the codes become zero. Specifically, LS codes exploit the properties of the so-called orthogonal complementary sets [48, 58]. An example of the design of LS spreading codes can be found in [40]. In the UTRA TDD mode, the uplink and downlink timeslots are transmitted on the same carrier frequency, which creates additional undesirable and grave interference infested scenarios compared to UTRA FDD. More explicitly, as argued in the context of Figure 3.6, both transmission directions may interfere with each other, resulting in MS $\rightarrow$ MS and BS $\rightarrow$ BS interference, respectively. The interference experienced at the mobile may be divided into two categories. Firstly, interference is imposed by the signals transmitted to other mobiles from the same base station, which is known as intra-cell interference. Secondly, interference is encountered owing to the signals transmitted to other mobiles from other basestations, as well as to other basestations from other mobiles, which is termed inter-cell interference.

The instantaneous SINR is obtained upon dividing the received signal powers by the total interference plus thermal noise power, and then by multiplying this ratio by the spreading factor, SF, yielding [43]

$$SINR_{DL} = \frac{SF \cdot P_{BS}}{(1-\alpha)I_{Intra} + I_{Inter} + N_0}, \tag{3.4}$$

where $\alpha = 1$ corresponds to the ideal case of perfectly orthogonal intra-cell interference and $\alpha = 0$ to completely asynchronous intra-cell interference. Furthermore, P_{BS} is the signal power received by the mobile user from the base station, N_0 is the thermal noise, I_{Intra} is the intra-cell interference and I_{Inter} is the inter-cell interference. Again, the interference plus noise power is scaled by the spreading factor, SF, since during the despreading process the associated low-pass filtering reduces the noise bandwidth by a factor of SF. The inter-cell interference is not only due to the MSs, but also due to the BSs illuminating the adjacent cells by co-channel signals. Owing to invoking LS spreading codes in our UTRA-like TDD/CDMA system, the intra-cell interference may be completely eliminated, hence we have $\alpha = 1$. Our current research is building on our previous findings recorded in the context of a UTRA-like TDD system [41], where we found that invoking adaptive modulation as well as beam-steering proved to be a powerful means of enhancing the capacity of TDD/CDMA. In the investigations of [41], OVSF codes were used as spreading codes. However, the intra-cell interference is only eliminated by employing orthogonal OVSF codes, if the system is perfectly synchronous and provided that the mobile channel does not destroy the OVSF codes' orthogonality. In an effort to prevent intra-cell interference, again, in this section we employ LS codes, which exhibit ideal auto-correlation and cross-correlation functions within the IFW. Thereby, the "near far effect" may be significantly reduced and hence the user capacity of the system can be substantially enhanced.

Parameter	Value	Parameter	Value
Noisefloor	-100dBm	Pilot power	-9dBm
Frame length	10ms	Cell radius	78m
Multiple access	TDD/CDMA	Number of basestations	49
Modulation scheme	4QAM/QPSK	Spreading factor	16
Min BS transmit power	-48dBm	Min MS transmit power	-48dBm
Max BS transmit power	17dBm	Max MS transmit power	17dBm
Low quality access SINR	5.2dB	Outage (1% BER) SINR	4.8dB
Pathloss exponent	-2.0	Target SINR	6.2dB
Average inter-call-time	300s	Max. new-call queue-time	5s
Average call length	60s	Pedestrian speed	3mph
Max consecutive outages	5	Signal bandwidth	5MHz

Table 3.5: Simulation parameters [40].

As a benefit of the LS codes' interference resilience, it was shown in [40] that the achievable BER performance of LS codes is better than that of OVSF codes. For a spreading factor of 16, the post-despreading SINR required for maintaining a BER of 1×10^{-3} was 6.2 dB in case of LS codes, which is almost 2 dB lower than that necessitated by the OVSF codes.

3.6.3 System Parameters

The cell-radius was 78 m, which was the maximum affordable cell radius for the IFW duration of ± 1 chip intervals at a chip rate of 3.84 Mchip/s. The mobiles were capable of moving freely, at a speed of 3mph, in random directions, selected at the start of the simulation from a uniform distribution, within the infinite simulation area of 49 wrapped-around traffic cells [43]. Furthermore, the post-despreading SINRs required for obtaining the target BERs were determined with the aid of physical-layer simulations using a 4QAM modulation scheme, in conjunction with 1/2-rate turbo coding for transmission over a COST 207 seven-path Bad Urban channel [61]. Using this turbo-coded transceiver and LS codes having a spreading factor (SF) of 16, the post-despreading SINR required for maintaining the target BER of 1×10^{-3} was 6.2 dB. The BER, which was deemed to correspond to low-quality access, was stipulated at 5×10^{-3}. This BER was exceeded for SINRs falling below 5.2 dB. Furthermore, a low-quality outage was declared, when the BER of 1×10^{-2} was exceeded, which was encountered for SINRs below 4.8 dB. These values can be seen along with the other system parameters in Table 3.5. All other experimental conditions were identical to those in [43].

3.6.4 Simulation Results

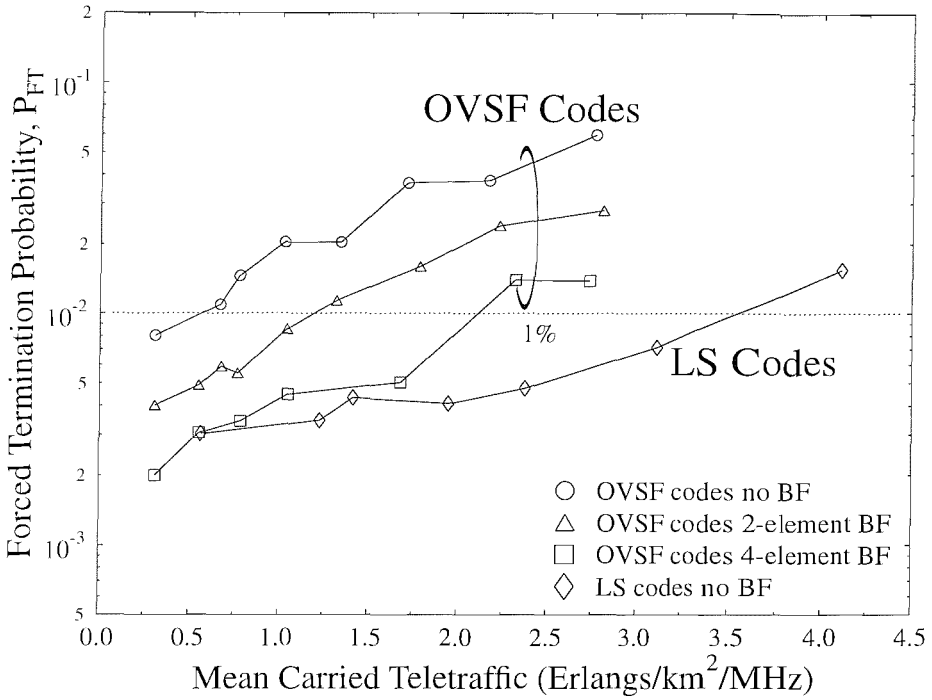

Figure 3.16: Forced termination probability versus mean carried traffic of the UTRA-like TDD cellular network using **LS codes and OVSF codes** both with as well as without beamforming in conjunction with shadowing having a frequency of 0.5 Hz and a standard deviation of 3dB for a spreading factor of SF=16.

Figure 3.16 shows the forced termination probability associated with a variety of traffic loads quantified in terms of the mean normalized carried traffic expressed in Erlangs/km^2/MHz, when subjected to 0.5 Hz frequency shadowing having a standard deviation of 3 dB. As observed in the figure, nearly an order of magnitude reduction of the forced termination probability has been achieved by employing LS spreading codes compared to those of using OVSF spreading codes. In conjunction with OVSF codes, the "No beamforming" scenario suffered from the highest forced termination probability of the four traffic scenarios characterized in the figure at a given load. Specifically, the network capacity was limited to 50 users, or to a teletraffic density of approximately 0.55 Erlangs/km^2/MHz. With the advent of employing 4-element adaptive antenna arrays at the base stations the number of users supported by the TDD system increased to 178 users, or a teletraffic density of 2.03 Erlangs/km^2/MHz. However, in conjunction with LS codes, and even without employing antenna arrays at the base stations, the TDD system was capable of supporting 306 users, or an equivalent traffic density of 3.45 Erlangs/km^2/MHz.

Figure 3.17 portrays the probability of low quality access versus various traffic loads. In conjunction

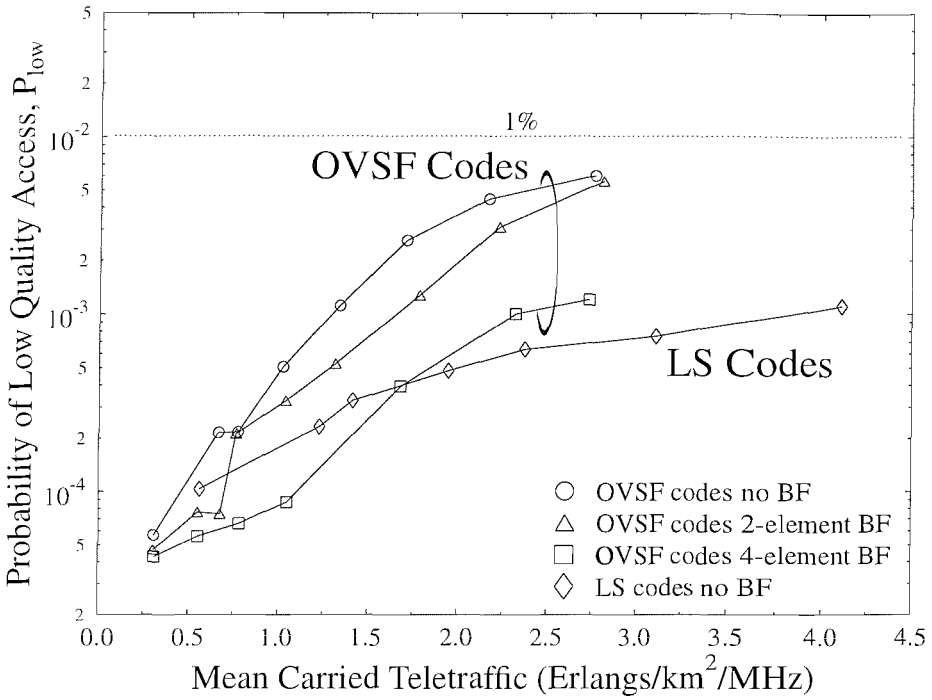

Figure 3.17: Probability of low quality access versus number of users of the UTRA-like TDD cellular network using **LS codes and OVSF codes** both with as well as without beamforming in conjunction with shadowing having a frequency of 0.5 and a standard deviation of 3dB for a spreading factor of SF=16.

with OVSF codes, it can be seen from the figure that without beamforming the system suffered from encountering more multiuser interference, as the traffic loads increased. Hence the probability of low quality access became higher. When invoking beamforming, both the intra- and inter-cell interference was reduced and hence the probability of low quality access was reduced as well. As a benefit of employing LS codes, the intra-cell interference was efficiently reduced and therefore the probability of low quality access was found to be lower even without beamforming, than that of the system using OVSF codes and employing 2-element beamforming. We also observed that at lower traffic loads the probability of low quality access for the "LS codes no BF" scheme is higher than that of "OVSF codes 4-element BF" scheme. This is a consequence of the associated high probability of forced termination for the "LS codes no BF" scheme, as shown in Figure 3.16, because the higher the probability of forced termination, the lower the number of users supported by the TDD system and hence the effects of co-channel interference imposed by the existing connections remain more benign when a new call starts.

For the sake of characterizing the achievable system performance also from a different perspective, the mean transmission power versus teletraffic performance is depicted in Figure 3.18. Again, as

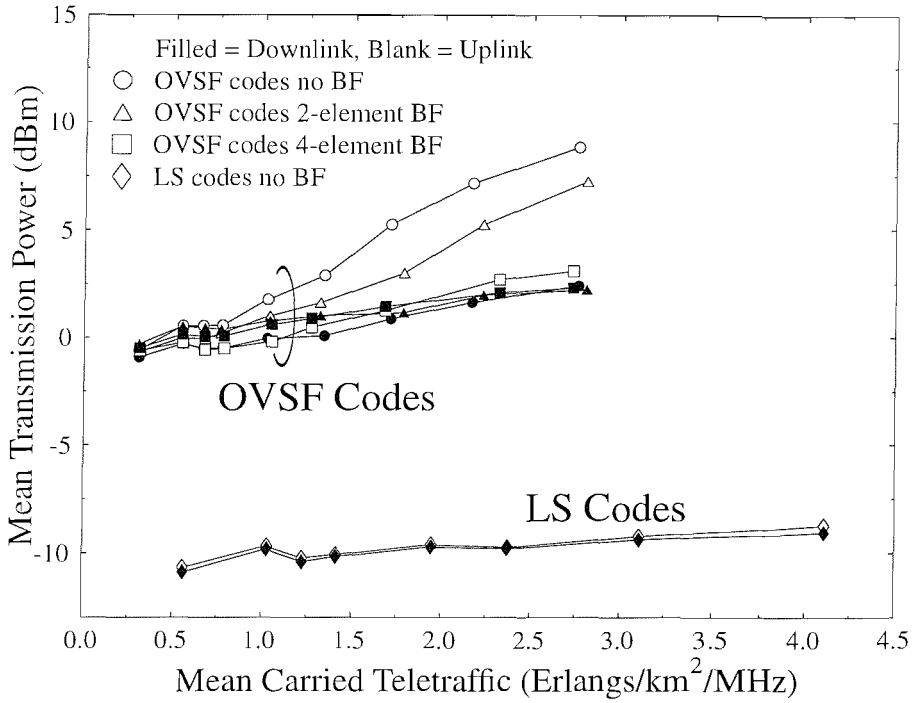

Figure 3.18: Mean transmission power versus number of users of the UTRA-like TDD cellular network using **LS codes and OVSF codes** both with as well as without beamforming in conjunction with shadowing having a frequency of 0.5 Hz and a standard deviation of 3dB for a spreading factor of SF=16.

Spreading Code	Beamforming	Users	Traffic (Erlangs /km^2/MHz)	Power (dBm) MS	BS
OVSF codes	No	50	0.55	0.54	-0.28
OVSF codes	2-elements	113	1.18	1.33	0.90
OVSF codes	4-elements	178	2.03	2.07	1.81
LS codes	No	306	3.45	-9.11	-9.21

Table 3.6: Maximum mean carried traffic and maximum number of mobile users that can be supported by the network, whilst meeting the network quality constraints of Section 3.6.3, namely $P_B \leq 3\%$, $P_{FT} \leq 1\%$, $P_{low} \leq 1\%$ and GOS $\leq 4\%$. The carried traffic is expressed in terms of normalized Erlangs (Erlang/km^2/MHz) using **OVSF codes and LS codes** in conjunction with shadow fading having a standard deviation of 3 dB and a frequency of 0.5 Hz for a spreading factor of SF=16.

a benefit of employing LS codes, both the required mean uplink and downlink transmission power are lower than that necessitated by OVSF codes. The TDD system using OVSF codes required an average 10 dBm to 20 dBm more signal power compared to the TDD system using LS codes. In [107] it was shown that the major source of interference is constituted by the BS-to-BS interference as a consequence of the BS's high signal power and the near-LOS propagation conditions prevailing between BSs. Even though the employment of LS codes can only reduce the intra-cell interference, it results in a substantial reduction of the BSs' power consumption, as shown in Figure 3.18. Hence the source of $BS \rightarrow BS$ inter-cell interference was also reduced. In other words, the employment of LS codes indirectly reduced the severe $BS \rightarrow BS$ inter-cell interference by keeping the BSs' transmission power at a low level.

Figure 3.19 shows the achievable Grade-Of-Service for a range of teletraffic loads. We observe similar trends regarding the probability of low quality access, as shown in Figure 3.17. In Equation 2.8, the GOS performance is jointly determined by P_B and P_{low}, which is interpreted as the probability of unsuccessful network access (blocking), or the probability of encountering a low quality, provided that a call is admitted to the system. The employment of the LS codes may cause the shortage of spreading codes and hence may lead to the blocking of a new call, since there are only 8 LS codes that can be used, when the IFW duration is ± 1 chip-length. The call duration and inter-call periods were Poisson distributed having the mean values shown in Table 3.5. When encountering this call arrival distribution, we observe that the new call blocking probability is negligible, as shown in Figures 3.17 and 3.19.

A summary of the maximum user capacities of the UTRA-like TDD/CDMA system using OVSF codes and LS codes in conjunction with log-normal shadowing having a standard deviation of 3dB and a shadowing frequency of 0.5 Hz as well as both with and without beamforming is given in Table 3.6. The teletraffic carried and the mean mobile and base station transmission powers required are also shown in Table 3.6.

3.6.5 Summary and Conclusions

In this section we studied the network performance of a UTRA-like TDD/CDMA system employing LS spreading codes. The computer simulation results provided showed that the TDD system invoking LS codes had a better performance compared to the system using OVSF codes. We designed a 49-cell "wrapped around" simulation area, constituted by sufficiently small 78 m radius cells, which guaranteed that the delayed asynchronous transmissions arrive within the IFW, where the auto-correlation and cross-correlation values of the LS codes became zero and hence eliminated the effects of intra-cell interference. The SINR required by the LS codes for the sake of maintaining a BER

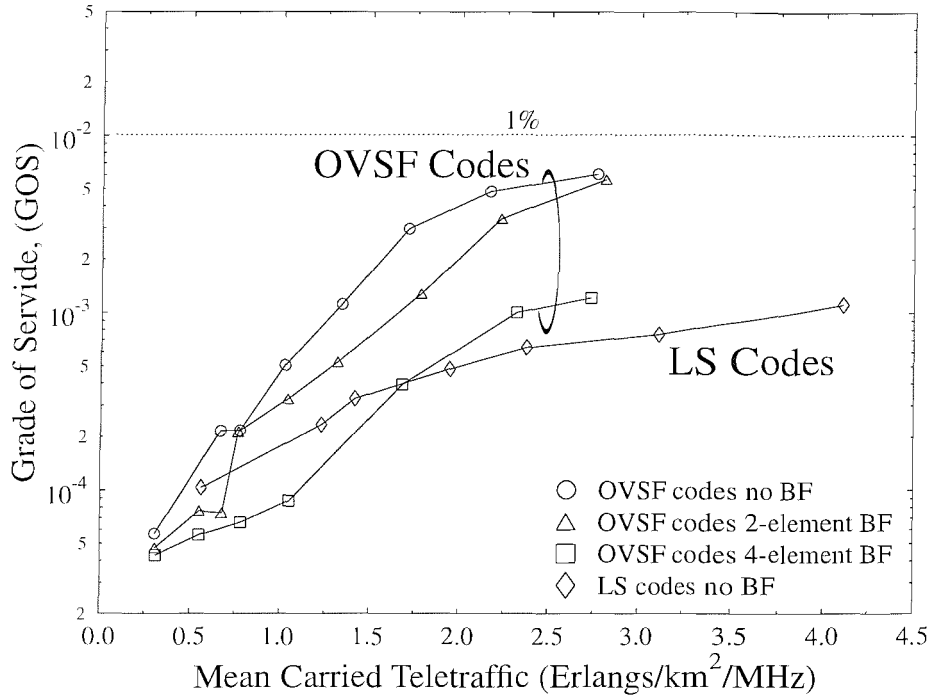

Figure 3.19: Grade-Of-Service (GOS) versus number of users of the UTRA-like TDD cellular network using **LS codes and OVSF codes** both with as well as without beamforming in conjunction with shadowing having a frequency of 0.5 Hz and a standard deviation of 3dB for a spreading factor of SF=16.

of 1×10^{-3} was almost 2 dB lower than that necessitated by the OVSF codes. Furthermore, a low mobile and base station transmission power has been maintained. Hence the average intra- and inter-cell interference level has become low, the severe $BS \rightarrow BS$ interference has been reduced and this resulted in TDD system performance improvements both in terms of the achievable call quality and the number of users supported. Our future research is focussed on further improving the performance of TDD systems using genetic algorithm based timeslot scheduling.

Chapter 4

The Effects of Power Control and Hard Handovers on the UTRA TDD/CDMA System

4.1 A Historical Perspective on Handovers

The terminology of handover [108] is synonymous in mobile communications to the process of transferring a MS from one BS or channel to another. It is typically initiated by experiencing a degraded signal quality in the current cell. Handovers may be divided into two broad categories, namely hard handovers and soft handovers, which are also often characterized informally by the terms 'break before make' and 'make before break', respectively. Therefore, in the context of hard handovers, the current transmission resources are released before the new resources are reserved, while in soft handovers, both the existing and new resources are engaged in the handover process. Poorly designed handover schemes may generate very heavy signaling traffic, hence potentially imposing a dramatic QoS degradation. The increasing interest and mass-market for mobile communications as well as the limited available spectrum has motivated the employment of cellular architectures based on small cells. As a result, the number of mobile users crossing the cell boundaries is increased and hence the resultant handover rate is also increased. Therefore the efficiency of handover algorithms is expected to play a crucial influence on the overall system performance [109–112]. This suggests that efficient handover algorithms constitute a cost-effective way of enhancing both the capacity and the QoS in cellular systems.

The radio propagation environment and the related handover algorithms are different in different cellular systems [113, 114]. Hence a particular handover algorithm endowed with a specific set of

parameters cannot perform equally well in different communication scenarios [115]. First- and second-generation cellular systems provide wide-area coverage even in cities using macro-cells [116–122]. The brief history of handover algorithms designed for cellular systems is summarized in Table 4.1.

4.2 Hard Handover in UTRA-like TDD/CDMA Systems

The UTRA network supports different types of HandOvers (HO), where the handover control procedure may be divided in the following types [90]:

- **Intra-system handover** [**127, 128**] occurring within a UTRA system, which can be further subdivided into
  - **Intra-frequency handovers** [**129**] between cells using to the same UTRA carriers,
  - **Inter-frequency handovers** [**14**] between cells employing different UTRA carriers.
- **Inter-system handover** [**130,131**] taking place between cells belonging to two different Radio Access Technologies (RAT) or different Radio Access Modes (RAM). The most typical case of inter-system HO is expected to take place between UTRA [43] and GSM/EDGE systems [88]. A typical example of inter-RAM HO is likely to take place between the UTRA FDD [43] and UTRA TDD [43] modes.

Furthermore, the following handover procedures can be identified [90]:

- **Hard handovers** [**132, 133**] represent a family of HO procedures, where the old radio link of a MS is released, before the new radio link is established. For real-time interactive voice-type bearers this hard HO procedure implies encountering a brief disconnection of the bearer. By contrast, for non-interactive data-type bearers hard HOs appear to be seamless. Invoking soft handovers is also a design option for the TDD mode, as suggested in [134]. Soft handovers improve the quality of service, since a diversity gain is provided by combining the signals received from both links [117]. However, being engaged in communications with two BSs introduces more interference [135], since in the TDD mode portrayed in Figure 3.6 a number of gravely detrimental interference scenarios may exist. The interference imposed is typically higher, if the network is asynchronous [136] or if the neighbouring cells carry different asymmetric traffic loads [23, 83, 91, 107]. Furthermore, in the UTRA system the legitimate spreading factor range of the FDD mode is 4 to 256 in the uplink and 4 to 512 in the downlink, while in the TDD mode the corresponding range is 1 to 16 in both the uplink and downlink [50, 137], as seen in Table 3.1. Hence soft handovers carried out in the TDD mode would need two of the 16 spreading codes,

Year	Author	Contribution
1992	Tekinay and Jabbari [121]	Studied the performance of non-preemptive priority queueing for handover calls.
1993	Vijayan and Holtzman [113]	A handover algorithm based on signal strength measurements made by the MSs in a lognormal fading environment was proposed.
1994	Viterbi, Gilhousen and Zehavi [117]	The effect of handover techniques on cell coverage and uplink capacity was investigated in a CDMA system.
1995	Nakano, Umeda and Ohno [118]	A BS-diversity aided handover algorithm was proposed for high capacity DS-CDMA cellular systems.
1996	Kim, Lee and Chin [119]	An adaptive handover algorithm taking into account the velocity of mobile stations was proposed.
1997	Calin and Zeghlache [122]	An analytical model characterizing a non-preemptive priority queueing system incorporating both voice and data users was proposed.
1998	Wong and Cox [120]	A handoff algorithm using pattern recognition was proposed.
1999	Benvenuto and Santucci [123]	A least squares path-loss estimation approach to handover algorithms was proposed.
2000	Santucci, Pratesi, Ruggieri and Graziosi [124]	A range of statistical parameters used in the performance analysis of a relative signal strength based handover algorithm.
2001	Yang, Ghaheri-Niri and Tafazolli [125]	The performance of power-triggered and E_c/N_0-triggered soft handover algorithms designed for UTRA was investigated.
2002	Wang, Sridhar and Green [126]	An adaptive soft handover algorithm using the location information of mobile stations was proposed.
2003	Wang, Liu and Cen [114]	Handover algorithms designed for a dynamic spreading aided WCDMA multimedia system were proposed.
2004	Lugara, Tartiere and Girard [115]	Inter-system handover algorithms supporting both UMTS and GSM were proposed.

Table 4.1: Contributions on handover algorithms designed for cellular systems.

because the communications between the MS and the serving as well as target BSs would have to take place concurrently via two air interface channels for distinguishing the signals [50] arriving from the serving and target BSs. This may be expected to severely limit the number of users supported. Hence hard handovers constitute a more appropriate solution for a TDD CDMA system, despite having no diversity gain.

- **Soft handovers [125, 138–140] and softer handovers [141, 142]** constitute a category of HO procedures in which a MS maintains at least one radio link all the time, typically establishing a new link to the target BS, before relinquishing the previous link. More explicitly, during soft HO the MS is simultaneously controlled by two or more BSs of the same or different Radio Network Controllers (RNC). Softer HOs constitute a special case of soft HOs, where the radio links that are added and removed belong to co-located BSs managed by the same BS controller. Soft and softer HOs are only possible, when using the same carrier frequency.

4.2.1 Relative Pilot Power Based Hard Handover

The UTRA TDD/CDMA system supports both inter-system HOs and intra-system HOs. All these handovers are mobile-assisted hard HOs and hence their philosophy is clearly different from that of the UTRA FDD mode, since in the latter protocol structure has been designed to support soft HOs. The generic HO procedure is typically described in four phases [143]: the related signal-quality measurements, HO initiation, HO decision and HO execution. A range of signal-quality related parameters, such as the received power, bit error rate and the MS's distance can be evaluated and processed as the related HO criteria. It is anticipated that the UTRA TDD system's hard HO is likely to be predominantly MS assisted HO, where the MS performs signal-quality measurements that are signalled to the RNC that makes the actual HO decisions. The conception of efficient HOs is one of the main challenges in UTRA TDD/CDMA networks, since it has a substantial impact on the system's performance and capacity. The philosophy of soft HO and macro diversity cannot be utilized in the TDD mode, since the active target BS set size is always equal to one during the HO procedure [144]. This is because handovers in the UTRA TDD mode are hard handovers, where the MS is connected to one basestation only [83].

In our simulations, we rely on a single radio access technology or a single radio access mode, hence we only consider intra-system hard HOs. Again, hard HOs cause a temporary disconnection of real-time interactive access bearers, but they appear to be seamless for non-interactive bearers. The hard HO algorithm used is based on the relative[1] pilot power of E_c/I_o in the serving cell and in the

[1]The reason for using a relative rather than absolute pilot power based hard HO procedure is, because it was found in [43] that in some cell areas all pilot signals may be weak, while in other locations they all may be strong, and this

neighbouring cells, where a minimum E_c/I_o handover margin is used as a threshold for preventing repetitive hard HOs between cells [50,145]. A hard HO can be processed when the following condition is satisfied [90]:

$$E_c/I_{o(serving\ cell)} + E_c/I_{o(margin)} < E_c/I_{o(new\ cell)}, \tag{4.1}$$

where $E_c/I_{o(serving\ cell)}$ is the average relative pilot power of the serving cell, while $E_c/I_{o(new\ cell)}$ is the average pilot power of the best potential target cell. The parameter $E_c/I_{o(margin)}$ is the margin by which the E_c/I_o value of the best HO-target cell has to exceed the E_c/I_o value of the serving cell, before the hard handover is activated. The so-called HO *acceptance threshold* T_{acc} and call *drop threshold* T_{drop} are the corresponding hard HO thresholds, where a HO is enabled and the call is dropped, respectively. Again, a relative rather than absolute received pilot power scheme is used in our investigations, which exhibits performance benefits in realistic propagation environments exposed to shadow fading [43]. The relative hard HO thresholds T_{acc} and T_{drop} are expressed in terms of dB, which are normalized to the received pilot strength E_c/I_o of the best potential neighbouring HO target cell. Again, when the E_c/I_o value of the best neighbouring HO target cell exceeds the E_c/I_o value of the serving cell, the hard HO may be enabled, provided that it is necessary due to the serving cell's signal quality degradation. Hence the relative *acceptance threshold* T_{acc} is set to 0 dB, which implies that the best neighbouring cell can be accepted as a candidate HO target cell for hard HO, provided that it has at least as high a pilot power as the serving cell. The call *drop threshold* T_{drop} is the $E_c/I_{o(margin)}$ value shown in Equation 4.1. When the received signal quality of the serving cell degrades and hence the relative pilot power E_c/I_o of the serving cell becomes by at least T_{drop} dB lower than the E_c/I_o value of the HO candidate cell, the hard handover will be activated.

4.2.2 Simulation Results

In this section the effect of having a hysteresis in the TDD system's hard HO candidate/active BS set update procedure is evaluated. The appropriate choice of the handover hysteresis threshold is critical for the sake of achieving an attractive tradeoff between the transmit power required for supporting the handover process and seamless call continuity [146]. Having a low HO hysteresis threshold would enable a mobile user to capture and register a larger number of pilots, hence creating a high number of potential target BSs, but if they tend to provide a relatively low signal quality, the undesirable 'ping-pong' effect of switching back and forth between calls may not be avoided. On the other hand, an excessive HO hysteresis threshold would practically eliminate the 'ping-pong' effect, hence reducing the

phenomenon may generate either too many or too few potential target HO cells. This potential deficiency may be overcome by normalizing the pilot powers of the potential HO target cells to that of the serving cell or to those of the other BSs in the active BS set, which allows the inclusion of at least one target HO BS.

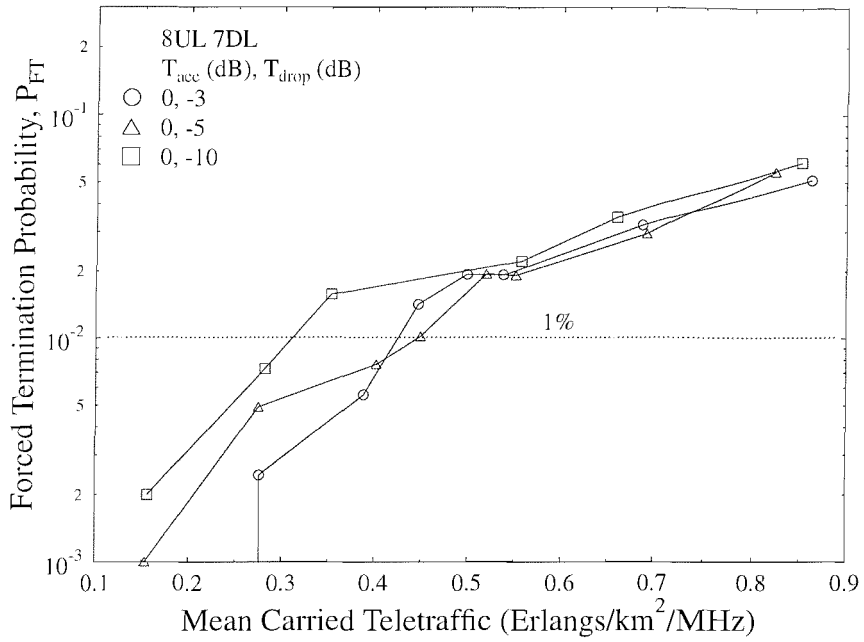

Figure 4.1: Forced termination probability versus mean carried traffic of the UTRA-like TDD/CDMA based cellular network with shadowing and using **relative received pilot power, E_c/I_o,** based hard-HO thresholds in conjunction with **a near-symmetric traffic load of 8:7 (UL:DL) timeslots.** The system parameters are summarized in Table 4.2.

HO-related signaling, but this is achieved at the risk of not finding any better-quality BSs. This would consequently generate an excessive call dropping rate. Three different traffic scenarios are studied, namely having a near-symmetric UL:DL traffic load of 8:7 timeslots, UL-dominated asymmetric traffic loads and DL-dominated asymmetric traffic loads.

Parameter	**Value**	**Parameter**	**Value**
Cell radius	150 m	Noisefloor	-100 dBm
Chip rate	3.84 Mcps	Spreading factor	16
BS/MS Minimum TX Power	-44 dBm	BS/MS Maximum TX Power	+21 dBm
Modulation scheme	4-QAM	Pathloss exponent	-3.5
Target E_b/N_o	8.0 dB	Low Quality (LQ) Outage E_b/N_o	7.0 dB
Outage E_b/N_o	6.6 dB	Handover margin	3,5,10 dB

Table 4.2: Parameters used for the hard handover investigations.

4.2.2.1 Near-Symmetric UL/DL Traffic Loads

The forced termination performance at the near-symmetric traffic load ratio of 8:7 (UL:DL) timeslots is shown in Figure 4.1, illustrating that reducing the absolute value of the HO threshold T_{drop} to -3 dB and -5 dB improved the forced termination performance compared to $T_{drop} = -10$ dB, in particular at low traffic loads. The reduced force termination probability is a benefit of handing over to potential target BSs earlier, without jeopardizing terminating the call. This phenomenon is also evident in Figure 4.2, which shows the probability of a low quality outage versus mean the carried teletraffic of a UTRA-like TDD/CDMA based cellular network carrying a near-symmetric traffic load of 8:7 (UL:DL). However, the reduction of the absolute value of T_{drop} from -10 to -3 dB led to increasing the number of handover events, as shown in Figure 4.3. This is predictable, since having higher hysteresis requires a higher received pilot power from the neighbouring HO target cells to be selected. Consequently, the rate of active BS set update becomes lower, leading to an increased average BS and MS transmission power, as shown in Figure 4.4. The increased BS and MS transmission power results in an increased co-channel interference level, and hence in a higher probability of outage associated with a low call quality. It was observed in Figure 4.3 that the number of handover events started to reduce, when the traffic loads exceeded 0.6 Erlang/km^2/MHz in Figure 4.3. This is a consequence of the associated high forced termination probability, as seen in Figure 4.1. This phenomenon ultimately led to the reduction of the number of supported users, while most users also suffered from experiencing a high level of interference.

4.2.2.2 Asymmetric Traffic loads

In this section the effects of both uplink-dominated as well as downlink-dominated asymmetric traffic loads on the achievable teletraffic performance are examined, while using different hard handover hysteresis thresholds.

Figures 4.5 and 4.6 demonstrate that the system's forced termination probability was improved, when T_{drop} was adjusted from -10 dB to -3 dB. It is observed in Figure 4.6 that when carrying predominantly downlink traffic loads associated with a traffic load ratio of 1:14 (UL:DL) the system benefitted more from reducing the absolute value of the hard HO hysteresis from -10 dB to -3 dB compared to the predominantly uplink traffic load scenario of 13:2 (UL:DL) timeslots, as seen in Figure 4.5. A carried traffic improvement of 0.2 $Erlangs/km^2/MHz$ was achieved in the 1:14 (UL:DL) timeslot scenario, which is twice as high as the performance gain observed in the 13:2 (UL:DL) scenario, when the handover hysteresis was reduced from -10 dB to -5 dB.

This is because the higher the handover hysteresis, the slower the handover process and hence a

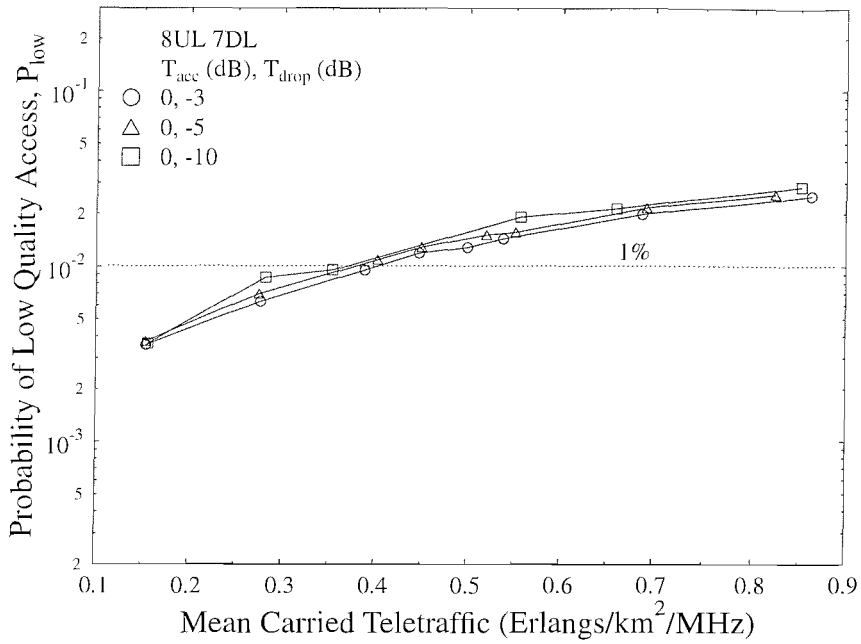

Figure 4.2: Probability of low quality access versus mean carried traffic of the UTRA-like TDD/CDMA based cellular network with shadowing and using **relative received pilot power,** E_c/I_o, based hard-HO thresholds in conjunction with **a near-symmetric traffic load of 8:7 (UL:DL) timeslots.** The system parameters are summarized in Table 4.2.

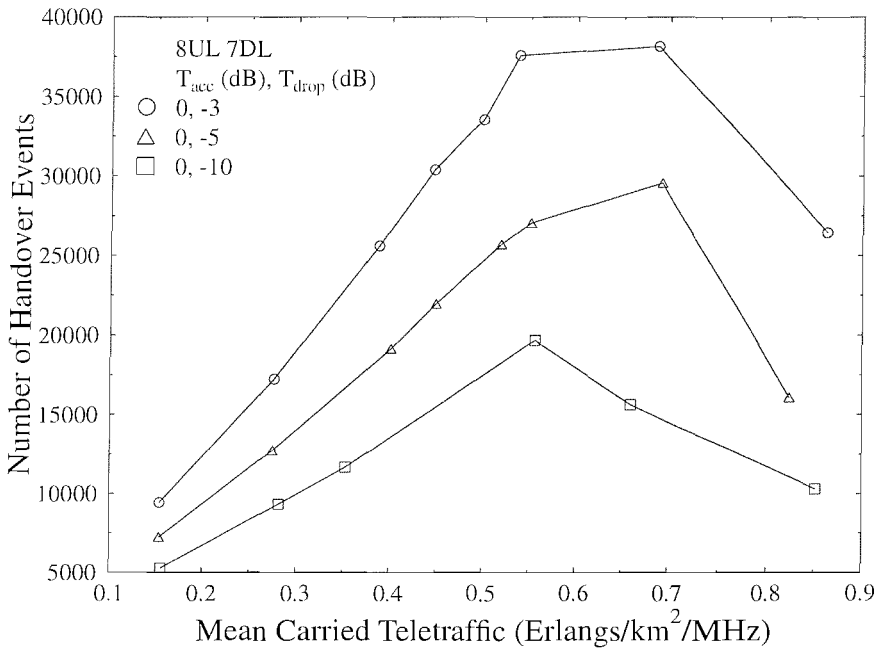

Figure 4.3: Number of handover events per 49-cell simulation area versus mean carried traffic of the UTRA-like TDD/CDMA based cellular network with shadowing and using **relative received pilot power,** E_c/I_o, based hard-HO thresholds in conjunction with **a near-symmetric traffic load of 8:7 (UL:DL) timeslots.** The system parameters are summarized in Table 4.2.

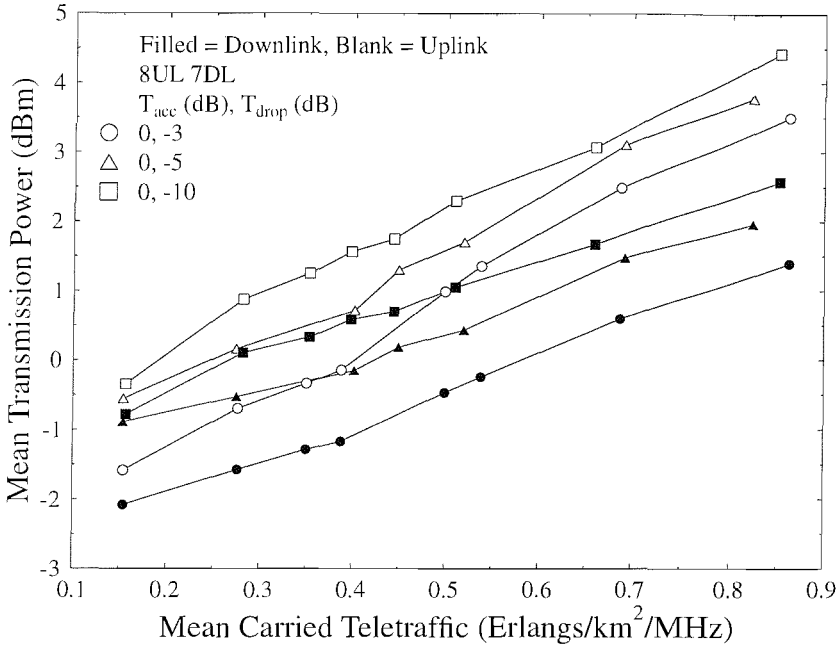

Figure 4.4: Mean BS and MS transmission power versus mean carried traffic of the UTRA-like TDD/CDMA based cellular network with shadowing and using **relative received pilot power,** E_c/I_o, based hard-HO thresholds in conjunction with **a near-symmetric traffic load of 8:7 (UL:DL) timeslots.** The system parameters are summarized in Table 4.2.

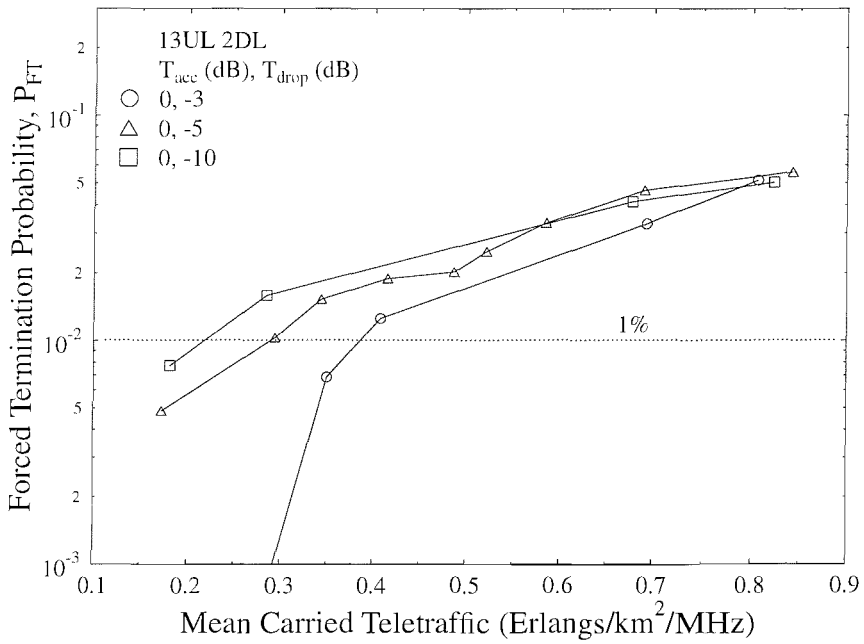

Figure 4.5: Forced termination probability versus mean carried traffic of the UTRA-like TDD/CDMA based cellular network with shadowing and using **relative received pilot power,** E_c/I_o, based hard-HO thresholds in conjunction with **an asymmetric traffic load of 13:2 (UL:DL) timeslots.** The system parameters are summarized in Table 4.2.

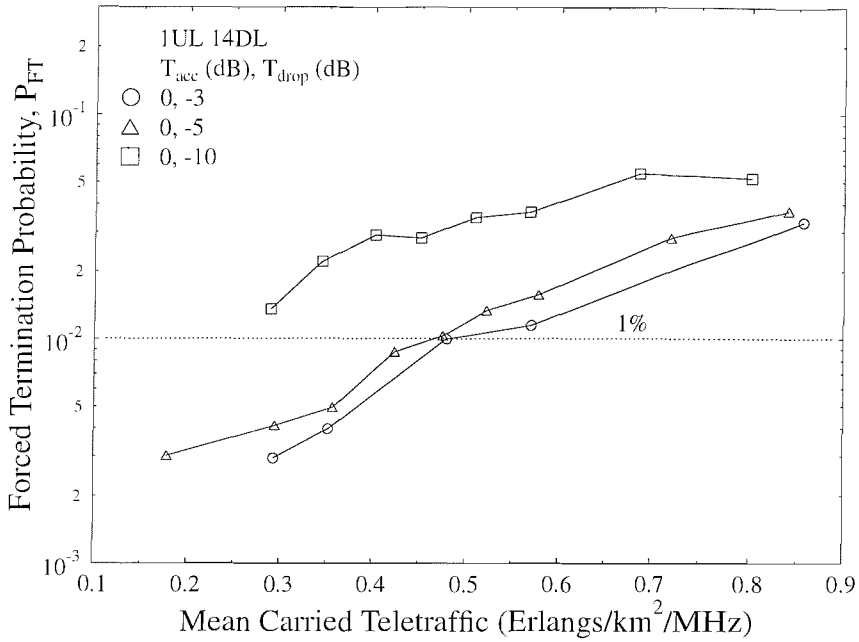

Figure 4.6: Forced termination probability versus mean carried traffic of the UTRA-like TDD/CDMA based cellular network with shadowing and using **relative received pilot power,** E_c/I_o, based hard-HO thresholds in conjunction with **an asymmetric traffic load of 1:14 (UL:DL) timeslots.** The system parameters are summarized in Table 4.2.

forced termination event may occur, before the hard-HO can be completed owing to the insufficiently high signal power received from the serving basestation. More explicitly, during the hard-HO process, the mobile station tends to recede from the serving basestation and approaching the HO target basestation. The received pilot signal level of the serving basestation may gradually reduce, while the received pilot signal level of the HO target basestation may be increased, as shown in Figure 4.7. The SINR of the mobile station was gradually reduced as it receded from the serving basestation. When the received pilot power approaches $T_{drop} = -10\ dB$, the SINR is often already below the outage SINR, before the mobile can be handed over to the HO target basestation, hence the call is likely to be terminated, as shown in Figure 4.7. However, still considering the same special case, if we have $T_{drop} = -5\ dB$, the mobile station may have been handed over to the HO target basestation, before the SINR degraded further and the call was terminated. For a predominantly downlink traffic load of 1:14 (UL:DL) timeslot scenario, most of the terminated calls encountered during the hard handover process occurred owing to encountering a poor uplink connection quality, which is typically caused by the routinely incurred severe BS to BS interference of the UTRA TDD mode. Only when the UL/DL TS allocation of the interfering cells is the as same as that of the serving cell, can the BS to BS interference be avoided, since in this scenario the serving BS is not receiving during the interfering BS's transmit TS. However, for the predominantly downlink traffic load of 1:14 (UL:DL) a grave BS

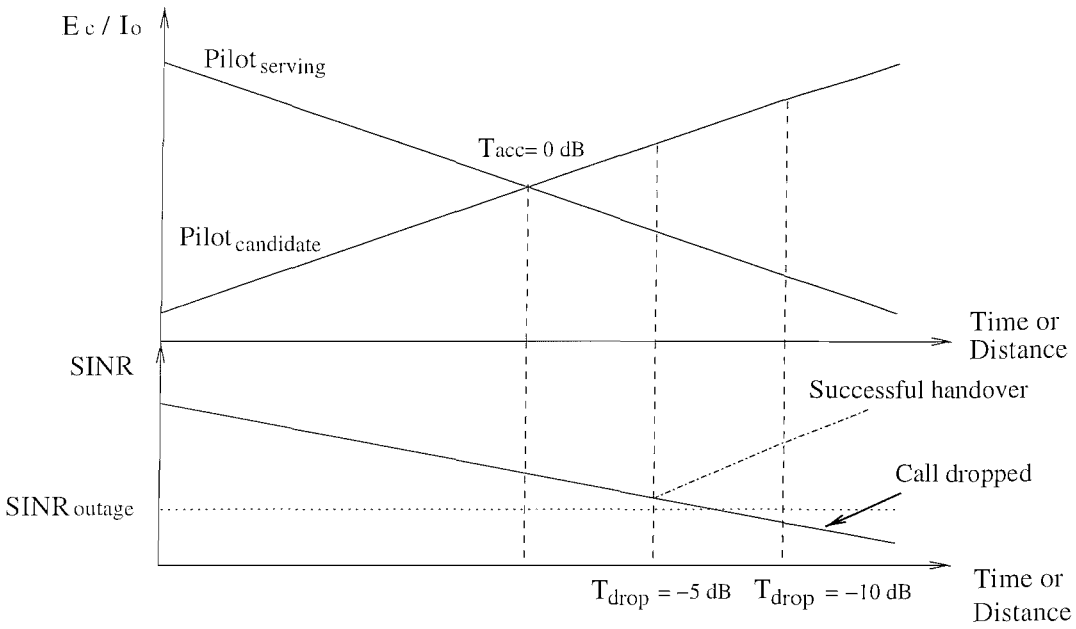

Figure 4.7: The hard-handover process in the UTRA/TDD CDMA system.

to BS interference is encountered with a probability of 93.33% = 14/15, when a mobile user invoking a hard HO is transmitting in a serving cell's uplink timeslot, since in the interfering cell 14 downlink timeslots out of the total 15 timeslots may be inflicting interference. For the predominantly uplink traffic load of 13:2 (UL:DL), the probability of BS to BS interference occurring is 13.33% = 2/15, when a mobile user invoking a hard HO is transmitting in a serving cell's uplink timeslot, and only two downlink timeslots may be contaminated by the BS to BS interference. Hence carrying a predominantly downlink traffic load is more beneficial, since it allows us to reduce the handover hysteresis, which in turn reduces the call dropping probability, as seen in Figure 4.6.

Figures 4.8 and 4.9 portray the probability of low quality access versus various traffic loads. It is observed that the specific choice of the HO hysteresis T_{drop} does not significantly affect the probability of low quality access. Similar trends were found for various traffic loads. The low quality access performance associated with predominantly uplink traffic loads is poorer than that recorded for predominantly downlink traffic loads. This is because the specific uplink and donwlink timeslot allocation is random in every cell and leads to a randomly fluctuating interference load for each timeslot. In case of closed-loop power control [147], it is difficult to accurately adjust the power level, if the received interfering signal is uncorrelated between timeslots. We will provide more detailed justifications for this issue in the next section.

The number of handover events recorded across the entire 49-cell simulation area is shown in Figures 4.10 and 4.11, illustrating that reducing the absolute value of the hard-HO hysteresis threshold T_{drop} leads to a higher number of handover events, which is beneficial in terms of reducing the call dropping probability. However, as a penalty, the associated HO signalling traffic is increased and a

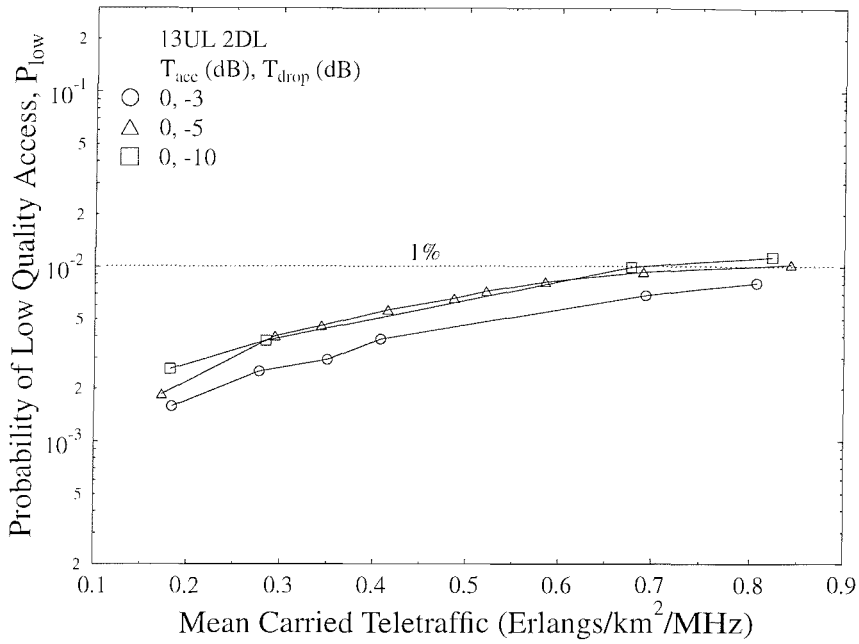

Figure 4.8: Probability of low quality access versus mean carried traffic of the UTRA-like TDD/CDMA based cellular network with shadowing and using **relative received pilot power,** E_c/I_o, based hard-HO thresholds in conjunction with **an asymmetric traffic load of 13:2 (UL:DL) timeslots.** The system parameters are summarized in Table 4.2.

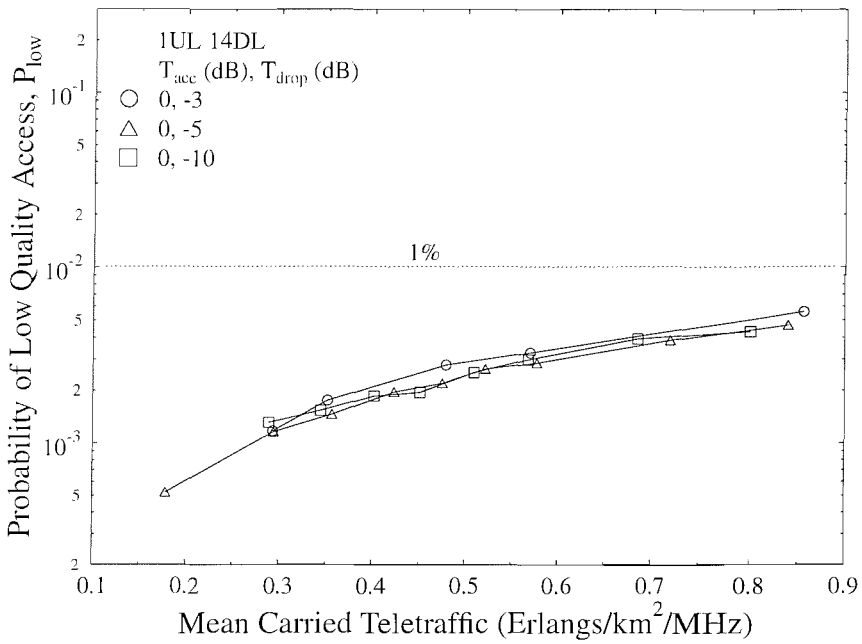

Figure 4.9: Probability of low quality access versus mean carried traffic of the UTRA-like TDD/CDMA based cellular network with shadowing and using **relative received pilot power,** E_c/I_o, based hard-HO thresholds in conjunction with **an asymmetric traffic load of 1:14 (UL:DL) timeslots.** The system parameters are summarized in Table 4.2.

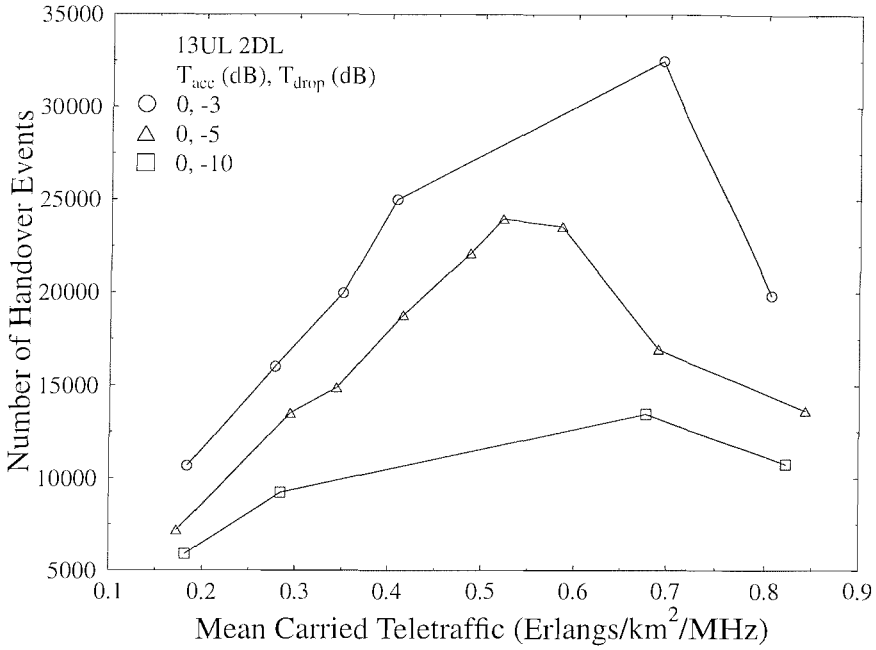

Figure 4.10: Number of handover events per 49-cell simulation area versus mean carried traffic of the UTRA-like TDD/CDMA based cellular network with shadowing and using **relative received pilot power,** E_c/I_o, based hard-HO thresholds in conjunction with **an asymmetric traffic load of 13:2 (UL:DL) timeslots.** The system parameters are summarized in Table 4.2.

higher proportion of the call duration is spent in the process of hard-HO. From the perspective of the radio resource management, a high number of handover events will decrease the overall available resources, since the control channels of both the serving basestations and the HO target basestations are more likely to be engaged by the mobile stations in handover [148, 149]. Having a high handover hysteresis also results in high BS and MS power consumption. The serving basestation and the mobile station have to increase their transmission powers in an effort to maintain the SINR value required for sustaining the current connection quality during the process of hard handover, as depicted in Figures 4.12 and 4.13. For example, it may be inferred from Figure 4.12 and 4.13 that a 7 dB increase of the hysteresis threshold T_{drop} results in an average transmission power increase of 1.5 dBm for both the basestation and mobile station.

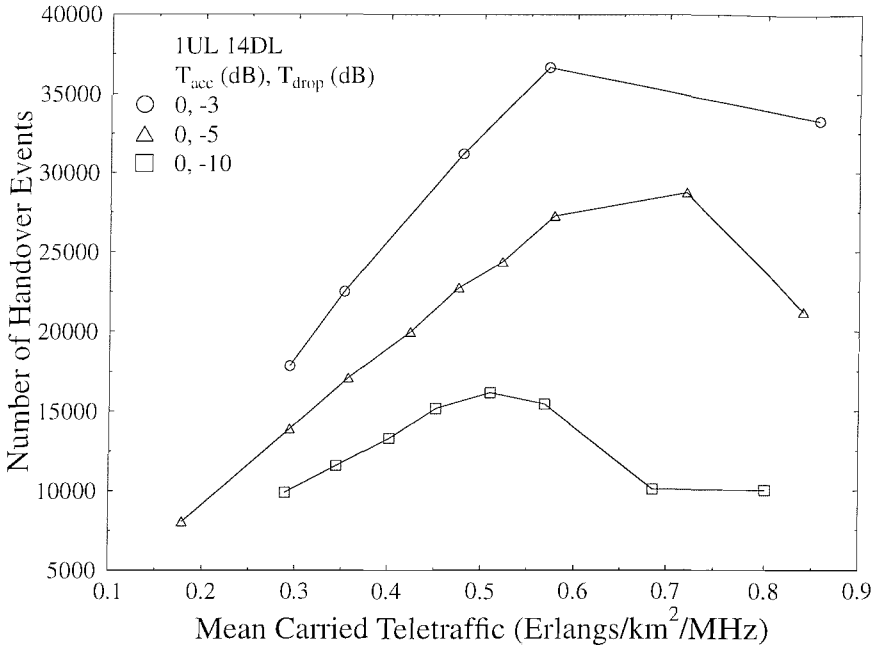

Figure 4.11: Number of handover events per 49-cell simulation area versus mean carried traffic of the UTRA-like TDD/CDMA based cellular network with shadowing and using **relative received pilot power,** E_c/I_o, based hard-HO thresholds in conjunction with **an asymmetric traffic load of 1:14 (UL:DL) timeslots.** The system parameters are summarized in Table 4.2.

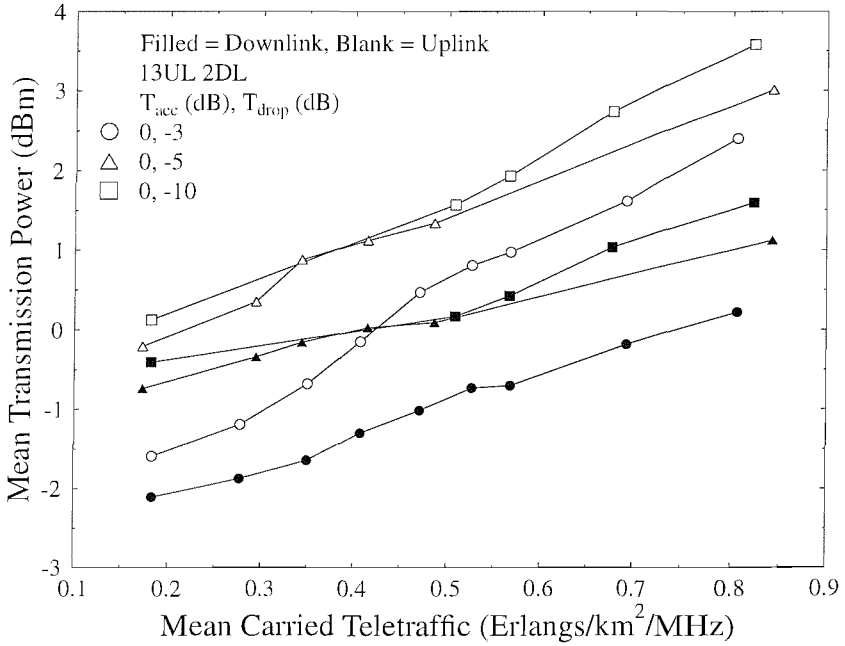

Figure 4.12: Mean transmission power versus mean carried traffic of the UTRA-like TDD/CDMA based cellular network with shadowing and using **relative received pilot power,** E_c/I_o, based hard-HO thresholds in conjunction with **an asymmetric traffic load of 13:2 (UL:DL) timeslots.** The system parameters are summarized in Table 4.2.

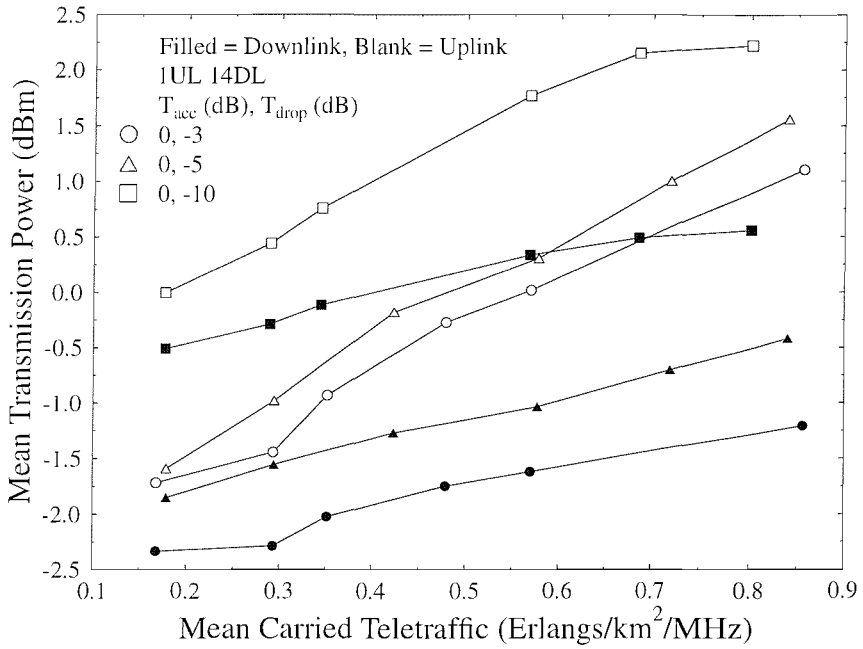

Figure 4.13: Mean transmission power versus mean carried traffic of the UTRA-like TDD/CDMA based cellular network with shadowing and using **relative received pilot power,** E_c/I_o, based hard-HO thresholds in conjunction with **an asymmetric traffic load of 1:14 (UL:DL) timeslots.** The system parameters are summarized in Table 4.2.

4.3 Power Control in UTRA-like TDD/CDMA Systems

Agile and accurate power control is one of the key factors predetermining the attainable performance of the UTRA TDD/CDMA system, where all users share the same frequency. The power control regime has a vital influence on controlling the interference. Without power control a MS roaming in the vicinity of the BS and transmitting at an excessive power may overwhelm mobiles that are at the cell edge, a phenomenon which is often referred to as the near-far problem [150–153]. It is essential to keep the transmission power at the minimum level ensuring adequate signal quality at the receiver end. Power control may be classified as open-loop power control, inner-loop power control sometimes also referred to as closed-loop power control and outer-loop power control, all of which may be used in both the UL and DL [50].

The preferred solution to power control in the UTRA FDD/CDMA system is based on the philosophy of inner-loop power control or fast closed-loop power control in both the UL and DL. In the UL the BS generates frequent estimates of the received SINR and compares it to the target SINR required for maintaining the quality of a specific service. If the measured SINR is higher than the target SINR, the BS will instruct the MS to decrease its power. This measure-instruct-react cycle is executed at a rate of 1500 times per second (1.5 kHz) for each mobile station and thus operates faster than any significant change of path loss could possibly happen. In fact, typically it is even faster than the typical Doppler frequency of fast Rayleigh fading for low to moderate mobile speeds. Hence closed-loop power control will prevent any power inbalance among all the uplink signals received at the base station.

In the DL the same closed-loop power control is used as in the UL. However, there is no near-far problem due to the one-to-many broadcast-type transmission scenario in the DL. All the signals received by the MS within a specific traffic cell originate from the same BS transmitting to all MSs. The motivation of using closed-loop power control in the DL is firstly to provide the minimum amount of additional power to mobile stations roaming at the cell edge, since they suffer from increased inter-cell interference. Secondly, closed-loop DL power control is capable of enhancing the signals attenuated by Rayleigh fading with the aid of transmitting an additional power with the aim of augmenting the action of error-correcting methods [50].

4.3.1 UTRA TDD Downlink Closed-loop Power Control

As argued in the previous section, the aim of the UTRA TDD downlink power control scheme is to limit the effects of interference. The transmitter typically uses a signal quality based power control on the DL [147]. Closed-loop power control facilitates for the BS transmitter to adjust the power in response

to the MS's specific request. Downlink closed-loop power control is based on SIR measurements at the MS receiver and the corresponding Transmit Power Control (TPC) commands are generated by the MS. The power control step size determines the change in the DL power in response to a TPC message received from the MS, where the legitimate DL power steps are 1, 2 and 3 dB [147].

The inter-cell interference encountered is not only due to the MSs, but also due to the BSs contaminating the adjacent cells by co-channel signals. The DL closed-loop power control adjusts the MSs' transmit power in order to maintain the DL SINR near the SINR target, namely near $SINR_{target}$. As discussed in Section 4.2, the handovers in the UTRA TDD mode are based on hard handovers [50]. The mobile communicates with a single BS, and only one TPC command will be received in each DL timeslot. When we have $SINR_{DL} > SINR_{target}$, the TPC command is set to 0, otherwise, if $SINR_{DL} < SINR_{target}$, then the TPC command is set to 1. When the MS receives a TPC command, the MS is instructed to power down or up according to the 'stepsize' typically expressed in dB. The tolerance of the transmit power and the highest average rate of change in code domain power according to the power control stepsize shall be within the range shown in Table 4.3 [147].

Stepsize	**Tolerance**	**Range of average rate of change in code domain power per 10 steps**	
		Minimum	**Maximum**
1 dB	± 0.5 dB	± 8 dB	± 12 dB
2 dB	± 0.75 dB	± 16 dB	± 24 dB
3 dB	± 1 dB	± 24 dB	± 36 dB

Table 4.3: TDD DL Power Control Stepsize Tolerance [147]

DL TPC commands	**Tolerance**		**Range of average rate of change in code domain power per 10 steps**	
	Lower	**Upper**	**Lower**	**Upper**
For powering up	+ 0.5 dB	+ 1.5 dB	+ 8 dB	+ 12 dB
For powering down	- 0.5 dB	- 1.5 dB	- 8 dB	- 12 dB

Table 4.4: FDD DL Power Control Tolerance for the 1 dB-Stepsize Mode [154]

For the sake of comparison, Table 4.4 shows the tolerance of the code domain power and the highest average rate of change in the UTRA FDD mode in conjunction with a power stepsize of 1 dB [154]. Upon comparing Tables 4.3 and 4.4, it can be seen that the tolerance and range of power control is the same in the FDD and TDD modes. However, the power control agility of the TDD and FDD modes is

different. In the FDD mode, there may be 15 dB power change across a 15-timeslot, 10 ms FDD frame. By contrast, in the TDD mode the achievable power control agility in the DL depends on the ratio of the number of UL/DL timeslots. To maintain the maximum possible flexibility, while facilitating closed-loop power control whenever deemed useful, the Synchronization CHannel (SCH) has two TSs per 15-timeslot, 10 ms TDD frame for DL transmission in cellular usage, which corresponds to the most extreme uplink asymmetry of TS allocation having a ratio of 2:13 DL:UL allocation. On the other hand, at least one TS has to be allocated for the UL transmission of the Random Access CHannel (RACH), which corresponds to a maximum DL asymmetry of 14:1 (DL:UL). The procedure of carrying out one power control step requires a pair of UL and DL TSs. Then a TPC command is transmitted in an UL TS, when the received signal power evaluated during the previous DL TS has to be adjusted. Hence the TDD power control rate in the DL ranges from 100 Hz to 700 Hz, corresponding to having access to 1...7 DL TSs. The ability to support asymmetric UL/DL capacity allocations is the most attractive feature of the TDD mode. However, the TDD mode imposes a problem in terms of the associated low power control rate. Hence the MS may require a relatively high BS transmitted power, when the mobile suffers from experiencing a high level of interference or when it enters a building, which substantially attenuates the signal power received from the BS. This phenomenon may also lead to a high call dropping probability, when the BS is unable to satisfy the MS's received power requirement owing to the relatively low power-control agility of the TDD mode. For example, in the FDD mode a 15 dB power change can be achieved within a 15-timeslot 10 ms frame, if the power control stepsize is 1 dB. By contrast, in the TDD mode a 15 times longer duration corresponding to 15 frames and 150 ms may be needed for the extreme DL asymmetry of 14:1 (DL:UL) TS allocation. A dropped call would be encountered, when there are five consecutive 10 ms frames having an SINR value below the target SINR value. For the above-mentioned extreme asymmetric TDD traffic situation, after requesting a power increase in five consecutive frames only 5 dB power change has been achieved, potentially requiring a further $10\ dB = 15\ dB - 5\ dB$ powering up, which eventually leads to this connection being terminated owing to having an insufficiently high received power level. One possible option of compensating for this relatively slow feedback loop is using a higher power control stepsize. In the 3GPP initiative [155], using 2 bits for the TPC command was proposed for the DL, allowing for a more flexible power control stepsize adjustment, ranging from 1 to 3 dB. Hence we could adjust the power control stepsize commensurately with the difference between the measured and target SINR, namely according to $\Delta SINR$:

$$\Delta SINR = |SINR_{target} - SINR_{DL}|. \tag{4.2}$$

The relationship between the stepsize and $\Delta SINR$ is shown in Table 4.5 based on Table 4.3 and the 3GPP initiative [156]. Using a flexible power control stepsize adjustment is a desirable feature in the

UTRA system's TDD mode due to the associated reduced power control feedback rate. However, a higher power control stepsize may impose a possible increase of the interference level inflicted upon other MSs in both the same as well as in the adjacent cells. In Section 4.3.3 we will provide a comparative study of using a 1 dB fixed power control stepsize and a flexible power control stepsize in order to investigate the achievable system performance, when invoking a higher PC stepsize.

Stepsize (dB)	**ΔSINR (dB)**	**The number of TPC bits needed**
+ 1	$0 < \Delta SINR \leq 1.5$	1
+ 2	$1.5 < \Delta SINR \leq 2.75$	2
+ 3	$2.75 < \Delta SINR \leq 4$	2
+ 4	$4 < \Delta SINR \leq 5.25$	3
+ 5	$5.25 < \Delta SINR \leq 6.5$	3
+ 6	$6.5 < \Delta SINR \leq 7.75$	3
. . .		
- 1	$1 < \Delta SINR \leq 2.5$	1
- 2	$2.5 < \Delta SINR \leq 3.75$	2
- 3	$3.75 < \Delta SINR \leq 5$	2
- 4	$5 < \Delta SINR \leq 6.25$	3
- 5	$6.25 < \Delta SINR \leq 7.5$	3
- 6	$7.5 < \Delta SINR \leq 8.75$	3
. . .		

Table 4.5: Closed-loop Power Control Stepsizes

4.3.2 UTRA TDD Uplink Closed-loop Power Control

Closed-loop power control may also be used in the UTRA TDD mode's 1.28 $Mchip/s$ option [156]. The uplink closed-loop power control is used to set the power of both the uplink Dedicated Physical Control CHannel (DPCH) and Physical Common Packet CHannel (PCPCH). Both the SINR measurement and power adjustment phase of the UTRA TDD UL closed-loop PC scheme is similar to that described in Section 4.3.1.

4.3.3 Closed-loop Power Control Simulation Results

In this section the effects of the closed-loop power control stepsize on the UTRA TDD/CDMA system's performance was studied. As we have discussed in Section 4.3.1, the asymmetric teletraffic load of

the UTRA TDD mode results in a potentially lower power control rate compared to the FDD mode. The slow feedback loop of the power control command may lead to calls being terminated due to the insufficiently high transmitted power [157]. The limited TPC command feedback rate can be compensated by an appropriate stepsize selection, since it is possible to use three different power control stepsizes in the UTRA TDD mode [155], as we have seen in Table 4.3. In our simulations both the symmetric and asymmetric traffic loads of the UTRA-like TDD/CDMA system are studied. Both the uplink and downlink use closed-loop power control. Three different power control stepsize algorithms are used in our simulations, namely:

- Fixed power control stepsize of 1 dB, 1 TPC bit is needed;
- Flexible power control stepsize of 1 dB to 3 dB, 2 TPC bits are needed;
- Flexible power control stepsize of 1 dB to 6 dB, 3 TPC bits are needed.

The stepsizes of the UL/DL commands and the required number of TPC bits are presented in Table 4.5 for each legitimate scenario.

4.3.3.1 UL/DL Symmetric Traffic Loads

For a near-symmetric traffic load, we used an 8:7 (UL:DL) TS allocation ratio in each 15-slot TDD frame, where the eight UL TSs and seven DL TSs are allocated randomly in each TDD frame. Hence the achievable power control rate is 700 Hz, allowing a 7 dB power correction range during the 15 slots of a 10 ms frame. Figure 4.14 portrays the forced termination probability versus mean carried traffic of the UTRA-like TDD/CDMA based cellular network in conjunction with the above-mentioned symmetric traffic load of 8:7 (UL:DL). It may be observed that the system's achievable traffic load did not benefit from invoking an adaptive PC stepsize in the scenario considered, in fact, it performed slightly worse compared to using a fixed 1 dB PC stepsize. The reason for this observation will be outlined below. For the "PC Stepsize 1 dB" scenario of Figure 4.14, the TDD system was capable of supporting 78 users at $P_{FT} = 1\%$, corresponding to a teletraffic density of 0.46 Erlang/km^2/MHz. The "Adaptive PC Stepsize 1 dB to 3 dB" and "1 dB to 6 dB" scenario of the TDD network was found to support 73 users and 70 users, corresponding to a normalized traffic load of 0.42 Erlang/km^2/MHz and 0.40 Erlang/km^2/MHz, respectively. The percentage of forced call terminations entirely deemed to be due to encountering an insufficiently high signal power-rather than due to violating any of the other performance requirements-within the total number of forced termination scenarios was found to be zero, although this is not explicitly demonstrated here. This is because for the near-symmetric traffic scenario considered, the TDD system was capable of

maintaining a relatively high power control feedback rate of 700 Hz, which prevented the calls from being dropped due to experiencing an insufficiently high signal power. This is why the adaptive power control stepsize adjustment algorithm failed to improve the achievable system performance.

Parameter	**Value**	**Parameter**	**Value**
Cell radius	150 m	Noisefloor	-100 dBm
Chip rate	3.84 Mcps	Spreading factor	16
BS/MS Minimum TX Power	-44 dBm	BS/MS Maximum TX Power	+21 dBm
Modulation scheme	4-QAM	Pathloss exponent	-3.5
Target E_b/N_o	8.0 dB	Low Quality (LQ) Outage E_b/N_o	7.0 dB
Outage E_b/N_o	6.6 dB	Handover margin	5 dB
Power control SINR hysteresis	1 to 6 dB		

Table 4.6: Parameters used for the simulation of the power control.

Figure 4.15 characterizes the mean transmission power versus mean carried traffic of the UTRA-like TDD/CDMA based cellular network. It may be observed in the figure that using the adaptive PC stepsize based algorithm required on average 0.1 dBm to 0.5 dBm more signal power as the traffic load became higher, which is the reason that invoking the adaptive PC stepsize based algorithm slightly degraded the overall carried traffic load of a near-symmetrically loaded TDD system, as shown in Figure 4.14. The higher PC stepsize based algorithm resulted in an increased average transmission power, which increased the system's interference level and led to the degradation of the TDD system's carried traffic.

Figure 4.16 portrays the probability of low quality access versus various traffic loads, where most of the connections appear to have a poor call quality. Even though the system is capable of potentially achieving 0.46 $Erlang/km^2/MHz$ normalized traffic density when judged purely on the basis of the 1% forced termination probability shown in Figure 4.14, the overall system's carried traffic is reduced to 0.27 $Erlang/km^2/MHz$, when considering the probability of low quality access, as shown in Figure 4.16. This is because the closed-loop power control algorithm is unable to sufficiently accurately compensate for the SINR variations imposed by the dynamically fluctuating timeslot allocations of the basestations. It was observed that the probability of low quality access is the limiting factor of the overall system throughput, rather than the forced termination probability values shown in Figure 4.14.

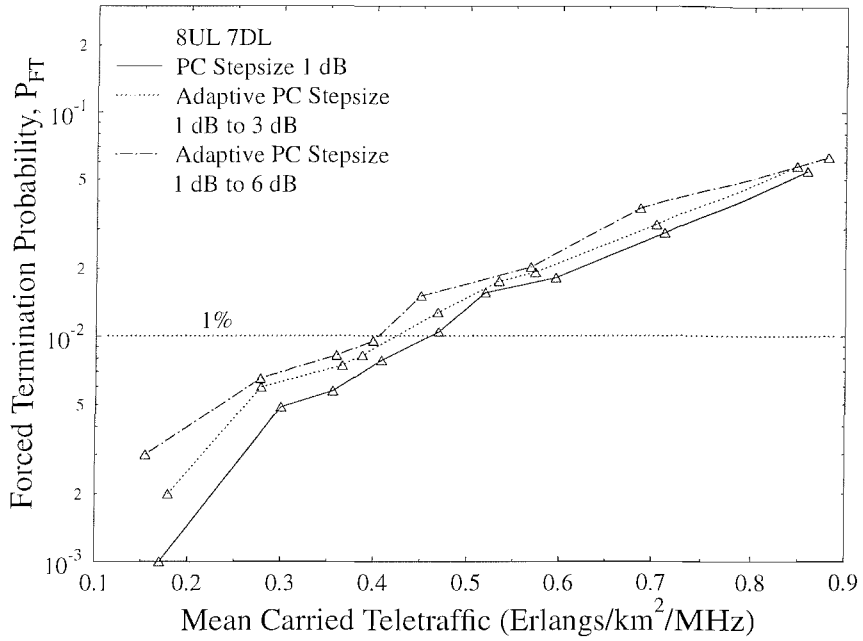

Figure 4.14: Forced termination probability versus mean carried traffic of the UTRA-like TDD/CDMA based cellular network with shadowing and using various closed-loop PC schemes in conjunction with **a near-symmetric traffic load of 8:7 (UL:DL) timeslots.** The system parameters are summarized in Table 4.6.

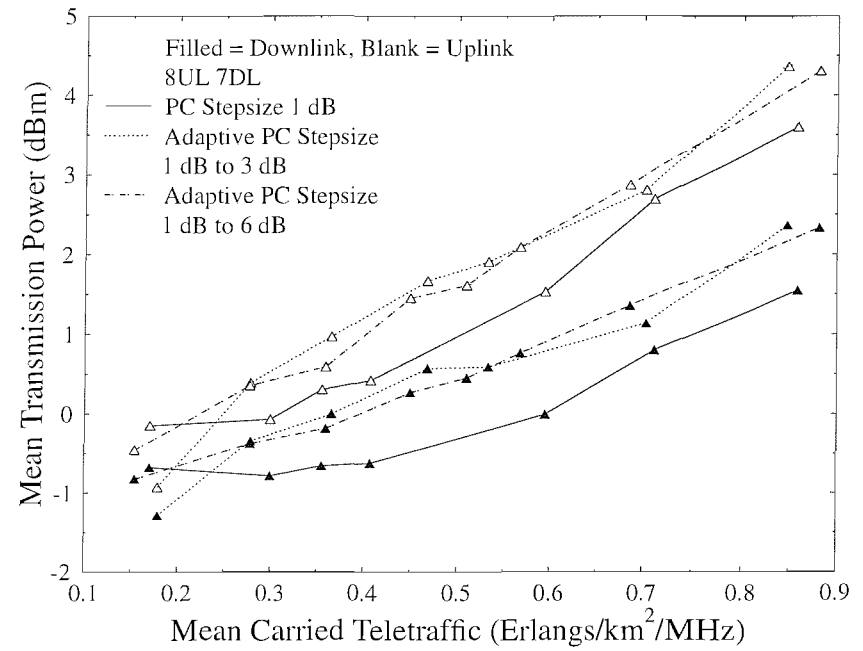

Figure 4.15: Mean MS and BS transmission power versus mean carried traffic of the UTRA-like TDD/CDMA based cellular network with shadowing and using various closed-loop PC schemes in conjunction with **a near-symmetric traffic load of 8:7 (UL:DL) timeslots.** The system parameters are summarized in Table 4.6.

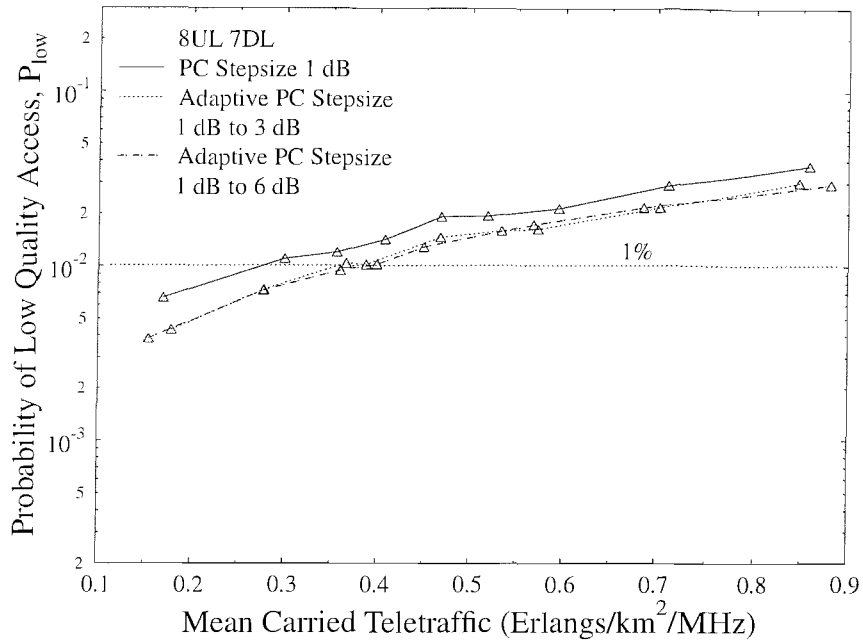

Figure 4.16: Probability of low quality access versus mean carried traffic of the UTRA-like TDD/CDMA based cellular network with shadowing and using various closed-loop PC schemes in conjunction with **a near-symmetric traffic load of 8:7 (UL:DL) timeslots.** The system parameters are summarized in Table 4.6.

4.3.3.2 Uplink Dominated Asymmetric Traffic Loads

The adaptive PC stepsize scenario of "1 dB to 3 dB" and "1 dB to 6 dB" summarized in Table 4.5 is employed to compensate for the slowly-acting power control feedback loop associated with the asymmetric TDD traffic loads, as highlighted in Section 4.3.1. In this section we present the achievable carried traffic improvement of the TDD system, when invoking the adaptive PC stepsize algorithm of Table 4.5. The UL:DL TS allocation ratio of 13:2 (UL:DL) was studied in our simulations.

The associated forced termination probability versus mean carried traffic of the UTRA-like TDD CDMA system conveying an asymmetric traffic load of 13:2 (UL:DL) is portrayed in Figure 4.17. Observe in the figure that a significant forced termination probability improvement was achieved by employing the adaptive PC stepsize algorithm of Table 4.5. When using the fixed 1 dB power control stepsize, the achievable performance of the TDD system was gravely degraded, because the MSs and BSs are unable to sufficiently increase the transmission power at the 200 Hz power control rate facilitated by having only two DL TSs, hence only allowing a 2 dB power correction range during the 15-slot 10 ms frame. More specifically, although not explicitly shown here for reasons of space economy, we observed that about 90% of the forced call terminations of the total number of dropped calls were due to the slowly-acting power control feedback, when the traffic load was low, which was

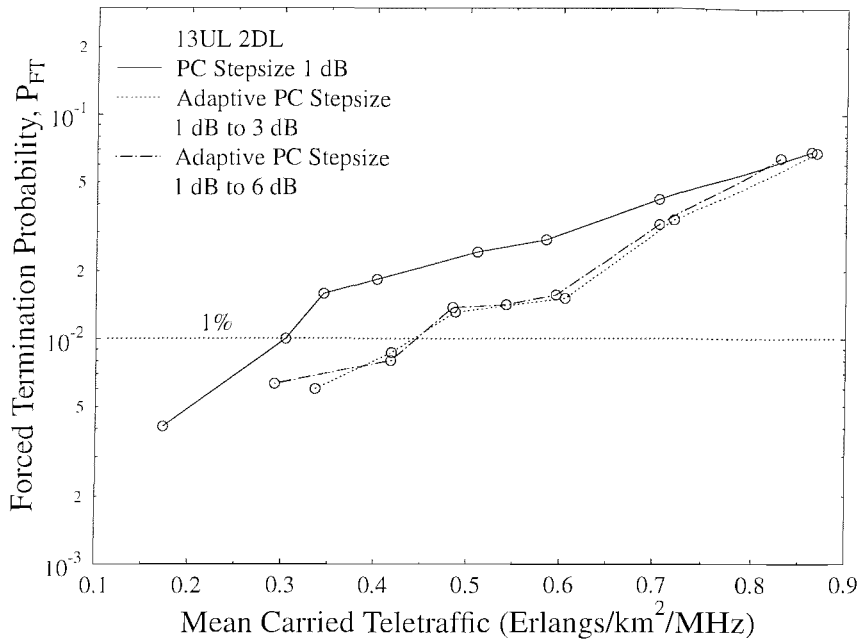

Figure 4.17: Forced termination probability versus mean carried traffic of the UTRA-like TDD/CDMA based cellular network with shadowing and using various closed-loop PC schemes in conjunction with **an asymmetric traffic load of 13:2 (UL:DL) timeslots.** The system parameters are summarized in Table 4.6.

reduced to about 21%, when the traffic load was high. When using the fixed 1 dB power control stepsize, the TDD system is capable of supporting only 50 users at $P_{FT} = 1\%$, corresponding to a normalized teletraffic density of 0.30 Erlang/km^2/MHz. In conjunction with the '1 dB to 3 dB adaptive PC stepsize' algorithm, the number of users supported by the network increased by 46% to 73 users, corresponding to a traffic load of 0.44 Erlang/km^2/MHz. When invoking the '1 dB to 6 dB adaptive PC stepsize' algorithm, the achievable forced termination probability becomes similar to that of the 'Adaptive PC Stepsize 1 dB to 3 dB' scenario. The number of users supported by the network was 72, corresponding to a normalized traffic load of 0.43 Erlang/km^2/MHz. Using the 'Adaptive PC Stepsize 1 dB to 3 dB' scheme, a maximum of 6 dB power correction range per TDD frame is possible, which is close to the power correction range of the near-symmetric traffic load of 8:7 (UL:DL) and statistically speaking avoids the forced termination events potentially inflicted by the provision of insufficient transmit power. Hence no further performance improvement is achieved by employing the higher power control stepsize of 6 dB, as seen in Figure 4.17.

Figure 4.18 portrays the mean transmission power versus mean carried traffic performance of the UTRA-like TDD network. Similar trends are observed to those seen in Figure 4.15. Using a high power control stepsize may promptly compensate for the associated signal power variations based on the estimated channel quality, but the increased transmit power inflicts an increased interference upon

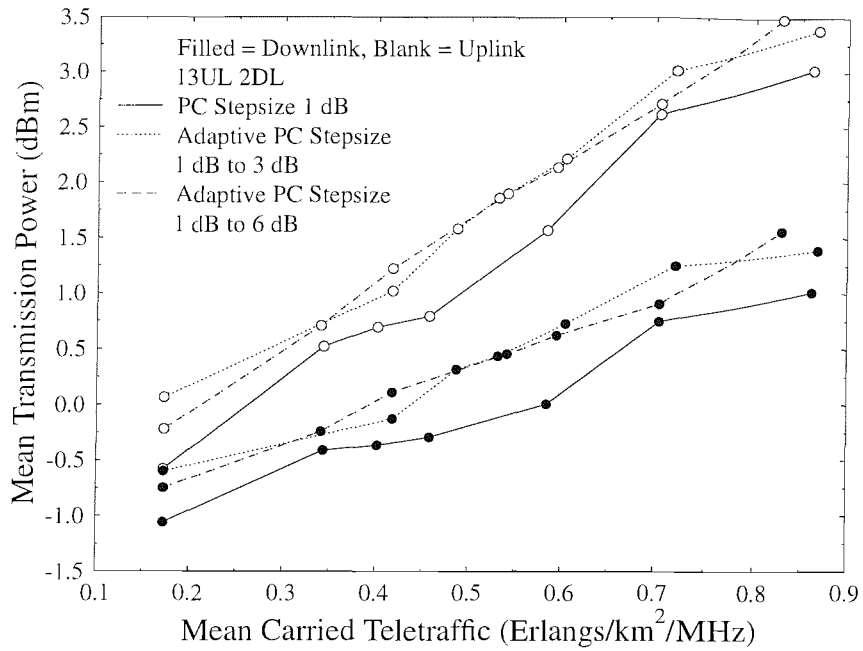

Figure 4.18: Mean MS and BS transmission power versus mean carried traffic of the UTRA-like TDD/CDMA based cellular network with shadowing and using various closed-loop PC schemes in conjunction with **an asymmetric traffic load of 13:2 (UL:DL) timeslots.** The system parameters are summarized in Table 4.6.

the other mobile users at the same time. Hence the other users may also have to increase their transmit power owing to this sudden interference change. An additional 0.3 dBm signal power is required, when invoking the adaptive PC stepsize algorithm. Figure 4.19 shows the associated low quality access performance, both with and without adaptive stepsize control. Regardless of the presence or absence of adaptive stepsize control, the various traffic loads result in a similar low quality access performance. Again, as we have discussed in Section 4.3.3.1, most of the low quality access events are imposed, because the closed-loop power control is incapable of accurately compensating for the SINR variations imposed by the erratically varying timeslot allocations of the different basestations. However, the the SINR fluctuation imposed by an asymmetric traffic load of 13:2 (UL:DL) for example is typically significantly smaller than that of the near-symmetric traffic load of 8:7 (UL:DL). Hence the overall probability of low quality access seen in Figure 4.19 is better than the corresponding performance associated with a near-symmetric traffic load, as seen in Figure 4.16.

4.3.3.3 Downlink Dominated Asymmetric Traffic Loads

For a TS allocation ratio of 1:14 (UL:DL), Figure 4.20 presents the forced termination probability versus the mean carried traffic performance of the UTRA-like TDD/CDMA system. In [107] it was shown that the major source of interference is constituted by the BS-to-BS interference as a con-

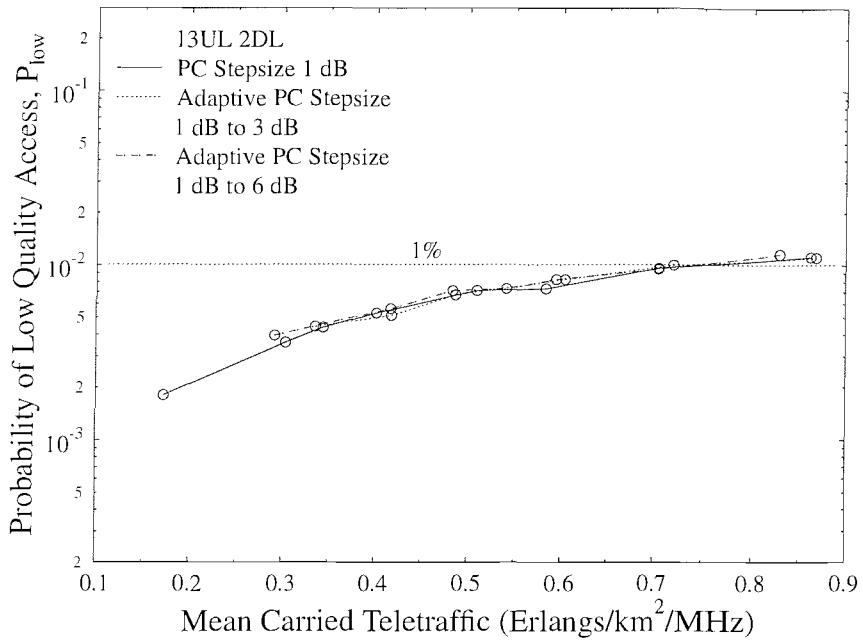

Figure 4.19: Probability of low quality access versus mean carried traffic of the UTRA-like TDD/CDMA based cellular network with shadowing and using various closed-loop PC schemes in conjunction with **an asymmetric traffic load of 13:2 (UL:DL) timeslots.** The system parameters are summarized in Table 4.6.

sequence of the near-LOS propagation conditions prevailing between the high-elevation BSs. The co-channel interference is typically more severe in urban areas, owing to the typically high number of interfering BSs and MSs. Hence, more frequent power adjustments may be needed for maintaining the target SINR in the uplink. In Figure 4.20 we can see that there is a high probability of forced termination, when using a low power control stepsize of 1 dB. Although not shown graphically, a nearly 98% outage probability was recorded due to the insufficiently high signal power received from the MSs, when the traffic load is as low as 0.25 Erlang/km^2/MHz, and 70% when the traffic load is as high as 0.5 Erlang/km^2/MHz. However, it is observed in Figure 4.20 that with the advent of the "1 dB to 3 dB" PC stepsize control regime, the TDD network can support a teletraffic density of 0.40 Erlang/km^2/MHz, corresponding to 72 users. As also seen in Figure 4.20, the employment of the "1 dB to 6 dB" regime led to a TDD network that supported a traffic load of 0.52 Erlang/km^2/MHz and handled 93 users. This corresponded to a relative gain of 26% over the performance improvement provided in the TDD mode by the "1 dB to 3 dB" PC stepsize control regime. This suggests again that a 6 dB power control correction range per TDD frame is needed for both symmetric and asymmetric TDD traffic loads for the sake of avoiding a high forced termination probability imposed by an insufficiently responsive power ramping. A TDD system using a TS allocation of 1:14 (UL:DL) has a rather limited 100 Hz power control rate imposed by the 1 dB transmit power adjustment per

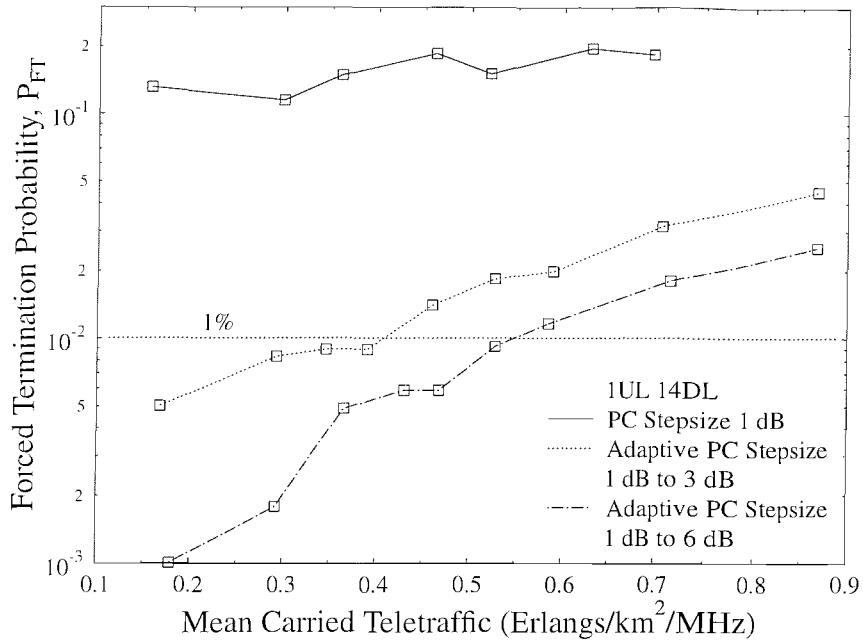

Figure 4.20: Forced termination probability versus mean carried traffic of the UTRA-like TDD/CDMA based cellular network with shadowing and using various closed-loop PC schemes in conjunction with **an asymmetric traffic load of 1:14 (UL:DL) timeslots.** The system parameters are summarized in Table 4.6.

TDD frame. In conjunction with a power control stepsize of 1 dB, this system can hardly handle any sudden power variations in excess of 5 dB, since a call is terminated within 50 ms or 5 TDD frames, if the target SINR cannot be maintained. Hence using a sufficiently high power control stepsize is the key factor in maintaining an adequate system performance in case of carrying downlink dominated traffic loads.

The mean transmission power versus teletraffic performance achieved in conjunction with the asymmetric traffic load of 1:14 (UL:DL) is depicted in Figure 4.21. Again, a higher than necessary power may increase the interference imposed upon other MSs supported by both the serving BS and by the BSs in the adjacent cells. Observe in Figure 4.21 that an additional 0.3 dBm signal power is needed for both UL and DL transmission, when invoking the adaptive PC stepsize scheme. Upon comparing Figure 4.22 to both Figure 4.19 and Figure 4.16 we observed that the probability of low quality access in Figure 4.22 has been reduced as a benefit of the reduced channel quality fluctuations imposed by the various TS allocations of the different cells, since only a single timeslot can be allocated to either the uplink or the downlink in conjunction with a TS allocation ratio of 1:14 (UL:DL). This TS-allocation ratio indirectly limits the rate of interference variation engendered by the TS allocation variations in the interfering cells.

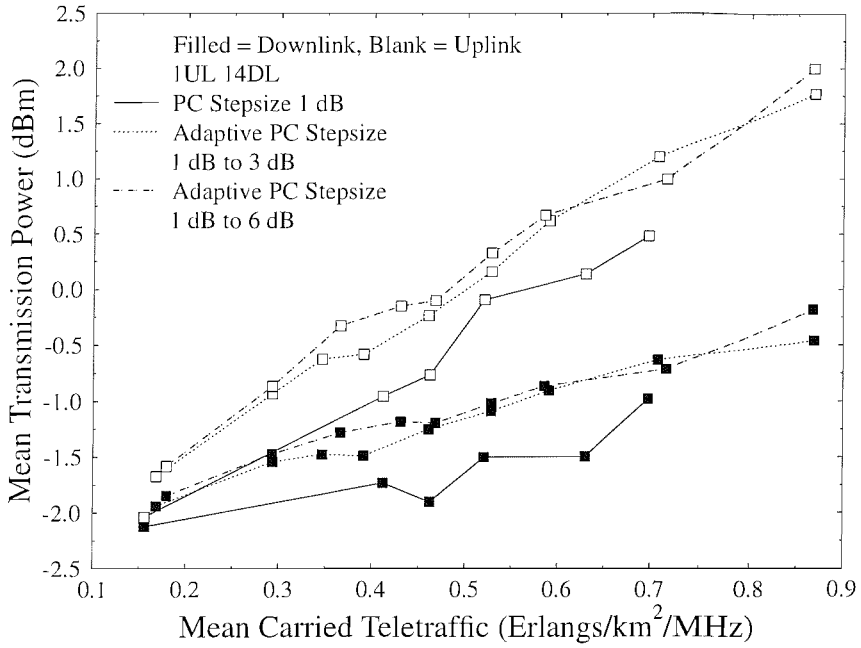

Figure 4.21: Mean transmission power versus mean carried traffic of the UTRA-like TDD/CDMA based cellular network with shadowing and using various closed-loop PC schemes in conjunction with **an asymmetric traffic load of 1:14 (UL:DL) timeslots.** The system parameters are summarized in Table 4.6.

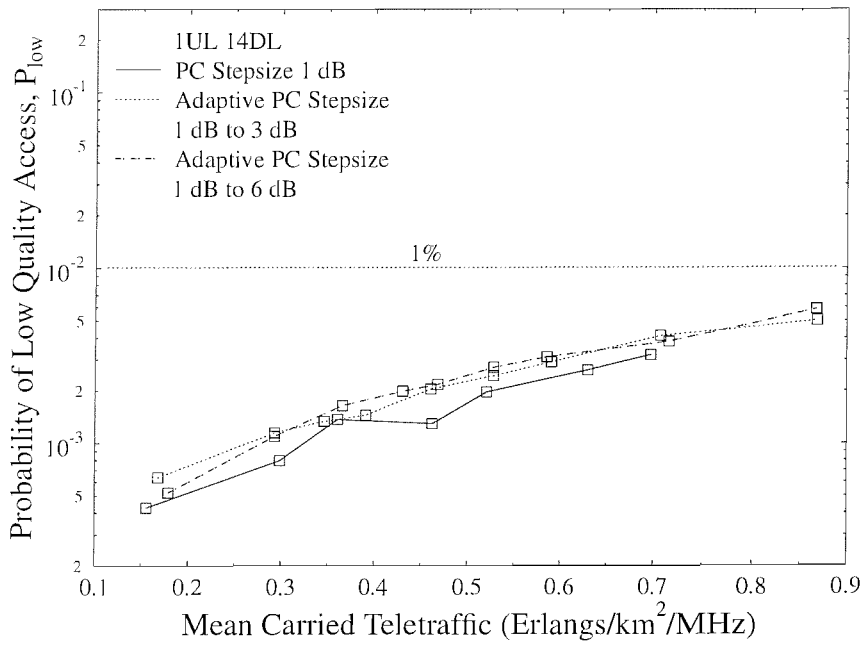

Figure 4.22: Probability of low quality access versus mean carried traffic of the UTRA-like TDD/CDMA based cellular network with shadowing and using various closed-loop PC scheme in conjunction with **an asymmetric traffic load of 1:14 (UL:DL) timeslots.** The system parameters are summarized in Table 4.6.

4.3.4 UTRA TDD Uplink Open-loop Power Control

One of the inherent benefits of open-loop power control is that it makes a rough estimate of the path loss encountered by means of a downlink beacon signal. However, in the UTRA FDD mode this pathloss estimation technique is far too inaccurate, because the fast fading is essentially uncorrelated between the uplink and downlink, owing to the large frequency separation of the uplink and downlink bands of the UTRA FDD mode. Hence in the UTRA FDD mode, open-loop power control is only used for providing a coarse initial power setting of the mobile station at the beginning of a call. By contrast, in the 3.84 *Mcps* UTRA TDD mode, the reciprocity of the UL/DL channel may be exploited for assisting the operation of the open-loop power control in the uplink. Based on the estimated interference level at the BS as well as on the path loss estimate of the DL, the mobile weights the path loss measurements by taking into account its interference estimate and sets the UL transmission power accordingly. The estimated interference level and the BS transmitter power used are signalled to the MS for the sake of calculating the required transmit power [147]. The transmitter power of the mobile is calculated according to [156]:

$$P_{UE} = \alpha L_{PCCPCH} + (1 - \alpha)L_0 + I_{BS} + SINR_{TARGET} + C, \tag{4.3}$$

where P_{UE} is the transmitter power level expressed in dBm, L_{PCCPCH} is the measured path loss in dB, L_0 is the long-term average path loss in dB, I_{BS} is the estimated interference power level at the BS's receiver quantified in terms of dBm, and finally α is a weighting parameter which represents the BS's confidence in the path loss measurements, which may be impaired by both interference and fading. Furthermore, $SINR_{TARGET}$ is the target SINR expressed in dB, while C is a constant to be set by the higher Open Systems Interconnection (OSI) layers. To elaborate a little further, the weighting factor α is a function of the time delay between the UL TS of the MS, for which the power is being calculated and the most recent DL PCCPCH TS. The specific value of the parameter α should also reflect the fading channel's Doppler frequency, which depends on the speed of the MS. More explicitly, the weighting factor α is defined as a function of the time delay, d, which is expressed in terms of the number of the TSs between the UL TS and the most recent DL TS [103], obeying

$$\alpha = 1 - \frac{(d-1)}{6}. \tag{4.4}$$

In our UTRA-like TDD system [41] a lognormally distributed slow fading obeying an average frequency of 0.5 Hz using the sum-of-sinusoid-like shadowing model of [43], and a pedestrian walking velocity of 3 mph were used. The MSs' positions and the fading parameters are updated on a frame-by-frame basis. The measured path loss L_{PCCPCH} is assumed to be constant during the 15 timeslots of a 10 ms frame. Hence we have $L_{PCCPCH} = L_0$, in Equation 4.3, yielding:

$$P_{UE} = L_{PCCPCH} + I_{BS} + SINR_{TARGET} + C. \tag{4.5}$$

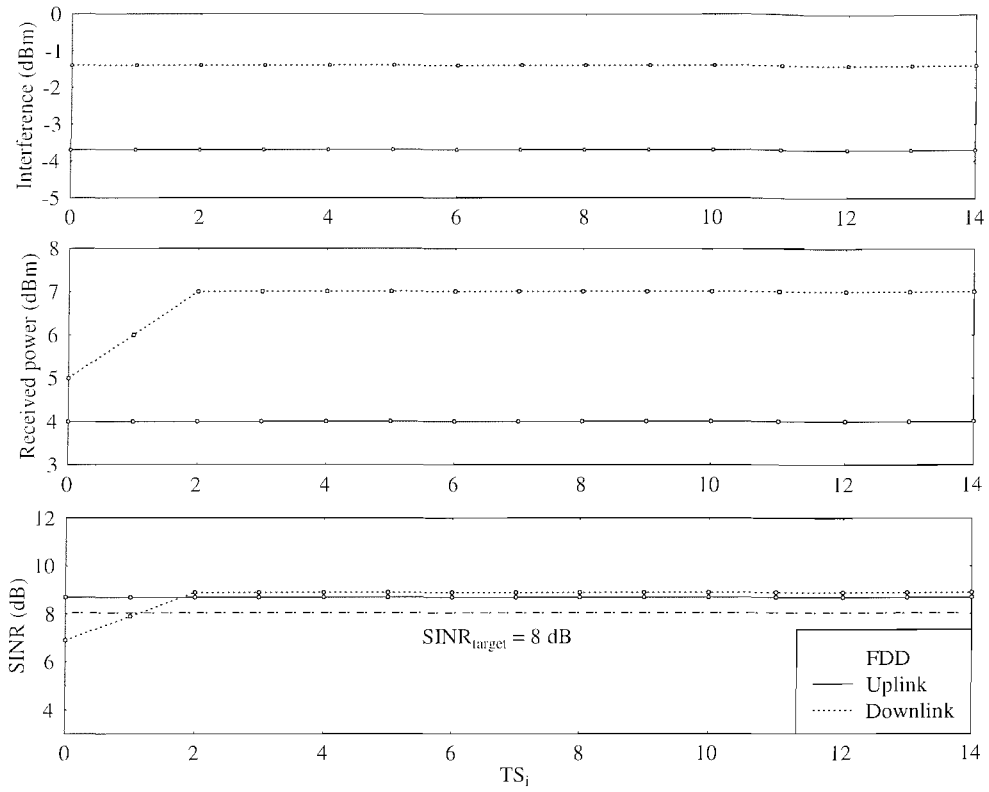

Figure 4.23: A 'snap-shot' of the interference, uplink and downlink received powers, extracted from simulations, also showing the uplink and downlink received SINRs, versus TS index in a FDD frame using closed-loop power control in conjunction with **a near-symmetric traffic load of 8:7 (UL:DL) timeslots.**

4.3.5 Frame-Delay Based Power Adjustment Model

In the FDD mode the uplink and downlink traffic is transmitted on different frequencies, which prevents encountering interference between the uplink and downlink. Hence only two different interference scenarios exist, namely the *BS to MS* interference encountered during downlink transmissions and the *MS to BS* interference engendered during uplink transmissions. The interference received from other cells is near-constant during an FDD 10 ms frame. Figure 4.23 illustrates this phenomenon, where the downlink SINR is below the target SINR of 8 dB at TS_0. Hence the closed-loop power control scheme starts to increase the downlink transmit power, seen in the middle trace of Figure 4.23, while the interference plotted at the top does not change between TS_1 and TS_2, as seen in the top trace of Figure 4.23. Therefore the SINR reaches the target SINR value of 8 dB at TS_2 and hence improves the call quality, as shown in the bottom trace of Figure 4.23.

By contrast, in TDD mode two additional interference scenarios exist, since the uplink and downlink TSs are transmitted on the same carrier frequency. The received interference is imposed either by a basestation or a mobile station in the interfering cell. Hence the interference level may change, for

example, due to the movement of the dominant interfering source, as shown in Figure 4.24(a). The table seen at the bottom of Figure 4.24(d) presents the uplink and downlink timeslots' allocation in both the interfered cell and the interfering cell. The basestation and mobile station of the interfered cell are denoted as BS_A and MS_A, while BS_B and MS_B represent the interfering cell's basestation and mobile station, respectively. Figure 4.24(a), 4.24(b) and 4.24(c) portray the interference level, the received power and the instantaneous SINR value at the receiver of both BS_A (solid line) and MS_A (dotted line), respectively. At TS_0 and TS_2, the transmit direction is the uplink in the interfered cell. By contrast, in the interfering cell the transmit direction is the downlink at TS_0 and the uplink at TS_2. Hence the UL and DL interference scenarios are different from each other, as seen in Figure 4.24(a), which results in having an uplink SINR that is below the target SINR of 8 dB at TS_2. Even though the closed-loop power control regime is capable of compensating for the interference degradation by increasing the transmit power at TS_4, the same scenario is encountered again in Figure 4.24(c) at TS_{10}, which results in an inadequate SINR value of 5 dB. The closed-loop power control scheme is incapable of predicting the interference level variations imposed by the various TS allocations of the different cells, potentially leading to a poor call quality, as shown in Figure 4.16.

As seen in Figure 4.24(d), for example, in TS_3 MS_A roaming in the interfered cell receives in the DL and its signal is contaminated by the dominant interfering BS_B of the interfering cell, which is also transmitting in TS_3 in the DL. Owing to the dominant interferer BS_B, MS_A would request BS_A to increase its power transmitted to MS_A. However, as depicted in Figure 4.24(d), during TS_5 the interference scenario has changed, since now BS_B is no longer interfering with MS_A, because it is also receiving. Therefore the previously requested BS_A transmit power is likely to become excessive, since in reality now a BS_A transmit power reduction would be required. In order to circumvent this problem it may be beneficial to postpone implementing the increased power request of MS_A until the same TS-namely TS_3 (TS_{18}) of the next TDD frame when the interference level may be expected to be similar to that experienced at TS_3 of MS_A during the previous frame, as seen in Figure 4.24(a), unless MS_A or MS_B become inactive, or alternatively, another dominant interferer initiates a call.

To elaborate on the related power control actions in little more detail, let us now consider Figures 4.24(a)–4.24(c), commencing from TS_0, where MS_A is transmitting in the UL and MS_B is receiving in the DL. During TS_0 the target SINR of 8 dB is met at both the serving BS's UL receiver, namely at BS_A and at the DL receiver of MS_A. More explicitly, the UL interference level at the receiver of BS_A in Figure 4.24(a) is -10.3 dBm and the received power (P_{RX}) of MS_A is -2 dBm in Figure 4.24(b), yielding an SINR of 8.3 dB at the input of BS_A, as seen in Figure 4.24(c). When the interference pattern changes during TS_1 in Figure 4.24(d), in the example considered in Figure 4.24(c) the target $SINR_A$ remained unchanged. To elaborate on the associated scenario, MS_A is receiving

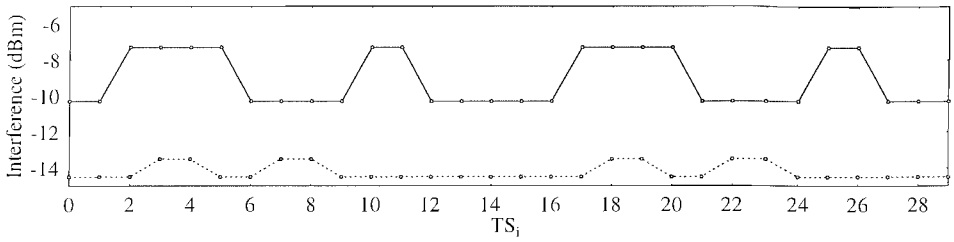

(a)

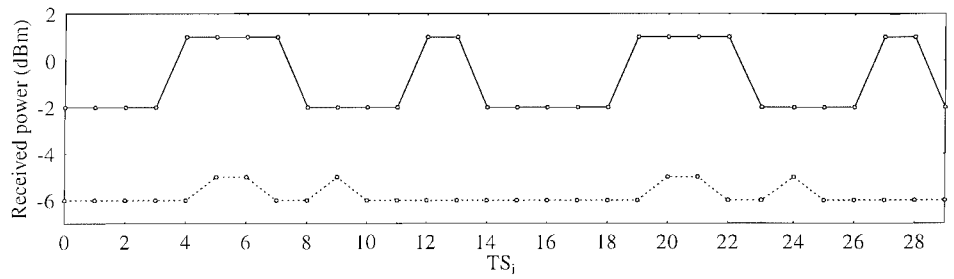

(b)

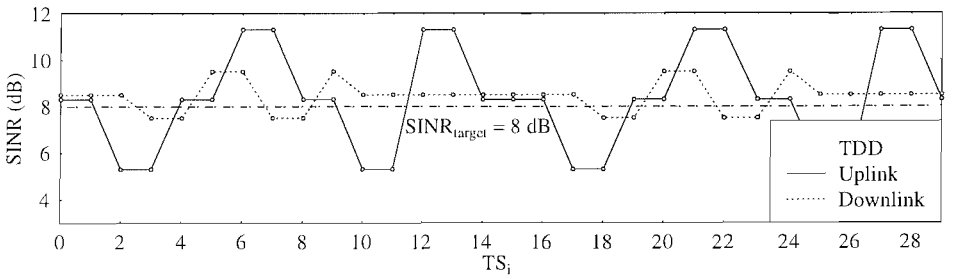

(c)

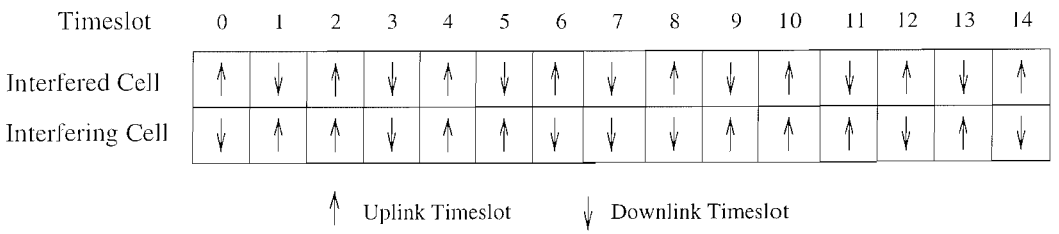

(d)

Figure 4.24: A 'snap-shot' of the interference, the uplink and the downlink received powers, extracted from our simulations, also showing the uplink and downlink received SINRs, versus the TS index in a TDD frame using closed-loop power control in conjunction with **a near-symmetric traffic load of 8:7 (UL:DL)**. The system parameters are summarized in Table 4.6.

in TS_1 of Figure 4.24(d), and the interference level at its input is -14.5 dBm in Figure 4.24(a). The corresponding received power of MS_A is -6 dBm in Figure 4.24(b), yielding an SINR of 8.5 dB at the input of MS_A.

Let us now proceed to TS_2, when MS_A is transmitting in the UL and so is MS_B. Observe in Figure 4.24(a) that as shown by the continuous line, the interference at the input of BS_A increases from -10.3 dBm to -7.3 dBm, which is an indication that MS_B is likely to be closer to BS_A than to MS_A, because in TS_1 MS_A was receiving and yet, its received interference level was lower, namely -14.5 dBm as printed using the dotted line. Therefore the SINR at the input of BS_A is reduced to 5.3 dB, as shown using the continuous line in Figure 4.24(c), which is below the target SINR of 8 dB, hence necessitating a transmit power increase by MS_A in time for its next UL transmission during TS_4. Hence the adaptive PC stepsize regime arranges for a 3 dB power increase in time for MS_A's transmission during TS_4 as seen in Figure 4.24(b), which meets the 8 dB target SINR requirement depicted in Figure 4.24(c), because the interference level plotted in Figure 4.24(a) remained unchanged.

By contrast, the interference scenario encountered during TS_3 and TS_5 will highlight a deficiency of this PC regime. Explicitly, in TS_3 both MS_A and MS_B are receiving in the DL, while in TS_5 MS_B switches to UL transmission. In TS_3 the interference level experienced by MS_A is seen to be increased in Figure 4.24(a) due to the interference imposed by BS_B transmitting to the DL receiver of MS_B. This degrades the SINR to 7.5 dB during TS_3 at the input of MS_A, which hence requests a higher transmit power from BS_A, as indicated by the ramp up of the dotted curve of Figure 4.24(b) to 5 dBm, showing an increased received power of -5 dBm during TS_5. The resultant DL SINR of TS_5 plotted using the dotted lines is increased to 9.5 dB. When MS_B switches to UL transmit mode in TS_5, BS_B has to switch to its receiver mode, inevitably seizing its transmission to MS_B and hence the interference level plotted by the dotted line is seen to decease to -14.5 dBm in Figure 4.24(a). At the same time the received power of MS_A printed using dotted lines in Figure 4.24(b) is seen to be increased to -5 dBm, which results in an unnecessarily high SINR of 9.5 dB, as plotted by the dotted line in Figure 4.24(c). This unnecessarily high SINR is a consequence of a change in the interference scenario between TS_3 and TS_5, which resulted in MS_A requesting an excessive transmit power from BS_A. An even more undesirable deficiency of this PC regime is encountered, when the power requested by MS_A becomes insufficient owing to an unexpected rise in the interference level. This deficiency may be mitigated by a less agile power control regime, which does not react prematurely on the basis of the erratically fluctuating UL/DL interference pattern, it rather acts during the same TS of the next TDD frame, which is likely to have the same SINR as the specific TS, when the SINR estimate was generated. More explicitly, the benefit of this deferred power control philosophy is that the UL/DL TS configuration as well as the received signal level are likely to be similar to those experienced,

when the SINR estimate was generated. Whilst the advantages of this frame-delay based PC regime might appear less tangible at this stage, the results of Section 4.3.5 will demonstrate its virtues in more quantitative terms. We will demonstrate namely that its benefits manifest themselves in terms of reducing the probability of low quality access, which became excessive due to the often deficient premature power adjustments imposed by the unpredictable UL/DL TS assignments.

As we have discussed above, the erratic interference level fluctuation imposed by the time-variant TS allocations governed by the different TDD cells results in a relatively high power control inaccuracy, as highlighted for example in Figure 4.24. However, the TSs having the same index in consecutive TDD frames typically have the same UL/DL TS allocation pattern and their associated interference load may also be expected to be similar. Hence, if the power adjustment takes place in the TS having the same index in the next frame, the accuracy of the power control may be improved, especially in the absence of shadowing. It can be observed in Figure 4.25 that the interference level fluctuation imposed by the interfering cells results in a low UL SINR between TS_2 and TS_5. When we invoke the above-mentioned 'frame-delay' based power control scheme, the transmitted power seen in Figure 4.25(b) is not adjusted in the current frame, namely in *Frame* N, it is rather postponed until frame *Frame* $(N+1)$. More specifically, TS_2 and TS_{17} are the third timeslots in *Frame* N and *Frame* $(N+1)$, respectively, and the associated TS allocation pattern as well as interference pattern are identical, as seen in the context of TS_2^{FrameN} and $TS_2^{FrameN+1}$ in Figure 4.25(d) and in terms of the interference level seen in Figure 4.25(a). Hence, a power adjustment carried out at TS_{17} based on the interference-related measurements conducted during TS_2 has the potential of compensating for the interference load increase experienced, as shown in Figure 4.25(c).

In the frame-delay based power control simulations open-loop power control was used in the uplink, as discussed in Section 4.3.4. The estimated interference level and the BS transmitter power used are signalled to the mobile station for the sake of calculating the required uplink transmit power. The required transmit power is calculated during each uplink TS based on the information generated during the TS having the same index in the previous frame. The DL power control also operates in a closed-loop fasion, but the power adjustment is frame-delayed. In other words, each TPC command is processed in the same TS of the next frame. In the next section we will embark on studying the achievable performance of the frame-delay based open-loop uplink power control regime in case of different near-symmetric as well as asymmetric traffic loads and compare the associated results to the best system performance obtained in Section 4.3.3, where closed-loop power control was used for both the uplink and the downlink without frame-delay power based adjustment.

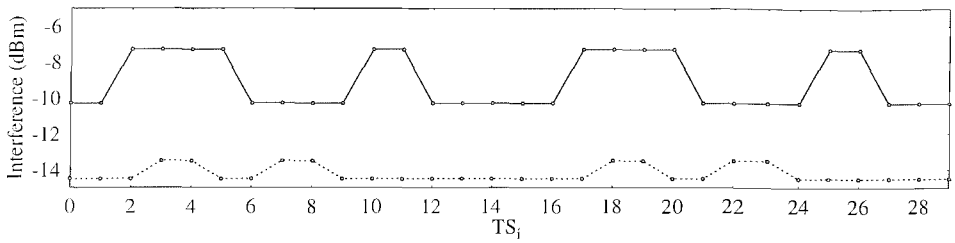

(a)

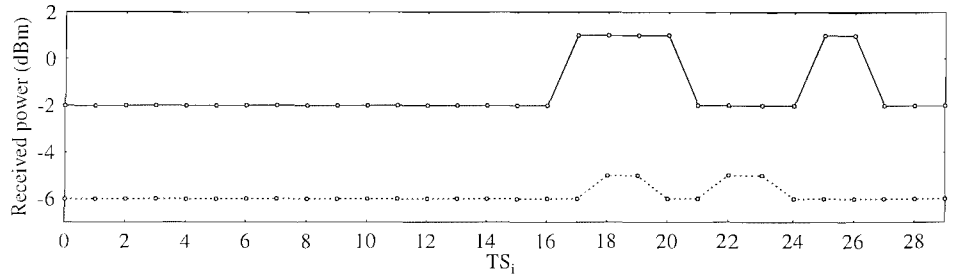

(b)

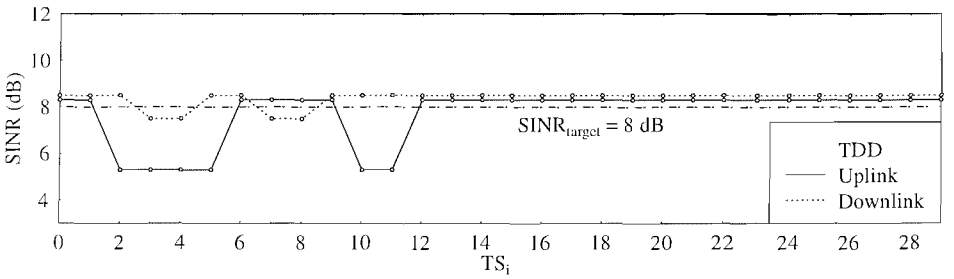

(c)

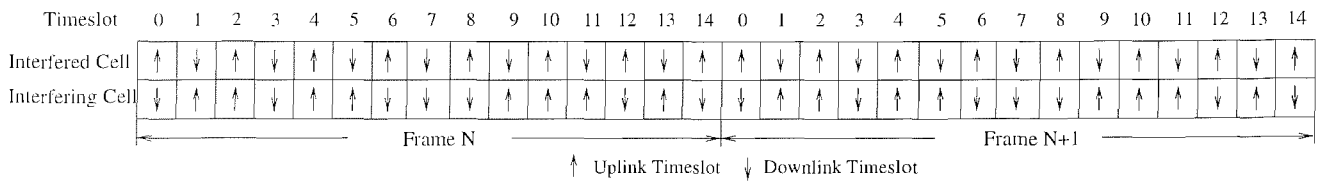

(d)

Figure 4.25: A 'snap-shot' of the interference, the uplink and the downlink received powers, extracted from our simulations, also showing the uplink and downlink received SINRs, versus the TS index in a TDD frame using **frame-delay based power control** in conjunction with **a near-symmetric traffic load of 8:7 (UL:DL) timeslots .** The system parameters are summarized in Table 4.6.

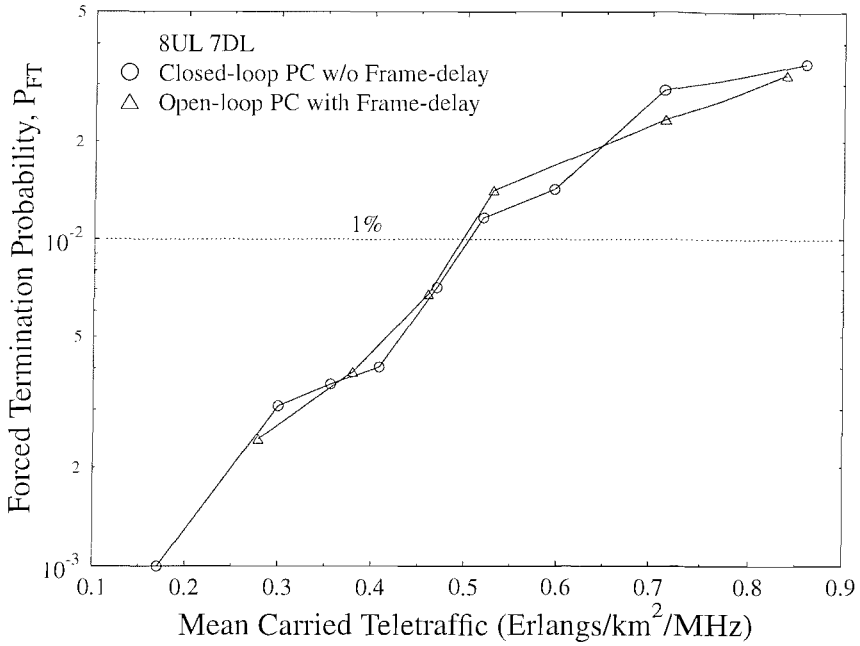

Figure 4.26: Forced termination probability versus mean carried traffic of the UTRA-like TDD/CDMA based cellular network with shadowing as well as with and without **frame-delay based power control** in conjunction with **a near-symmetric traffic load of 8:7 (UL:DL) timeslots.** The system parameters are summarized in Table 4.6.

4.3.5.1 UL/DL Symmetric Traffic Loads

Recall from the simulation results of Section 4.3.3.1 that the system's performance was seriously limited by the poor probability of low quality access in case of supporting near-symmetric traffic loads, as evidenced by Figure 4.16. Again, the reason for this phenomenon was that the power control was unable to compensate for the erratic interference level variations imposed by the rapidly fluctuating TS allocations of the interfering cells. For a traffic load ratio of 8:7 (UL:DL), there are $C_{15}^{7} = 6435$ possible TS allocations in a TDD frame. In Figure 4.26 the forced termination probability of the system using closed-loop uplink power control was found to be close to the one using open-loop uplink power control. By contrast, using open-loop power control instead of closed-loop power control in the uplink did not reduce the number of users supported. Explicitly, at $P_{FT} = 1\%$, a teletraffic density of 0.46 Erlang/km^2/MHz was achieved, corresponding to 78 users.

It is observed in Figure 4.27 that the probability of low quality access reduced dramatically, when invoking the frame-delay based power control scheme in comparison to the system without frame-delay based power control scheme. The system's performance is no longer dominated by the excessive number of low quality outage events, which is a valuable benefit of the frame-delay based power adjustment. This phenomenon was confirmed by examining Figure 4.28, which portrays the discrete

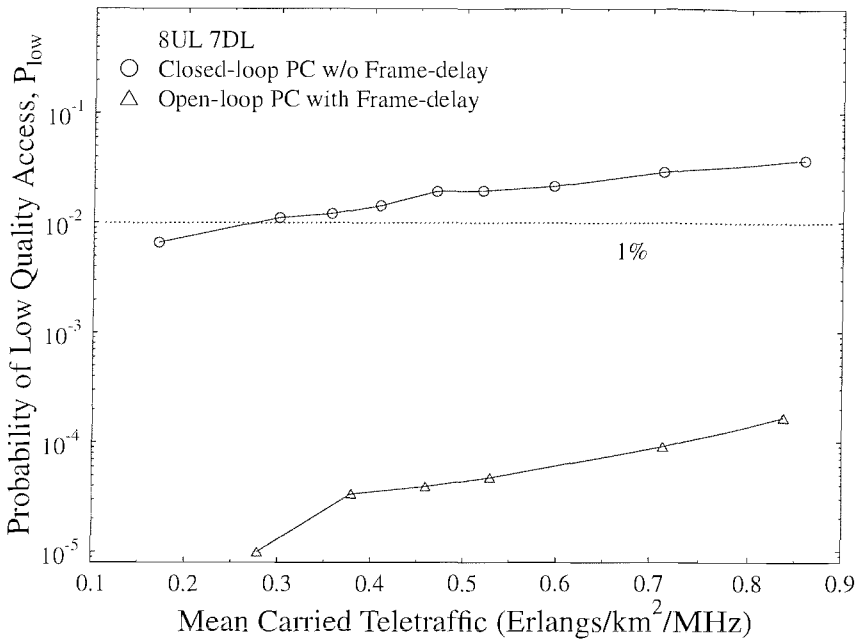

Figure 4.27: Probability of low quality access versus mean carried traffic of the UTRA-like TDD/CDMA based cellular network with shadowing as well as with and without using **frame-delay based power control** in conjunction with **a near-symmetric traffic load of 8:7 (UL:DL) timeslots.** The system parameters are summarized in Table 4.6.

histogram modelling the probability density function of the instantaneous SINR. A high number of signal quality reaches to the target SINR of 8 dB by employing the frame-delay based power control scheme. The enhanced call quality associated with a 10^{-4} low quality access probability has the benefit of a low probability of retransmission requests and enhances the system's carried traffic.

4.3.5.2 Asymmetric Traffic Loads

Figure 4.29 characterizes the forced termination probability versus asymmetric traffic loads of 13:2 and 1:14 (UL:DL) timeslots using different power control schemes. The uplink versus downlink traffic load ratio of 13:2 is characteristic of uploading data files from mobile users to the basestation, which typically requires a higher channel quality than the classic speech service, if an excessive retransmission probability is to be avoided. In Figure 4.29 both the closed-loop power control refraining from frame-delay based power adjustment and the uplink open-loop power control employing frame-delay based power control have similar forced termination performances, which suggests that invoking the frame-delay based power adjustment does not degrade the system's overall performance, quite the opposite. There are three propagation-related phenomena, which may affect the accuracy of the power control in our system, namely the shadow fading, pathloss and the interference variations. Since power update is carried out only once per 10 ms frame duration, the effects of channel quality fluctuations due to

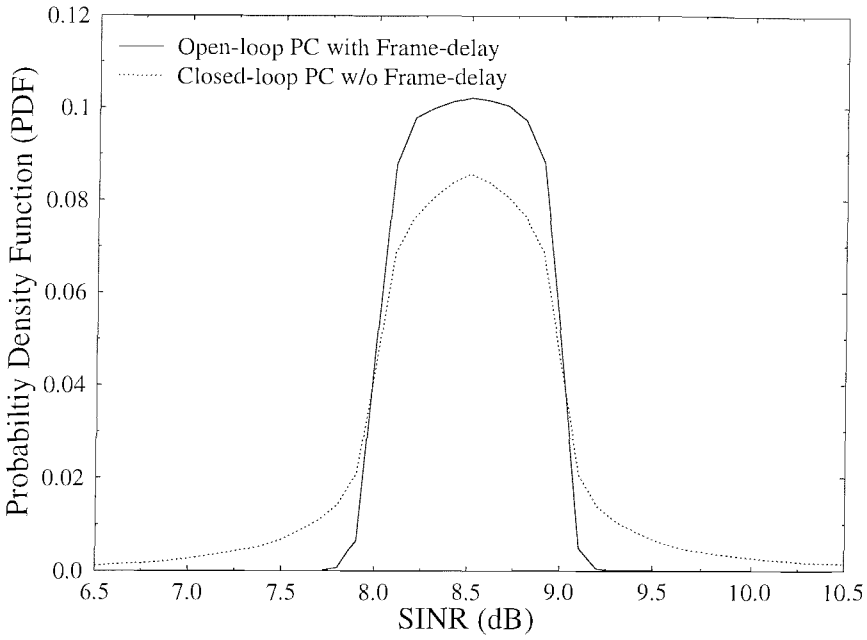

Figure 4.28: The SINR histogram modelling the probability density function of the UTRA-like TDD/CDMA cellular network's SINR both with and without using **frame-delay based power control** in conjunction with **a near-symmetric traffic load of 8:7 (UL:DL) timeslots.**

both shadowing and pathloss are similar [158] in a TDD frame. The interference variations may be compensated by the frame-delay based power adjustment, hence both the closed-loop and open-loop power control have a similar forced termination probability in Figure 4.29.

Similar trends are observed regarding the probability of forced termination call at an asymmetric traffic load ratio of 1:14 (UL:DL) in Figure 4.29 to those found for the traffic load of 13:2 (UL:DL) scenario. Again, the specific choice of employing the uplink open-loop power control and the frame-delay based power adjustment does not dramatically influence the system's performance. However, the mean downlink dominated carried teletraffic corresponds to a better total throughput than the uplink dominated traffic load. The TDD network carrying uplink dominated traffic is found to support a traffic load of 0.43 Erlang/km^2/MHz at $P_{FT} = 1\%$, corresponding to 72 users. By contrast, the TDD network conveying DL dominated traffic supports an equivalent traffic load of 0.52 Erlang/km^2/MHz, corresponding to 93 users. The difference is mainly caused by the co-channel interference imposed by the uplink. In Figure 4.30 the mean uplink transmission power associated with a traffic load of 13:2 (UL:DL) requires on average 1.2 dBm higher power than the traffic loads of 1:14 UL:DL). Since 86.7% of the total traffic load is generated for uplink transmission, the interference engendered by the mobile users degrades the achievable system performance.

The probability of low quality access recorded for the asymmetric traffic loads of 13:2 and 1:14 (UL:DL) versus the mean carried teletraffic load is portrayed in Figure 4.31. Observe that a substantial

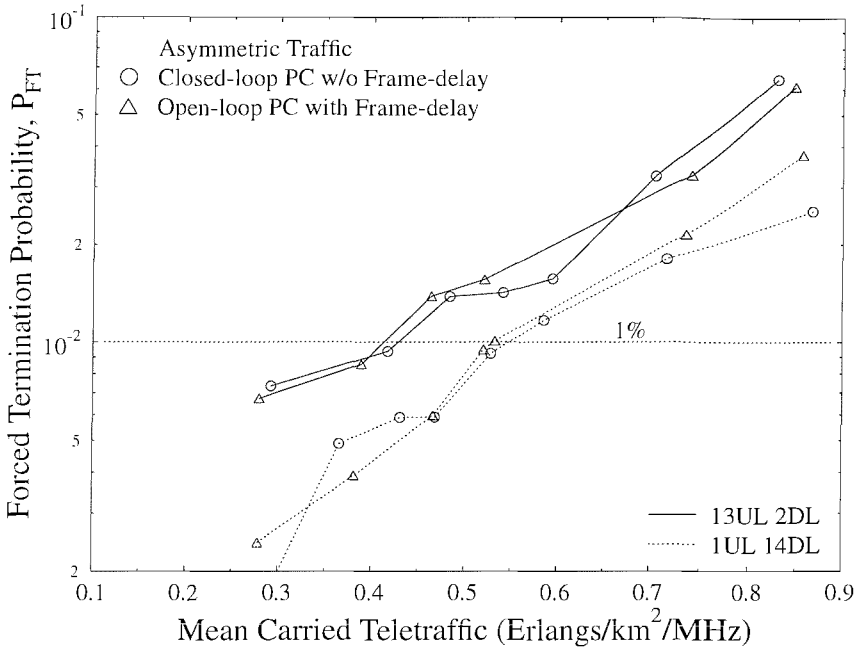

Figure 4.29: Forced termination probability versus mean carried traffic of the UTRA-like TDD/CDMA based cellular network with shadowing as well as with and without **frame-delay based power control** in conjunction with **an asymmetric traffic load of 13:2 and 1:14 (UL:DL) timeslots.** The system parameters are summarized in Table 4.6.

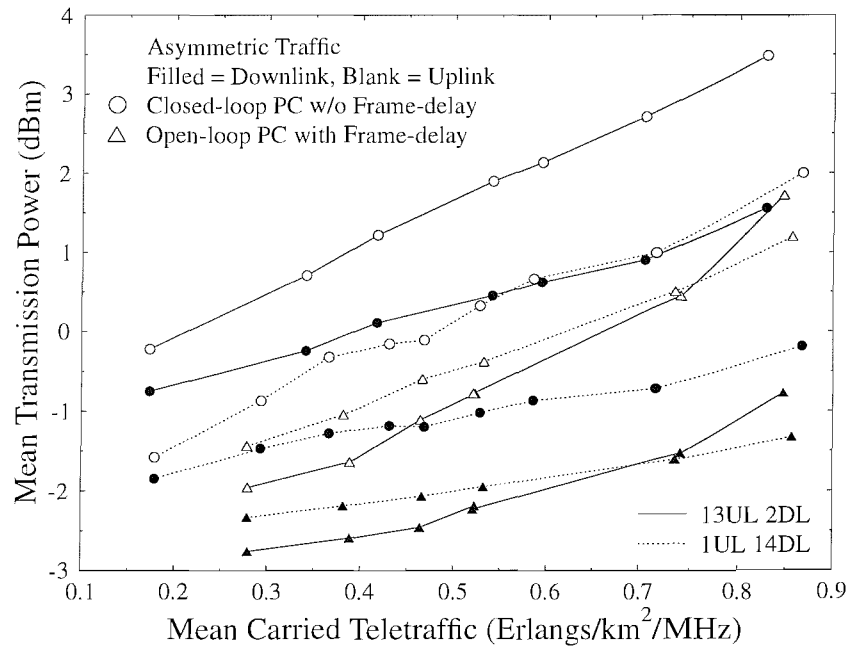

Figure 4.30: Mean transmission power versus mean carried traffic of the UTRA-like TDD/CDMA based cellular network with shadowing as well as with and without **frame-delay based power control** in conjunction with **an asymmetric traffic load of 13:2 and 1:14 (UL:DL) timeslots.** The system parameters are summarized in Table 4.6.

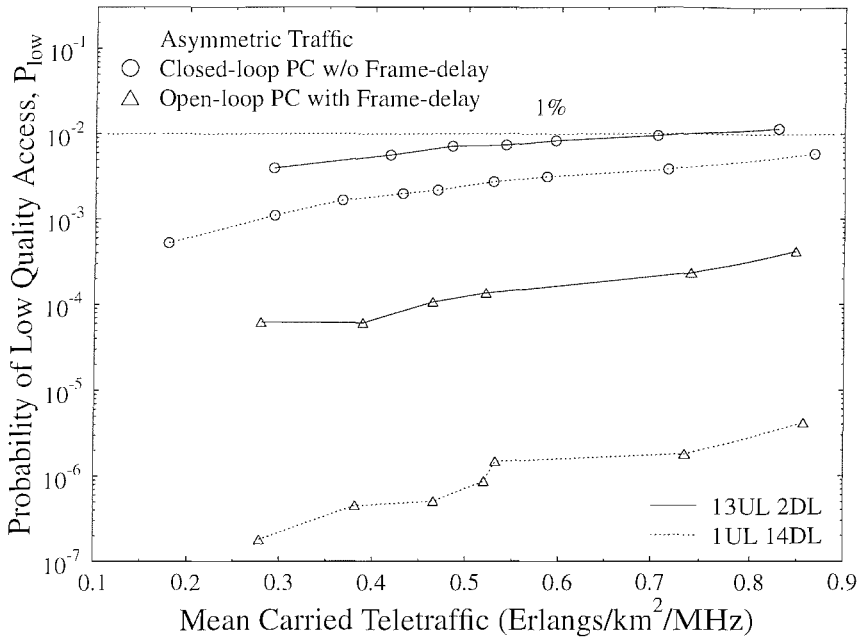

Figure 4.31: Probability of low quality access versus mean carried traffic of the UTRA-like TDD/CDMA based cellular network with shadowing as well as with and without **frame-delay based power control** in conjunction with **an asymmetric traffic load of 13:2 and 1:14 (UL:DL) timeslots.** The system parameters are summarized in Table 4.6.

performance improvement has been achieved, when invoking the frame-delay based power adjustment scheme, which is a benefit of the significantly higher call quality shown in Figure 4.31. The low quality outage probability was seen in Figure 4.31 to be below $10^{-}5$-10^{-6} for a traffic load ratio of 1:14, when supporting 72 users or a traffic load of 0.43 Erlang/km^2/MHz. This phenomenon was observed, because the mean uplink transmission power is higher than that of the downlink, as seen in Figure 4.31, and the more symmetric the traffic load, the lower the overall co-channel interference level. Hence typically a better link quality is achieved.

A summary of the maximum number of users supported by the UTRA-like TDD/CDMA system at various traffic load ratios using both closed-loop power control and uplink open-loop power control in conjunction with log-normal shadowing having a standard deviation of 3 dB and a shadowing frequency of 0.5 Hz was summarised in Table 4.7 both with as well as without frame-delay based power adjustment. The teletraffic carried and the mean mobile as well as base station transmission powers required are also shown in Table 4.7.

PC mode	Traffic Ratio (UL:DL)	Stepsize	Users	Traffic (Erlangs /km^2/MHz)	Limiting Factor	Power (dBm) MS	Power (dBm) BS
Closed-loop	8 : 7	1 dB	45	0.27	P_{low}	-0.09	-0.66
Closed-loop	13 : 2	1 to 3 dB	73	0.44	P_{FT}	1.19	0.01
Closed-loop	1 : 14	1 to 6 dB	93	0.52	P_{FT}	0.43	-0.98
Open-loop	8 : 7	1 to 6 dB	78	0.46	P_{FT}	-1.05	-2.33
Open-loop	13 : 2	1 to 6 dB	72	0.43	P_{FT}	-1.54	-2.60
Open-loop	1 : 14	1 to 6 dB	93	0.52	P_{FT}	-0.43	-1.98

Table 4.7: Maximum mean carried traffic and maximum number of mobile users that can be supported by the network, whilst meeting the network quality constraints of Section 3.6.3, namely $P_B \leq 3\%$, $P_{FT} \leq 1\%$, $P_{low} \leq 1\%$ and GOS $\leq 4\%$. The carried traffic is expressed in terms of Erlang/km^2/MHz) using **both closed-loop and open-loop power control** with as well as without **frame-delay power adjustment.** Shadow fading having a standard deviation of 3 dB and a frequency of 0.5 Hz was encountered and a spreading factor of SF=16 was used.

4.4 Summary and Conclusion

In this chapter, we studied the effects of both the hard handover margin and different power control schemes on the UTRA TDD/CDMA system's performance. In Sections 4.3.1–4.3.4 both closed-loop power control as well as open-loop power control schemes were developed, respectively. In Section 4.3.5 a frame-delay based power adjustment algorithm was proposed to overcome the channel quality variations imposed by the erratically fluctuating timeslot allocations in the different interfering radio cells. To elaborate a little further, we commenced our discourse in Sections 4.1 and 4.2 with a brief introduction to hard handovers in the context of the UTRA TDD/CDMA system. In Section 4.2.1 a relative pilot power based hard handover algorithm [50, 145] was employed. The related simulation results were provided in Section 4.2.2. A handover margin range of 3-10 dB was considered in three different near-symmetric and asymmetric traffic load scenarios. The best hard handover margin was found to be 5 dB in conjunction with $T_{acc} = 0\ dB$ and $T_{drop} = -5\ dB$, whilst meeting the network quality constraints of Section 3.6.3, as evidenced by Figures 4.1, 4.5 and 4.6 of Section 4.2.2.

We then continued our discourse with a power control study of the UTRA-like TDD/CDMA system in Section 4.3. We described a closed-loop power scheme designed for the downlink and uplink in Sections 4.3.1 and 4.3.2, respectively. Although it is a beneficial feature of the UTRA TDD mode that it is capable of supporting both asymmetric traffic and a flexible timeslot allocation, the associated low power control rate often results in a high forced termination probability owing to the associated

insufficiently high transmit power. However, this deficiency may be compensated by employing a flexible power control stepsize, as evidenced by the simulation results of Section 4.3.3. Furthermore, An open-loop uplink power control scheme was also developed based on the 3GPP standard [159] in Section 4.3.4. Again, the main advantage of the TDD mode is its flexible timeslot allocation regime capable of adopting to the prevalent traffic requirements. However, this may impose erratic channel quality fluctuations and result in inaccurate power control. As a countermeasure, in Section 4.3.5, we proposed a frame-delay based power adjustment algorithm, which substantially improved the system's performance, as evidenced by Figures 4.27 and 4.31 of Section 4.3.5.

Chapter 5

Genetically Enhanced UTRA/TDD Network Performance

5.1 Introduction

In Chapter 3 we demonstrated that although the UTRA/TDD mode was contrived for the sake of improving the achievable network performance by assigning all the timeslots on a demand basis to the uplink and downlink, this measure may result in an excessive BS-to-BS interference and hence in a potentially reduced number of system users. In Section 3.5 we therefore invoked both adaptive modulation and adaptive beamforming for the sake of mitigating this TDD-specific problem and demonstrated that with their advent the number of users supported may become similar but still somewhat inferior in comparison to that of an FDD system. In this chapter our research evolves further and as a design alternatives, we will apply a Genetic Algorithm (GA) for improving the achievable performance of the UTRA-TDD mode. More specifically, in Figure 3.13 we demonstrated that the employment of adaptive arrays in conjunction with AQAM limited the detrimental effects of co-channel interference on the UTRA-like TDD/CDMA system and resulted in performance improvements both in terms of the achievable call quality and the number of users supported. However, in comparison to a UTRA-like FDD/CDMA system, the capacity of the UTRA-like TDD/CDMA cellular system was shown to remain somewhat poorer than that of the UTRA-like FDD/CDMA system under the same propagation conditions. It was shown for example in Figure 3.10 of Chapter 3 that the TDD mode is more prone to avalanche-like teletraffic overload and its carried teletraffic is up to a factor two lower than that of the FDD mode. Again, this is because in the TDD mode mobile stations (MSs) can interfere both with base stations (BSs) as well as with each other. The same holds for BSs, which can interfere with both MSs and other BSs [107] owing to using all timeslots in both the uplink and

downlink. The resultant additional interference has a significant detrimental impact on the system's capacity due to the employment of the interference-limited CDMA technique. These conclusions were also corroborated by Wu [107], who also pointed out that the inter-cell BS-to-BS interference substantially decreases the system's user capacity. Hence we can increase the total system capacity by reducing the BS-to-BS interference. One way of achieving a reduced BS-to-BS interference is by invoking beamforming, since the BS can focus its transmitted signal energy on the MSs, while creating a radiation null in the direction of the adjacent BSs, as we have investigated in Chapter 3. However, this can only be achieved, if there are no MSs roaming in the immediate vicinity of the line between the serving BS and the neighbouring BS. Hence the achievable capacity of the beamforing aided UTRA-like TDD/CDMA system remains limited.

In order to mitigate these performance limitations, in this chapter we design a GA-assisted UTRA-like TDD/CDMA system. A Dynamic Channel Allocation (DCA) algorithm is developed, which minimizes the amount of Multiuser Interference (MUI) experienced at the BSs by employing GAs [61, 160–166].

The structure of this chapter is as follows. We will first study the effect of timeslots allocation to the system performance. Then the GA-aided UTRA-like TDD/CDMA system model used in this chapter is described in Section 5.2. The numerical results characterizing the various interference scenarios and the number of users supported by the GA-assisted TDD/CDMA system is quantified and compared to that of the TDD/CDMA system displusing with GAs in Section 5.3. Let us now commence our discourse by briefly highlighting how GAs may be used for enhancing the UTRA/TDD system's performance.

5.2 The Genetically Enhanced UTRA-like TDD/CDMA System

Recently substantial advances have been made in the context of diverse wireless receivers, such as in CDMA multiuser detectors [61], beamforming [167] and Space Division Multiple Access (SDMA) aided OFDM [168]. Genetic algorithms have been used as robust guided stochastic search algorithms for solving various optimization problems, such as multiprocessor scheduling [169], topology design and bandwidth allocation in ATM networks [170], for improving the performance of channel allocation in cellular networks [171], for code design [172] and code set selection in optical CDMA networks [173]. Despite establishing themselves as useful optimization tools in numerous applications, the employment of GAs in the network layer of mobile communications, has been extremely rare. In order to probe further in this promising field, in this chapter genetic algorithms have been utilized by a UTRA-like TDD/CDMA system, where the GA-assisted timeslot allocator assigns either uplink or downlink

timeslots to MSs or BSs, while maintaining certain Quality of Service (QoS) guarantees.

The aim of this design is to maximize the achievable UTRA-like TDD/CDMA network's capacity, measured in terms of the mean normalized carried traffic expressed in units of Erlang/km^2/MHz. The performance metrics used to quantify the quality of service have been described in Section 2.1.5. Recall that the call dropping probability, P_{FT}, quantifies the probability that a call is forced to be prematurely terminated. This may be the consequence of an insufficiently high SINR encountered during the call, which is not remedied by an intra-cell handover, either due to the lack of available channels, or owing to an insufficient improvement of the SINR, which leads to successive outages and eventually to a dropped call. Calls may also suffer from forced termination, when a mobile enters a heavily loaded cell, which either suffers from a poor average SINR or has no available channels for the mobile to handover to. The main limiting factors are the number of available spreading or OVSF codes, or high interference levels and low maximum affordable transmit power, resulting in excessive call dropping rates. Since a dropped call constitutes an annoyance from a user's viewpoint, the users' SINR value has to be maintained safely above the target SINR value.

The interference experienced at the mobile can be divided into interference due to the signals transmitted to other mobiles from the same base station, which is known as intra-cell interference, and that encountered owing to the signals transmitted to other mobiles from other basestations as well as to other basestations from other mobiles, which is termed inter-cell interference.

The instantaneous SINR is obtained by dividing the received signal powers by the total interference plus thermal noise power, and then by multiplying this ratio by the spreading factor, SF, yielding [43]

$$SINR_{DL} = \frac{SF \cdot P_{BS}}{(1-\alpha)I_{Intra} + I_{Inter} + N_0}, \tag{5.1}$$

where $\alpha = 1$ corresponds to the ideal case of perfectly orthogonal intra-cell interference and $\alpha = 0$ to completely asynchronous intra-cell interference. Furthermore, P_{BS} is the signal power received by the mobile user from the base station, N_0 is the thermal noise, I_{Intra} is the intra-cell interference and I_{Inter} is the inter-cell interference. Again, the interference plus noise power is scaled by the spreading factor, SF, since during the despreading process low-pass filtering reduces the noise bandwidth by a factor of SF. The inter-cell interference is not only due to the MSs, but also due to the BSs illuminating the adjacent cells by co-channel signals.

Following the above introductory considerations, let us represent the GA's solution space F as $n \times m$-dimensional binary matrix, where n is the number of radio cells and m is the total number of timeslots. Explicitly, the total number of timeslots is the product of the number of traffic cells, the number of RF carriers per cell and the number of timeslots per carrier. Each element f_{ij} in the matrix is either one or zero, as shown in Figure 5.1.

f_{ij} Timeslot Index

Cell Index	1	2	3	4	5	...						m
1	0	1	0	0	1	...	0	0	0	0	0	1
2	0	0	0	0	0	...	0	1	0	0	0	0
3	0	0	1	0	0	...	0	0	0	1	0	0
...						⋮						
	1	0	1	0	0	...	0	0	1	0	1	0
	0	0	0	1	0	...	1	0	0	0	0	0
n	1	0	0	0	0	...	0	0	0	1	0	0

Figure 5.1: Timeslot allocation matrix used by the GA

The uplink differs from the downlink in that the multiple access interference is asynchronous in the uplink due to the un-coordinated transmissions of the mobile stations, whereas it may remain quasi-synchronous in the downlink. To elaborate a little further, all the synchronous downlink signals of the users sharing a given timeslot are assumed to arrive at the MS via the same propagation channel. The pathloss and shadow fading are updated on a 10 ms frame by frame basis every 15 timeslots. If this channel is dispersive, it does affect the orthogonality of each of the OVSF codes, but the amount of interference inflicted remains lower than in case of the asynchronous uplink, where all multipath components of the asynchronous users arrive at different times at the BS, as discussed in [174]. A possible solution for mitigating the problem of OVSF code orthogonality degradation imposed by channel induced linear distortion is employing Multi-User Detectors (MUDs) [61, 63] at the base stations.

Thus, we define β as the MUD's efficiency, which quantifies the percentage of the intra-cell interference that is removed by the MUD. Setting $\beta = 0.0$ implies 0% efficiency, implying that the intra-cell interference is not reduced by the MUD, whereas $\beta = 1.0$ results in perfect suppression of all the intra-cell interference. Therefore, based on Equation 5.1 uplink SINR expression becomes:

$$SINR_{UL} = \frac{SF \cdot P_{MS}}{(1-\beta)I_{Intra} + I_{Inter} + N_0}, \tag{5.2}$$

in conjunction with a MUD, where P_{MS} is the signal power received by basestation from the mobile user. Again, the inter-cell interference is imposed by the MSs and the BSs in the adjacent cells.

In our previous investigations [41] we quantified the achievable performance of the UTRA TDD/CDMA

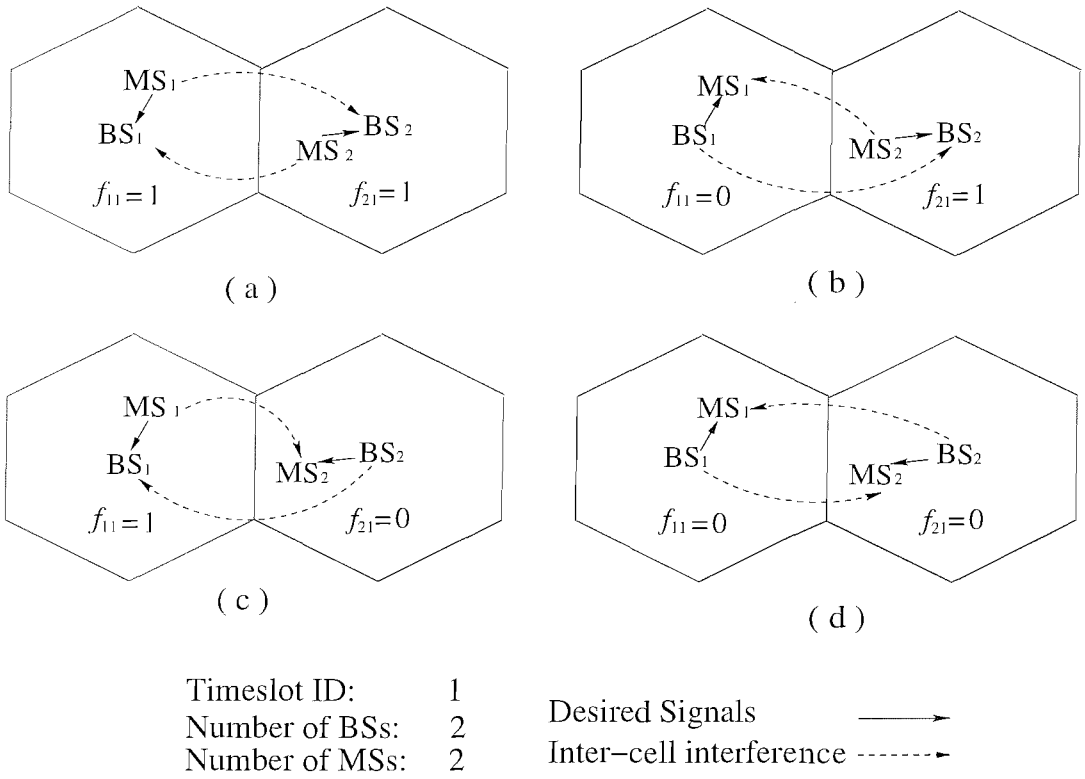

Figure 5.2: An example of UL/DL timeslot allocation options.

system, demonstrating that significant performance improvements can be achieved as a direct result of the interference rejection capabilities of the adaptive antenna arrays and adaptive modulation invoked. Hence the reduction of the interference improved the system's performance. The amount of inter-cell interference imposed depends on the angle of arrival of the interference imposed by the adjacent radio cell. If the timeslot in the interfering cell is used as an uplink timeslot, then we have $f_{ij} = 1$ in Table 5.1, vice versa.

A simple example of the possible timeslot allocation scenarios is given in Figure 5.2, portraying four possible timeslot allocation scenarios for two BSs and two MSs. More specifically in the scenario of Figure 5.2 (a) and (c), BS_1 experiences two types of inter-cell interference, namely $MS_2 \rightarrow BS_1$ and $BS_2 \rightarrow BS_1$ respectively. Similarly, in the scenario seen in Figure 5.2 (b) and (d), MS_1 also experiences two different types of inter-cell interferences imposed by the neighbouring cell, which is experienced as $MS_2 \rightarrow MS_1$ and $BS_2 \rightarrow MS_1$ respectively. In [107] it was shown that the major source of interference is constituted by the BS-to-BS interference as a consequence of the BS's high signal power and the near-LOS propagation conditions prevailing between BSs. Hence we can avoid BS's encountering a high $BS \rightarrow BS$ inter-cell interference by appropriately scheduling the allocation of timeslots. Interference is inherent in cellular systems, and it is challenging to control it in practice due to the presence of random propagation effects. Interference is more severe in urban areas, due

to the typically large number of interfering BSs and MSs. If there are n BSs in an area, for each timeslot, there are 2^n ways of allocating it to a specific BS either in the uplink or downlink. An optimal timeslot allocation algorithm would have to tentatively invoke all possible 2^n TS allocations, in order to find the best one, when a new TS has to be allocated to a user, who is initiating a new call. However, since this new TS allocation affects the entire system's interference patterns, the complexity of the optimum full-search algorithm would become excessive. In order to reduce the complexity of the associated decision, we invoked a genetic algorithm for determining the advantageous scheduling of uplink and downlink timeslots. The genetic algorithm uses an objective function to determine how 'fit' each UL/DL TS allocation is for survival in the consecutive generations of the GA. For instance, the aim of the GA is to determine in our example provided in Section 5.2, which UL/DL TS allocation of the total of four different options has the best overall connection quality, lower UL/DL average power consumption and lower interference level. The GA's objective function will be evaluated for a small fraction of the entire set of possible TS allocations, while aiming for a near-optimum solution.

In the following, several definitions are introduced for the sake of describing the GA's objective function. There are n radio cells and each radio cell is illuminated by a BS belonging to the set:

$$BS \stackrel{def}{=} \{BS_1, BS_2, \cdots, BS_n\}. \tag{5.3}$$

Several actively communicating mobile users belong to a radio cell and there are n sets of MSs, where each set is constituted by the MSs roaming in a specific cell and the entire set of MSs is defined as:

$$M \stackrel{def}{=} \{M_1, M_2, \cdots, M_n\}. \tag{5.4}$$

The GA-assisted timeslot allocation scheme decides the UL/DL transmit direction of each timeslot of a carrier, as shown in each column of Figure 5.1. Then an individual of the GA, which is also often referred to as a genome, can be defined as:

$$f \stackrel{def}{=} \{f_1, f_2, \cdots, f_n\}, \tag{5.5}$$

where f_j $(j = 1, 2, \cdots, n)$ denotes the UL/DL transmit direction of each timeslot of a carrier in a radio cell. As mentioned earlier in Section 5.2, each gene f_j of an individual is either one or zero, where

$$f_j = \begin{cases} 1 & \text{if } cell_j \text{ is dedicated to uplink transmission,} \\ 0 & \text{if } cell_j \text{ is assigned to downlink transmission.} \end{cases}$$

Hence, in Equation 5.1 and Equation 5.2, I_{Inter} can now be written as:

$$I^k_{Inter} = \sum_{j=1:j\neq k}^{n} (f_j \cdot I_{M_j} + (1 - f_j) \cdot I_{BS_j}), \tag{5.6}$$

where I_{M_j} and I_{BS_j} are the inter-cell interference received from the mobile stations and basestation of cell j, respectively. When experiencing an instantaneous $SINR_{UL}^k$ or $SINR_{DL}^k$ for the kth active connection, the received signal power, the amount of intra-cell interference and thermal noise power cannot be readily altered. However, the inter-cell interference can be minimized by advantageously scheduling the UL/DL transmit direction in other radio cells, which maintains the value of $SINR^k$ above the target $SINR$. The performance of the network may be characterized on the basis of the probability of having a sufficiently high SINR for a timeslot. This is defined as:

$$P_{Satisfied} = \frac{N_{adequate}}{N_{outage} + N_{low-quality} + N_{adequate}}, \tag{5.7}$$

where N_{outage}, $N_{low-quality}$ and $N_{adequate}$ are the number of timeslots experiencing an outage, a low quality and adequate SINRs. More explicitly, the probability of $P_{Satisfied}$ quantifies, how 'fit' a specific GA-assisted timeslot allocation is. The values of N_{outage}, $N_{low-quality}$ and $N_{adequate}$ will be determined by comparing each slot's SINR to the thresholds of 6.6, 7.0 and 8.0 dBs. The flowchart of the GA invoked in this chapter is depicted in Figure 5.3. Firstly, an initial population consisting P number of so-called individuals is created in the 'Initialisation' block, where P is known as the population size. Each individual is defined according to Equation 5.5, which represents a legitimate timeslot allocation. The size of each individual of the GA is n ($0 < n \leqslant 49$), which is the number of active BSs in the simulation area containing binary flags corresponding the specific UL/DL TS allocation. There are 49-cells in the simulation area, hence the size of the full search space is 2^{49}. However since not all the BSs are in active status, the GA-assisted TS allocation mechanism will detect the number of active BSs and decide upon the specific size of the search space given by 2^n, which reduces the complexity, when we have $n < 49$. Each binary bit of an individual represents the transmission direction in a cell, and it is a logical if '1', it is dedicated to uplink transmission, and vice versa. This initial population of individuals is generated randomly. The fitness value is evaluated by substituting the candidate solution into the objective function, as indicated by the 'Evaluation' block of Figure 5.3. The evaluation process is invoked according to Equation 5.7. The SINR value of each active connection is calculated according to Equations 5.1 and 5.2. Then the SINR value is classified by comparing it to the SINR thresholds of outage, low quality access and adequate SINRs. The probability of $P_{Satisfied}$ in Equation 5.7 is the individual's fitness value.

5.3 Simulation Results

In our initial investigations we do not impose any user requirements concerning the number of uplink and dowlink TSs requested, we simply aim for determining the best possible UL/DL system configuration, which would allow us to estimate the capacity of the system. The associated UTRA/TDD

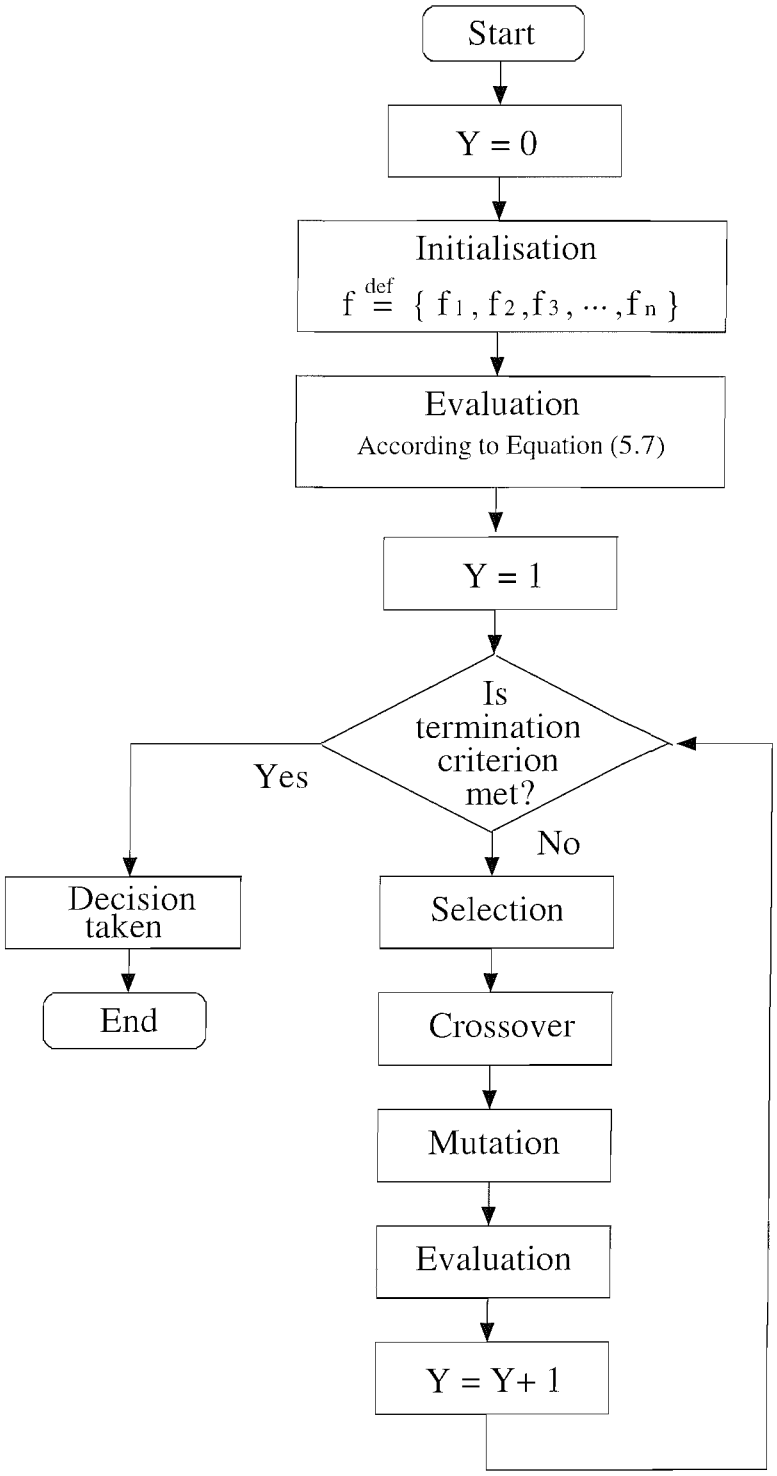

Figure 5.3: A flowchart depicting the structure of a genetic algorithm used for function optimization.

Set-up/Parameter	Method/Value
Individual initialization method	Uniform Random
Selection method	Fitness-Proportionate
Cross-over operation	Single point
Mutation operation	Uniform random bit flip
Population size	Variable P= 4,10,20
Generation size	Variable Y=25,10,5
Probability of Mutation	0.1
Probability of Crossover	0.9
Computational complexity	100

Table 5.1: Configuration of the GA used to obtain the results of Figure 5.4.

system parameters are described in Table 3.2 of Section 3.5.1. These investigations were conducted using a spreading factor of 16. Given that the chip rate of UTRA is 3.84 Mchips/sec, this spreading factor corresponds to a channel data rate of $3.84 \times 10^6/16 = 240$ kbps. Applying 1/2 rate error correction coding would result in an effective data throughput of 120 kbps. A cell radius of 150 m was assumed and a pedestrian walking velocity of 3 mph was used. The simulation area was constituted of 49 traffic cells using the wrapped-around structure of Section 2.2.2.

It was shown for example in Chapter 9 of [61] that the GA's performance is dependent on numerous factors, such as the population size P, the number of generations Y, the choice of the parents' selection method, as well as on a number of other genetic operations employed. In this section, we will quantify the system's achievable performance with the advent of GAs, and attempt to find an appropriate GA set-up and parameter configuration that are best suited for our optimization problem. The GA's parameters are summarized in Table 5.1. Our performance metrics are, as before, the call dropping or forced termination probability P_{FT}, the probability of low quality access P_{low} and the mean transmission power, which were defined in Section 2.1.5. The complexity of the GA is governed by the number of generations Y required, in order to achieve a reliable decision. For the sake of simplicity, the computational complexity of the GA is quantified here in the context of the total number of objective function evaluations, given by $P \times Y$.

Figure 5.4 shows the forced termination probability associated with a variety of traffic loads quantified in terms of the mean normalized carried traffic expressed in Erlangs/km^2/MHz, when subjected to 0.5 Hz frequency shadowing having a standard deviation of 3 dB. As observed in the figure nearly

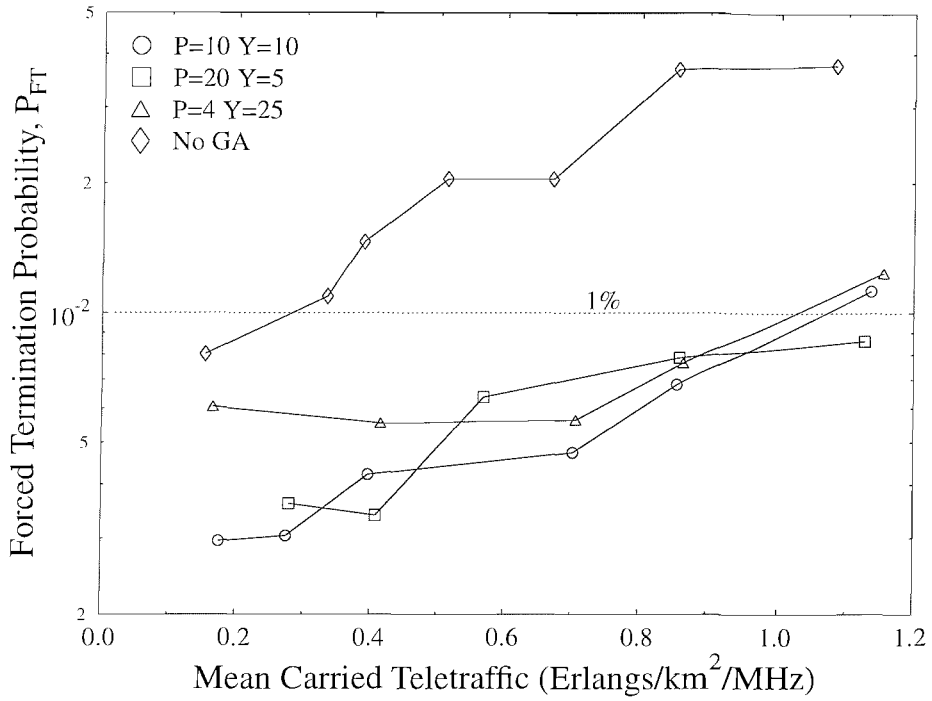

Figure 5.4: Forced termination probability versus mean carried traffic of the UTRA-like TDD/CDMA based cellular network both **with and without GA-assisted timeslots allocation as well as with shadowing having a standard deviation of 3 dB** for SF=16.

an order of magnitude reduction of the forced termination probability has been achieved by employing GA-assisted timeslots scheduling compared to the "No GA" scheme refraining from using UL/DL TS optimization. In the context of the "No GA" scheme, the allocation of the uplink and downlink timeslots for each BS was fixed to a ratio 7:8 (UL:DL). This fixed timeslot allocation may inflict a high BS→BS interference, when the serving cell is using uplink timeslots and the interfering cell is using downlink timeslots, as portrayed in Figure 5.2 (b) or (c). The associated high inter-cell interference may result in a poor SINR, which fails to satisfy the system's target SINR required for maintaining a high-quality connection and hence increases the probability of forced termination. By contrast, in the GA-assisted UTRA TDD/CDMA system each timeslot in a frame can be allocated to either the uplink or downlink, depending on the associated slot-SINR potentially, allowing us to allocate the timeslot by minimizing the inter-cell interference. Inflicted, as we mentioned in the previous section, for a UTRA/TDD system having n BSs, there are 2^n possible UL/DL TS allocation schemes for each timeslot. In our simulated scenario there are 49 wrapped-around traffic cells, as was shown in Figure 2.11, creating a search space of size 2^{49}. As argued before, the size of this search-space is excessive, preventing a full search. As a more attractive design option, a GA is utilized for finding a suboptimum, but highly beneficial uplink or downlink TS allocation. The computational complexity of GA-aided search was set to $P \cdot Y = 100$, while using different P and Y values. The "No GA"

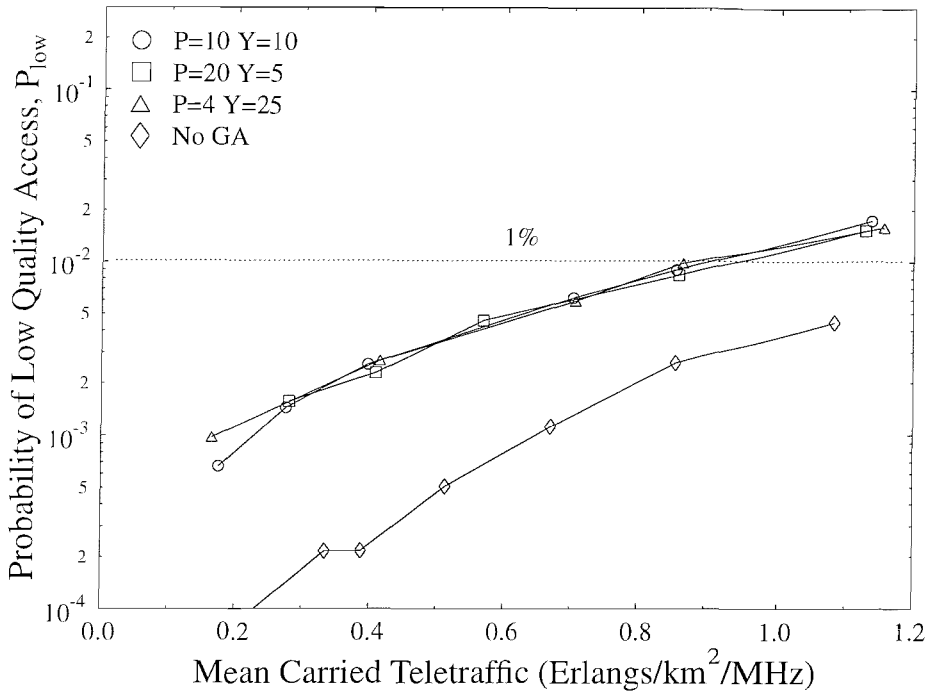

Figure 5.5: Probability of low quality access versus mean carried traffic of the UTRA-like TDD/CDMA based cellular network both **with and without GA-assisted UL/DL TS-allocation as well as with shadowing having a standard deviation of 3dB** for SF=16.

based TDD network was found to support 58 users, at P_{FT} = 1%, corresponding to a traffic load of 0.3 Erlang/km^2/MHz. Upon employing GA-assisted UL/DL timeslot allocation, the number of users supported by the TDD network increased to 185 users, or to an equivalent traffic load of 1.05 Erlang/km^2/MHz, when invoking a population size of 10 and 10 generations. When the population size was reduced to 4 in conjunction with 25 generations, the TDD system was capable of supporting 174 users, corresponding to a teletraffic density of 1.01 Erlang/km^2/MHz.

Figure 5.5 portrays the probability of low quality access versus various traffic loads. It can be seen from the figure that the probability of low quality access for the "No GA" scheme becomes better than that of systems using GA-assisted UL/DL timeslot scheduling. This is a consequence of the associated high probability of forced termination "No GA" scheme, as shown in Figure 5.4, because the higher the probability of forced termination, the lower the number of users supported by the TDD system and hence the effects of co-channel interference imposed by the existing connections remain more benign when a new call starts. Hence a better connection quality is maintained compared to that of the "GA-assisted" scheme. From the figure we observe that the GA-aided TDD system's teletraffic density was limited to 0.87 Erlangs/km^2/MHz, corresponding to 151 users, which was limited by the performance metric P_{low}, as mentioned in Section 2.1.5.

For the sake of characterizing the achievable system performance also for a different perspective,

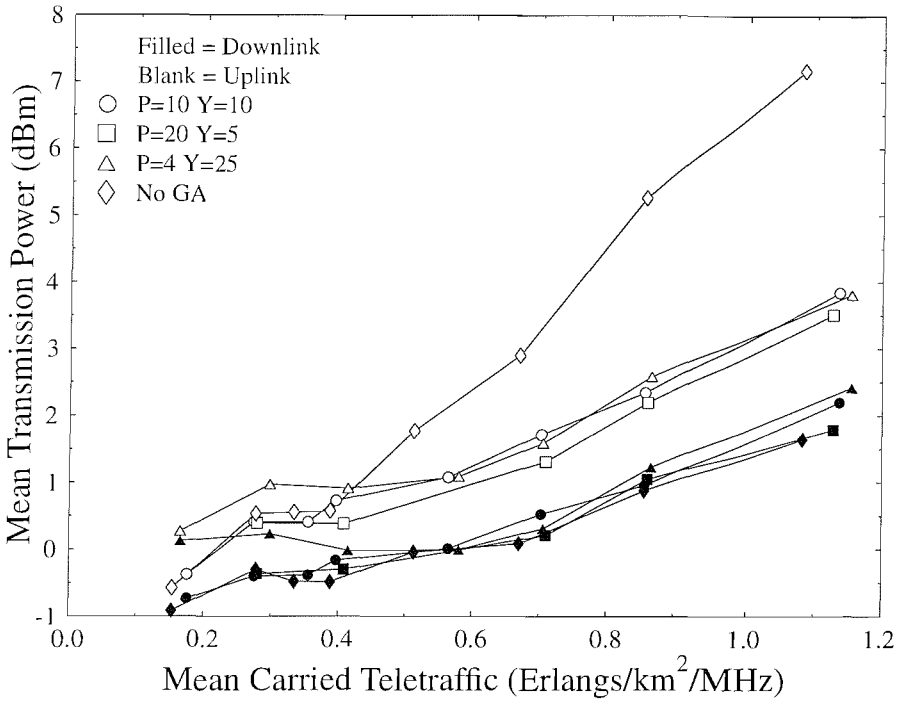

Figure 5.6: Mean transmission power versus mean carried traffic of the UTRA-like TDD/CDMA based cellular network both **with and without both with as well as without GA-assisted UL/DL TS-allocation as well as with shadowing having a standard deviation of 3dB** for a spreading factor of SF=16.

the mean transmission power versus teletraffic performance is depicted in Figure 5.6. We observe in the figure that both the "GA-assisted" and "No GA" scenario obey a similar trend in terms of their downlink power consumption. However, in terms of uplink power consumption, the "No GA" scheme requires an average 2 dB to 5 dB more signal power than the "GA-assisted" scheme, as the traffic load becomes higher. Again, this is because the severe $BS \rightarrow BS$ inter-cell interference degrades the quality of the call. Hence, for the sake of achieving the target SINR and maintain the existing connections, the MSs have to increase their transmission power, which results in an increased interference level imposed on other connections, hence inflicting a performance degradation upon the whole system. The "GA-assisted" system is capable of avoiding the presence of severe interference by advantageously scheduling the UL/DL timeslots, and keep the system's average power as low as possible for the sake of supporting more MSs.

Figure 5.7 shows the ratio of uplink to downlink timslots versus various traffic loads. In the context of the "No GA" scheme we fixed the uplink to downlink timeslot utilization ratio to 0.875, since there are seven uplink timeslots and eight downlink timeslots in each frame. By contrast, in the "GA-assisted" scheme we did not specify the uplink to downlink timeslots ratio. The GA-assisted timeslot scheduling scheme determined whether a timeslot was used in the uplink or downlink of the system.

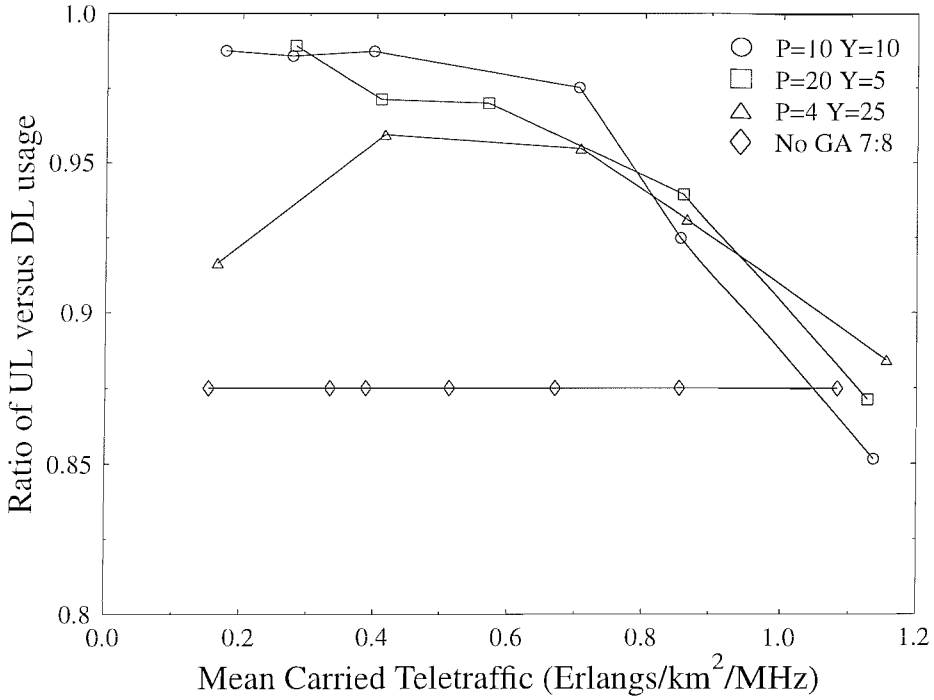

Figure 5.7: Ratio of uplink timeslots to downlink timeslots versus the mean carried traffic of the UTRA-like TDD/CDMA based cellular network both **with and without GA-assisted UL/DL TS allocation and with shadowing having a standard deviation of 3dB** for a spreading factor of SF=16.

From the resultant statistical results we observe that the UL/DL ratio of the "GA-assisted" schemes was between 0.9 and 1.0, which is close to the symmetric traffic load allocation.

5.4 Summary and Conclusion

In this chapter, we introduced a GA-assisted UL/DL timeslot scheduling scheme for the sake of avoiding the severe inter-cell interference caused by using the UTRA TDD/CDMA air interface. The system model and simulation parameters used in this chapter were highlighted in Section 5.2. The GA aided UTRA TDD/CDMA system's performance was then examined using computer simulations in Section 5.3. Summaries of the various parameters and the GA configuration that were used in our simulations were listed in Table 5.1. Significant system performance gains have been achieved by employing the GA-aided UL/DL TS scheduling scheme, as seen in Figure 5.4. The "No GA" based TDD network was found to support 58 users at P_{FT} = 1%, corresponding to a traffic load of 0.6 Erlang/km^2/MHz. Upon employing GA-assisted UL/DL timeslot allocation in conjunction with the computational complexity of $P \cdot Y$ = 100 objective function evaluations, while using a population size of 10 and 10 generations, the number of users supported by the TDD network increased to 185,

or to an equivalent traffic load of 2.11 Erlang/km^2/MHz. In Figure 5.5 we observed that it was the probability of low quality access, not the probability of forced termination, which imposed the more severe constraint on the system's capacity. In Figure 5.6, we compared the power consumption between the "No GA" and the "GA-assisted" TDD system. We observed a similar trend in terms of their downlink power consumption. However, in terms of uplink power consumption the "No GA" scheme requires on average 2 dB to 5 dB more signal power than the "GA-assisted" scheme, as the traffic load is increased.

Chapter 6

Conclusions and Further Work

6.1 Summary and Conclusions

In this thesis we have investigated the performance of a CDMA based cellular mobile network, similar in its nature to the FDD and TDD mode of the UTRA standard.

Chapter 2 examined the performance of an FDD/CDMA based cellular mobile network. In Section 2.1 we characterized the achievable capacity of a UTRA-like FDD CDMA system employing Loosely Synchronized (LS) spreading codes. In our previous investigations presented in [43], OVSF codes were used as spreading codes. However, the intracell interference may only be eliminated by employing orthogonal OVSF codes, if the system is perfectly synchronous and provided that the mobile channel does not destroy the OVSF codes' orthogonality. Current CDMA systems are interference limited, suffering from Inter-Symbol-Interference (ISI), since the orthogonality of the spreading sequences is destroyed by the dispersive channel. They also suffer from Multiple-Access-Interference (MAI) owing to the non-zero cross-correlations of the spreading codes. LS codes exhibit a so-called Interference Free Window (IFW), where both the auto-correlation and cross-correlation values of the codes become zero. Therefore LS codes have the promise of mitigating the effects of both ISI and MAI in time dispersive channels. Hence, LS codes have the potential of increasing the attainable capacity of CDMA networks. A comparison of the OVSF and LS codes was provided in Section 2.1.6. In conjunction with OVSF codes, the number of users supported by the "No beamforming" scenario was limited to 152 users, or to a teletraffic load of approximately 2.65 Erlangs/km^2/MHz. With the advent of employing four-element adaptive antenna arrays at the base stations the number of users supported by the network increased to 428 users, or almost to 7.23 Erlangs/km^2/MHz. However, in conjunction with LS codes, and even without employing antenna arrays at the base stations, the network capacity was dramatically increased to 581 users, or 10.10 Erlangs/km^2/MHz, provided that the cell-size was

sufficiently small for ensuring that all multipath components of the interfering users arrived within the IFW of the code. When four-element adaptive antenna arrays were employed in the above-mentioned LS-code based scenario, the system was capable of supporting 800 users, which is equivalent to a teletraffic load of 13.39 Erlang/km^2/MHz. It was demonstrated that the network performance of the UTRA-like system employing LS spreading codes was substantially better than that of the system using OVSF codes. Explicitly, as evidenced by Figures 2.7, 2.8, 2.10, respectively, a low call dropping probability, low mobile and base station transmission power and high call quality has been maintained. In Section 2.2 we studied the network performance of different FDD/CDMA systems having various cell sizes, i.e. a cell radius of 78 m, 150 m, 300 m, 500 m and 800 m. The simulation results were compared for the sake of quantifying how the cell size affects the achievable system performance. From the results of Figure 2.13 we observed that, as expected, the network's performance became worse, when the cell radius increased and a further improvement of the system's performance was achieved by using adaptive antenna arrays and adaptive modulation, as evidenced by Figure 2.18. The teletraffic density of the scenario having a cell radius of 78 m and employing no antenna arrays at the basestation reached 2.65 Erlang/km^2/MHz, which is about 94 times higher than that of the system having a cell radius of 800 m, which supported a traffic density of 0.028 Erlang/km^2/MHz. When using "2- or 4-element beamforming", the adaptive antenna arrays have considerably reduced the levels of interference, leading to a higher network capacity, as seen in Figure 2.18. In practice, the coverage and capacity requirements within suburban and dense urban environments lead directly to high BS site densities. Hence microcells constitute attractive practical solutions in terms of their relative ease of site acquisition and increased air interface capacity. In Section 2.3 the performance of a UTRA-like FDD/CDMA cellular network was investigated as a function of various target SINR thresholds. As expected, the comparisons seen in Figure 2.23 illustrate that the network's traffic-density performance became worse, when the target SINR was increased, resulting in supporting less links at a better quality. When the target SINR threshold was set to 6 dB, without employing antenna arrays the achievable traffic density reached 1.87 Erlang/km^2/MHz, which is about 27 times higher than that of the scenario, when the SINR value was set to 12 dB, which yielded 0.069 Erlang/km^2/MHz. When using "2- or 4-element beamforming", the adaptive antenna arrays have considerably reduced the levels of interference, leading to a higher network capacity, as evidenced by Figure 2.23. When the SINR threshold was set to 6 dB, with the advent of employing 2-element adaptive antenna arrays at the basestations the achievable traffic density increased by 33% to 2.80 Erlang/km^2/MHz. Replacing the 2-element adaptive antenna arrays with 4-element arrays led to a further traffic density increase of 35%, which is associated with a density of 4.34 Erlangs/km^2/MHz, as seen in Figure 2.23. When the target SINR threshold was increased to 12 dB, we observed in Figure 2.23 that the user-capacity became extremely poor without the employment of adaptive antenna arrays, and only a total of 9

users can be supported in the whole area of 49 base stations. This is because the target SINR was excessive and hence the required transmitted power increased rapidly, which then increased the interference level imposed on other users, until the system became unstable. Hence the receivers' SINR cannot reach the target SINR and hence the vast majority of the calls have to be dropped. The great advantage of using adaptive antenna arrays was clearly demonstrated in this scenario. In conjunction with 2- or 4-element beamforming the number of users supported by the system became a factor four or eight higher than that of 'no beamforming', supporting 43 and 78 users, respectively. Hence, a low value of the target SINR results in a substantially increased number of supported users, additionally benefiting from a superior call quality and from a reduced transmission power at a given number of adaptive antenna array elements installed at the base stations. When the target SINR is excessive, the overall required transmitted power rapidly increases, imposing an increased interference level and hence resulting in a degradation of the network capacity.

We continued our discourse in Section 3.2 by studying the characteristics of UTRA. The UTRA system supports two modes, the FDD mode, where the uplink and downlink signals are transmitted on different frequencies, and the TDD mode, where the uplink and the downlink signals are transmitted on the same carrier frequency, but multiplexed in time [43]. The operating principles of these two schemes were described in Figure 3.2. The UTRA TDD system was then further detailed in Section 3.3 and a comparison between the UTRA TDD system and FDD system was carried out. The UTRA TDD physical layer and physical channels were highlighted in Sections 3.3.1 and 3.3.2, while the power control regime of the TDD system was discussed in Section 3.3.3. One of the major attractions of the UTRA TDD mode is that it allows the uplink and downlink capacities to be adjusted asymmetrically. Recall from Figure 3.6 that the uplink and downlink are supported by the same carrier frequency, which creates additional interference compared to the UTRA FDD mode of the system. Two additional interference scenarios were described in Section 3.4.

We then conducted simulations in Section 3.5.1 for the sake of investigating the achievable performance of the TDD mode in both non-shadowed and shadowed propagation environments, in conjunction with both adaptive antenna arrays and adaptive modulation techniques. As seen in Figure 3.7, the TDD network supported 256 users when experiencing no log-normal shadow fading and using no adaptive antenna arrays. However, with the advent of 2-element adaptive antenna arrays the number of users supported was increased by 27% to 325 users, and when upgrading the system to 4-element arrays, the TDD network supported a further 47% more users, increasing their number to 480 users. As seen in Figure 3.10, when subjected to log-normal shadow fading having a standard deviation of 3 dB in conjunction with a maximum fading frequency of 0.5 Hz, the TDD mode supported about 150 users without adaptive antennas. Again, invoking adaptive antenna arrays at the base stations in-

creased the number of users supported to 203, and 349, when employing two and four array elements, respectively. These results were then improved by applying adaptive modulation techniques, both with and without adaptive antenna arrays. The beamforming based investigations were performed in conjunction with log-normal shadow fading having a standard deviation of 3 dB as well as maximum fading frequencies of both 0.5 Hz and 1.0 Hz. As seen in Figure 3.13, without adaptive antenna arrays the AQAM-aided TDD network supported 223 users at a mean uplink modem throughput of 2.86 BPS. The mean throughput of the downlink was 2.95 BPS. Upon increasing the maximum shadowing frequency from 0.5 Hz to 1.0 Hz the number of users supported by the TDD network reduced slightly to 218 users, whilst the mean modem throughput remained essentially unchanged. However, invoking 2-element adaptive antenna arrays enhanced the TDD network's user population by 64% upon encountering 0.5 Hz shadow fading, and by 56% when subjected to 1.0 Hz shadowing, as evidenced by Figure 3.13. In both cases the mean TDD throughput dropped by approximately 0.3 BPS. A further 0.2 BPS reduction of the mean TDD throughput occurred, when applying 4-element adaptive antenna arrays. However, this allowed an extra 30% of TDD users to be supported, when subjected to shadow fading fluctuating at a maximum frequency of 0.5 Hz and 35% in conjunction with 1.0 Hz frequency shadowing, as supported by Figure 3.13. Therefore, the results of Table 3.4 have shown the significant TDD user-population increases achieved by invoking adaptive modulation techniques, which allowed us to achieve an FDD-like network performance. In Section 2.4 our discussions evolved further by examining the achievable network performance of a MC-CDMA based cellular network benefiting from both adaptive antenna arrays and adaptive modulation techniques. A brief introduction of MC-CDMA was given in Section 2.4.1. The adaptive beamforming and adaptive modulation assisted MC-CDMA network's performance was quantified in Section 2.4.2.

In Chapter 4, we studied the effects of both the hard handover margin and of different power control schemes on the UTRA TDD/CDMA system's performance. In Sections 4.3.1–4.3.4 both closed-loop power control as well as open-loop power control schemes were developed, respectively. In Section 4.3.5 a frame-delay based power adjustment algorithm was proposed to overcome the channel quality variations imposed by the erratically fluctuating timeslot allocations in the different interfering radio cells. To elaborate a little further, we commenced our discourse in Sections 4.1 and 4.2 with a brief introduction to hard handovers in the context of the UTRA TDD/CDMA system. In Section 4.2.1 a relative pilot power based hard handover algorithm [50, 145] was employed. The related simulation results were provided in Section 4.2.2. A handover margin range of 3-10 dB was considered in three different near-symmetric and asymmetric traffic load scenarios. The best hard handover margin was found to be 5 dB in conjunction with $T_{acc} = 0\ dB$ and $T_{drop} = -5\ dB$, whilst meeting the network quality constraints of Section 3.6.3, as evidenced by Figures 4.1, 4.5 and 4.6 of Section 4.2.2.

We then continued our discourse with a power control study of the UTRA-like TDD/CDMA system in Section 4.3. We described a closed-loop power scheme designed for the downlink and uplink in Sections 4.3.1 and 4.3.2, respectively. Although it is a beneficial feature of the UTRA TDD mode that it is capable of supporting both asymmetric traffic and a flexible timeslot allocation, the associated low power control rate often results in a high forced termination probability owing to the associated insufficiently high transmit power. However, this deficiency may be compensated by employing a flexible power control stepsize, as evidenced by the simulation results of Section 4.3.3. Furthermore, An open-loop uplink power control scheme was also developed based on the 3GPP standard [159] in Section 4.3.4. Again, the main advantage of the TDD mode is its flexible timeslot allocation regime capable of adopting to the prevalent traffic requirements. However, this may impose erratic channel quality fluctuations and result in inaccurate power control. As a countermeasure, in Section 4.3.5, we proposed a frame-delay based power adjustment algorithm, which substantially improved the system's performance, as evidenced by Figures 4.27 and 4.31 of Section 4.3.5.

In Chapter 5, we introduced a GA-assisted UL/DL timeslot scheduling scheme for the sake of avoiding the severe inter-cell interference caused by using the UTRA TDD/CDMA air interface. The system model and simulation parameters used in this chapter were highlighted in Section 5.2. The GA aided UTRA TDD/CDMA system's performance was then examined using computer simulations in Section 5.3. Summaries of the various parameters and the GA configuration that were used in our simulations were listed in Table 5.1. Significant system performance gains have been achieved by employing the GA-aided UL/DL TS scheduling scheme, as seen in Figure 5.4. The "No GA" based TDD network was found to support 58 users at $P_{FT} = 1\%$, corresponding to a traffic load of 0.6 Erlang/km^2/MHz. Upon employing GA-assisted UL/DL timeslot allocation in conjunction with the computational complexity of $P \cdot Y = 100$ objective function evaluations, while using a population size of 10 and 10 generations, the number of users supported by the TDD network increased to 185, or to an equivalent traffic load of 2.11 Erlang/km^2/MHz. In Figure 5.5 we observed that it was the probability of low quality access, not the probability of forced termination, which imposed the more severe constraint on the system's capacity. In Figure 5.6, we compared the power consumption between the "No GA" and the "GA-assisted" TDD system. We observed a similar trend in terms of their downlink power consumption. However, in terms of uplink power consumption the "No GA" scheme requires on average 2 dB to 5 dB more signal power than the "GA-assisted" scheme, as the traffic load is increased.

The number of users and the corresponding Erlang capacities of the various cellular systems and various system environments considered are given in Tables 6.1 and 6.2.

Duplex method	Spreading codes	Cell radius	Target SINR	No. of AAA elements	Extracted from Fig.	Modulation mode	Users	Erlang Traffic/ km^2/MHz
FDD	OVSF	78m	8dB	1	2.7	4QAM	152	2.65
FDD	OVSF	78m	8dB	2	2.7	4QAM	242	4.12
FDD	OVSF	78m	8dB	4	2.7	4QAM	428	7.23
FDD	LS	78m	6dB	1	2.7	4QAM	581	10.1
FDD	LS	78m	6dB	2	2.7	4QAM	622	10.6
FDD	LS	78m	6dB	4	2.7	4QAM	802	13.39
FDD	OVSF	150m	8dB	1	2.12	4QAM	150	0.87
FDD	OVSF	150m	8dB	2	2.12	4QAM	239	1.39
FDD	OVSF	150m	8dB	4	2.12	4QAM	348	1.99
FDD	OVSF	300m	8dB	1	2.12	4QAM	139	0.19
FDD	OVSF	300m	8dB	2	2.12	4QAM	229	0.32
FDD	OVSF	300m	8dB	4	2.12	4QAM	385	0.54
FDD	OVSF	500m	8dB	1	2.12	4QAM	142	0.07
FDD	OVSF	500m	8dB	2	2.12	4QAM	222	0.10
FDD	OVSF	500m	8dB	4	2.12	4QAM	370	0.19
FDD	OVSF	800m	8dB	1	2.12	4QAM	138	0.02
FDD	OVSF	800m	8dB	2	2.12	4QAM	217	0.04
FDD	OVSF	800m	8dB	4	2.12	4QAM	371	0.07
FDD	OVSF	150m	6dB	1	2.22	4QAM	320	1.87
FDD	OVSF	150m	6dB	2	2.22	4QAM	489	2.81
FDD	OVSF	150m	6dB	4	2.22	4QAM	758	4.34
FDD	OVSF	150m	10dB	1	2.22	4QAM	53	0.30
FDD	OVSF	150m	10dB	2	2.22	4QAM	113	0.65
FDD	OVSF	150m	10dB	4	2.22	4QAM	156	0.89
FDD	OVSF	150m	12dB	1	2.22	4QAM	9	0.07
FDD	OVSF	150m	12dB	2	2.22	4QAM	43	0.25
FDD	OVSF	150m	12dB	4	2.22	4QAM	78	0.44

Table 6.1: Summary of network performance results using the system parameters of Tables 2.1 and 2.3.

Duplex method	Spreading codes	Cell radius	Target SINR	No. of AAA elements	Extracted from Fig.	Modulation mode	Users	Erlang Traffic/ km^2/MHz
TDD	OVSF	150m	8dB	1	3.10	4QAM	72	0.41
TDD	OVSF	150m	8dB	2	3.10	4QAM	151	0.87
TDD	OVSF	150m	8dB	4	3.10	4QAM	245	1.39
GA-TDD	OVSF	150m	8dB	1	5.4	4QAM	185	1.05
TDD	OVSF	78m	8dB	1	3.16	4QAM	50	0.55
TDD	OVSF	78m	8dB	2	3.16	4QAM	113	1.18
TDD	OVSF	78m	8dB	4	3.16	4QAM	178	2.03
TDD	LS	78m	6dB	1	3.16	4QAM	306	3.45
FDD	OVSF	150m	variable	1	2.17	AQAM	223	1.27
FDD	OVSF	150m	variable	2	2.17	AQAM	366	2.11
FDD	OVSF	150m	variable	4	2.17	AQAM	476	2.68
TDD	OVSF	150m	variable	1	3.13	AQAM	153	0.88
TDD	OVSF	150m	variable	2	3.13	AQAM	320	1.83
TDD	OVSF	150m	variable	4	3.13	AQAM	420	2.41
MC-CDMA	OVSF	150m	6dB	1	2.32(a)	4QAM	323	1.83
MC-CDMA	OVSF	150m	6dB	2	2.32(a)	4QAM	466	2.72
MC-CDMA	OVSF	150m	6dB	4	2.32(a)	4QAM	733	4.18
MC-CDMA	OVSF	150m	variable	1	2.32(b)	AQAM	517	2.95
MC-CDMA	OVSF	150m	variable	2	2.32(b)	AQAM	594	3.50
MC-CDMA	OVSF	150m	variable	4	2.32(b)	AQAM	869	4.98

Table 6.2: Summary of network performance results using the system parameters of Tables 2.7, 3.2 and 3.5.

6.2 Further Work

Our further research includes increasing the achievable total system capacity by invoking space-time coding aided sophisticated Multi-Carrier CDMA networks [175–179]. Additionally, the performance evaluation of AD-HOC networks [180–186] is a promising unexplored area of research.

In the context of the interference limited 3G CDMA system LS codes might hold the promise of an increased network capacity without dramatic changes of the 3G standards. However, LS codes exhibit two impediments. Firstly, the number of spreading codes exhibiting a certain IFW is limited and hence under high user-loads the system may become code-limited, rather than interference-limited. The number of LS codes may be increased using the procedure proposed in [55], but further research is required for increasing the number of codes. A particularly attractive solution is to invoke both DS-CDMA time-domain (TD) and frequency-domain (FD) spreading [187] to multiple carriers in MC-CDMA. This can be achieved for example using LS and OVSF codes in the TD and FD, respectively. Then no multiuser detection (MUD) is required in the TD and the MUD employed in the FD has a low complexity owing to using an OVSF code having a low SF. The total number of users supported becomes the product of the number of LS and OVSF codes.

The second deficiency of LS codes is that they tend to exhibit a short IFW duration. However, this deficiency is also eliminated with the aid of the above-mentioned joint TD and FD spreading regime, because upon spreading to information to multiple carriers the TD chip-duration may be commensurately extended by a factor corresponding to the number of carriers.

We have concentrated our efforts on studying the performance of a UTRA-like TDD/CDMA system in both symmetric and asymmetric traffic scenarios by employing various GA-assisted timeslot scheduling schemes. The most influential factor in determining the achievable system performance is the specific choice of the GA's objective function invoked for capable of determining the near-optimum UL/DL TS allocation based user scheduling. With the aid of a properly designed objective function it is possible to incorporate additional information about the UTRA TDD/CDMA system in the context of different system constraints, such as handover algorithms, user mobility, power control algorithms, average power consumption, call connection quality, symmetric or asymmetric traffic load requirements and etc. Since the system's performance depends on the dimensionality of the GA, it is a meritorious future research item to document the achievable network performance as a function of the GA's affordable complexity. It is also informative to determine the histogram of various network performance metrics for different GA configurations. The further GA-assisted UTRA TDD/CDMA system's achievable performance under asymmetric traffic load constitutes the subject of our further interest.

6.2.1 Advanced Objective Functions

The employment of appropriate objective functions and fitness scaling aided genetic algorithms is often more attractive in network optimization than using the family of classic gradient search based methods, because they do not require the solution of differential equations or a smooth search surface. The genetic algorithm requires only a single measure of how meritorious a single individual is compared to the other individuals [61, 160, 188]. The objective function provides a goodness measure, given a single solution to a problem. In Section 5.3 our objective function evaluates how meritorious a genome is based on two aspects, the average power consumption and the call's connection quality. The mean uplink and downlink transmission power are calculated and compared to that of the previous timeslot, respectively. A mean transmission power value, which requires the lowest power increment compared to that of the previous timeslot is deemed to have a better fitness. To estimate the call's connection quality, the SINR of each uplink/downlink timeslot is compared to the target SINR and the number of low quality outages is monitored. The lower the number of low-quality outages, the better the fitness of an individual . From Figure 5.4 and Figure 5.6 we observe that significant system performance gains have been achieved and in terms of uplink power consumption, since the "No GA" scheme requires on average of 2 dB to 5 dB more signal power than the "GA-assisted" scheme, as the traffic load is increased by employing the GA-aided UL/DL TS scheduling scheme. Hence we may conclude that our scheduling scheme is capable of maintaining a low average power consumption in the context of a UTRA-like TDD/CDMA system. Furthermore, we speculate that a higher system capacity gain can be achieved by invoking more advanced objective functions, since only two aspects of the TDD system, namely its average power consumption and call connection quality were taken into account in optimizing the attainable TDD system performance. In our future research the effects of handovers, power control, the users' movement and other factors on the TDD system's achievable performance will be studied. The effects of the GA's population size, the probability of mutation, the choice of crossover operation, incest prevention and elitism will also be studied with the aid of computer simulations.

6.2.2 Other Types of Genetic Algorithms

In Section 5.3 we used a 'simple' genetic algorithm, employing so-called non-overlapping populations [160]. Some other types of genetic algorithms, namely Steady-State GAs and so-called Deme GAs [188] may be worth investigating.

To elaborate a little further, 'Steady-State' GAs using overlapping populations are similar to the algorithms described by DeJong [189], where the amount of population overlap may be controlled

for the sake of adjusting the GA's properties. The algorithm creates a new temporary population of individuals and adds these to the previous population, then removes the lowest-fitness individuals in order to reduce the population to its original size. Again, the amount of overlap between generations may be controlled. Newly generated offspring are added to the population, then the lowest-fitness individuals are removed, hence the new offspring may or may not survive until the new generation, depending on whether they are more meritorious than the least promising individuals in the current population.

The so-called 'Deme' genetic algorithm [188] has multiple independent populations. Each population evolves using a steady-state genetic algorithm, but in each generation some individuals migrate from one population to another. More specifically, each population migrates a fixed number of its best individuals to the neighboring population. The master population is updated in each generation with the best individuals from each population. Our future work may investigate a range of migration methods or migration operators.

Our computer simulations will comparatively study the above-mentioned types of genetic algorithms at different complexities of $P \cdot Y = C$.

Bibliography

[1] P.-G. Andermo and L.-M. Ewerbring, "A CDMA-based radio access design for UMTS," *IEEE Personal Communications*, vol. 2, pp. 48–53, February 1995.

[2] J. Rapeli, "UMTS: Targets, system concept, and standardization in a global framework," *IEEE Personal Communications*, vol. 2, pp. 20–28, February 1995.

[3] E. Dahlman, B. Gudmundson, M. Nilsson, and A. Skold, "UMTS/IMT-2000 based on wideband cdma," *IEEE Communications Magazine*, vol. 36, pp. 70–80, September 1998.

[4] P. Baier, P. Jung, and A. Klein, "Taking the challenge of multiple access for third-generation cellular mobile radio systems - a European view," *IEEE Communications Magazine*, vol. 34, pp. 82–89, February 1996.

[5] E. Berruto, M. Gudmundson, R. Menolascino, W. Mohr, and M. Pizarroso, "Research activities on UMTS radio interface, network architectures and planning," *IEEE Communications Magazine*, vol. 36, pp. 82–95, February 1998.

[6] H. Aghvami and B. Jafarian, "A vision of UMTS/IMT-2000 evolution," *IEE Journal on Electronics and Communication Engineering*, vol. 12, pp. 148–152, June 2000.

[7] K. Buchanan, R. Fudge, D. McFarlane, T. Phillips, A. Sasaki, and H. Xia, "IMT-2000: service provider's perspective," *IEEE Personal Communications*, vol. 4, pp. 8–13, Augest 1997.

[8] R. Pandya, D. Grillo, E. Lycksell, P. Mieybegue, H. Okinaka, and M. Yabusaki, "IMT-2000 standards: network aspects," *IEEE Personal Communications*, vol. 4, pp. 20–29, Augest 1997.

[9] L. Hanzo, P. J. Cherriman, and J. Streit, *Wireless Video Communications*. John Wiley and IEEE Press, New York, 2001.

[10] D. G. Jeong and W. S. Jeon, "CDMA/TDD system for mobile multimedia communications," in *Proceedings of the IEEE International Conference on Communication, ICC1998*, vol. 2, (Atlanta, GA, USA), pp. 994 – 998, June 1998.

[11] D. G. Jeong and W. S. Jeon, "CDMA/TDD system for wireless multimedia services with traffic unbalance between uplink and downlink," *IEEE Journal on Selected Areas in Communications*, vol. 17, pp. 939–946, May 1999.

[12] *The UMTS Forum website.* http://www.umts-forum.org/.

[13] T. Ojanpera and R. Prasad, "An overview of third-generation wireless personal communications: a european perspective," *IEEE Personal Communications*, vol. 5, pp. 59 – 65, December 1998.

[14] E. Dahlman, B. Gudmundson, M. Nilsson, and A. Skold, "UMTS/IMT-2000 based on wideband CDMA," *IEEE Communications Magazine*, vol. 39, pp. 70–80, September 1998.

[15] B. Brand and A. Aghvami, "Multidimensional PRMA with prioritized Bayesian broadcast-a MAC strategy for multiservice traffic over UMTS," *IEEE Transactions on Vehicular Technology*, vol. 47, pp. 1148–1161, November 1998.

[16] J. Markoulidakis, R. Menolascino, F. Galliano, and M. Pizarroso, "Network planning methodology applied to the UTRA specifications," in *Proceedings of the IEEE International Symposium on Personal, Indoor and Mobile Radio Communications*, vol. 2, (Boston USA), pp. 1009–1013, September 1998.

[17] X. Mestre, M. Najar, C. Anton, and J. Fonollosa, "Adaptive beamforming for high bit rate services in the FDD mode of UTRA," in *Proceedings of the IEEE Vehicular Technology Conference 1999 Fall*, vol. 4, (Amsterdam, Netherlands), pp. 1951–1955, 19-22 September 1999.

[18] S. Akhtar and D. Zeghlache, "Capacity evaluation of the UTRA WCDMA interface," in *Proceedings of the IEEE Vehicular Technology Conference 1999 Fall*, vol. 2, (Amsterdam, Netherlands), pp. 914–918, 19-22 September 1999.

[19] F. Berens, T. Bing, H. Michel, A. Worm, and P. Baier, "Performance of low complexity turbo-codes in the UTRA-TDD-mode," in *Proceedings of the IEEE Vehicular Technology Conference 1999 Fall*, vol. 5, (Amsterdam, Netherlands), pp. 2621–2625, 19-22 September 1999.

[20] N. Haardt and W. Mohr, "The complete solution for third-generation wireless communications: two modes on air, one winning strategy," *IEEE Personal Communications*, vol. 7, pp. 18 – 24, December 2000.

[21] H. Holma, S. Heikkinen, O.-A. Lehtinen, and A. Toskala, "Interference considerations for the time division duplex mode of the UMTS Terrestrial Radio Access," *IEEE Journal on Selected Areas in Communications*, vol. 18, pp. 1386–1393, August 2000.

[22] L. Aguado, T. O'Farrell, and J. Harris, "Evaluation of impact of mixed traffic on UTRA performance," *IEE Electronics Letters*, vol. 36, pp. 1876–1877, October 2000.

[23] H. Haas and S. McLaughlin, "A Dynamic Channel Assignment Algorithm for a Hybrid TDMA/CDMA-TDD Interface Using the TS-Opposing Technique," *IEEE Journal on Selected Areas in Communications*, vol. 19, pp. 1831–1846, October 2001.

[24] M. Guenach and L. Vandendorpe, "Downlink performance analysis of a BPSK-based WCDMA using conventional RAKE receivers with channel estimation," *IEEE Journal on Selected Areas in Communications*, vol. 19, pp. 2165–2176, November 2001.

[25] M. Poza, A. Heras, J. Lablanca, and E. Lopez, "Downlink interference estimation in UMTS," *IEE Electronics Letters*, vol. 37, pp. 590–591, April 2001.

[26] J. Perez-Romero, O. Sallent, R. Agusti, and J. Sanchez, "Managing radio network congestion in UTRA-FDD," *IEE Electronics Letters*, vol. 38, pp. 1384–1386, October 2002.

[27] B. Allen, M. Beach, and P. Karlsson, "Analysis of smart antenna outage in UTRA FDD networks," *IEE Electronics Letters*, vol. 38, pp. 2–3, January 2002.

[28] M. Ruiz-Garcia, J. Romero-Jerez, and A. Diaz-Estrella, "Quality of service support of MAC protocols for multimedia traffic in UTRA," *IEE Electronics Letters*, vol. 38, pp. 139–141, January 2002.

[29] A. Ebner, H. Rohling, R. Halfmann, and M. Lott, "Synchronization in ad hoc networks based on UTRA TDD," in *Proceedings of the IEEE International Symposium on Personal, Indoor and Mobile Radio Communications*, vol. 4, (Lisbon, Portugal), pp. 1650–1654, 15-18 September 2002.

[30] A. Agnetis, G. Brogi, G. Ciaschetti, P. Detti, and G. Giambene, "Optimal packet scheduling in UTRA-TDD," *IEEE Communications Letters*, vol. 7, pp. 112–114, March 2003.

[31] C. Kao and J. Mar, "Intelligent MBWIMA/UMTS protocol using cascade fuzzy logic control for UTRA TDD mode," *IEEE Transactions on Vehicular Technology*, vol. 52, pp. 1663–1674, November 2003.

[32] J. Blogh and L. Hanzo, "Adaptive modulation and adaptive antenna array assisted network performance of multi-user detection aided UTRA-like FDD/CDMA," in *Proceedings of the IEEE Vehicular Technology Conference 2002 Fall*, vol. 3, (Vancouver, Canada), pp. 1806–1810, 24-28 September 2002.

[33] R. Rummler, Y. W. Chung, and H. Aghvami, "A new multicast protocol for UMTS," in *Proceedings of the IEEE Global Telecommunications Conference*, vol. 2, (San Francisco, USA), pp. 687–691, 1-5 December 2003.

[34] Y. Yang and T.-S. Yum, "Maximally flexible assignment of orthogonal variable spreading factor codes for multirate traffic," *IEEE Transactions on Wireless Communications*, vol. 3, pp. 781–792, May 2004.

[35] K. Sivarajah and H. Al-Raweshidy, "Dynamic channel allocation for ongoing calls in UTRA TDD system," *IEE Electronics Letters*, vol. 40, pp. 1197–1198, September 2004.

[36] Y. Yang and T.-S. P. Yum, "UTRA TDD handover performance," in *Proceedings of the IEEE Global Telecommunications Conference*, vol. 5, (Dallas, Texas USA), pp. 3305–3309, 29 Nov. - 3 Dec. 2004.

[37] S. Ni and L. Hanzo, "Genetic algorithm aided timeslot scheduling for UTRA TDD CDMA networks," *IEE Electronics Letters*, vol. 41, pp. 422 – 424, March 2005.

[38] T. Rouse, S. McLaughlin, and I. Band, "Congestion-based routing strategies in multihop TDD-CDMA networks," *IEEE Journal on Selected Areas in Communications*, vol. 23, pp. 668–681, March 2005.

[39] P. Zhang, X. Tao, J. Zhang, Y. Wang, L. Li, and Y. Wang, "A vision from the future: beyond 3g tdd," *IEEE Communications Magazine*, vol. 43, pp. 38–44, January 2005.

[40] S. Ni, H. Wei, J. S. Blogh, and L. Hanzo, "Network Performance of Asynchronous UTRA-like FDD/CDMA Systems using Loosely Synchronised Spreading Codes," in *Proceedings of the IEEE Vehicular Technology Conference 2003 Fall*, vol. 2, (Orlando, USA), pp. 1359 – 1363, October, 2003.

[41] S. Ni, J. S. Blogh, and L. Hanzo, "On the network performance of UTRA-like TDD and FDD CDMA systems using adaptive modulation and adaptive beamforming," in *Proceedings of the IEEE Vehicular Technology Conference 2003 Spring*, vol. 1, (Jeju, Korea), pp. 606 – 610, April, 2003.

[42] S. Ni and L. Hanzo, "Genetically enhanced performance of a UTRA-like time-division duplex CDMA network," in *To appear in the proceedings of the IEEE Vehicular Technology Conference 2005 Spring.*

[43] J. S. Blogh and L. Hanzo, *Third-Generation Systems and Intelligent Wireless Networking - Smart Antennas and Adaptive Modulation.* John Wiley and IEEE Press, 2002.

[44] J. S. Blogh and L. Hanzo, "Adaptive Antenna Assisted Network Performance of FDD-Mode UMTS," in *Proceedings of the IEEE Vehicular Technology Conference 2001 Spring*, (Rhodes, Greece), pp. 2455–2459, May, 2001.

[45] J. S. Blogh and L. Hanzo, "The Network Performance of Multi-Rate FDD-Mode UMTS," in *Proceedings of the IEEE Vehicular Technology Conference 2001 Fall*, (Atlantic City, USA), pp. 1294–1298, October, 2001.

[46] L. Hanzo, C. Wong, and M. Yee, *Adaptive wireless transceivers: Turbo-Coded, Turbo-Equalised and Space-Time Coded TDMA, CDMA and OFDM systems*. John Wiley and IEEE Press, 2002.

[47] F. Adachi, M. Sawahashi, and K. Okawa, "Tree-structured Generation of Orthogonal Spreading Codes with Different Lengths for Forward Link of DS-CDMA Mobile," *IEE Electronics Letters*, vol. 33, no. 1, pp. 27–28, 1997.

[48] S. Stańczak, H. Boche, and M. Haardt, "Are LAS-codes a miracle?," in *Proceedings of the IEEE Global Telecommunications Conference, GLOBECOM '01*, (San Antonio, Texas, USA), pp. 589–593, November, 2001.

[49] D. Li, "A high spectrum efficient multiple access code," *Chinese Journal of Electronics*, vol. 8, pp. 221–226, July 1999.

[50] H. Holma and A. Toskala, eds., *WCDMA for UMTS: Radio Access for Third Generation Mobile Communications*. John Wiley & Sons, Ltd., 2000.

[51] N. B. Mehta, L. J. Greenstein, T. M. Willis, and Z. Kostic, "Analysis and Results for the Orthogonality Factor in WCDMA Downlinks," in *Proceedings of the IEEE Vehicular Technology Conference 2002 Spring*, vol. 1, (Birmingham, AL, USA), pp. 100–104, 6-9 May 2002.

[52] M. Hunukumbure, M. Beach, and B. Allen, "Downlink Orthogonality Factor in UTRA FDD Systems," *IEE Electronics Letters*, vol. 38, pp. 196–197, February 2002.

[53] R. Assarut, K. Kawanishi, R. Deshpande, U. Yamamoto, and Y. Onozato, "Performance evaluation of Orthogonal Variable-Spreading-Factor Code Assignment Schemes in W-CDMA," in *Proceeding of the IEEE International Conference on Communications ICC'2002*, vol. 5, (New York, USA), pp. 3050–3054, 28 April - 2 May 2002.

[54] K. I. Pedersen and P. E. Mogensen, "The Downlink Orthogonality Factors Influence on WCDMA System Performance," in *Proceedings of the IEEE Vehicular Technology Conference 2002 Fall*, vol. 4, (Vancouver, Canada), pp. 2061–2065, 24-28 September 2002.

[55] B. J. Choi and L. Hanzo, "On the Design of LAS Spreading Codes," in *Proceedings of the IEEE Vehicular Technology Conference 2002 Fall*, vol. 4, (Vancouver, Canada), pp. 2172–2176, 24-28 September 2002.

[56] H. Wei, L. Yang, and L. Hanzo, "Interference-free broadband single- and multicarrier ds-cdma," *IEEE Communications Magazine*, vol. 43, pp. 68–73, February 2005.

[57] H. Wei and L. Hanzo, "On the Uplink Performance of LAS-CDMA," in *To appear in the IEEE Vehicular Technology Conference 2005 Spring*, (Stockholm, Sweden), 30 May-1 June 2005.

[58] C.-C. Tseng and C. L. Liu, "Complementary Sets of Sequences," *IEEE Transactions on Information Theory*, vol. 18, pp. 644–652, September 1972.

[59] R. L. Frank, "Polyphase Complementary Codes," *IEEE Transactions on Information Theory*, vol. 26, pp. 641–647, November 1980.

[60] R. Sivaswamy, "Multiphase Complementary Codes," *IEEE Transactions on Information Theory*, vol. 24, pp. 546–552, September 1987.

[61] L. Hanzo, L. L. Yang, E. L. Kuan, and K. Yen, *Single- and Multi-carrier DS-CDMA*. John Wiley and IEEE Press, 2003.

[62] M.-L. Cheng and J.-I. Chuang, "Performance evaluation of distributed measurement-based dynamic channel assignment in local wireless communications," *IEEE Journal on Selected Areas in Communications*, vol. 14, pp. 698–710, May 1996.

[63] S. Verdú, *Multiuser Detection*. Cambridge University Press, 1998.

[64] P. J. Cherriman, E. L. Kuan, and L. Hanzo, "Burst-by-burst adaptive joint-detection CDMA/H.263 based video telephony," in *IEEE Transactions on Circuits and Systems for Video Technology*, vol. 12, pp. 342–348, May 2002.

[65] H. Wei, L. Yang, and L. Hanzo, "Interference-free broadband single- and multicarrier ds-cdma," *IEEE Communications Magazine*, vol. 43, pp. 68–73, February 2005.

[66] B. Walke, *Mobile Radio Networks - Networking, Protocols and Traffic Performance, 2nd Edition*. John Wiley and Sons, IEEE Press, New York, 2002.

[67] G. J. Foschini and Z. Miljanic, "Distributed Autonomous Wireless Channel Assignment Algorithm with Power Control," *IEEE Transactions on Vehicular Technology*, vol. 44, pp. 420–429, August 1995.

[68] J. Chuang and N. R. Sollenberger, "Spectrum Resource Allocation for Wireless Packet Access with Application to Advanced Cellular Internet Service," *IEEE Journal on Selected Areas in Communications*, vol. 16, pp. 820–829, August 1998.

[69] M. Soleimanipour, W. Zhuang, and G. H. Freeman, "Modelling and resource allocation in wireless multimedia CDMA system," in *Proceedings of the IEEE Vehicular Technology Conference 1998 Spring*, vol. 2, (Ottawa, Canada), pp. 1279–1283, 18-21 May 1998.

[70] A. S. Acampora and M. Naghshinen, "Control and Quality-of-Service Provisioning in High-Speed Microcellular Networks," *IEEE Personal Communications*, vol. 1, pp. 36–43, 2nd Quarter 1994.

[71] L. Hanzo, M. Muenster, B. Choi, and T. Keller, *OFDM and MC-CDMA for Broadband Multi-user Communications, WLANs and Broadcasting.* John Wiley and IEEE Press, 2003.

[72] N. Yee, J.-P. Linnartz, and G. Fettweis, "Multicarrier CDMA in indoor wireless radio networks," in *Proceedings of the IEEE Personal, Indoor and Mobile Radio Communications, PIMRC'93*, vol. 1, pp. 109–113, 1993.

[73] K. Fazel and L. Papke, "On the performance of convolutionally-coded CDMA/OFDM for mobile communication system," in *Proceedings of the IEEE Personal, Indoor and Mobile Radio Communications, PIMRC'93*, vol. 1, pp. 468–472, 1993.

[74] A. Chouly, A. Brajal, and S. Jourdan, "Orthogonal multicarrier techniques applied to direct sequence spread spectrum CDMA systems," in *Proceedings of the IEEE Global Telecommunications Conference 1993*, (Houston, TX, USA), pp. 1723–1728, 29 November – 2 December 1993.

[75] V. M. DaSilva and E. S. Sousa, "Performance of orthogonal CDMA codes for quasi-synchronous communication systems," in *Proceedings of the IEEE International Conference on Universal Personal Communications, ICUPC '93*, (Ottawa, Canada), pp. 995–999, October 1993.

[76] L. Vandendorpe, "Multitone direct sequence CDMA system in an indoor wireless environment," in *Proceedings of the IEEE Symposium on Communications and Vehicular Technology, SCVT1993*, (Delft, The Netherlands), pp. 4.1.1–4.1.8, October 1993.

[77] R. Prasad and S. Hara, "Overview of multicarrier CDMA," *IEEE Communications Magazine*, vol. 35, pp. 126–133, December 1997.

[78] R. Prasad and S. Hara, "Overview of multi-carrier CDMA," in *Proceedings of the IEEE International Symposium on Spread Spectrum Techniques and Applications ISSSTA'1996*, (Mainz, Germany), pp. 107–114, 22–25 September 1996.

[79] D. I. Scott, P. M. Grant, S. McLaughlin, G. Povey, and D. Cruickshank, "Research in reconfigurable terminal design for mobile and personal communications," tech. rep., Department of Electrical Engineering, The University of Edinburgh, March 1997.

[80] N. Yee and J. P. Linnartz, "MICRO 93-101: Multi-carrier CDMA in an indoor wireless radio channel," tech. rep., University of California at Berkeley, 1994.

[81] L. Hanzo, S. Ng, W. Webb, and T. Keller, *Quadrature Amplitude Modulation: From Basics to Adaptive Trellis-Coded, Turbo-Equalised and Space-Time Coded OFDM, CDMA and MC-CDMA Systems.* John-Wiley, IEEE Press, September 2004.

[82] "COST 207 : Digital land mobile radio communications, final report," tech. rep., Office for Official Publications of the European Communities, Luxembourg, 1989.

[83] M. Haardt, A. Klein, R. Koehn, S. Oestreich, M. Purat, V. Sommer, and T. Ulrich, "The TD-CDMA Based UTRA TDD Mode," *IEEE Journal on Selected Areas in Communications*, vol. 18, pp. 1375–1385, August 2000.

[84] J. Gibson, *The Mobile Communications Handbook.* CRC PRESS, 1996.

[85] W. Lu, B. Walke, and X. Shen, "4G mobile communications: toward open wireless architecture," *IEEE Personal Communications*, vol. 11, pp. 4–6, April 2004.

[86] T. Le and H. Aghvami, "Fast channel access and DCA scheme for connection and connectionless-oriented services in UMTS," *IEE Electronics Letters*, vol. 35, pp. 1048–1049, June 1999.

[87] B. Walke, M. Althoff, and P. Seidenberg, *UMTS - A Comprehensive Introduction.* John Wiley and Sons, IEEE Press, New York, 2002.

[88] R. Steele and L. Hanzo, *Mobile Radio Communications.* Piscataway, NJ: IEEE Press, 1999.

[89] T. Kriengchaiyapruk and I. Forkel, "Adaptive switching point allocation in TD/CDMA systems," in *Proceedings of the IEEE Vehicular Technology Conference 2002 Fall*, vol. 3, (Vancouver, Canada), pp. 1456–1460, 24-28 September 2002.

[90] J. Laiho, A. Wacker, and T. Novosad, *Radio Network Planning and Optimisation for UMTS.* John Wiley & Sons, Ltd. and IEEE Press, 2002.

[91] H. Holma, G. J. R. Povey, and A. Toskala, "Evaluation Interference Between Uplink and Downlink in UTRA/TDD," in *Proceedings of the IEEE Vehicular Technology Conference 1999 Fall*, vol. 5, (Amsterdam, the Netherlands), pp. 2616–2620, 19-22 September 1999.

[92] J. Laiho-Steffens, A. Wacker, and P. Aikio, "The Impact of the Radio Network Planning and Site Configuration on the WCDMA Network Capacity and Quality of Service," in *Proceedings of the IEEE Vehicular Technology Conference 2000 Spring*, vol. 2, (Tokyo, Japan), pp. 1006–1010, 2000.

[93] K. Hiltunen and R. de Bernadi, "WCDMA Downlink Capacity Estimation," in *Proceedings of the IEEE Vehicular Technology Conference 2000 Spring*, vol. 2, (Tokyo, Japan), pp. 992–996, 2000.

[94] K. Sipilä, Z. C. Honkasalo, J. Laiho-Steffens, and A. Wacker, "Estimation of Capacity and Required Transmission Power of WCDMA Downlink Based on a Downlink Pole Equation," in *Proceedings of the IEEE Vehicular Technology Conference 2000 Spring*, vol. 2, (Tokyo, Japan), pp. 1002–1005, 2000.

[95] H. Haas, S. McLaughlin, and G. J. R. Povey, "A Novel Interference Resolving Algorithm for the TDD TD-CDMA Mode in UMTS," in *Proceedings of the IEEE International Symposium on Personal, Indoor and Mobile Radio Communications*, vol. 2, (London, UK), pp. 1231–1235, September 2000.

[96] T. Kriengchaiyapruk, *Dynamic Channel Allocation in UTRA-TDD.* PhD thesis, Lehrstuhl für Kommunikationsnetze, July 2004.

[97] Q. Y. Miao, W. B. Wang, and D. C. Yang, "The Coexistence of UTRA-TDD and FDD System In the Adjacent Channel," in *Proceedings of the IEEE Global Telecommunications Conference, Globecom 2001*, vol. 6, (San Antonio, U.S.A.), pp. 3714–3718, November 2001.

[98] T. L. Lee, C. Faure, and D. Grandblaise, "Impact of FDD/TDD Co-Existence on Overall UMTS System Performance," in *Proceedings of the IEEE Vehicular Technology Conference 2001 Spring*, vol. 4, (Rhodes, Greece), pp. 2655–2659, May 2001.

[99] H. Haas, S. McLaughlin, and G. Povey, "Capacity-coverage analysis of TDD and FDD Mode in UMTS at 1920MHz," *IEE Electronics and Communication Engineering Journal*, vol. 149, pp. 51–57, February 2002.

[100] I. Forkel, P. Seidenberg, R. Pabst, and G. Heidelberger, "Performance Evaluation of Power Control Algorithms in Cellular UTRA Systems," *3G Mobile Communication Technologies (3G 2001)*, pp. 11–15, March 2001.

[101] J. Kurjenniemi, S. Hämäläinen, T. Ristaniemi, O. Lehtinen, and P. Patronen, "Convergence of UTRA TDD Uplink Power Control," in *Proceedings of the IEEE Vehicular Technology Conference 2001 Spring*, vol. 4, (Rhodes, Greece), pp. 2908–2912, May 2001.

[102] J. Wen, J. Sheu, and J. Chen, "An Optimum Downlink Power Control Method for CDMA Cellular Mobile Systems," in *Proceedings of the IEEE International Conference on Communication, ICC2001*, vol. 6, (Helsinki, Finland), pp. 1738–1742, Jun 2001.

[103] J. Kurjenniemi, S. Hämäläinen, and T. Ristaniemi, "Uplink Power Control in UTRA TDD," in *Proceedings of the IEEE International Conference on Communication, ICC2001*, vol. 5, (Helsinki, Finland), June 2001.

[104] Q. Wu, "Performance of optimum transmitter power control in CDMA cellular mobile systems," *IEEE Transactions on Vehicular Technology*, vol. 48, pp. 571–575, March 1999.

[105] R. Choi and R. Murch, "Evaluation of a Pre-Rake Smart Antenna System for TDD CDMA Systems," in *Proceedings of the IEEE Vehicular Technology Conference 2002 Fall*, vol. 1, (Vancouver, Canada), pp. 346–350, September 2002.

[106] R. Machauer, M. Iurascu, and F. Jondral, "FFT Speed Multiuser Detection for High Rate Data Mode in UTRA-FDD," in *Proceedings of the IEEE Vehicular Technology Conference 2001 Fall*, vol. 1, (Atlantic U.S.A.), pp. 502–505, October 2001.

[107] X. Wu, L.-L. Yang, and L. Hanzo, "Uplink capacity investigations of TDD/CDMA," in *Proceedings of the IEEE Vehicular Technology Conference, VTC Spring 2002*, vol. 2, (Birmingham, Alabama, USA), pp. 997 – 1001, 6-9 May 2002.

[108] S. Tekinay and B. Jabbari, "Handover and channel assignment in mobile cellular networks," *IEEE Communications Magazine*, vol. 29, pp. 42–46, November 1991.

[109] E. Berruto, M. Gudmundson, R. Menolascino, W. Mohr, and M. Pizarroso, "Research activities on UMTS radio interface, network architectures, and planning," *IEEE Communications Magazine*, vol. 36, pp. 82–95, Feburary 1998.

[110] I. Katzela and M. Naghshineh, "Channel assignment schemes for cellular mobile telecommunication systems: a comprehensive survey," *IEEE Personal Communications*, vol. 3, pp. 10–31, June 1996.

[111] B. Jabbari, "Teletraffic aspects of evolving and next-generation wireless communication networks," *IEEE Personal Communications*, vol. 3, pp. 4–9, December 1996.

[112] N. D. Tripathi, J. H. Reed, and H. F. VanLandinoham, "Handoff in cellular systems," *IEEE Personal Communications*, vol. 5, pp. 26–37, December 1998.

[113] R. Vijayan and J. Holtzman, "A model for analyzing handoff algorithms," *IEEE Transactions on Vehicular Technology*, vol. 42, pp. 351–356, August 1993.

[114] J. Wang, J. Liu, and Y. Cen, "Handoff algorithms in dynamic spreading WCDMA system supporting multimedia traffic," *IEEE Journal on Selected Areas in Communications*, vol. 21, pp. 1652–1662, December 2003.

[115] D. Lugara, J. Tartiere, and L. Girard, "Performance of UMTS to GSM handover algorithms," in *Proceedings of the IEEE International Symposium on Personal, Indoor and Mobile Radio Communications*, vol. 1, (Barcelona, Spain), pp. 444–448, 5-8 September 2004.

[116] O. Grimlund and B. Gudmundson, "Handoff strategies in microcellular," in *Proceedings of the IEEE Vehicular Technology Conference*, pp. 505–510, 19-22 May 1991.

[117] A. Viterbi, A. Viterbi, K. Gilhousen, and E. Zehavi, "Soft handoff extends CDMA cell coverage and increases reverse link capacity," *IEEE Journal on Selected Areas in Communications*, vol. 12, pp. 1281–1288, October 1994.

[118] E. Nakano, N. Umeda, and K. Ohno, "Performance of diversity handover in DS-CDMA cellular systems," in *Proceedings of the IEEE 4th International Conference on Universal Personal Communications*, (Tokyo, Japan), pp. 421–425, November 1995.

[119] Y.-I. Kim, K.-J. Lee, and Y.-O. Chin, "Analysis of multi-level threshold handoff algorithm," in *Proceedings of the IEEE Global Telecommunications Conference, GLOBECOM '96*, vol. 2, (London, UK), pp. 1141–1145, November 1996.

[120] D. Wong and D. Cox, "A handoff algorithm using pattern recognition," in *Proceedings of the IEEE International Conference on Universal Personal Communications*, vol. 1, (Florence, Italy), pp. 759–763, October 1998.

[121] S. Tekinay and B. Jabbari, "A measurement-based prioritization scheme for handovers in mobile cellular networks," *IEEE Journal on Selected Areas in Communications*, vol. 10, pp. 1343–1350, October 1992.

[122] D. Calin and D. Zeghlache, "Performance and handoff analysis of an integrated voice-data cellular system," in *Proceedings of the IEEE 8th International Symposium on Personal, Indoor and Mobile Radio Communications*, vol. 2, (Helsinki, Finland), pp. 386–390, 1997.

[123] N. Benvenuto and F. Santucci, "A least squares path-loss estimation approach to handover algorithms," *IEEE Transactions on Vehicular Technology*, vol. 48, pp. 437–447, March 1999.

[124] F. Santucci, M. Pratesi, M. Ruggieri, and F. Graziosi, "A general analysis of signal strength handover algorithms with cochannel interference," *IEEE Transactions on Communications*, vol. 48, pp. 231–241, February 2000.

[125] X. Yang, S. Ghaheri-Niri, and R. Tafazolli, "Performance of power-triggered and E_c/N_0-triggered soft handover algorithms for UTRA," in *Second International Conference on 3G Mobile Communication Technologies*, no. 477, (London, UK), pp. 7–10, 2001.

[126] S. Wang, S. Sridhar, and M. Green, "Adaptive soft handoff method using mobile location information," in *Proceedings of the IEEE Vehicular Technology Conference 2002 Spring*, vol. 4, (Birmingham, Alabama, USA), pp. 1936 – 1940, 6-9 May 2002.

[127] H. Persson and J. Karlsson, "Maintaining QoS by utilizing hierarchical wireless systems," in *Proceedings of The 9th Asia-Pacific Conference on Communications*, vol. 1, (Penang, Malaysia), pp. 292–296, 21-24 September 2003.

[128] A. Tolli, I. Barbancho, J. Gomez, and P. Hakalin, "Intra-system load balancing between adjacent GSM cells," in *Proceedings of the IEEE Vehicular Technology Conference*, vol. 1, (Jeju Island, Korea), pp. 393 – 397, 22-25 April 2003.

[129] J. Kim, D. H. Kim, P. jung Song, and S. Kim, "Design of optimum parameters for handover initiation in WCDMA," in *Proceedings of the IEEE Vehicular Technology Conference*, vol. 4, (Atlantic City, NJ, USA), pp. 2768 – 2772, 7-11 October 2001.

[130] B. Singh, K. Aggarwal, and S. Kumar, "An analytical model for intersystem handover," in *Proceedings of the IEEE Conference on Convergent Technologies for Asia-Pacific Region*, vol. 4, (Bangalore, India), pp. 1311–1315, 15-17 October 2003.

[131] G. Durastante and A. Zanella, "An efficient monitoring strategy for intersystem handover from TD-SCDMA to GSM networks," in *Proceedings of the IEEE International Symposium on Personal, Indoor and Mobile Radio Communications (PIMRC) 2002*, vol. 4, (Lisbon, Portugal), pp. 1555 – 1560, 15-18 September 2002.

[132] M. Iwamura and A. Aghvami, "Impact of handover blocking on control load, capacity and coverage of W-CDMA downlink," in *Proceedings of the IEEE International Symposium on Personal, Indoor and Mobile Radio Communications (PIMRC) 2004*, vol. 1, (Barcelona, Spain), pp. 350 – 354, 5-8 September 2004.

[133] K. Hiramatsu, K. Miya, O.Kato, and K. Homma, "Transmit diversity applied on the CDMA/TDD cellular systems," in *Proceedings of the IEEE Vehicular Technology Conference*, vol. 2, (Tokyo, Japan), pp. 1170 – 1174, 15-18 May 2000.

[134] P. Chaudhury, W. Mohr, and S. Onoe, "The 3gpp proposal for imt-2000," *IEEE Communications Magazine*, vol. 37, pp. 72–81, December 1999.

[135] J. Rodriguez, X. Yang, R. Tafazolli, D. Huy, V. Monteiro, and A. Gameiro, "Dynamic System Level Performance for MC-CDMA Scheme," in *Proceedings of the European Wireless Conference 2004*, (Barcelona, Spain), 24-27 February 2004.

[136] S. H. Hwang and L. Hanzo, "Effects of multipath propagation delay on uplink performance of synchronous DS-CDMA systems communicating in dispersive Rayleigh fading channels," *IEE Electronics Letters*, vol. 40, pp. 1589 – 1591, December 2004.

[137] TS25.201, "Technical Specification Group Radio Access Network; Physical layer - General description," *3GPP TSG R6, v6.0.0*, 2003-12.

[138] X. Yang, S. Ghaheri-Niri, and R. Tafazolli, "Evaluation of soft handover algorithms for UMTS," in *Proceedings of the IEEE International Symposium on Personal, Indoor and Mobile Radio Communications (PIMRC) 2000*, vol. 2, (London, UK), pp. 772 – 776, 18-21 September 2000.

[139] N. Binucci, K. Hiltunen, and M. Caselli, "Soft handover gain in WCDMA," in *Proceedings of the IEEE Vehicular Technology Conference*, vol. 3, (Boston, MA, USA), pp. 1467 – 1472, 24-28 September 2000.

[140] K. Sipila, M. Jasberg, J. Laiho-Steffens, and A. Wacker, "Soft handover gains in a fast power controlled WCDMA uplink," in *Proceedings of the IEEE Vehicular Technology Conference 1999 Spring*, vol. 2, (Houston, Texas, USA), pp. 1594 – 1598, 16-20 May 1999.

[141] W. L. Lim, Y. C. Foo, and R. Tafazolli, "Adaptive softer handover algorithm for high altitude platform station UMTS with onboard power resource sharing," in *Proceedings of the IEEE International Symposium on Wireless Personal Multimedia Communications*, vol. 1, (Hawaii, USA), pp. 52 – 56, 27-30 October 2002.

[142] W.-U. Pistelli and R. Verdone, "Downlink capacity for WCDMA with soft and softer handover; advantages of unbalanced received powers," in *Proceedings of the IEEE International Symposium on Wireless Personal Multimedia Communications*, vol. 1, (Hawaii, USA), pp. 77 – 81, 27-30 October 2002.

[143] R. Verdone and A. Zanella, "Performance of received power and traffic driven handover algorithms in urban cellular networks," *IEEE Transactions on Wireless Communications*, vol. 9, pp. 60 – 70, February 2002.

[144] TS25.331, "Technical Specification Group Radio Access Network; Radio Resource Control (RRC)," *3GPP TSG R6, v6.0.1*, 2004-01.

[145] R. Owen, P. Jones, and S. D. adn D. Lister, "Uplink WCDMA capacity and range as a function of inter-to-intra cell interference: theory and pratice," in *Proceedings of the IEEE Vehicular Technology Conference 2000 Spring*, vol. 1, (Tokyo, Japan), pp. 298–303, 2000.

[146] D. Calin and M. Areny, "Impact of Radio Resource Allocation Policies on the TD-CDMA System Performance: Evaluation of Major Critical Parameters," *IEEE Journal on Selected Areas in Communications*, vol. 19, pp. 1847–1859, October 2001.

[147] TS25.105, "Technical Specification Group Radio Access Network; Base Station (BS) radio transmission and reception (TDD)," *3GPP TSG R6, v6.0.0*, 2003-12.

[148] J. Kurjenniemi, S. Hämäläinen, and T. Ristanlemi, "UTRA TDD handover performance," in *Proceedings of the IEEE Global Telecommunications Conference, GLOBECOM '01*, vol. 1, (San Antonio, Texas, USA), pp. 533–537, 2001.

[149] TS25.123, "Technical Specification Group Radio Access Network; Requirements for support of radio resource management," *3GPP TSG R6, v6.0.0*, 2003-12.

[150] A. Chockalingam, P. Dietrich, L. Milstein, and R. Rao, "Performance of closed-loop power control in DS-CDMA cellular systems," *IEEE Transactions on Vehicular Technology*, vol. 47, pp. 774–789, August 1998.

[151] R. Gejji, "Forward-link-power control in CDMA cellular-systems," *IEEE Transactions on Vehicular Technology*, vol. 41, pp. 532–536, November 1992.

[152] J. Dunlop, J. Irvine, and B. Manzanedo, "Power control in a cellular adaptive air interface," *IEE Electronics Letters*, vol. 32, pp. 1968–1969, October 1996.

[153] B. Manzanedo, P. Cosimini, J. Irvine, and J. Dunlop, "Implementation and assessment of adaptive power control in a 3rd generation cellular system," in *Proceedings of the IEEE Vehicular Technology Conference 1996 Spring*, vol. 2, (Atlanta, USA), pp. 1135 – 1139, 28 April-1 May 1996.

[154] TS25.104, "Technical Specification Group Radio Access Network; Base Station (BS) radio transmission and reception (FDD)," *3GPP TSG R6, v6.7.0*, 2004-09.

[155] TS25.222, "Technical Specification Group Radio Access Network; Multiplexing and channel coding (TDD)," *3GPP TSG R6, v6.0.0*, 2003-12.

[156] TS25.224, "Technical Specification Group Radio Access Network; Physical layer procedures (TDD)," *3GPP TSG R6, v6.2.0*, 2004-09.

[157] J. Kurjenniemi, O. Lehtinen, and T. Ristaniemi, "Signaled step size for downlink power control of dedicated channels in UTRA TDD," in *4th International Workshop On Mobile and Wireless Communications Network, 2002*, vol. 1, (Stockholm, Sweden), pp. 675–679, 2002.

[158] J. D. Gibson, *The Communications Handbook*. CRC Press and IEEE Press, Boca Ration, Florida, 1997.

[159] "3rd Generation Partnership Project; Technical Specification Group Radio Access Network; Physical layer procedures (TDD)." 3G TS 25.224 V4.3.0 (2001-12).

[160] D. Goldberg, *Genetic Algorithms in Search, Optimization, and Machine Learning*. ISBN 0201157675, MA USA: Addison-Wesley, August 2001.

[161] J. Holland, *Adaptation in Natural and Artificial Systems*. Ann Arbor, Michigan: University of Michigan Press, 1975.

[162] M. Mitchell, *An Introduction to Genetic Algorithms*. Cambridge, Massachusetts: MIT Press, 1996.

[163] D. Whitley, "A Genetic Algorithm Tutorial," *Statistics and Computing*, vol. 4, pp. 65 – 85, June 1994.

[164] S. Forrest, "Genetic algorithms: Principles of natural selection applied to computation," *Science*, vol. 261, pp. 872 – 878, August 1993.

[165] H. Mühlenbein, *Foundations of Genetic Algorithms*, ch. Evolution in time and space – The Parallel Genetic Algorithm, pp. 316–337. California, USA: G. Rawlins, ed., Morgan Kaufmann, 1991.

[166] J. J. Grefenstette and J. E. Baker, "How genetic algorithms work: A critical look at implicit parallelism," in *Proceedings of the IEEE Third International Conference on Genetic Algorithms* (J. D. Schaffer, ed.), (California, USA), pp. 20–27, Morgan Kaufmann, 1989.

[167] A. Wolfgang, N. N. Ahmad, S. Chen, and L. Hanzo, "Genetic algorithm assisted minimm bit error rate beamforming," in *CDROM of the IEEE 59th Vehicular Technology Conference*, vol. 1, (Milan Italy), pp. 142 – 146, 17-19 May, 2004.

[168] M. Alias, A. Samingan, S. Chen, and L. Hanzo, "Multiple antenna aided OFDM employing minimum bit error rate multiuser detection," *IEE Electronics Letters*, vol. 39, pp. 1769–1770, November 2003.

[169] E. Hou, N. Ansari, and H. Ren, "A Genetic Algorithm for Multiprocessor Scheduling," *IEEE Transaction on Parallel and Distributed Systems*, vol. 5, pp. 113 – 120, February 1994.

[170] K.-S. Tang, K.-T. Ko, K. F. Man, and S. Kwong, "Topology Design and Bandwidth Allocation of Embedded ATM Networks Using Genetic Algorithms," *IEEE Communications Letters*, vol. 2, pp. 171 – 173, June 1998.

[171] C. Y. Ngo and V. O. K. Li, "Fixed Channel Assignment in Cellular Radio Network Using a Modified Genetic Algorithm," *IEEE Transactions on Vehicular Technology*, vol. 47, pp. 163 – 172, February 1998.

[172] D. Sadot, U. Mahlab, and V. Natan-Bar, "New method for developing optical CDMA address code sequences using the genetic algorithm," in *Proceedings of the IEEE International Conference on Communication, ICC1998*, vol. 3, (Atlanta, GA, USA), pp. 7–11, June 1998.

[173] Y. H. Lee, S. T. Sheu, and M. H. Chen, "Application of Genetic Algorithm for Optimal Simultaneous Code Set Selection in Optical CDMA," in *Modelling and Simulation, MS99*, vol. 3, (Philadelphia, USA), pp. 5 – 8, May 1999.

[174] S. H. Hwang and L. Hanzo, "Reverse-link performance of synchronous DS-CDMA systems in dispersive Rician multipath fading channels," *IEE Electronics Letters*, vol. 39, pp. 1682–1684, November 2003.

[175] S. Hara and R. Prasad, "Overview of Multicarrier CDMA," *IEEE Communications Magazine*, vol. 35, pp. 126–133, December 1997.

[176] B. Abdool-Rassool, F. Heliot, L. Revelly, R. Nakhai, and H. Aghvami, "4-PSK space-time trellis codes with five and six transmit antennas for slow Rayleigh fading channels," *IEE Electronics Letters*, vol. 39, pp. 297–299, February 2003.

[177] B. Rassool, B. Allen, R. Nakhai, R. Roberts, and P. Sweeney, "Error statistics of optimal and sub-optimal space-time trellis codes: concatenation requirements," in *Proceedings of the IEEE International Symposium on Personal, Indoor and Mobile Radio Communications*, vol. 2, (Beijing, China), pp. 1007–1011, 7-10 September 2003.

[178] B. Rassool, F. Heliot, L. Revelly, M. Dohler, R. Nakhai, and H. Aghvami, "Fast search techniques for obtaining space-time trellis codes for Rayleigh fading channels and its performance in CDMA systems," in *Proceedings of the IEEE Vehicular Technology Conference 2003 Spring*, vol. 1, (Jeju, Korea), pp. 66–69, 22-25 April 2003.

[179] F. Heliot, M. Ghavami, R. Nakhai, and A. Aghvami, "Performance of space-time block coding and space-time trellis coding for impulse radio," in *Proceedings of the IEEE Global Telecommunications Conference*, vol. 5, (Dallas, Texas USA), pp. 3225–3229, 29 Nov. - 3 Dec. 2004.

[180] B. G. Evans and K. Baughan, "Visions of 4G," *IEE Electronics and Communication Engineering Journal*, vol. 12, pp. 293–303, December 2000.

[181] C. K. Toh, *Wireless ATM and AD-HOC Networks Protocols and Architectures*. Kluwer Academic Publishers, 1997.

[182] A. Jardosh, E. Belding-Royer, K. Almeroth, and S. Suri, "Real-world environment models for mobile network evaluation," *IEEE Journal on Selected Areas in Communications*, vol. 23, pp. 622–632, March 2005.

[183] X. Liu and L. Hanzo, "Effects of rate adaptation on the throughput of random ad hoc networks," in *To appear in the IEEE Vehicular Technology Conference 2005 Fall*, (Dallas, Texas, USA), 25-28 September 2005.

[184] H. Luo and S. Lu, "A topology-independent wireless fair queueing model in ad hoc networks," *IEEE Journal on Selected Areas in Communications*, vol. 23, pp. 585–597, March 2005.

[185] V. Srinivasan, P. Nuggehalli, C.-F. Chiasserini, and R. Rao, "An Analytical Approach to the Study of Cooperation in Wireless Ad Hoc Networks," *IEEE Transaction on Wireless Communications*, vol. 4, pp. 722–733, March 2005.

[186] M. Ghassemian, P. Hofmann, C. Prehofer, V. Friderikos, and H. Aghvami, "Performance analysis of Internet gateway discovery protocols in ad hoc networks," in *Proceedings of the IEEE Wireless Communications and Networking Conference*, vol. 1, pp. 120–125, 21-25 March 2004.

[187] L. Yang, H. Wei, and L. Hanzo, "A Multicarrier DS-CDMA System Using Both Time-Domain and Frequency-Domain Spreading," in *Proceedings of the IEEE Vehicular Technology Conference 2003 Fall*, vol. 4, (Orlando, Florida, USA), pp. 2426 – 2430, 6-9 October 2003.

[188] M. Wall, *GAlib Genetic Algorithm Package version 2.45*. Massachusetts Institute of Technology: http://lancet.mit.edu/ga/, 1996.

[189] W. Spears and K. DeJong, *Foundations of Genetic Algorithms*. California, USA: G. Rawlins ed., Morgan Kaufmann, 1991.

Glossary

3G	Third generation mobile communications systems
3GPP	Third Generation Partnership Project
AAA	Adaptive Antenna Arrays
ABS	Active Base station Set
Adaptive Modulation	A modulation scheme, where the actual modulation mode of transmitter 'A' is adjusted according to the near-instantaneous channel quality perceived by receiver 'B'
AQAM	Adaptive Quadrature Amplitude Modulation
BER	Bit Error Ratio, the ratio of the number of bits received incorrectly normalized to the total number of received bits
BS	Base Station
CCI	CoChannel Interference
CDMA	Code Division Multiple Access
DCA	Dynamic Channel Allocation
DECT	Digital Enhanced Cordless Telecommunications
DL	DownLink
DPCH	Dedicated Physical Control CHannel
ETS ISMG	European Telecommunications Institute's - Special Mobile Group
FDD	Frequency Division Duplex
FTP	File Transfer Protocol

GA	Genetic Algorithm
GOS	Grade-Of-Service
GP	Guard Period
HO	HandOver
HQS	Handover Queueing System
IBEP	Instantaneous Bit Error Probability
IFW	Interference Free Window
IS-95	Pan-American DS-CDMA cellular communication system developed by Qualcomm
ISI	Inter Symbol Interference
LOS	Line-Of-Sight
LS	Loosely Synchronized
MAI	Multiple Access Interference
MC-CDMA	A version of Multi-Carrier CDMA, which spreads an information symbol over several subcarriers and uses an OFDM-like scheme to transmit the signal, also known as OFDM-CDMA
MC-DS-CDMA	A version of Multi-Carrier CDMA, which uses a set of orthogonal subcarriers conveying a time-domain-spread information signal
MMSE-BDFE	Minimum Mean Square Error Block Decision Feedback Equalized
MS	Mobile Station
MUD	Multi-User Detector
MUI	Multiple User Interference, an interference inflicted by the other users' signal
OFDM	Orthogonal Frequency Division Multiplexing
OPC	Optimum Power Control
OSI	Open Systems Interconnection
OVSF	Orthogonal Variable Spreading Factor

PC	Power Control
PCPCH	Physical Common Packet CHannel
PDF	Probability Density Function
QAM	Quadrature Amplitude Modulation
QOS	Quality of Service
RAM	Radio Access Mode
RAT	Radio Access Technology
RF	Radio Frequency
RNC	Radio Network Controller
SCH	Synchronization CHannel
SDMA	Space Division Multiple Access
SF	Spreading Factor
SINR	Signal to Interference plus Noise Ratio, same as Signal to Noise Ratio (SNR) when there is no interference
SMI	Sample Matrix Inversion
TDD	Time Division Duplex
TPC	Transmit Power Control
UL	UpLink
UMTS	Universal Mobile Telecommunication System
UTRA	UMTS Terrestrial Radio Access. This is a 3G standard advocated by ETSI
UTRAN	UMTS Terrestrial Radio Access Network
VAD	Voice Activity Detector
WCDMA	Wideband CDMA

Author Index

H

I

J

K

L

M

N

O

P

R

S

T

U

V

W

X

Y

Z